Study on Selective Oxygen Transfer Reactions with Hydrogen Peroxide by Polyoxometalate Catalysts

Keigo KAMATA

Department of Applied Chemistry
School of Engineering
The University of Tokyo
2006

CONTENTS

Chapter I General Introduction 1

1.1. Background 2
1.1.1. Catalytic Oxidation of Hydrocarbons 2
1.1.1.1. Catalytic Oxidation with Hydrogen Peroxide 6
1.1.1.2. Catalytic Oxidation with Molecular Oxygen 11
1.1.2. Polyoxometalates 14
1.1.2.1. Properties of Polyoxometalates 14
1.1.2.2. Liquid-Phase Oxidation Catalyzed by POMs 15
(a) Homogeneous Oxidation with POM-based Compounds 18
(i) Mixed-Addenda POMs 18
(ii) Transition-Metal-Substituted POMs 19
(iii) Peroxometalates 23
(b) Heterogeneous Catalysts with POM-based Compounds 24
1.2. Purpose of This Thesis 33
1.3. References 37

Chapter II Synthesis, Structural Characterization, and Catalytic Performance of Dititanium-Substituted γ-Keggin Silicotungstate 44

2.1. Introduction 45
2.2. Experimental 46
2.2.1. Instruments 46
2.2.2. Syntheses and Characterization of POMs 46
2.2.3. Acid/base Titration 49
2.2.4. Catalytic Oxidation 50
2.2.5. X-Ray Crystallography 50
2.3. Results and Discussion 51
2.3.1. Synthesis of Dititanium-Substituted Silicotungstate 51
2.3.2. Formation of Methoxo Derivative 59
2.3.3. Synthesis of Monotitanium-Substituted Silicotungstate 61

2.3.4. Mono-Oxygenation of Olefins and Sulfides 61
2.4. Conclusion 67
2.5. References 68

Chapter III Oxygen Transfer Reaction with Hydrogen Peroxide Catalyzed by Divacant Lacunary Polyoxometalate 71

3.1. Introduction 72
3.2. Experimental 76
3.2.1. Instruments 76
3.2.2. Syntheses and Characterization of POMs 76
3.2.3. Catalytic Oxidation 79
3.2.4. ^{18}O-Labeling Experiments 82
3.2.5. Kinetic Derivations 82
3.2.6. X-ray Crystallography 83
3.3. Results and Discussion 84
3.3.1. Epoxidation of Mono-Olefins and Oxidation of Sulfides 84
3.3.1.1. Effect of Catalyst 84
3.3.1.2. Effect of Solvent 86
3.3.1.3. X-Ray Crystallographic Structure 87
3.3.1.4. Catalytic Activity for Epoxidation of Mono-Olefins 87
3.3.1.5. Catalytic Activity for Oxidation of Sulfides 90
3.3.1.6. Structural Stability 91
3.3.2. Epoxidation of Non-Conjugated Dienes 92
3.3.2.1. Comparison of Regioselectivity 92
3.3.2.2. Epoxidation of C_6-Olefins 100
3.3.3. Reaction Mechanism for Olefin Epoxidation 102
3.3.3.1. Electronic and Steric Characters of Active Oxygen Species 102
3.3.3.2. Reactivity of Divacant Lacunary POM with Hydrogen Peroxide 105
3.3.3.3. Reactivity of Diperoxo Derivative with Olefins 112
3.3.3.4. ^{18}O-Labeling Experiments 116
3.3.3.5. Reaction Mechanism 116

3.3.3.6. Kinetics 117
3.4. Conclusion 123
3.5. References 124

Chapter IV Epoxidation of Allylic Alcohols in Water with Hydrogen Peroxide Catalyzed by Dinuclear Peroxotungstate 130

4.1. Introduction 131
4.2. Experimental 133
4.2.1. Instruments 133
4.2.2. Materials 133
4.2.3. Oxidation of Allylic Alcohols 134
4.2.4. Kinetic Studies 134
4.2.5. Stability of Catalyst 135
4.3. Results and Discussion 136
4.3.1. Catalytic Epoxidation of Allylic Alcohols 136
4.3.1.1. Effect of Solvent 136
4.3.1.2. Effect of Catalyst 136
4.3.1.3. Catalytic Activity for Epoxidation of Allylic Alcohols 138
4.3.2. Kinetics and Mechanism 141
4.4. Conclusion 146
4.5. References 150

General Conclusions 153

List of Publications 158

Acknowledgements 160

Chapter I

General Introduction

1.1. Background

1.1.1. Catalytic Oxidation of Hydrocarbons

Chemical industries have been contributing to worldwide economic development over the past century, and yet they are often taken to task for many serious environmental problems. Worldwide demands for environmentally friendly chemical processes and products require the development of novel and cost-effective approaches to pollution prevention. One of the most attractive concepts for pollution prevention is green chemistry, which is best defined as the utilization of a set of principles that reduces or eliminates the use or generation of hazardous substances in the design, manufacture, and applications of chemical products.[1a] Advances in green chemistry can solve the obvious hazards associated with global issues such as climate change, energy production, availability of a safe and adequate water supply, food production, and the presence of toxic substances in the environment. The challenge of sustainability will be met with new technologies that provide society with the products we depend on in an environmentally responsible manner.[1]

For fine chemicals manufacture, antiquated "stoichiometric" technologies (e.g., stoichiometric reductions with metals (Na, Mg, Fe, Zn) and metal hydrides ($LiAlH_4$, $NaBH_4$) and oxidations with permanganate or chromium (VI) reagents) are still widely used.[1b] The replacement of these stoichiometric methodologies with cleaner catalytic alternatives can reduce the use and generation of toxic and hazardous substances. For example, the atom efficiencies of the stoichiometric epoxidation of propylene (the chlorohydrin process) and catalytic epoxidation with H_2O_2 are compared (Scheme 1-1). In contrast to the stoichiometric process, the catalytic process offers economical and environmental advantages due to the high atom efficiency and no output of chloride laden sewage. In these contexts, catalysis can be expected to remain a cornerstone in building a sustainable chemical community through green chemistry.[2]

New analytical methods, high-level theoretical studies, and various mechanistic experiments are producing important information on factors which contribute to a catalyst's activity, selectivity, and stability. Especially, the valuable information on the correlations between active sites and catalytic performance can lead to new generation

of catalysts. For the oxidation reaction, mono-, di-, and polynuclear sites of various fine catalysts such as well-defined molecular catalysts, bio-mimetic catalysts relating to the heme enzyme of cytochrome P-450 and the non-heme enzyme of methane monooxygenase, and isolated single site heterogeneous catalysts can effectively activate oxidant and/or substrate, resulting in the specific reactivity and chemo-, regio-, and stereoselectivity. However, some degradation of organic ligands almost invariably occurs under oxidative conditions and the catalytic activity and lifetime are limited. Therefore, the development of selective oxidation reactions by the inorganic catalysts with structurally well-defined active sites can contribute to the construction of "green" and "environmentally-conscious" chemical processes.

Catalytic oxidation is a key technology for converting petroleum-based feedstocks to useful chemicals such as diols, epoxides, alcohols, and carbonyl compounds.[3] Millions of tons of these compounds are annually produced worldwide and applied to all areas of chemical industries, ranging from pharmaceutical to large-scale commodities. The oxidation processes of bulk chemical industries predominantly involve the use of O_2 as the primary oxidant. Their success depends largely on the use of metal catalysts to promote both reaction rate and selectivity to partial oxidation products. The production of ethylene oxide from ethylene by supported silver catalyst, maleic anhydride from *n*-butane by $(VO)_2P_2O_7$ catalyst, terephthalic acid from *p*-xylene by manganese and cobalt salts (Scheme 1-2), and the carbonyl compounds from olefins by palladium salts (Wacker oxidation, Scheme 1-3) are examples of successful commercial oxidation processes with O_2. Since propylene oxide cannot be obtained directly using O_2 in the same manner as the production of ethylene oxide, propylene oxide is produced by metal-catalyzed liquid phase oxidation with hydroperoxides produced by hydrocarbon autoxidaiton (Scheme 1-4).

During recent years, much attention has been focused on the development of catalytic oxidations with environmentally benign oxidants. The choice of the oxidant determines the practicability and efficiency of the oxidation reaction. A large number of oxidants have been extensively investigated in context with catalytic liquid-phase oxidation processes. Some of major oxidants are summarized in Table 1-1. The oxidants such as ClO^-, ClO_2, and ClO_3^- which lead in varying yields to chlorinated organic compounds such as the highly toxic and carcinogenic dioxins are becoming

Stoichiometric:

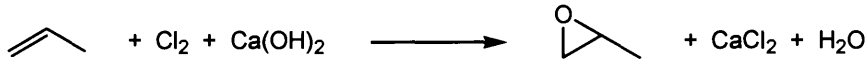

Atom efficiency
= (moloecular weight of the desired product)/(total molecular weights of all substances) x 100
= (58.1)/(42.1+70.9+74.1) x 100 = ***31.1%***

Catalytic:

Atom efficiency
= (58.1)/(42.1+34.0) x 100 = ***76.3%***

Scheme 1-1. Atom efficiencies of stoichiometric and catalytic epoxidation.

$$\text{R-H} \rightarrow \text{R}\bullet + \text{H}\bullet \quad (\textit{or}\ \text{R-H} + \text{M}^{n+} \rightarrow \text{R}\bullet + \text{M}^{(n-1)+} + \text{H}^{+})$$
$$\text{R}\bullet \rightarrow \text{ROO}\bullet$$
$$\text{ROO}\bullet + \text{R-H} \rightarrow \text{ROOH} + \text{R}\bullet$$

Scheme 1-2. Free radical autoxidation.

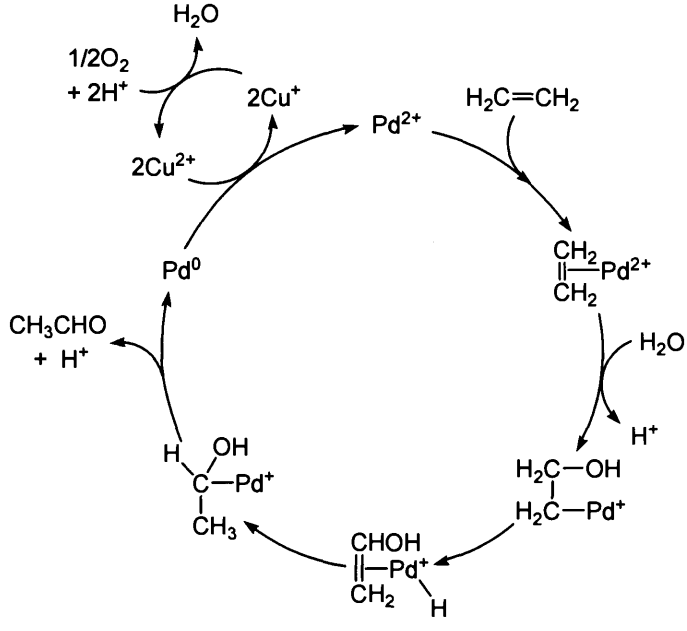

Scheme 1-3. Wacker type oxidation.

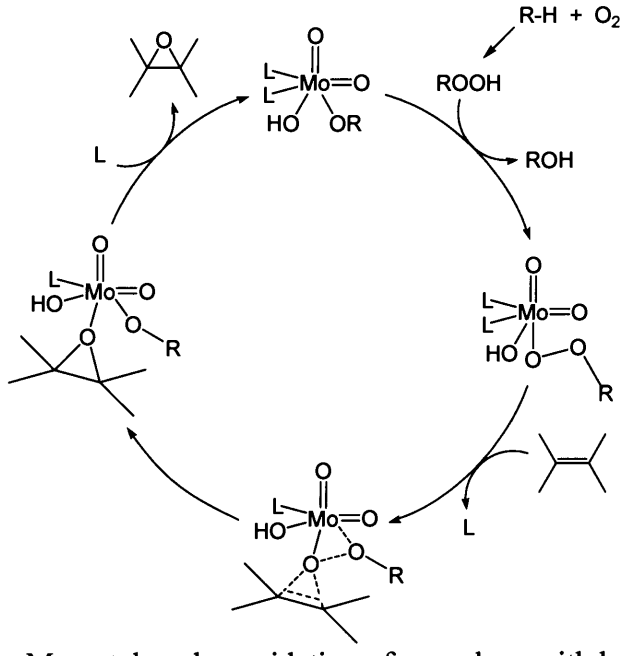

Scheme 1-4. Mo-catalyzed epoxidation of propylene with hydroperoxide.

Table 1-1. Various oxidants used for liquid-phase oxidation processes

oxidants	active oxygen (%)	by-product
O_2 (dioxygenase type)	100	none[a]
O_2 (monooxygenase type)	50	H_2O, CO_2, and carboxylic acid, *etc.*
H_2O_2	47	H_2O
N_2O	36	N_2
O_3	33	O_2
ClO_2	24	ClO^-, Cl^-
ClO^-	22	Cl^-
$(CH_3)_2CO_2$	22	$(CH_3)_2CO$
t-BuOOH (TBHP)	18	*t*-BuOH
$C_5H_{11}NO_2$[b]	14	$C_5H_{11}NO$
ClO_3^-	13	ClO_2^-, Cl^-
HSO_5^-	11	HSO_4^-
$ClC_6H_4CO_3H$ (*m*-CPBA)	10	ClC_6H_4COOH
$NCC_6H_4N(CH_3)_2O$	10	$NCC_6H_4N(CH_3)_2$
IO_4^-	8	IO_3
C_6H_5IO (PhIO)	7	C_6H_5I
C_6F_5IO (PFIB)	5	C_6F_5I

[a] No by-products should be observed provided reducing agent-free non-radical-chain aerobic oxygenation can be achieved. [b] *N*-Methylmorpholine *N*-oxide.

environmentally, politically, and economically unacceptable. In addition, active oxygen contents of most oxidants are relatively low (≤30%). In these contexts, the most attractive oxidants are H_2O_2 and O_2 (or air) because of their high contents of active oxygen species and co-production of only water.[4]

The ideal system for "green" oxidation is the use of environmentally-friendly oxidants together with recyclable catalysts in nontoxic solvents. Thus, the current goal of the research and industry is the development of effective metal catalysts that can activate H_2O_2 or O_2 at ambient conditions and transfer to various substrates with high chemo-, regio-, diastereo-, and stereoselectivity. In the following section, the selective hydrocarbon oxidations in liquid phase by the structurally well-defined catalysts with O_2 and H_2O_2 are described. The homogeneous and heterogeneous oxidation catalyses by polyoxometalate-related compounds are mentioned later (section 1.1.2.2.).

1.1.1.1. Catalytic Oxidation with Hydrogen Peroxide

H_2O_2 is an attractive oxidant due to the following advantages; (i) H_2O_2 has a high content of active oxygen species (47% of its weight), which is more than those of the other common oxidants such as NaClO, $KHSO_5$, and ROOH, (ii) water is the only by-product, and (iii) aqueous H_2O_2 is a stable reagent. Therefore, much attention has been paid to the development of the metal catalysts for the oxidation with H_2O_2.

Methyltrioxorhenium (MTO) has been reported to be an active catalyst for the oxidation of various substrates including olefins, alkynes, aromatic compounds, sulfides using H_2O_2 as an oxidant.[5a] Among them, the epoxidation of olefins was extensively studied. MTO could activate H_2O_2 through an equilibrium formation of the catalytically active η^2-peroxo species of $CH_3ReO_2(O_2)$ and $CH_3ReO(O_2)_2(H_2O)$ (Scheme 1-5). Initially, anhydrous H_2O_2 in *t*-BuOH was used as an oxidant but low selectivities were reported for acid sensitive epoxides due to the high acidity of the MTO-H_2O_2 system.[5b] The addition of a base, such as pyridine, in large excess to MTO (>10:1) enhanced the rate and selectivity for the epoxidation of di-, tri- and tetrasubstituted olefins using commercially available 30% aqueous H_2O_2, as the base protected the epoxide from ring opening [Eq. (1-1)].[5c–5e]

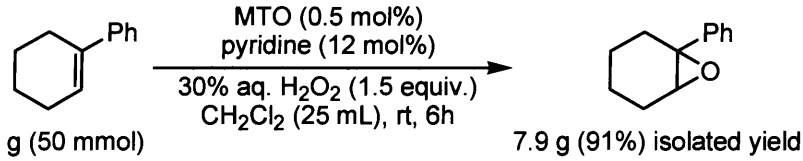

(1-1)

Titanium silicalite-1 (TS-1) is a microporous solid material with the MFI structure modified by isomorphous substitution of Si(IV) with Ti(IV).[4f,4g,6a,6b] Its remarkable activity in oxidation of various substrates with aqueous H_2O_2 (Scheme 1-6) is attributed to site isolation of Ti(IV) centers in the hydrophobic pores of silicalite, which enables the simultaneous adsorption of the oxidant and the hydrophobic substrate in the presence of water. Owing to the relatively small pore diameter of the 10-member ring of TS-1, efforts have been made to synthesize large pore 12-member ring Ti zeolites such as BEA (Ti-β),[6c] MTW (Ti-ZSM-12),[6d] ISV (Ti-ITQ-7),[6e] and MWW (Ti-MCM-22).[6f] Although the complete mechanism for TS-1-catalyzed epoxidation was not known, the rate enhancement due to methanol suggested a tight association at the Ti active site as shown in Scheme 1-7. This coordination of methanol was proposed to increase the electrophilicity of the Ti-coordinated peroxide species and facilitate oxygen transfer to the olefins.

Al-free Sn-Beta was able to catalyze the Baeyer-Villiger oxidation of cyclic ketones with diluted H_2O_2 with good activities and very high selectivity to the corresponding lactone.[7] Even when a double bond was present in the reactant cyclic ketone, a very high chemoselectivity for the Baeyer-Villiger reaction was observed with Sn-Beta catalyst [Eq. (1-2)]. The Baeyer-Villiger oxidation with H_2O_2 on Sn-Beta was reported to proceed *via* a "Criegee" adducts, where H_2O_2 added to a ketone activated by the Sn-Beta, without formation of dioxiranes or carbonyl oxides as intermediates.

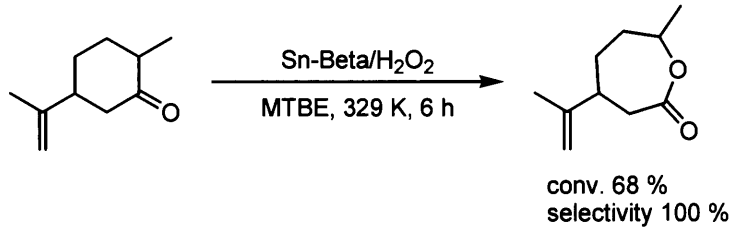

(1-2)

Tilley and co-workers developed the molecular precursor route to isolated catalytic sites supported on various forms of silica.[8] Advantages of this approach include the molecular-level control over the structure of the catalytic site and the generation of site-isolated catalysts (Scheme 1-8). The active sites which were introduced *via*

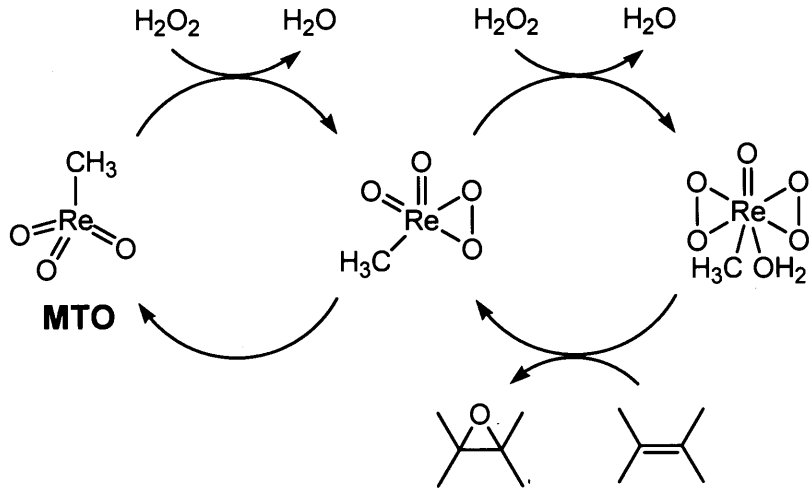

Scheme 1-5. Epoxidation mechanism catalyzed by MTO.

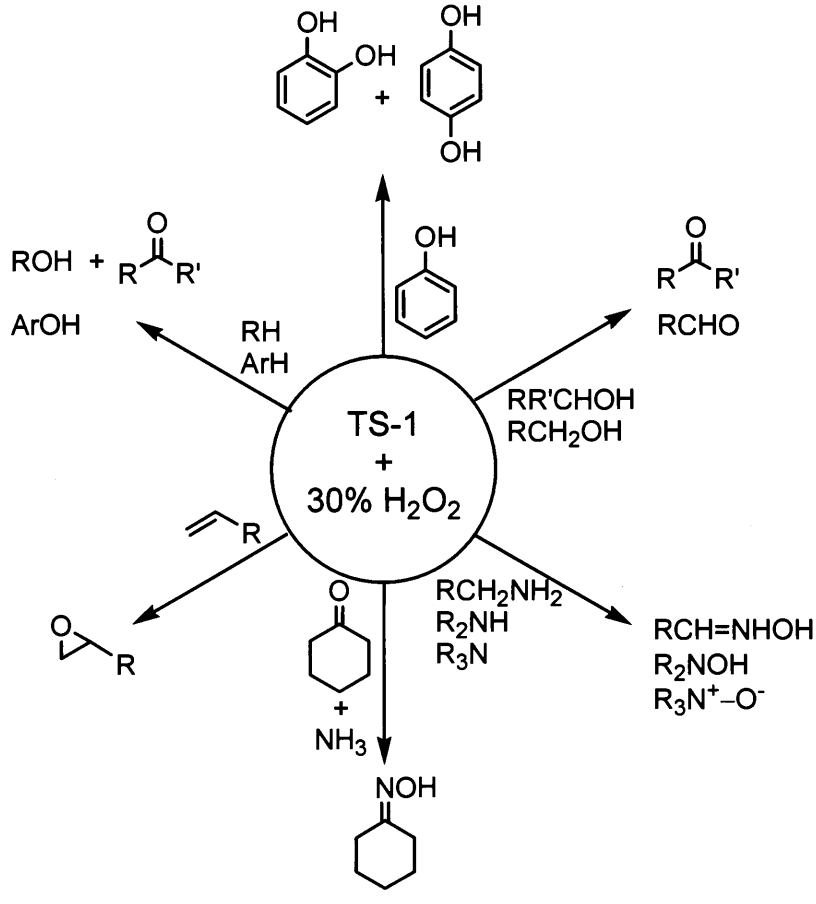

Scheme 1-6. Various oxidation reactions catalyzed by TS-1.

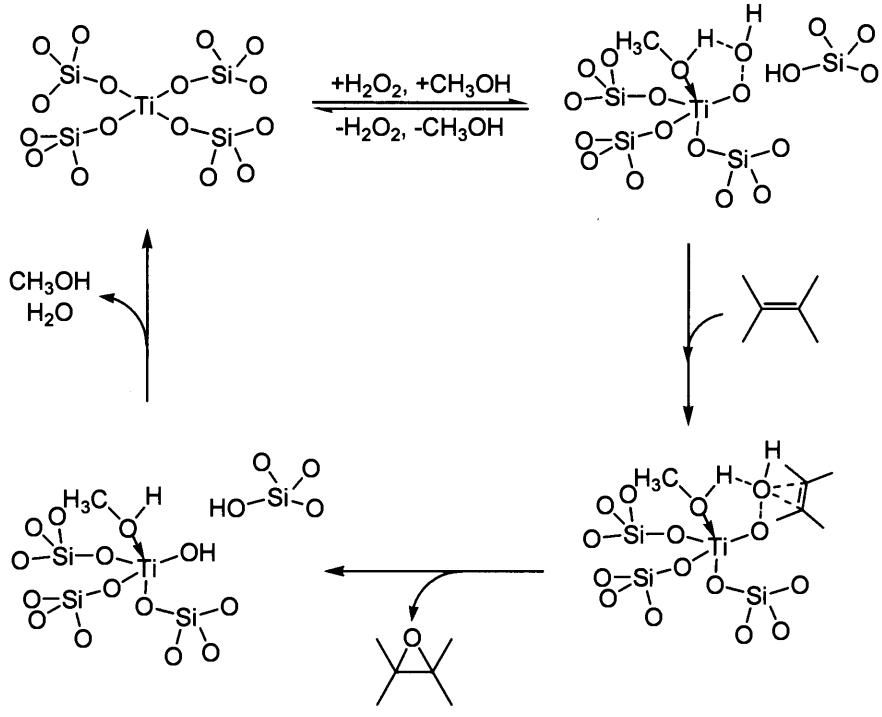

Scheme 1-7. Epoxidation mechanism catalyzed by TS-1.

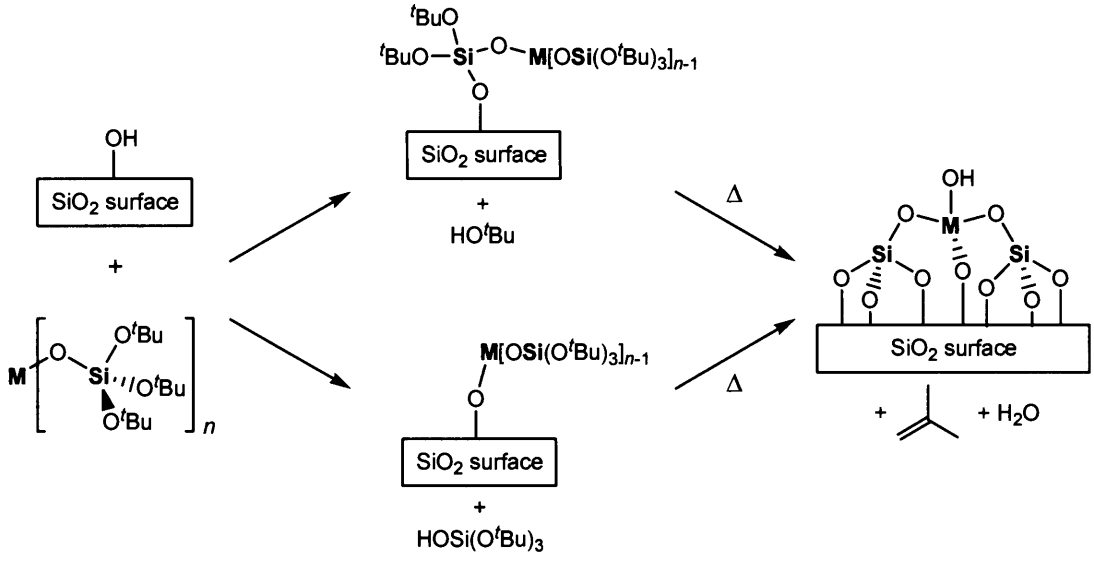

Scheme 1-8. Thermolytic molecular precursor route to site-isolated active site.

grafting reactions of the molecular precursors such as $MO_2[OSi(O^tBu)_3]_2$ (M = Mo, W),[8b] $Fe[OSi(O^tBu)_3]_3(THF)$,[8c] and $(^iPrO)Ti[OSi(O^tBu)_3]_3$[8d] with SBA-15 could catalyze various hydrocarbon oxidations with H_2O_2.

The oxidant activation mechanisms for hydrocarbon oxidations catalyzed by iron centers in heme (e.g., cytochrome P450) and non-heme iron enzymes (e.g., methane monooxygenase and Rieske dioxygenase) has been a subject of persistent interest in bioinorganic chemistry.[9] According to the structure of the iron center, iron-peroxo and/or high-valent iron-oxo species have been proposed as the possible oxidizing species (Scheme 1-9). The selective oxidation systems by biomimetic metalloporphyrins, mainly iron(III) and manganese(III), with various oxidants have been developed. While the use of H_2O_2 as an oxidant in metalloporphyrin-catalyzed oxidations caused fast destruction of the catalysts and the non-productive decomposition of oxidant, co-catalysts such as carboxylic acids, ammonium acetate, and imidazole significantly enhanced the catalytic activity.[10]

Non-heme iron complexes based on a tetradentate ligand have been reported to epoxidize aliphatic olefins at high yields (60–90%) with 50% H_2O_2. The addition of acetic acid (30 mol%) significantly favored the epoxide production due to the formation of a μ-oxo, carboxylate-bridged diiron (III) complex. This complex was easily formed *in situ* and the epoxidation completed within 5 min [Eq. (1-3)].[11a] Similarly, a μ-oxo-iron(III) dimer $[((phen)_2(H_2O)Fe^{III}{}_2)_2(\mu\text{-}O)](ClO_4)_4$ was an efficient epoxidation catalyst for a wide range of olefins including terminal ones using peracetic acid as an oxidant.[11b] These iron complexes mimicked the methane monooxygenase enzyme.

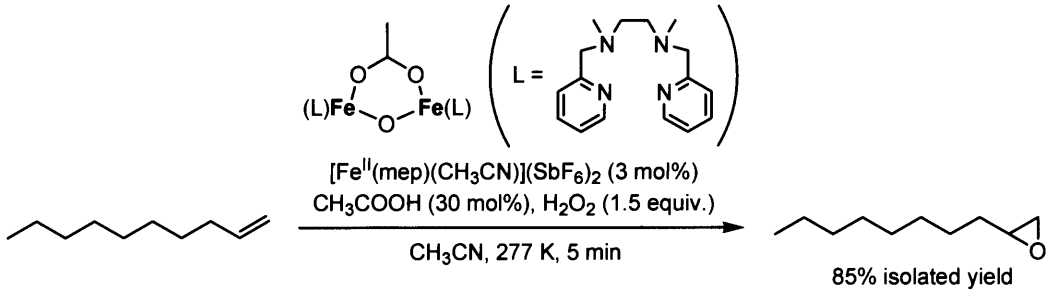

(1-3)

Some dimeric manganese complexes based on the *N,N',N''*-trimethyl-1,4,7-triazacyclononane ligand also showed high conversions and turnover numbers for epoxidation.[12] The use of additive ligands, 1,3-diones and dicarboxylic acids, significantly increased the yield of epoxide and decreased the

decomposition of H_2O_2.[12a] Acetic acid also enhanced the catalytic activity, resulting in >4000 turnover numbers for epoxidation of 1-decene [Eq. (1-4)].[12b]

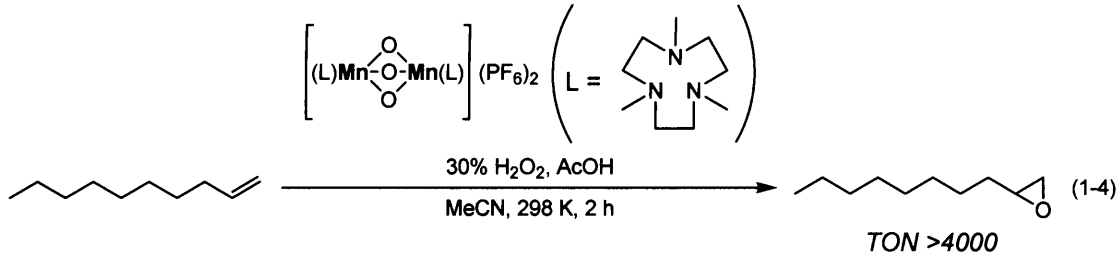

(1-4)

1.1.1.2. Catalytic Oxidation with Molecular Oxygen

Enzymes which activate O_2 to oxidize organic substrates into oxygenates are classified into two groups according to the mode of oxygen incorporation (Scheme 1-10). Dioxygenase incorporates two oxygen atoms of an O_2 molecule into the substrate, whereas monooxygenase transfers only one oxygen atom. The latter usually requires reducing agents such as NADH and other chemicals as a cofactor and the other oxygen atom in O_2 is converted to water. Based on this concept of monooxygenase enzymes, activation of O_2 by artificial reducing agents such as H_2, CO, and aldehyde established new oxidation systems with O_2 under mild reaction condition.[13] However, the artificial monooxygenase systems typically require an excess amount of reducing agents in order to obtain the oxygenated products selectively. In these contexts, there is a need to develop effective O_2-based catalytic and controllable oxidation systems without reducing agents. Next, some successful examples for oxidation with O_2 as a sole oxidant are stated.

Thomas and co-workers developed "single-site heterogeneous catalysts" based on metal-substituted mesoporous silicas such as MCM-41 and SBA-15 and microporous aluminophosphates.[14] For *n*-alkane oxyfunctionalization with Co- and Mn-AlPO-18, the oxidation at the terminal carbon was highly preferred [Eq. (1-5)]. Because of the end-on approach of the *n*-alkane in AlPO-18, owing to the pore dimensions and topology of this molecular sieve, only the C_1 and C_2 positions were preferentially oxidized. When other structures with larger pore dimensions (AlPO-36 and AlPO-5) were used, oxyfunctionalization was predominant at the C_3 and C_4 positions.

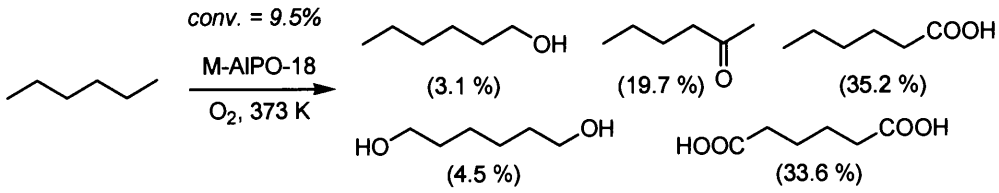

(1-5)

An aerobic oxidation of hydrocarbons through catalytic carbon radical generation under mild conditions was achieved by using *N*-hydroxyphthalimide (NHPI).[15] The reaction of NHPI in benzonitrile with O_2 leaded to the generation of a phthalimide *N*-oxyl (PINO) radical [Eq. (1-6)]. A catalytic system of NHPI and a transition metal salts such as Co or Mn applied to various functionalizations of hydrocarbons including oxygenation, nitration, sulfoxidation, epoxidation, carboxylation, and oxyalkylation.

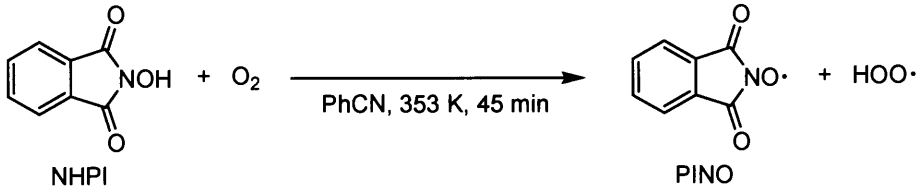

(1-6)

The formation of P-450-like active species from O_2 without any reducing agents was examined by several groups.[16] It was reported that ruthenium (II) porphyrin complex could oxidize by O_2 to dioxo ruthenium (VI) complex, which oxidized tetramethylethylene to the corresponding epoxide at room temperature accompanied by the formation of the starting ruthenium (II) complex (Scheme 1-11). Because of low turnover numbers of the system, more efficient aerobic epoxidation without radical initiators or reducing agents are still desired.

The oxidation of primary and secondary alcohols into the corresponding carbonyl compounds plays a central role in organic synthesis.[17] Recent developments of the reusable heterogeneous catalysts consisting of Ru and Pd provided atom-efficient methods with clean oxidant of O_2. Nanoclustered Pd^0 species could effectively promote the alcohol oxidation under an atmospheric O_2 pressure, giving a remarkably high turnover number of ≥236000 with an excellent turnover frequency of approximately 9800 h^{-1} for a 250-mmol-scale oxidation of 1-phenylethanol under solvent-free conditions [Eq. (1-7)].[17d]

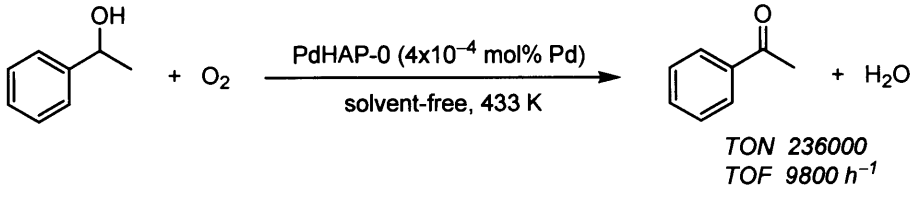

(1-7)

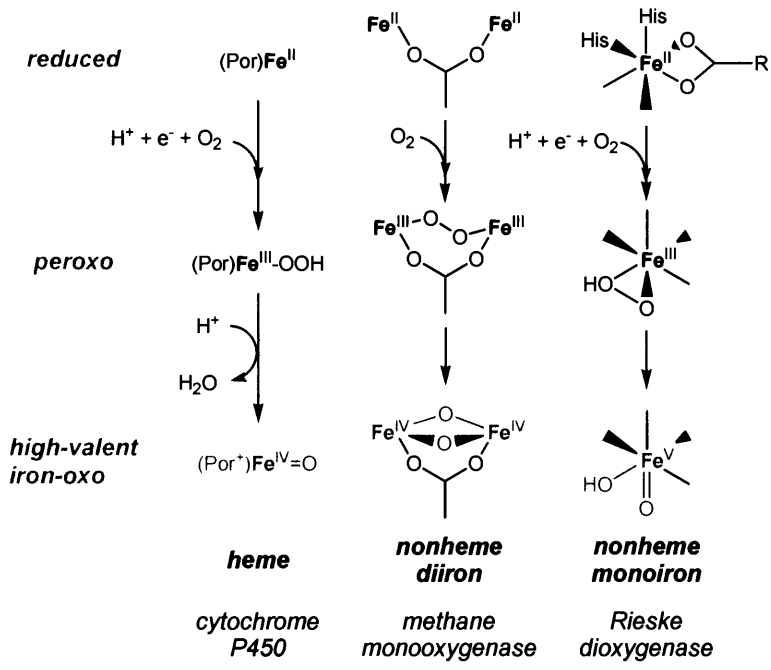

Scheme 1-9. Mechanistic scheme for O_2-activating iron enzymes.

<u>Dioxygenase</u>

$$S + O_2 \rightarrow SO_2$$
$$2S + O_2 \rightarrow 2SO$$

<u>Monooxygenase</u>

$$S + O_2 + 2H^+ + 2e^- \rightarrow SO + H_2O$$

(S: Substrate, SO: oxygenated product)

Scheme 1-10. Classification of oxygenases.

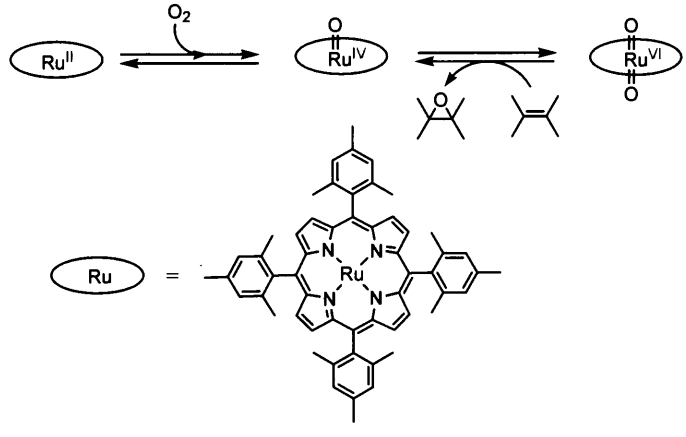

Scheme 1-11. O_2 activation by Ru-porphyrin complex.

1.1.2. Polyoxometalates

1.1.2.1. Properties of Polyoxometalates

Polyoxometalates (POMs) belong to a large class of nano-sized metal-oxygen cluster anions (Figure 1-1).[18,19] POMs form by a self-assembly process, typically in an acidic aqueous solution and can be isolated as solids with an appropriate counter cation (e.g., H^+, alkaline metal, NH_4^+, alkylammonium, *etc.*). Generally, two types of POMs are distinguishing as based on chemical composition; isopolyoxometalates (IPAs) and heteropolyoxometalates (HPAs). These anions can be represented by the following general formulas:

$$[M_mO_y]^{p-} \qquad \text{(IPAs)}$$

$$[X_xM_mO_y]^{q-}\ (x < m) \qquad \text{(HPAs)}$$

where M is the addenda atom and X is the hetero atom. The most common addenda atoms are the d^0-early-transition-metal ions such as W^{VI}, Mo^{VI}, and V^V. The heteroatoms can be *p*-, *d*-, or *f*-block elements such as P^V, As^V, Si^{IV}, Ge^{IV}, and B^{III}. Typical reactions are given in Eqs. (1-8) and (1-9) for preparation of heptamolybdate (IPA) and dodecatungstophosphate (HPA), respectively.

$$7MoO_4^{2-} + 8H^+ \rightarrow Mo_7O_{24}^{6-} + 4H_2O \qquad (1\text{-}8)$$

$$12WO_4^{2-} + HPO_4^{2-} + 23H^+ \rightarrow PW_{12}O_{40}^{3-} + 12H_2O \qquad (1\text{-}9)$$

Among a wide variety of HPA compounds, the Keggin structures are the most stable and more easily available. The Keggin anions (typically represented by the formula $[X^{n+}M_{12}O_{40}]^{(8-n)-}$) contain one central heteroatom and 12 addenda atoms that surround it in four M_3O_{13} triads. Each of the M_3O_{13} groups can be rotated 60° about its 3-fold axis, leading to geometrical isomers. Rotation of one, two, three, and all four M_3O_{13} groups of the most common α-isomer Keggin structure produces the β, γ, δ, and ε isomers, respectively. Another typical HPA is the Wells-Dawson type POM. The Wells-Dawson structure (typically represented by the formula $[X_2^{n+}M_{18}O_{62}]^{(16-2n)-}$) consists of two trivacant A-type lacunary Keggin species, which generated by the loss of corner-shared group of MO_6 octahedra, linked directly across the lacunae.

The generation of lacunary derivatives of the POM anion results from the removal of one or more addenda atoms. The most stable lacunary compounds are obtained

with Si^{IV} as the heteroatom. While the dodecatungstosilicates are stable in acidic solution, hydrolytical cleavages of W-O bonds occur and well-defined lacunary POMs with 11, 10, 9 tungsten atoms are produced when the pH increases. Lacunary species can act as ligands with numerous metal cations, leading to mono-, di-, trinuclear transition-metal-substituted POM complexes according to the number of vacant sites. The metal incorporation involves reaction of aquated first-row and occasionally second-row *d*-block metal ions, $M(H_2O)_6^{z+}$, with a lacunary POM derived from the Keggin [Eq. (1-10)], Wells-Dawson, and other POM families. In addition, lacunary species assemble into large POM structures, either directly or with incorporation of metal ion linkers.[19h,19i]

$$M(H_2O)_6^{z+} + X^{n+}M_{11}O_{39}^{(4-n)-} \rightarrow (MOH_2^{z+})X^{n+}M_{11}O_{39}^{(12-n-z)-} \quad (1\text{-}10)$$

These anion structures of POMs are called "primary structure". The "secondary structure" is the three-dimensional (usually regular) arrangement consisting of polyanions, counter cations, and additional molecules. The tertiary structure represents the manner in which the secondary structure assembles into solid particles and relates to properties such as particle size, surface area, and pore structure (Figure 1-2). The presence of hierarchical structures (primary, secondary and tertiary structures) could lead to three unique modes for heterogeneous acid and oxidation catalysis—surface-type, pseudoliquid (or bulk-type I) and bulk-type II (Figure 1-3).[19a,19b] In the following section, the liquid-phase oxidation by POM compounds with H_2O_2 and O_2 are described.

1.1.2.2. Liquid-Phase Oxidation Catalyzed by POMs

The versatility and accessibility of POMs have led to the various applications in the fields of structural chemistry, analytical chemistry, surface science, medicine, electrochemistry, photochemistry, and catalysis. POMs have especially received much attention in the area of oxidation and acid catalysis. Several categories of POMs are formed by proper selection of the starting components and by the adjustment of pH and temperature. Typical examples are shown in Figure 1-1; (i) IPAs, (ii) HPAs, (iii) mixed-addenda POMs, (iv) transition metal substituted POMs, (v) lacunary POMs, and (vi) peroxometalates. Various types of POMs are effective homogeneous catalysts for the H_2O_2- and O_2-based environmentally-friendly oxidations. In addition, the

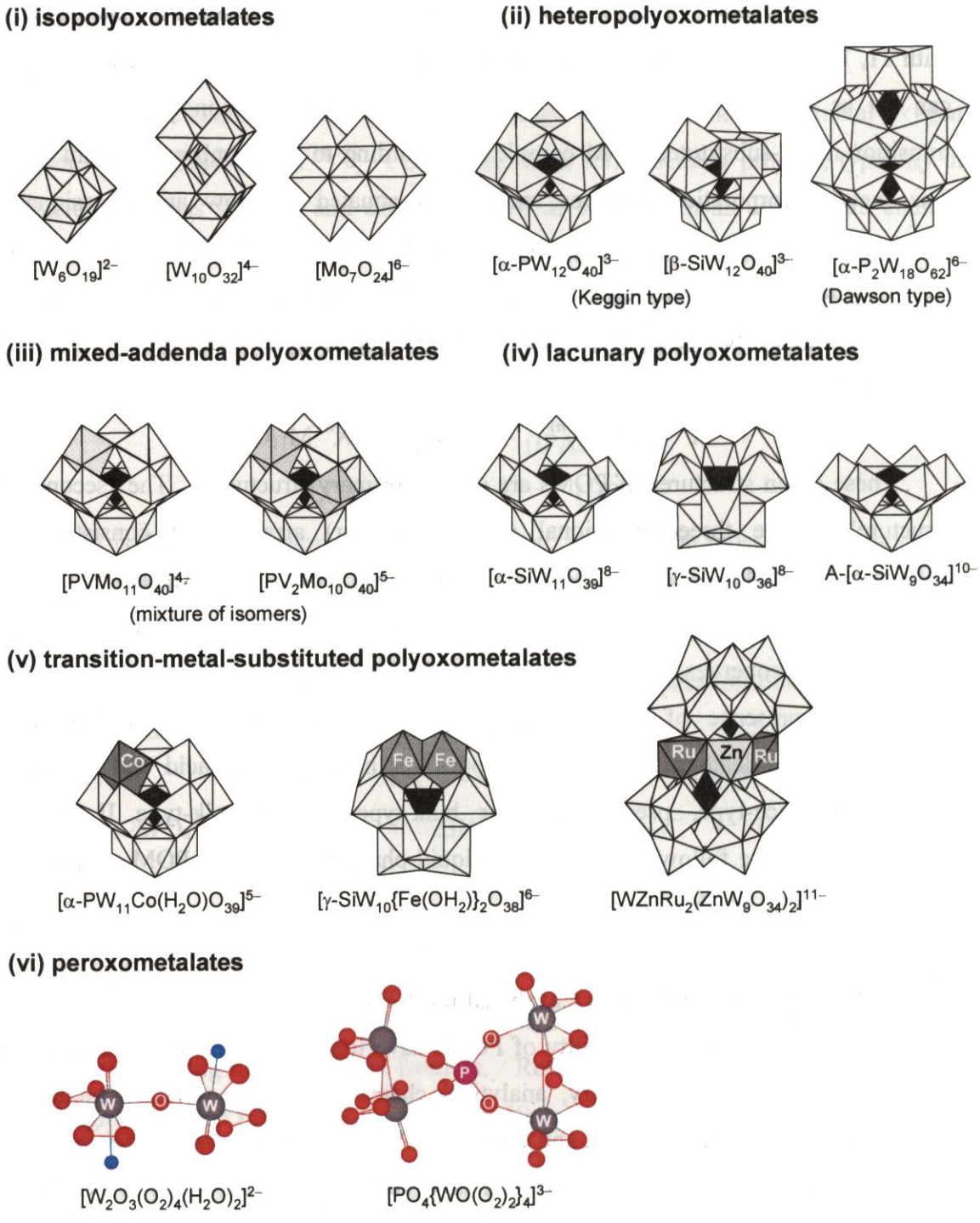

Figure 1-1. Structures of POMs.

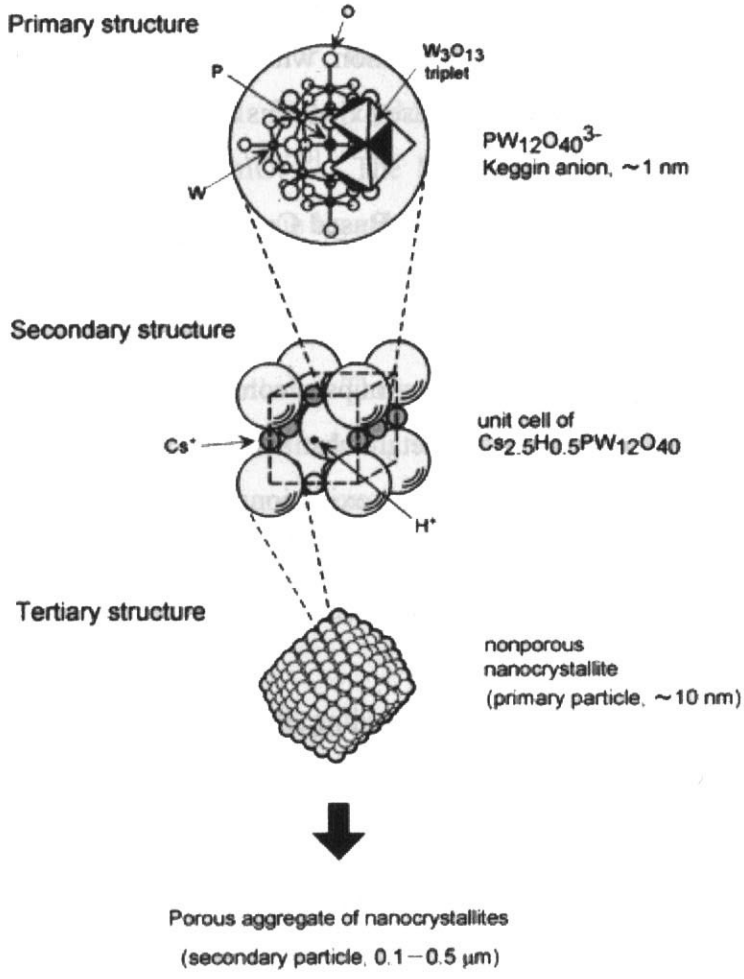

Figure 1-2. Primary, secondary and tertiary structures; hierarchical structures of HPAs in the solid state.

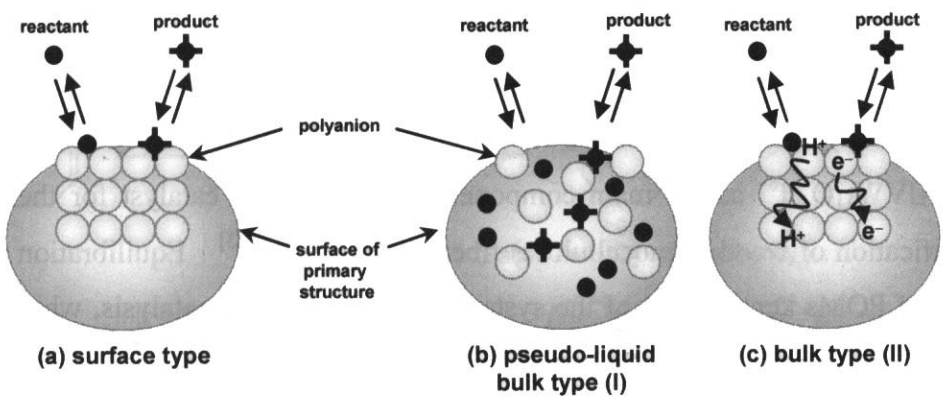

Figure 1-3. Three types of catalysis for solid HPAs; (a) surface type, (b) pseudoliquid: bulk type (I), and (c) bulk type (II).

heterogenization of POMs can improve the catalyst recovery and recycling. Next, the development of (a) homogeneous oxidation with POM-based compounds and (b) heterogenization of POMs for liquid phase oxidations are described.

(a) Homogeneous Oxidation with POM-Based Compounds

Many catalytic systems for H_2O_2- and O_2-based oxidations catalyzed by POMs have been developed. Typical examples of oxidation reactions are listed in Table 1-2. The systems can be classified into three groups according to the structures of POMs; (i) mixed-addenda POMs, (ii) transition-metal-substituted POMs, and (iii) peroxometalates. In this section, liquid-phase homogeneous oxidations by POMs with H_2O_2 and O_2 are described according to the above classification.

(i) Mixed-Addenda POMs

A wide variety of hydrocarbons including alkanes, alcohols, amines, and arenes could be oxidized with O_2 in the presence of mixed-addenda POMs $[PMo_{12-n}V_nO_{40}]^{(3+n)-}$.[20] The oxidation mechanism included one (or more) electron oxidation of the substrate by $[PMo_{12-n}V_nO_{40}]^{(3+n)-}$ to give the product and the reduced form of $[PMo_{12-n}V_nO_{40}]^{(3+n)-}$, followed by reoxidation of the reduced form by O_2. The $[PMo_{12-n}V_nO_{40}]^{(3+n)-}/O_2$/hydrocarbon redox system can be used to oxidize a wide variety of hydrocarbons since the redox potential of $[PMo_{12-n}V_nO_{40}]^{(3+n)-}$ (ca. 0.7 V vs. SHE) is lower than that of O_2 and is higher than that of a wide variety of hydrocarbons.[19f,19g,21] It is noted that the system consisting of $[PMo_{12-n}V_nO_{40}]^{(3+n)-}$ and Pd^{2+} salts could catalyze the Wacker oxidation and Moritani-Fujiwara reaction with the use of O_2.[19f,19g,20a,20j,20k,22]

Thermodynamically controlled self-assembly of an equilibrated ensemble of POMs with $[AlVW_{11}O_{40}]^{6-}$ as the main component could act as a catalyst for the selective delignification of wood (lignocellulose) fibers (Figure 1-4).[23] Equilibration reactions typical of POMs kept the pH of the system near 7 during the catalysis, which avoided acid or base degradation of cellulose.

(ii) Transition-Metal-Substituted POMs

In 1986, it was reported for the first time by Hill and Brown that transition-metal-substituted POMs $[PW_{11}O_{39}M'(OH_2)]^{5-}$ (M' = Mn^{2+}, Co^{2+}) catalyzed the oxidation of olefins with PhIO.[24] The M' atom easily becomes coordinatively unsaturated by elimination of the aquo ligand, and the resulting polyanion is regarded as an inorganic metalloporphyrin analogue.[25] Transition-metal-substituted POMs are oxidatively and hydrolytically stable compared with organometallic complexes, and their active sites can be controlled. These advantages have been applied to the development of biomimetic catalysis relating to the heme enzyme, cytochrome P-450, and the nonheme enzyme, methane monooxygenase analogues (Figure 1-5). Until now, numerous catalytic oxidations by transition-metal-substituted POMs have been developed and some transition-metal substituted POMs can activate H_2O_2 and O_2 as described below.

Transition-metal-substituted Keggin-type POMs sometimes promoted the non-productive decomposition of H_2O_2, while Zn, Ti, Fe, and Mn-substituted POMs could act as effective catalysts for H_2O_2-based epoxidation.[26] Zinc-containing $[PZn^{II}W_{11}O_{39}]^{5-}$ and $[PZnMo_2W_9O_{39}]^{5-}$ have been reported to show moderate activity for the epoxidation although the stability has not been unclear.[26a,27] Yamase and co-workers proposed that the η^2-peroxo $Ti(O_2)$ species formed by the reaction of $[PTi_xW_{12-x}O_{40}]^{(3+2x)-}$ with H_2O_2 was an active intermediate for epoxidation of olefins.[28] Mizuno and co-workers synthesized *di*-iron-substituted silicotungstate, $[\gamma\text{-}SiW_{10}\{Fe(OH_2)\}_2O_{38}]^{6-}$, by the reaction of $[\gamma\text{-}SiW_{10}O_{36}]^{8-}$ with $Fe(NO_3)_3$ in an acidic aqueous solution.[29a] This compound could catalyze the selective oxidation of olefins as well as alkanes with highly efficient utilization of H_2O_2 [Eqs. (1-11) and (1-12)].[29]

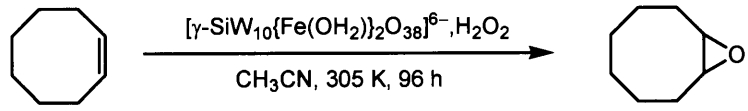

(1-11)

96%
(Based on H_2O_2, 99% effciency)

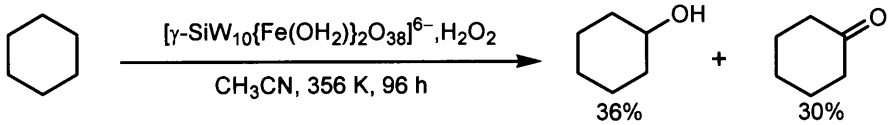

(1-12)

36% 30%
(Based on H_2O_2, 95% effciency)

Neumann and co-workers reported that the nickel-substituted quasi-Wells-Dawson

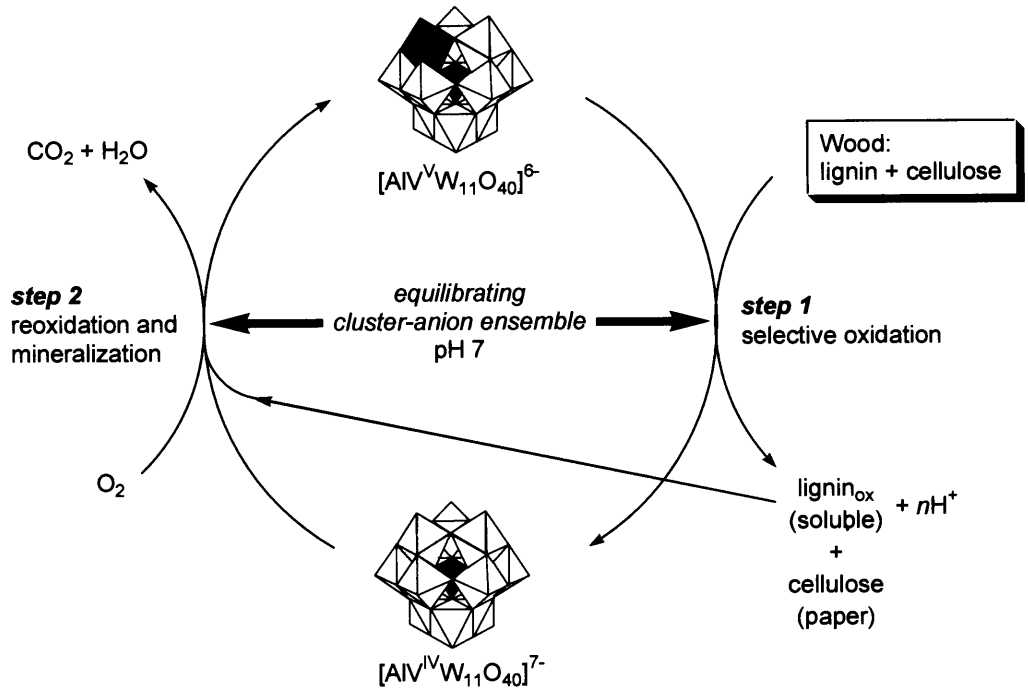

Figure 1-4. Proposed catalytic cycle for the selective delignification of wood (lignocellulose) fibres with an equilibrated ensemble of POMs.

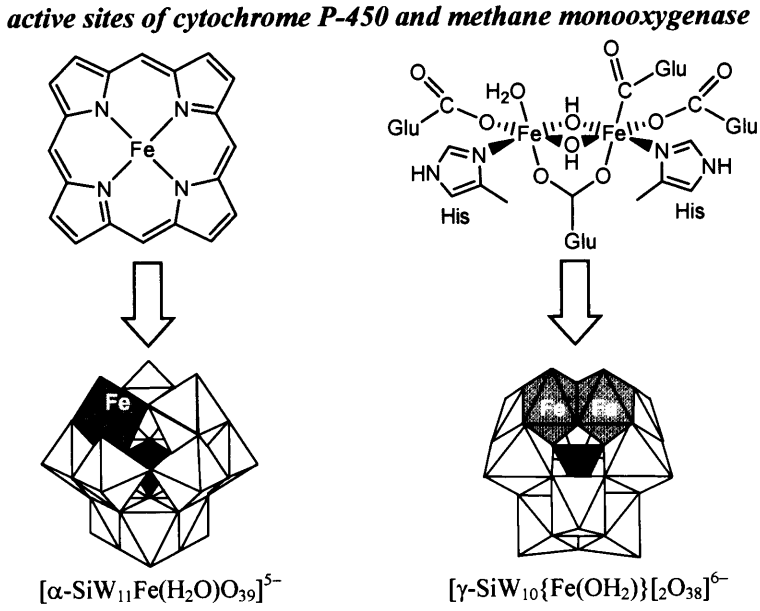

Figure 1-5. Application of transition-metal-substituted POMs as bio-mimetic catalysts.

type polyfluorooxometalate, $[Ni^{II}(H_2O)H_2F_6NaW_{17}O_{55}]^{9-}$, was the most active for epoxidation of olefins and allylic alcohols with H_2O_2 among various polyfluorooxometalates, $[M(L)H_2F_6NaW_{17}O_{15}]^{q-}$ (M = Zn^{II}, Co^{II}, Mn^{II}, Fe^{II}, Ru^{II}, Ni^{II}, and V^{V}).[30]

Among the complexes synthesized by the reactions of *d*-electron transition metals with trivacant lacunary POMs, the sandwich-type POMs have received much attention because of their superior catalytic performance for the oxidation with H_2O_2 and O_2.[31] In addition, sandwich-type POMs have been considered to be more thermodynamically stable than Wells-Dawson and Keggin-type POMs.[31a,31b,31c,32] An efficient biphasic H_2O_2-based epoxidation system catalyzed by $[WZnM_2(H_2O)_2(ZnW_9O_{34})_2]^{q-}$ (M=Mn^{II}, Zn^{II}, *etc.*), first synthesized by Tourné,[33] was reported. Manganese containing $[WZnMn_2(H_2O)_2(ZnW_9O_{34})_2]^{12-}$ was oxidatively and hydrolytically stable over a range of ≥12500 turnovers for the epoxidation of cyclooctene.[31a,31b] A series of new manganese(II)-substituted POMs, $[(Mn(H_2O)_3)_2(WO_2)_2(BiW_9O_{33})_2]^{10-}$, $[(Mn(H_2O))_3(SbW_9O_{33})_2]^{12-}$, and $[(Mn(H_2O)_3)_2(Mn(H_2O)_2)_2(TeW_9O_{33})_2]^{8-}$ could also catalyze regioselective epoxidation of *R*-(+)-limonene to 1,2-epoxide at ambient temperature in a biphasic system.[31d] Recently, a new family of transition-metal substituted POMs, $[((MOH_2)M_2PW_9O_{34})_2(PW_6O_{26})]^{17-}$ (M=Mn^{II}, Co^{II}), were synthesized by the decomposition of the sandwich-type POMs.[34] The methyltricaprylammonium salt of $[((Mn^{II}OH_2)Mn^{II}{}_2PW_9O_{34})_2(PW_6O_{26})]^{17-}$ effectively catalyzed the epoxidation of cyclooctene, cyclohexene, and 1-hexene.

A tetranuclear ferric Wells-Dawson-type sandwich POM, $[Fe^{III}{}_4(H_2O)_2(P_2W_{15}O_{56})_2]^{12-}$, showed low selectivity to the corresponding epoxides because of the progress of the allylic oxidation or oxidative cleavage of double bonds similar to Keggin-type analogues. In contrast to tetraferric species, a triferric sandwich-type POM, $[(NaOH_2)(Fe^{III}OH_2)Fe^{III}{}_2(P_2W_{15}O_{56})_2]^{14-}$, exhibited high selectivity to the corresponding epoxides.[35] A *di*-iron containing sandwich-type POM, $[Fe^{III}{}_2(NaOH_2)_2(P_2W_{15}O_{56})_2]^{16-}$, was synthesized using $FeCl_2$ in place of $FeCl_3$ followed by air oxidation in aqueous media, and the Na^+ center could easily be replaced with Cu^{II}, Co^{II}, and Ni^{II} because Na centers were weakly bonded and labile.[32c,36] Among these compounds, $[Fe^{III}{}_2(NaOH_2)_2(P_2W_{15}O_{56})_2]^{16-}$ and $[Fe^{III}{}_2(NiOH_2)_2(P_2W_{15}O_{56})_2]^{16-}$

exhibited higher activity for the epoxidation of cyclooctene.

The ruthenium-substituted sandwich type POM $[WZnRu_2(OH)(H_2O)(XW_9O_{34})_2]^{11-}$ (X = Zn^{2+} or Co^{2+}) catalyzed the selective hydroxylation of adamantane with O_2 as an oxidant [Eq. (1-13)].[37] The catalyst oxygenated selectively tertiary C-H bond of adamantane, giving only 1-adamantanol. The oxidation featured an adamantane:O_2 stoichiometry of 2:1. On the basis of the stoichiometry, spectroscopic evidence, and kinetic studies, a dioxygenase-type mechanism was proposed; activation of O_2 *via* complexation to a Ru^{2+} species followed by the formation of a Ru^{4+}=O species *via* a Ru^{3+}–O–O–Ru^{3+} intermediate (Scheme 1-12). *Di*-iron-substituted silicotungstate of $[\gamma\text{-}SiW_{10}\{Fe(OH_2)\}_2O_{38}]^{6-}$ catalyzed the selective epoxidation of olefins with only 1 atm of O_2 as an oxidant [Eq. (1-14)].[38a] The epoxidation was also proposed to proceed *via* a dioxygenase-type mechanism. *Di*-manganese-substituted silicotungstate, $[\gamma\text{-}SiW_{10}\{Mn^{III}(OH_2)\}_2O_{38}]^{6-}$, could also catalyze the oxidation of alkanes with only 1 atm of O_2.[38b]

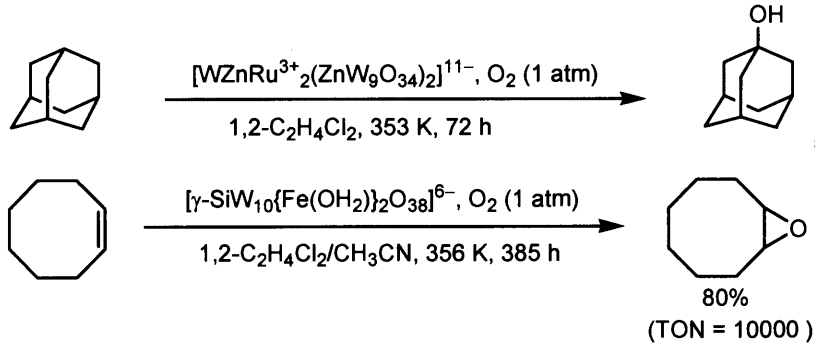

(1-13)

(1-14)

Finke and Weiner have reported that vanadium- and iron-containing polyanion-based precatalysts showed high catalytic activity for catechol dioxygenation with O_2.[39] For example, 3,5-di-*tert*-butylcatechol was oxidized in the presence of $(n\text{-}Bu_4N)_5[(CH_3CN)_xFe{\cdot}SiW_9V_3O_{40}]$ with extremely high turnover number (100000) and the value was far superior to those for man-made and natural enzymes [Eq. (1-15)].

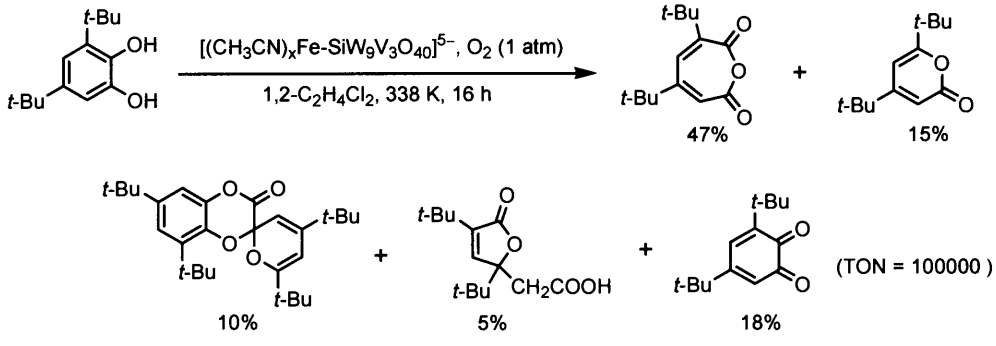

(1-15)

(iii) Peroxometalates

The transition metal peroxo complexes have attracted much interest in the fields of structural chemistry, biological chemistry, and material science.[40] Especially, the oxidation catalysis by d^0-transition metal peroxo complexes is of great importance because group IV–VII metals have been employed for industrial olefin epoxidation with organic hydroperoxides. Among the d^0-transition metal peroxo complexes, tungsten-based oxidation systems with H_2O_2 have received much attention because of the high reactivities compared with other analogues and inherent poor activity for decomposition of H_2O_2. Ishii and co-workers found effective H_2O_2-based epoxidation of terminal olefins catalyzed by $H_3PW_{12}O_{40}$ combined with cetyl pyridinium chloride (CPC) as a phase transfer agent [Eq. (1-16)].[41a] Other POMs such as $H_3PMo_{12}O_{40}$, $H_4SiW_{12}O_{40}$, and $H_3PMo_6W_6O_{40}$ were much less active than $H_3PW_{12}O_{40}$. Use of biphasic system prevented the hydrolytic cleavage of oxirane rings, resulting in high selectivity to epoxides. This Ishii-system could be applied to the epoxidation of allylic alcohols, monoterpenes, and α,β-unsaturated carboxylic acids, oxidation of alcohols, amines, and alkynes, and oxidative transformation of diols.[41]

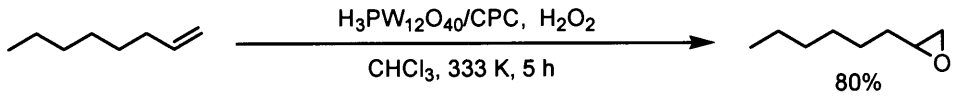

(1-16)

The $[PO_4\{WO(O_2)_2\}_4]^{3-}$ peroxotungstate was isolated and characterized crystallographically by Venturello and co-workers. The anion consisted of the PO_4^{3-} anion and two $[W_2O_2(O_2)_4]$ species. The peroxo species has been postulated to be a catalytically active species for the $H_3PW_{12}O_{40}/H_2O_2$ system because $[PO_4\{WO(O_2)_2\}_4]^{3-}$ exhibited a very similar catalytic reactivity to that of Ishii-system.[42a] The spectroscopic and kinetic investigations by Brégeault, Griffith, Thouvenot, and Hill show that the $[PO_4\{WO(O_2)_2\}_4]^{3-}$ is a catalytically important species among various peroxotungstates generated by the reaction of $H_3PW_{12}O_{40}$ with excess H_2O_2 (Scheme 1-13).[26a,43]

Not only *in-situ* generated peroxo species but also isolated peroxotungstates showed a catalytic activity for epoxidation. Various peroxo species have been isolated and characterized crystallographically.[42a,43a,44] Peroxotungstates containing phosphorous or arsenic ligands are generally much more active than $[W_2O_3(O_2)_4]^{2-}$ for

the catalytic epoxidation of olefins, especially terminal olefins, while the sulfate species, $[SO_4\{WO(O_2)_2\}_2]^{2-}$, was the most active for stoichiometric epoxidation of (*R*)-(+)-limonene among $[XO_4\{WO(O_2)_2\}_2]^{2-}$ (X=HAs, HP, and S) peroxotungstates.[44,45] While the effects of XO_4 ligands on the reactivity of epoxidation have not yet been clarified, the pH of an aqueous phase and solubility of catalyst to an organic phase have been reported to play an important role in these biphasic epoxidation systems because the structures of peroxo species in aqueous solution depend on the pH, concentration of tungsten and H_2O_2, and molar ratio of H_2O_2 to tungsten.[46] A biphasic epoxidation system in the presence of phosphate or arsenate, tungstate, and phase transfer agents (Q^+X^-) under acidic conditions was also reported by Venturello and co-workers.[42b] Recently, Noyori and co-workers reported an H_2O_2-based epoxidation system without halides and organic solvents using a catalytic system consisting of tungstate, (aminomethyl)phosphonic acid, and methyltrioctylammonium hydrogensulfate [Eq. (1-17)].[47] Although (aminomethyl)phosphonic acid was decomposed into phosphoric acid under the reaction conditions, it facilitated the epoxidation more than phosphoric acid.

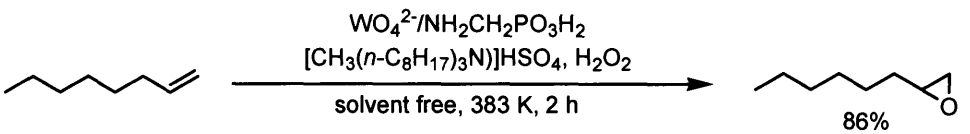

(1-17)

(b) Heterogeneous Catalysts with POM-based Compounds

As mentioned above, POMs could act as very effective catalysts for environmentally-friendly oxidations with H_2O_2 and O_2, and these oxidations are homogeneous in many cases. Heterogeneous catalysts are more desirable than the homogeneous catalysts from the standpoints of the catalyst/product separation and catalyst recycling. Therefore, the development of efficient heterogeneous catalysts with POMs and the related compounds for the liquid-phase oxidations has been attempted according to the classification as shown in Figure 1-6. In this section, some examples of heterogeneous oxidation catalysts with POMs are described.

Dispersion of POMs onto inert solid supports with high surface areas is very important for catalytic application because the surface areas of unsupported POMs are

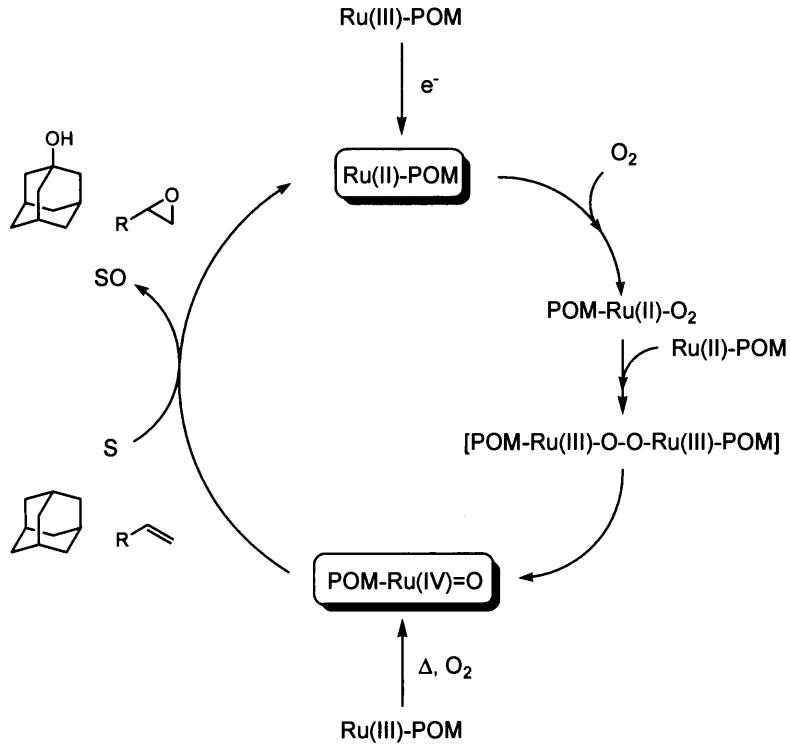

Scheme 1-12. Proposed catalytic cycle for activation of O_2 and substrate by the ruthenium-substituted sandwich type $[WZnRu^{3+}{}_2(XW_9O_{34})_2]^{11-}$ ($X = Zn^{2+}$ or Co^{2+}).

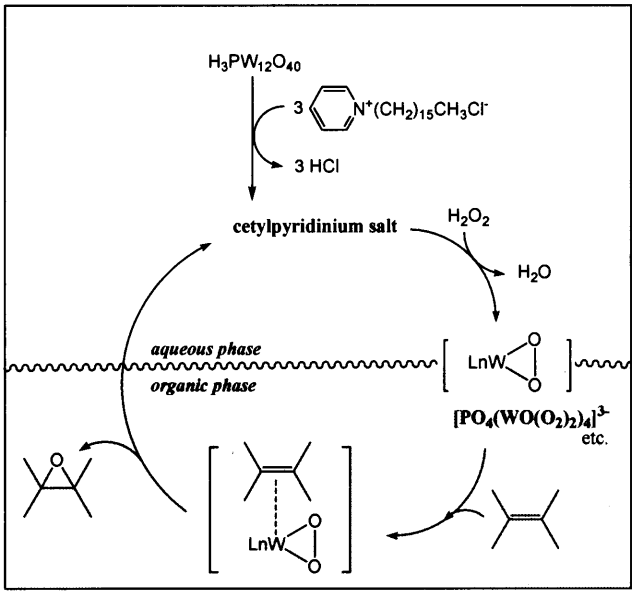

Scheme 1-13. Proposed catalytic cycle for the epoxidation of olefins with H_2O_2 by $H_3PW_{12}O_{40}$.

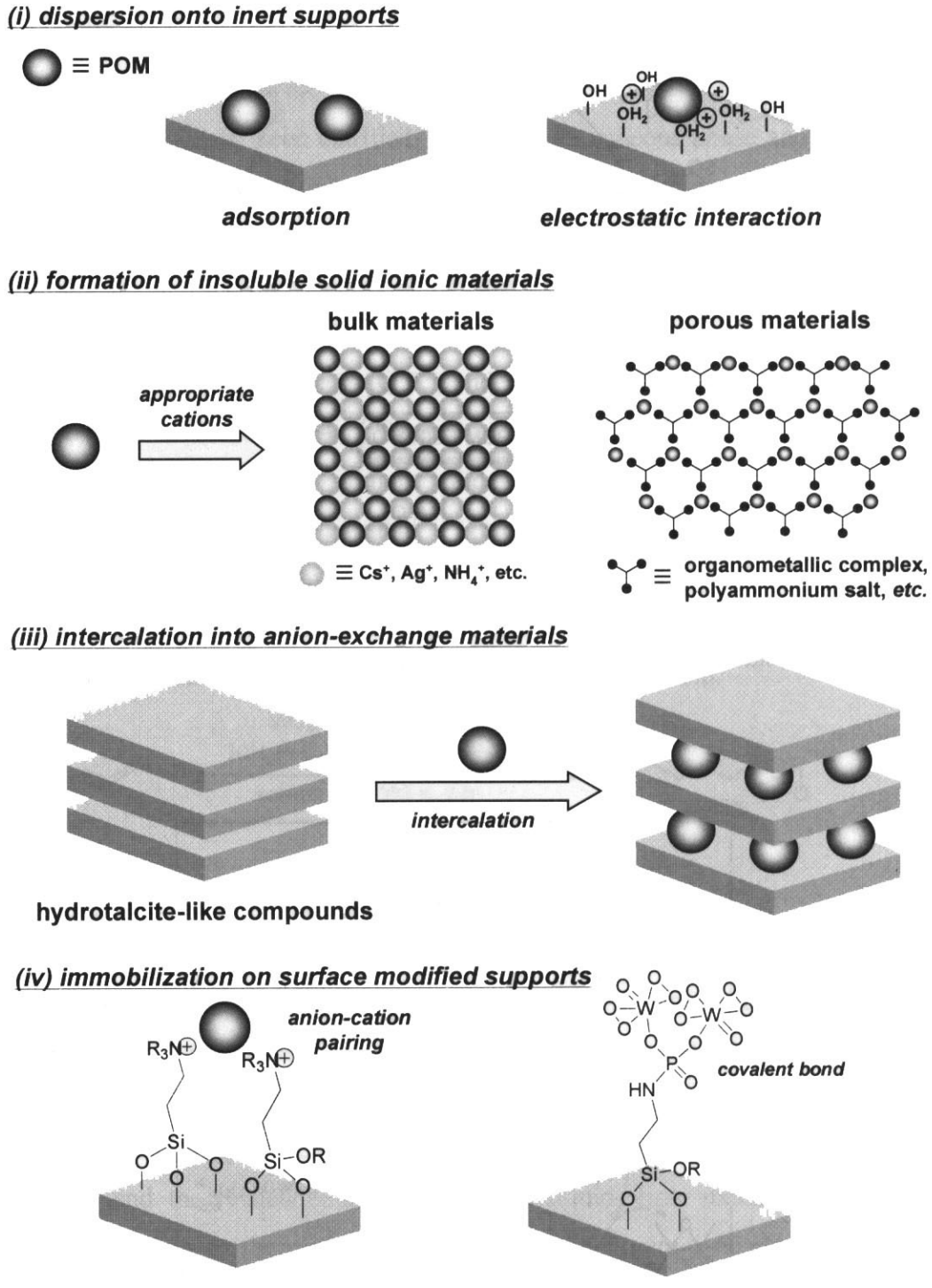

Figure 1-6. Schematic representation of strategies for heterogenization of POMs.

usually very low (~10 $m^2 \cdot g^{-1}$). Another advantage of dispersion of POMs onto inert supports is improvement of the stability. Therefore, immobilization of POMs on a number of supports has been extensively studied. The sandwich type Fe containing POM, $[(Fe(OH_2)_2)_3(A\text{-}\alpha\text{-}PW_9O_{34})_2]^{9-}$, was electrostatically immobilized on the surface of cationic silica/alumina nanoparticles ($(Si/AlO_2)Cl$).[48] In this case, there were ≈58 POM molecules per nanoparticle bound to the surface $\equiv Al\text{-}OH_2^+$ groups. This material efficiently catalyzed the aerobic oxygenation of sulfides and autoxidation of aldehydes. Interestingly, the activity per POM was higher than that of the parent POM.

Selection of appropriate counter cations can control the solubility of POMs. Xi and co-workers reported on the epoxidation of olefins performed with $(CP)_3[PO_4(WO_3)_4]$ catalyst.[49] This insoluble catalyst formed soluble active species, $(CP)_3[PO_4\{WO_2(O_2)\}_4]$, by the reaction with H_2O_2. When H_2O_2 was completely consumed, the catalyst became insoluble again, resulting in the simple catalyst recovery. When coupled with the 2-ethylanthraquinone/2-ethylanthrahydroquinone redox process for H_2O_2 production, O_2 could be used as an oxidant for the epoxidation of propylene in 85% yield based on 2-ethylanthrahydroquinone which was obtained without any by-products (Scheme 1-14).

Cross-linking of the copolymer was achieved by the presence of POMs and insoluble materials with micro- or mesopores were formed. Ikegami and co-workers prepared a novel insoluble catalyst of a cross-linked complex consisting of $PW_{12}O_{40}^{3-}$ and *N*-isopropylacrylamide with ammonium cations (PWAA) (Figure 1-7).[50] This PWAA catalyst heterogeneously catalyzed the oxidations of various substrates including allylic alcohols, amines, and sulfides with 30% aqueous H_2O_2 under mild reaction conditions without organic solvents [Eq. (1-18)].

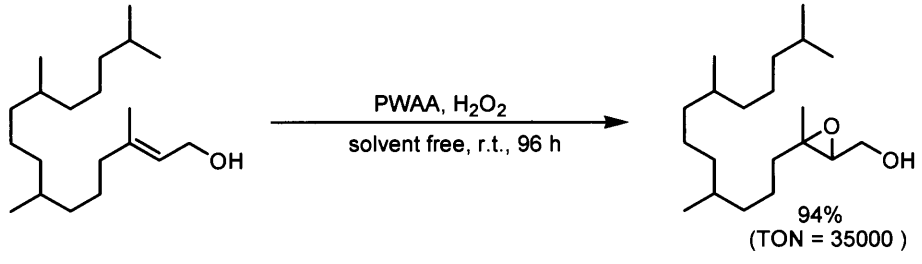

(1-18)

Hydrotalcite-like compounds (HTs) have anion-exchange ability and various kinds of anions including POMs can be intercalated.[51] Monomeric oxoanions such

as WO_4^{2-} and MoO_4^{2-} were also intercalated into the interlayer of HTs. These materials could act as efficient oxidation catalysts with H_2O_2. MgAl- or NiAl-HT intercalated with WO_4^{2-} (HT-WO_4^{2-}) showed excellent activities for oxidative bromination of unsaturated hydrocarbons using bromide-H_2O_2 as a bromine source under very mild reaction conditions (Scheme 1-15).[52]

POMs can be immobilized on surface modified supports *via* appropriate spacer ligands. The peroxotungstate $[W_2O_3(O_2)_4(H_2O)_2]^{2-}$ (**W2**) was immobilized on dihydroimidazolium based ionic liquid-modified SiO_2 (**1**-SiO_2) (Scheme 1-16).[53] Epoxidation was completely terminated by the catalyst **W2**/**1**-SiO_2 removal and no tungsten species could be detected in the filtrate. The catalysis was truly heterogeneous in nature and homogeneous catalysis could be heterogenized with retention of the **W2** catalyst performance by using ionic liquid-modified SiO_2 as a support.

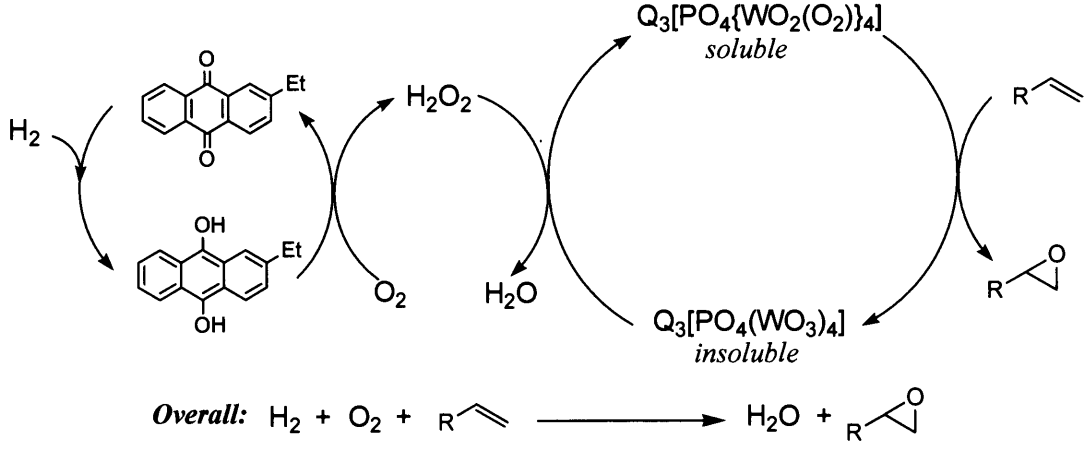

Scheme 1-14. Proposed catalytic cycle for the epoxidation of olefins by $[\pi\text{-}C_5H_5NC_{16}H_{33}]_3[PO_4(WO_3)_4]$ catalyst coupled with the 2-ethylanthraquinone/2-ethylanthrahydroquinone redox process.

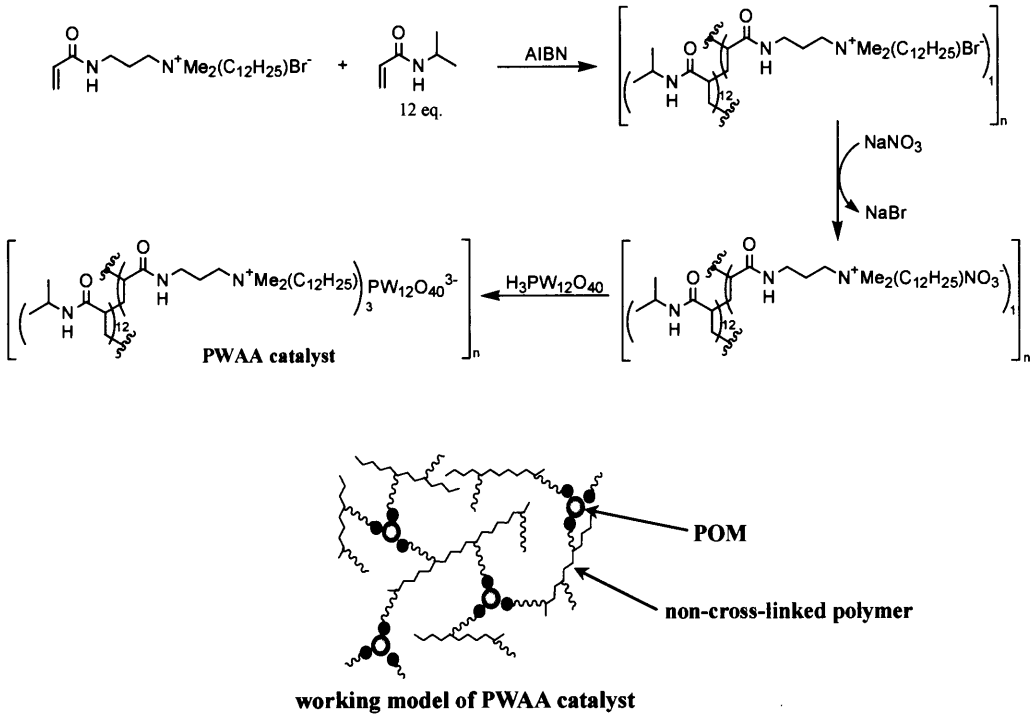

Figure 1-7. Preparation of PWAA catalyst.

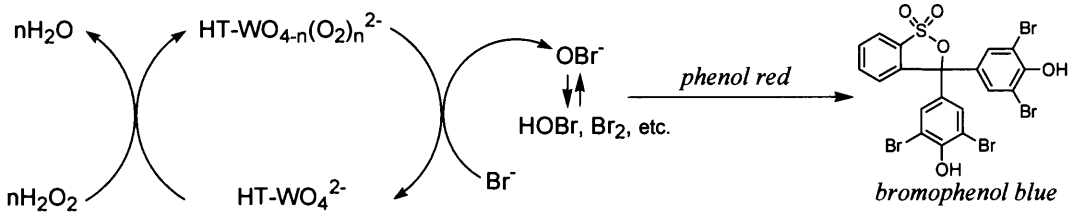

Scheme 1-15. Catalytic cycle of bromination with HT-WO_4^{2-} catalyst.

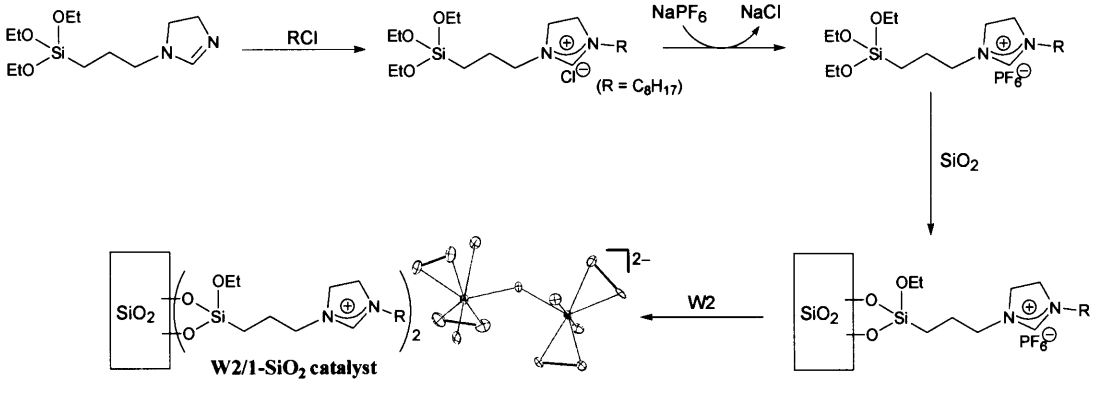

Scheme 1-16. Procedures for the preparation of **W2/1**-SiO_2 catalyst.

Table 1-2. Examples of H_2O_2- and O_2-based oxidations catalyzed by POMs

catalyst	reaction	oxidant	solvent	temp. (K)	ref.
$[PV_2Mo_{10}O_{40}]^{5-}$	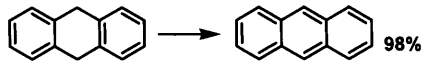 98%	O_2	tetraglyme /$ClCH_2CH_2Cl$	343	[20c]
$[PV_2Mo_{10}O_{40}]^{5-}$	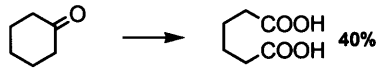 40%	O_2	AcOH /H_2O	343	[20d]
$[PV_6Mo_6O_{40}]^{9-}$	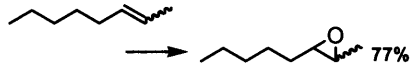 77%	O_2 /aldehyde	$ClCH_2CH_2Cl$	298	[20e]
$[PV_2Mo_{10}O_{40}]^{5-}$	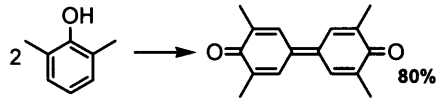 80%	O_2	*n*-hexanol	363	[20f]
$[PV_2Mo_{10}O_{40}]^{5-}$	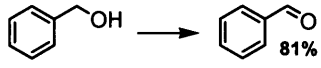 81%	O_2 /quinone	dacalin /H_2O	363	[20g]
$PdSO_4/CuSO_4/$ $[PV_6Mo_6O_{40}]^{9-}/\beta$-CD	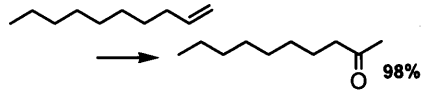 98%	O_2	H_2O	363	[20h]
$Pd(OAc)_2/$ $[PMo_{12-n}V_nO_{40}]^{(3+n)-}$	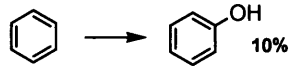 10%	O_2	AcOH /H_2O	403	[20i]
$Pd(OAc)_2/NaOAc$ /$[PMo_8V_4O_{40}]^{7-}$	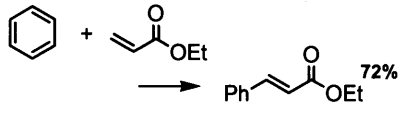 72%	O_2	AcOH	363	[20j]
$[PV_2Mo_{10}O_{40}]^{5-}$	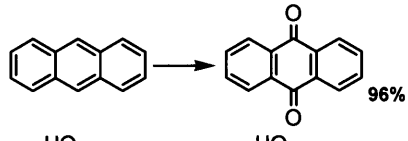 96%	O_2	CH_3CN	333	[20l]
$[AlV^VW_{11}O_{40}]^{6-}$	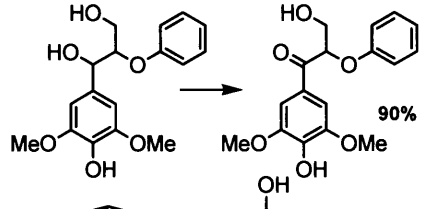 90%	O_2	H_2O	403	[23]
$[WZnRu^{III}_2(ZnW_9O_{34})_2]^{11-}$	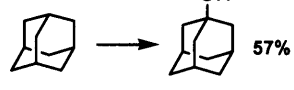 57%	O_2	$ClCH_2CH_2Cl$	353	[37]
$[WZnMn^{II}_2(ZnW_9O_{34})_2]^{12-}$	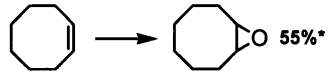 55%*	H_2O_2	$ClCH_2CH_2Cl$	275	[31b]
$[WZnMn^{II}_2(ZnW_9O_{34})_2]^{12-}$	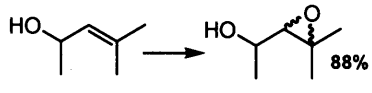 88%	H_2O_2	$ClCH_2CH_2Cl$	rt	[31e]
$[WZn_3(ZnW_9O_{34})_2]^{12-}$	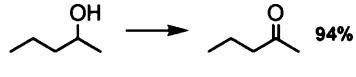 94%	H_2O_2	H_2O	358	[31f]
$[(Mn^{II}(H_2O))_3(SbW_9O_{33})_2]^{12-}$	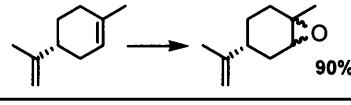 90%	H_2O_2	$ClCH_2CH_2Cl$	rt	[31d]

*Based on H_2O_2.

Table 2. (*continued*)

catalyst	reaction	oxidant	solvent	temp. (K)	ref.
$[Fe^{III}_4(H_2O)_2(PW_9O_{34})_2]^{6-}$	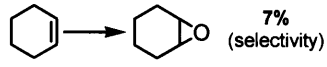 7% (selectivity)	H_2O_2	CH_3CN	298	[31c]
$[Fe^{III}_4(H_2O)_2(P_2W_{15}O_{56})_2]^{12-}$	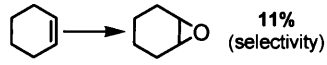 11% (selectivity)	H_2O_2	CH_3CN	298	[32b]
$[\alpha\beta\beta\alpha\text{-}(Mn^{II}OH_2)_2(Mn^{II})_2(AsW_{15}O_{62})_2]^{16-}$	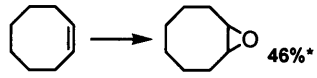 46%*	H_2O_2	CH_3CN	298	[36b]
$[Fe^{III}_2(NaOH_2)_2(P_2W_{15}O_{56})_2]^{12-}$	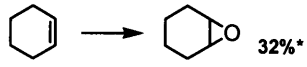 32%*	H_2O_2	CH_3CN	298	[32c]
$[(MOH_2)_2Fe^{III}_2(P_2W_{15}O_{56})(P_2M_2(OH_2)_4W_{13}O_{52}]^{16-}$ (M = Cu^{II} or Co^{II})	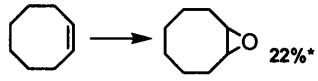 22%*	H_2O_2	CH_3CN	298	[36a]
$[((Mn^{II}OH_2)Mn^{II}PW_9O_{34})_2(PW_6O_{26})]^{17-}$	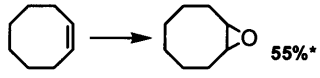 55%*	H_2O_2	CH_3CN	353	[34]
$[\gamma\text{-}SiW_{10}\{Fe^{III}(OH_2)\}_2O_{38}]^{6-}$	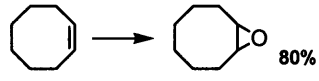 80%	O_2	$ClCH_2CH_2Cl$ /CH_3CN	356	[38a]
$[\gamma\text{-}SiW_{10}\{Mn^{III}(OH_2)\}_2O_{38}]^{6-}$	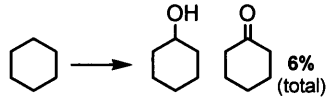 6% (total)	O_2	$ClCH_2CH_2Cl$ /CH_3CN	356	[38b]
$[\gamma\text{-}SiW_{10}\{Fe^{III}(OH_2)\}_2O_{38}]^{6-}$	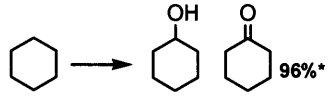 96%*	H_2O_2	CH_3CN	356	[29b]
$[\gamma\text{-}SiW_{10}\{Fe^{III}(OH_2)\}_2O_{38}]^{6-}$	$CH_4 \longrightarrow HCOOCH_3$ 7%*	H_2O_2	CH_3CN	353	[29e]
$[Ni(H_2O)H_2F_6NaW_{17}O_{35}]^{9-}$	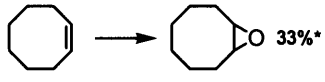 33%*	H_2O_2	CH_3CN	333	[30a]
$[H_2F_6NaVW_{17}O_{56}]^{8-}$	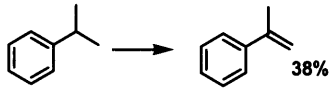 38%	O_2	$ClCH_2CH_2Cl$	363	[30b]
$[(CH_3CN)_xFeSiW_9V_3O_{40}]^{5-}$	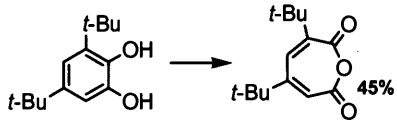 45%	O_2	$ClCH_2CH_2Cl$	338	[39]

*Based on H_2O_2.

Table 2. (*continued*)

catalyst	reaction	oxidant	solvent	temp. (K)	ref.
$H_3PW_{12}O_{40}$/CPC (CPC =cetyl pyridinium chloride)	80%	H_2O_2	$CHCl_3$	333	[41a]
$H_3PW_{12}O_{40}$/CPC	96%	H_2O_2	$CHCl_3$	rt	[41a,41b]
$H_3PW_{12}O_{40}$/CPC	90%	H_2O_2	H_2O	333-338	[41d]
$H_3PW_{12}O_{40}$/CPC	99%	H_2O_2	*t*-BuOH	reflux	[41a,41b]
$H_3PW_{12}O_{40}$/CPC	90%	H_2O_2	$CHCl_3$	rt	[41e]
$H_3PW_{12}O_{40}$/CPC	93%	H_2O_2	$CHCl_3$	rt	[41a]
$WO_4^{2-}/PO_4^{3-}/Q^+X^-$	82%*	H_2O_2	$ClCH_2CH_2Cl$ or C_6H_6	343	[42]
$WO_4^{2-}/NH_2CH_2PO_3H_2/[(CH_3(C_8H_{17})_3N]HSO_4$	86%	H_2O_2	without	363	[47b,47c]
$WO_4^{2-}/[(CH_3(C_8H_{17})_3N]HSO_4$	97%	H_2O_2	without	363	[47d,47e]
$WO_4^{2-}/[(CH_3(C_8H_{17})_3N]HSO_4$	93%	H_2O_2	without	348-363	[47a]
$[HPO_4\{WO(O_2)_2\}_2]^{2-}$	72%	H_2O_2	$CHCl_3$	274	[43c]
$[\beta_3\text{-}Co^{II}W_{11}O_{35}(O_2)_4]^{10-}$	91% (total)	H_2O_2	$CHCl_3$ /buffered H_2O	rt	[44e]

*Based on H_2O_2.

1.2. Purpose of This Study

Oxidation reactions are industrial core technologies for converting bulk chemicals to useful products. Selective oxygen transfer to olefins remains an important research objective in industry and synthetic chemistry because epoxides are widely used as epoxy resins, paints, surfactants, and intermediates in various organic syntheses. For the present processes in the production of propylene oxide, a chlorine-using non-catalytic process (the chlorohydrin process) and catalytic processes based on organic hydroperoxides are still used extensively. In contrast to such classical processes, catalytic epoxidation systems using H_2O_2 as a terminal oxidant might offer some advantages because H_2O_2 can oxidize organic compounds with relatively high atom efficiency and generates theoretically only water as a co-product.

POMs are early transition metal (V, Nb, Ta, W, and Mo, *etc.*) oxygen anion clusters and have the following advantages as oxidation catalysts: (i) Their redox and acid-base properties can be varied over a wide range by changing the chemical composition, (ii) they are not susceptible to oxidative and thermal degradation compared with the organometallic complexes such as metalloporphyrins, and (iii) their catalytically active sites can be designed by the combination of transition metals and inorganic ligands of lacunary POMs. Because of the superior properties, the POMs-based oxidation catalysts can be designed at the atomic and molecular levels.

The oxidation catalysis by d^0-transition metal peroxo complexes is of grest importance because group IV–VII metals have been employed for industrial olefin epoxidation with organic hydroperoxides. While it has been accepted that the oxygen transfer reaction proceeds *via* an intermediate that has η^2-coordination of the peroxide to the Lewis acid metal center, it is still controversial whether these η^2-peroxo complexes function as the actual catalytic species or as the catalyst precursors. Therefore, it is important to reveal the relationship between the structure of the peroxo species and their oxidation activity. It is expected that the activation of η^2-peroxo species by electrophiles (e.g., H^+, CMe_3^+, $SiMe_3^+$, and d^0-metals) can polarize the O-O bond and much enhance the catalytic activity.

The main purpose of this thesis is to design the highly functionalized POMs for the green catalytic oxidation systems with H_2O_2 as a sole oxidant. The polynuclear

structures of POMs lead to remarkable reactivity and selectivity which can not be observed for bulk metal oxides and mononuclear compounds. In addition, the designed POMs can allow using "green oxidant" such as H_2O_2 and "green solvent" such as water, which contribute to the solution of the environmental problems. The strategies for the design of POMs are summarized in Figure 1-8: (i) The introduction of transition metal elements in lacunary POMs, (ii) the formation of vacant sites for the activation of oxidant and/or substrate, and (iii) the application to the catalyst precursor for organic synthesis in aqueous phase.

In chapter II, the synthesis, characterization, and oxidation catalysis of the dititanium-substituted γ-Keggin silicotungstate, $[\{\gamma\text{-}SiTi_2W_{10}O_{36}(OH)_2\}_2(\mu\text{-}O)_2]^{8-}$, are described. Titanium is recognized to be an active element of an oxidation catalyst in both heterogeneous and homogeneous reaction systems. However, the details of reaction mechanism as well as relationship between the structure of the active site and reactivity are still unclear. The silicodititanodecatungstate dimer, $[\{\gamma\text{-}SiTi_2W_{10}O_{36}(OH)_2\}_2(\mu\text{-}O)_2]^{8-}$, with edge-shared dinuclear $Ti_2(\mu\text{-}OH)_2$ cores is found to be an effective homogeneous catalyst for the oxygen transfer reactions of various substrates including olefins and sulfides. The monotitanium-substituted silicotungstate of $[\alpha\text{-}H_2SiTiW_{11}O_{40}]^{4-}$ is inactive for epoxidation, showing that the structures of the active titanium sites influence the catalytic activity.

In chapter III, the design and oxidation catalysis of lacunary POMs are described. While lacunary POMs have been used as precursors for various complexes such as transition-metal-substituted POMs and organic-inorganic hybrid materials, scarcely is known of the catalysis by lacunary POMs themselves. Silicotungstates are suitable polynuclear peroxometalate precursors because they are rather stable in water compared with phosphotungstates and consist of the tungsten elements which are active for homogeneous epoxidation with H_2O_2. The novel compound $[\gamma\text{-}SiW_{10}O_{34}(H_2O)_2]^{4-}$, synthesized by the protonation of $[\gamma\text{-}SiW_{10}O_{36}]^{8-}$, shows high catalytic activity for the monooxygenation type reactions (i.e., epoxidation of mono-olefins, non-conjugated dienes, allylic alcohols, and oxidation of sulfides) with H_2O_2 as an oxidant. The catalytic performance of $[\gamma\text{-}SiW_{10}O_{34}(H_2O)_2]^{4-}$ is much superior to those of conventional peroxotungstates such as $[W_2O_3(O_2)_4(H_2O)_2]^{2-}$ and $[PO_4\{WO(O_2)_2\}_4]^{3-}$

from the standpoints of activity, selectivity, stereospecificity, and reusability in the above oxidations.

Use of water solvent instead of explosive, hazardous, and carcinogenic organic solvents is desirable, since water is a safe, harmless, and environmentally benign solvent. Description in chapter IV is the epoxidation of allylic alcohols *in water* catalyzed by simple dinuclear peroxotungstate, $[W_2O_3(O_2)_4(H_2O)_2]^{2-}$. Various primary and secondary allylic alcohols can effectively be epoxidized in water by $[W_2O_3(O_2)_4(H_2O)_2]^{2-}$ with high efficiency of H_2O_2 utilization. In addition, the dinuclear peroxotungstate can be reused with retention of the high catalytic activity, stereospecificity and chemo-, regio-, and diastereoselectivity for the epoxidation.

Finally, general conclusions of the present thesis and the scope for the extensive design of the POMs catalysts are stated.

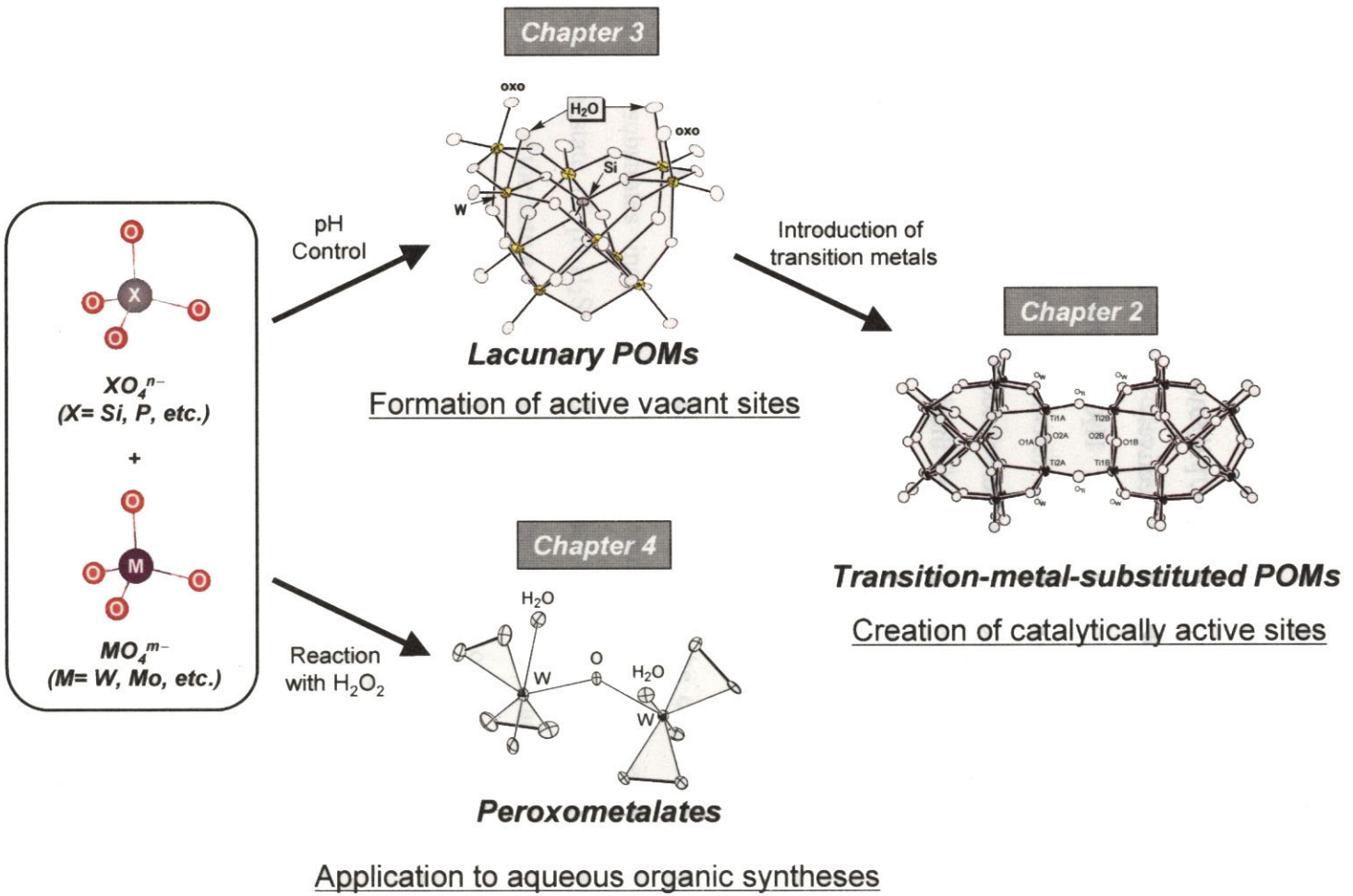

Figure 1-8. Strategies for catalyst design of polyoxometalate compounds.

1.3. References

[1] a) P. T. Anastas, J. C. Warner, *Green Chemistry: Theory and Practice*; Oxford University Press, **1998**; b) R. A. Sheldon, *Pure Appl. Chem.* **2000**, *72*, 1233; c) J. H. Clark, *Green Chem.* **1999**, *1*, 1; d) R. A. Sheldon, *Green Chem.* **2000**, *2*, G1; e) P. T. Anastas, L. B. Bartlett, M. M. Kirchhoff, T. C. Williamson, *Catal. Today* **2000**, *55*, 11.

[2] Special issues on "Green Chemistry": a) *Acc. Chem. Res.* **2002**, *35*, 685–816; b) *Pure Appl. Chem.* **2000**, *72*, 1207–1403.

[3] a) R. A. Sheldon, J. K. Kochi, *Metal Catalyzed Oxidations of Organic Compounds*, Academic Press, New York, **1981**; b) C. L. Hill in *Advances in Oxygenated Processes, Vol. 1* (Eds.: A. L. Baumstark), JAI Press, London, **1988**, p. 1–30; c) M. Hudlucky, *Oxidations in Organic Chemistry*, ACS Monograph Series, American Chemical Society, Washington, DC, **1990**; d) J.-E. Bäckvall, *Modern Oxidation Methods*, Wiley-VCH, Weinheim, **2004**.

[4] Recent reviews on "Oxidation catalysis": a) A. E. Shilov, G. B. Shul'pin, *Chem. Rev.* **1997**, *97*, 2879; b) M. Akita, Y. Moro-oka, *Catal. Today* **1998**, *44*, 183; c) Y. Moro-oka, *Catal. Today* **1998**, *45*, 3; d) R. A. Sheldon, I. W. C. E. Arends, A. Dijksman, *Catal. Today* **2000**, *57*, 157; e) Y. Ishii, S. Sakaguchi, T. Iwahama, *Adv. Synth. Catal.* **2001**, *343*, 393; f) D. E. de Vos, B. F. Sels, P. A. Jacobs, *Adv. Catal.* **2001**, *46*, 1; g) A. Corma, H. Garcia, *Chem. Rev.* **2002**, *102*, 3837; h) B. S. Lane, K. Burgess, *Chem. Rev.* **2003**, *103*, 2457; i) R. Noyori, M. Aoki, K. Sato, *Chem. Commun.* **2003**, 1977; j) D. E. De Vos, B. F. Sels, P. A. Jacobs, *Adv. Synth. Catal.* **2003**, *345*, 457; k) J.-M. Brégeault, *Dalton Trans.* **2003**, 3289; l) G.-J. ten Brink, I. W. C. E. Arends, R. A. Sheldon, *Chem. Rev.* **2004**, *104*, 4105; m) B. De Bruin, P. H. M. Budzelaar, A. W. Gal, *Angew. Chem. Int. Ed.* **2004**, *43*, 4142; n) T. Punniyamurthy, S. Velusamy, J. Iqbal, *Chem. Rev.* **2005**, *105*, 2329.

[5] a) C. C. Romao, F. E. Kuehn, W. A. Herrmann, *Chem. Rev.* **1997**, *97*, 3197; b) W. A. Herrmann, R. W. Fischer, M. U. Rauch, W. Scherer, *J. Mol. Catal.* **1994**, *86*, 243; c) J. Rudolph, K. L. Reddy, J. P. Chiang, K. B. Sharpless, *J. Am. Chem. Soc.* **1997**, *119*, 6189; d) C. Copéret, H. Adolfsson, K. B. Sharpless, *Chem. Commun.* **1997**, 1565; e) M. C. A. Van Vliet, I. W. C. E. Arends, R. A. Sheldon, *Chem. Commun.* **1999**, 821.

[6] a) B. Notari, *Adv. Catal.* **1996**, *41*, 253; b) I. W. C. E. Arends, R. A. Sheldon, M. Wallau, U. Schuchardt, *Angew. Chem. Int. Ed. Engl.* **1997**, *36*, 1144; c) M. A. Camblor,

M. Constantine, A. Corma, A. Gilbert, P. Esteve, A. Martinez; S. Valencia, *Chem. Commun.* **1996**, 1339; d) A. Tuel, *Zeolites* **1995**, 236; e) M.-J. Diaz-Cabanas, L. A. Villaescusa, M. A. Camblor, *Chem. Commun.* **2000**, 761; f) M. Sasidharan, P. Wu, T. Tatsumi, *J. Catal.* **2002**, *205*, 332.

[7] a) A. Corma, L. T. Nemeth, M. Renz, S. Valencia, *Nature* **2001**, *412*, 423; b) M. Renz, T. Blasco, A. Corma, V. Fornés, R. Jensen, L. Nemeth, *Chem. Eur. J.* **2002**, *8*, 4708.

[8] a) K. L. Fujdala, T. D. Tilley, *J. Catal.* **2003**, *216*, 265; b) J. Jarupatrakorn, M. P. Coles, T. D. Tilley, *Chem. Mater.* **2005**, *17*, 1818; c) C. Nozaki, C. G. Lugmair, A. T. Bell, T. D. Tilley, *J. Am. Chem. Soc.* **2002**, *124*, 13194; d) R. L. Brutchey, D. A. Ruddy, L. K. Anderson, T. D. Tilley, *Langumuir* **2005**, *21*, 9576.

[9] a) J. S. Valentine, C. S. Foote, A. Greenberg, J. F. Liebman, *Active Oxygen in Biochemistry*, Chapman and Hall, Glasgow, **1995**; b) B. J. Wallar, J. D. Lipscomb, *Chem. Rev.* **1996**, *96*, 2625; c) L. Que, Jr., R. Y. N. Ho, *Chem. Rev.* **1996**, *96*, 2607; d) M. Sono, M. P. Roach, E. D. Coulter, J. H. Dawson, *Chem. Rev.* **1996**, *96*, 2841; e) E. I. Solomon, T. C. Brunold, M. I. Davis, J. N. Kemsley, S.-K. Lee, N. Lehnert, F. Neese, A. J. Skulan, Y.-S. Yang, J. Zhou, *Chem. Rev.* **2000**, *100*, 235.

[10] a) S. Banfi, F. Legramandi, F. Montanari, G. Pozzi, S. Quici, *J. Chem. Soc., Chem. Commun.* **1991**, 1285; b) P. L. Anelli, L. Banfi, F. Legramandi, F. Montanari, G. Pozzi, S. Quici, *J. Chem. Soc., Perkin Trans. 1* **1993**, 1345; c) A. M. d. A. R. Gonsalves, R. A. W. Johnstone, M. M. Pereira, *J. Chem. Soc., Perkin Trans. 1* **1991**, 645; d) A. Thellend, P. Battioni, D. Mansuy, *J. Chem. Soc., Chem. Commun.* **1994**, 1035.

[11] a) M. C. White, A. G. Doyle, E. N. Jacobsen, *J. Am. Chem. Soc.* **2001**, *123*, 7194; b) G. Dubois, A. Murphy, T. D. P. Stack, *Org. Lett.* **2003**, *5*, 2469.

[12] a) D. E. De Vos, B. F. Sels, M. Reynaers, Y. V. Subba Rao, P. A. Jacobs, *Tetrahedron Lett.* **1998**, *39*, 3221; b) C. B. Woitiski, Y. N. Kozlov, D. Mandelli, G. V. Nizova, U. Schuchardt, G. B. Shul'pin, *J. Mol. Catal. A: Chem.* **2004**, *222*, 103; c) K. F. Sibbons, K. Shastri, M. Watkinson, *Dalton. Trans.* **2006**, 645.

[13] a) D. H. R. Barton, D. Doller, *Acc. Chem. Res.* **1992**, *25*, 504: b) I. Tabushi, A. Yazaki, *J. Am. Chem. Soc.* **1991**, *102*, 1991; c) T, Mukaiyama, T. Yamada, *Bull. Chem. Soc. Jpn.* **1995**, *103*, 7371; d) S. Murahashi, *Angew. Chem. Int. Ed. Engl.* **1995**, *34*, 2443.

[14] a) J. M. Thomas, R. Raja, *Chem, Commun.* **2001**, 675; b) J. M. Thomas, R. Raja, G. Sanker, R. G. Bell, *Acc. Chem. Res.* **2001**, *34*, 191; c) J. M. Thomas, R. Raja, D. W. Lewis, *Angew. Chem. Int. Ed.* **2005**, *44*, 6456.

[15] Y. Ishii, S. Sakaguchi, T. Iwahama, *Adv. Synth. Catal.* **2001**, *343*, 393.

[16] a) F. Montanari, L. Casella, *Metalloporphyrin Catalyzed Oxidations*, Kluwer, Dordrecht, **1994**; b) J. T. Groves, R. Quinn, *Inorg. Chem.* **1984**, *23*, 3844; c) J. T. Groves, R. Quinn, *J. Am. Chem. Soc.* **1985**, *107*, 5790.

[17] a) T. Mallat, A. Baiker, *Chem. Rev.* **2004**, *104*, 3037; b) R. A. Sheldon, I. W. C. E. Arends, A. Dijksman, *Catal. Today* **2000**, *57*, 157; c) K. Yamaguchi, N. Mizuno, *Chem. Eur. J.* **2003**, *9*, 4353; d) K. Mori, T. Hara, T. Mizugaki, K. Ebitani, K. Kaneda, *J. Am. Chem. Soc.* **2004**, *126*, 10657.

[18] Thematic issue on "Polyoxometalates", *Chem. Rev.* **1998**, *98*, 1–389.

[19] a) T. Okuhara, N. Mizuno, M. Misono, *Adv. Catal.* **1996**, *41*, 113; b) N. Mizuno, M. Misono, *Chem. Rev.* **1998**, *98*, 199; c) R. Neumann, *Prog. Inorg. Chem.* **1998**, *47*, 317; d) C. L. Hill, C. Chrisina, M. Prosser-McCartha, *Coord. Chem. Rev.* **1995**, *143*, 407; e) C. L. Hill in *Comprehensive Coordination Chemistry II, Vol. 4* (Eds.: J. A. McCleverty, T. J. Meyer), Elsevier Pergamon, Amsterdam, **2004**, pp. 679; f) I. V. Kozhevnikov, *Chem. Rev.* **1998**, *98*, 171; g) I. V. Kozhevnikov, *Catalysis by Polyoxometalates*, John Wiley & Sons, Ltd, Chichester, England, **2002**; h) M. T. Pope, in *Comprehensive Coordination Chemistry II, Vol. 4* (Eds.: J. A. McCleverty, T. J. Meyer), Elsevier Pergamon, Amsterdam, **2004**, pp. 635; i) M. T. Pope, *Heteropoly and Isopoly Oxometalates*, Springer-Verlag, Berlin, **1983**.

[20] a) K. I. Matveev, *Kinet. Katal.* **1977**, *18*, 862; b) A. M. Khenkin, A. Rosenberger, R. Neumann, *J. Catal.* **1999**, *182*, 82; c) R. Neumann, M. Lissel, *J. Org. Chem.* **1989**, *54*, 4607; d) A. Atlamsani, J.-M. Brégeault, M. Ziyad, *J. Org. Chem.* **1993**, *58*, 5663; e) M. Hamamoto, K. Nakayama, Y. Nishiyama, Y. Ishii, *J. Org. Chem.* **1993**, *58*, 6421; f) M. Lissel, H. J. in de Wal, R. Neumann, *Tetrahedron Lett.* **1992**, *33*, 1795; g) R. Neumann, A. M. Khenkin, I. Vigdergauz, *Chem. Eur. J.* **2000**, *6*, 875; h) E. Monflier, E. Blouet, Y. Barbaux, A. Mortreux, *Angew. Chem. Int. Ed. Engl.* **1994**, *33*, 2100; i) L. C. Passoni, A. T. Cruz, R. Buffon, U. Shuchardt, *J. Mol. Catal. A* **1997**, *120*, 117; j) T. Yokota, M. Tani, S. Sakaguchi, Y. Ishii, *J. Am. Chem. Soc.* **2003**, *125*, 1476; k) T. Yokota, S. Sakaguchi, Y.

Ishii, *Adv. Syhth. Catal.* **2002**, *344*, 849; l) A. M. Khenkin, L. Weiner, Y. Wang, R. Neumann, *J. Am. Chem. Soc.* **2001**, *123*, 8531.

[21] I. V. Kozhevnikov, K. I. Matveev, *Appl. Catal.* **1983**, *5*, 135.

[22] J. H. Grate, *J. Mol. Catal. A* **1996**, *106*, 57.

[23] I. A. Weinstock, E. M. G. Barbuzzi, M. W. Wemple, J. J. Cowan, R. S. Reiner, D. M. Sonnen, R. A. Heintz, J. S. Bond, C. L. Hill, *Nature* **2001**, *414*, 191.

[24] C. L. Hill, R. B. Brown, Jr., *J. Am. Chem. Soc.* **1986**, *108*, 536.

[25] C. L. Hill in *Activation and Functionalization of Alkanes*, (Eds.: C. L. Hill), Wiley, New York, **1989**, p. 243.

[26] a) D. C. Duncan, R. C. Chambers, E. Hecht, C. L. Hill, *J. Am. Chem. Soc.* **1995**, *117*, 681; b) M. W. Droege, R. G. Finke, *J. Mol. Catal.* **1991**, *69*, 323; c) I. C. M. S. Santos, M. M. Q. Simões, M. M. M. S. Pereira, R. R. L. Martins, M. G. P. M. S. Neves, J. A. S. Cavaleiro, A. M. V. Cavaleiro, *J. Mol. Catal. A: Chem.* **2003**, *195*, 253; d) N. I. Kuznetsova, L. I. Kuznetsova, V. A. Likholobov, *J. Mol. Catal. A: Chem.* **1996**, *108*, 135.

[27] S. Tangestaninejad, B. Yadollahi, *Chem. Lett.* **1998**, 511.

[28] a) T. Yamase, E. Ishikawa, Y. Asai, S Kanai, *J. Mol. Catal. A: Chem.* **1996**, *114*, 237; b) E. Ishikawa, T. Yamase, *J. Mol. Catal. A: Chem.* **1999**, *142*, 61.

[29] a) C. Nozaki, I. Kiyoto, Y. Minai, M. Misono, N. Mizuno, *Inorg. Chem.* **1999**, *38*, 5724; b) N. Mizuno, C. Nozaki, I. Kiyoto, M. Misono, *J. Am. Chem. Soc.* **1998**, *120*, 9267; c) N. Mizuno, C, Nozaki, I. Kiyoto, M. Misono, *J. Catal.* **1999**, *182*, 285; d) N. Mizuno, I. Kiyoto, C. Nozaki, M. Misono, *J. Catal.* **1999**, *184*, 171; e) N. Mizuno, Y. Seki, Y. Nishiyama, I. Kiyoto, M. Misono, *J. Catal.* **1999**, *184*, 550.

[30] a) R. Ben-Daniel, A. M. Khenkin, R. Neumann, *Chem. Eur. J.* **2000**, *6*, 3722; b) A. M. Khenkin, R. Neumann, *Inorg. Chem.* **2000**, *39*, 3455.

[31] a) R. Neumann, M. Gara, *J. Am. Chem. Soc.* **1994**, *116*, 5509; b) R. Neumann, M. Gara, *J. Am. Chem. Soc.* **1995**, *117*, 5066; c) X. Zhang, Q. Chen, D. C. Duncan, R. J. Lachicotte, C. L. Hill, *Inorg. Chem.* **1997**, *36*, 4381; d) M. Bösing, A. Nöh, I. Loose, B. Krebs, *J. Am. Chem. Soc.* **1998**, *120*, 7252; e) W. Adam, P. L. Alsters, R. Neumann, C. R. Saha-Möller, D. Sloboda-Rozner, R. Zhang, *J. Org. Chem.* **2003**, *68*, 1721; f) D. Sloboda-Rozner, C. R. Saha-Möller, R. Neumann, *J. Am. Chem. Soc.* **2003**, *125*, 5280.

[32] a) R. G. Finke, M. W. Droege, P. J. Domaille, *Inorg. Chem.* **1987**, *26*, 3886; b) X.

Zhang, Q. Chen, D. C. Duncan, C. F. Campana, C. L. Hill, *Inorg. Chem.* **1997**, *36*, 4208; c) X. Zhang, T. M. Anderson, Q. Chen, C. L. Hill, *Inorg. Chem.* **2001**, *40*, 418.

[33] C. M. Tourné, G. F. Tourné, F. Zonnevijlle, *J. Chem. Soc., Dalton Trans.* **1991**, 143.

[34] M. D. Ritorto, T. M. Anderson, W. A. Neiwert, C. L. Hill, *Inorg. Chem.* **2004**, *43*, 44.

[35] T. M. Anderson, X. Zhang, K. I. Hardcastle, C. L. Hill, *Inorg. Chem.* **2002**, *41*, 2477.

[36] a) T. M. Anderson, K. I. Hardcastle, N. Okun, C. L. Hill, *Inorg. Chem.* **2002**, *40*, 6418; b) I. M. Mbomekalle, B. Keita, L. Nadjo, P. Berthet, W. A. Neiwert, C. L. Hill, M. D. Ritorto, T. M. Anderson, *Dalton Trans.* **2003**, 2646.

[37] a) R. Neumann, M. Dahan, *Nature* **1997**, *388*, 353; b) R. Neumann, M. Dahan, *J. Am. Chem. Soc.* **1998**, *120*, 11969.

[38] a) Y. Nishiyama, Y. Nakagawa, N. Mizuno, *Angew. Chem. Int. Ed.* **2001**, *40*, 3639; b) T. Hayashi, A. Kishida, N. Mizuno, *Chem. Commun.* **2000**, 381.

[39] H. Weiner, R. G. Finke, *J. Am. Chem. Soc.* **1999**, *121*, 9831.

[40] a) M. H. Dickman, M. T. Pope, *Chem. Rev.* **1994**, *94*, 569; b) A. Butler, M. J. Clague, G. E. Meister, *Chem. Rev.* **1994**, *94*, 62; c) E. Y. Tshuva, S. J. Lippard, *Chem. Rev.* **2004**, *104*, 987; d) L. M. Mirica, X. Ottenwaelder, T. D. Stack, *Chem. Rev.* **2004**, *104*, 1013.

[41] a) Y. Ishii, K. Yamawaki, T. Ura, H. Yamada, T. Yoshida, M. Ogawa, *J. Org. Chem.* **1988**, *53*, 3587; b) Y. Ishii, K. Yamawaki, T. Yoshida, T. Ura, M. Ogawa, *J. Org. Chem.* **1987**, *52*, 1868; c) S. Sakaguchi, Y. Nishiyama, Y. Ishii, *J. Org. Chem.* **1996**, *61*, 5307; d) T. Oguchi, Y. Sakata, N. Takeuchi, K. Kaneda, Y. Ishii, M. Ogawa, *Chem. Lett.* **1989**, 2053; e) S. Sakaue, Y. Sakata, Y. Nishiyama, Y. Ishii, *Chem. Lett.* **1992**, 289; f) Y. Ishii, Y. Sakata, *J. Org. Chem.* **1990**, *55*, 5545; g) Y. Ishii, T. Yoshida, K. Yamawaki, M. Ogawa, *J. Org. Chem.* **1988**, *53*, 5549; h) Y. Sakata, Y. Ishii, *J. Org. Chem.* **1991**, *56*, 6233; i) Y. Sakata, Y. Katayama, Y. Ishii, *Chem. Lett.* **1992**, 671; j) T. Iwahama, S. Sakaguchi, Y. Nishiyama, Y. Ishii, *Tetrahedron Lett.* **1995**, *36*, 1523.

[42] a) C. Venturello, R. D'Aloisio, J. C. J. Bart, M. Ricci, *J. Mol. Catal.* **1985**, *32*, 107; b) C. Venturello, E. Alneri, M. Ricci, *J. Org. Chem.* **1983**, *48*, 3831.

[43] a) C. Aubry, G. Chottard, N. Platzer, J.-M. Brégeault, R. Thouvenot, F. Chauveau,

C. Huet, H. Ledon, *Inorg. Chem.* **1991**, *30*, 4409; b) A. C. Dengel, W. P. Griffith, B. C. Parkin, *J. Chem. Soc., Dalton Trans.* **1993**, 2683; c) L. Salles, C. Aubry, R. Thouvenot, F. Robert, C. Dorémieux-Morin, G. Chottard, H. Ledon, Y. Jeannin, J.-M. Brégeault, *Inorg. Chem.* **1994**, *33*, 871.

[44] a) J.-Y. Piquemal, L. Salles, G. Chottard, P. Herson, C. Ahcine, J.-M. Bregeault, *Eur. J. Inorg. Chem.* **2006**, 939 ; b) J.-Y. Piquemal, L. Salles, C. Bois, F. Robert, J.-M. Bregeault, *C. R. Acad. Sci., Série II*, **1994**, 1481; c) J.-Y. Piquemal, C. Bois, J.-M. Brégeault, *Chem. Commun.* **1997**, 473; d) L. Salles, F. Robert, V. Semmer, Y. Jeannin, J.-M. Brégeault, *Bull. Soc. Chim. Fr.* **1996**, *133*, 319; e) J. Server-Carrió, J. Bas-Serra, M. E. González-Núnez, A. García-Gastaldi, G. B. Jameson, L. C. W. Baker, R. Acerete, *J. Am. Chem. Soc.* **1999**, *121*, 977.

[45] a) A. J. Bailey, W. P. Griffith, B. C. Parkin, *J. Chem. Soc., Dalton Trans.* **1995**, 1833; b) L. Salles, J.-Y. Piquemal, R. Thouvenot, C. Minot, J.-M. Brégeault, *J. Mol. Catal. A: Chem.* **1997**, *117*, 375.

[46] a) H. Nakajima, T. Kudo, N. Mizuno, *Chem. Mater.* **1999**, *11*, 691; b) A. F. Ghiron, R. C. Thompson, *Inorg. Chem.* **1988**, *47*, 4766; c) N. J. Campbell, A. C. Dengel, C. J. Edwards, W. P. Griffith, *J. Chem. Soc., Dalton Trans.* **1989**, 1203; d) V. Nardello, J. Marko, G. Vermeersch, J. M. Aubry, *Inorg. Chem.* **1998**, *37*, 5418; e) O. W. Howarth, *Dalton Trans.* **2004**, 476.

[47] a) K. Sato, M. Aoki, R. Noyori, *Science*, **1998**, *281*, 1646; b) K. Sato, M. Aoki, M. Ogawa, T. Hashimoto, R. Noyori, *J. Org. Chem.* **1996**, *61*, 8310; c) K. Sato, M. Aoki, M. Ogawa, T. Hashimoto, D. Panyella, R. Noyori, *Bull. Chem. Soc. Jpn.* **1997**, *70*, 905; d) K. Sato, M. Aoki, J. Takagi, R. Noyori, *J. Am. Chem. Soc.***1997**, *119*, 12386; e) K. Sato, M. Aoki, J. Takagi, K. Zimmermann, R. Noyori, *Bull. Chem. Soc. Jpn.* **1999**, *72*, 2287.

[48] a) N. M. Okun, T. M. Anderson, C. L. Hill, *J. Am. Chem. Soc.* **2003**, *125*, 3194; b) N. M. Okun, T. M. Anderson, C. L. Hill, *J. Mol. Catal. A: Chem.* **2003**, *197*, 283; c) N. M. Okun, M. D. Ritorto, T. M. Anderson, R. P. Apkarian, C. L. Hill, *Chem. Mater.* **2004**, *16*, 2551.

[49] a) Z. Xi, N. Zhou, Y. Sun, K. Li, *Science* **2001**, *292*, 1139; b) Y. Sun, Z. Xi, G. Cao, *J. Mol. Catal. A: Chem.* **2001**, *166*, 219; c) Z. Xi, H. Wang, Y. Sun, N. Zhou, G. Cao, M. Li, *J. Mol. Catal. A: Chem.* **2001**, *168*, 299.

[50] a) Y. M. A. Yamada, M. Ichinohe, H. Takahashi, S. Ikegami, *Org. Lett.* **2001**, *3*,

1837; b) Y. M. A. Yamada, H. Tabata, M. Ichinohe, H. Takahashi, S. Ikegami, *Tetrahedron*, **2004**, *60*, 4087.

[51] F. Cavani, F. Trifiró, A. Vaccari, *Catal. Today* **1991**, *11*, 173.

[52] a) B. F. Sels, D. E. de Vos, M. Buntinx, F. Pierard, A. K.-D. Mesmaeker, P. A. Jacobs, *Nature*, **1999**, *400*, 855; b) B. F. Sels, D. E. de Vos, P. A. Jacobs, *J. Am. Chem. Soc.* **2001**, *123*, 8350.

[53] a) K. Yamaguchi, C. Yoshida, S. Uchida, N. Mizuno, *J. Am. Chem. Soc.* **2005**, *127*, 530; b) J. Kasai, Y. Nakagawa, S. Uchida, K. Yamaguchi, N. Mizuno, *Chem. Eur. J.* **2006**, *12*, 4176.

Chapter II

Synthesis, Structural Characterization, and Catalytic Performance of Dititanium-substituted γ-Keggin Silicotungstate

2.1. Introduction

Metal-oxygen cluster molecules, polyoxometalates (POMs) are attractive compounds for the wide range of chemistry including fundamental coordination chemistry and applied chemistry in catalysis, medicine, and material science due to the controllability of the molecular properties (composition, size, shape, acidity, and redox potential).[1] Recently, the interest in the catalysis of partially metal-substituted polyoxometalates (metal-substituted POMs), which are synthesized by the introduction of substituent metal ions into the vacant site of lacunary POMs, has been much growing because of the unique reactivity depending on the composition and structure of the molecules. Especially, dimetal-substituted γ-Keggin POMs containing an edge-shared dinuclear $M_2(\mu\text{-}O_2)$ site, $H_X[\gamma\text{-}SiM_2W_{10}O_{40}]^{n-}$ (where M = Mn, Fe, V), exhibited remarkable catalytic activities for hydrocarbon oxidations with "*green oxidants*" such as H_2O_2 and O_2.[2] These dimetal-substituted POMs were synthesized by the reaction of a divacant silicodecatungstate, $[\gamma\text{-}SiW_{10}O_{36}]^{8-}$,[3-5] with an appropriate metal source. In some cases, however, the reaction of with first-row transition metal species resulted in the re-organization of cluster frameworks giving some unexpected compounds.[6] Therefore, the selective syntheses of dimetal-substituted γ-Keggin clusters of various metal derivatives as well as the studies on their chemical properties including catalytic activities are still attractive subjects.

Titanium has been recognized to be an active element of an oxidation catalyst in both heterogeneous and homogeneous reaction systems. For example, a family of titanosilicates was extensively applied to various oxidation reactions including olefin epoxidation.[7,8] It has been proposed that tetrahedral Ti^{IV} center efficiently activated hydrogen peroxide, although the details of reaction mechanism as well as relationship between the structure of the active site and reactivity have been unclear. Titanium-containing POMs are attractive compounds because of their structural diversity of Ti centers. Several titanium-substituted phosphotungstates, $[PTi_XW_{12-X}O_{40}]^{(3+2X)-}$ (x = 1, 2) and their peroxo derivatives, were known to catalyze olefin epoxidation.[9] The structures of the Ti centers could be regarded as mononuclear sites (i.e., two titanium ions do not adjacently locate in $[PTi_2W_{10}O_{40}]^{7-}$). Recently, the tetrameric Ti-containing silicotungstate composed of β-Keggin subunits, $[\{\beta\text{-}SiTi_2W_{10}O_{39}\}_4]^{24-}$, has been synthesized from $[\gamma\text{-}SiW_{10}O_{36}]^{8-}$: The molecular

structure of this composed was revealed by the single crystal X-ray analysis, while the catalytic activity of this compound has not been reported.[10] In this context, the catalysis by various titanium-containing POMs, which are composed of multinuclear Ti sites and the other heteroatoms, should be investigated in order to reveal the structure-dependent reactivity.

In this chapter, a novel di-titanium-substituted γ-Keggin POM, $[\{\gamma\text{-}SiTi_2W_{10}O_{36}(OH)_2\}_2(\mu\text{-}O)_2]^{8-}$ (**1**), containing edge-shared dinuclear Ti site, has been synthesized and its molecular structure has been successfully determined. The dinuclear titanium core of **1** catalyzes mono-oxygenation reactions such as epoxidation of olefins and sulfoxidation of sulfides with H_2O_2.

2.2. Experimental

2.2.1. Instruments

IR spectra were measured on Jasco FT/IR-460 Plus using KBr disks. NMR spectra were recorded at 298 K on JEOL JNM-EX-270 (^{1}H, 270.0 MHz; ^{13}C, 67.8 MHz; ^{29}Si, 53.45 MHz; ^{183}W, 11.20 MHz) spectrometer. Chemical shifts (δ) were reported in ppm downfield from external $SiMe_4$ (solvent, $CDCl_3$) for ^{1}H, ^{13}C, and ^{29}Si NMR spectra and Na_2WO_4 (solvent, D_2O) for ^{183}W NMR spectra. CSI-TOFMS spectra of the polyoxometalates were recorded on a JEOL JMS-T100CS spectrometer. UV-vis spectra were recorded on a JASCO V-570 spectrometer. GC analyses were performed on Shimadzu GC-14B with a flame ionization detector equipped with a SE-30 packed column and GC-17A with a flame ionization detector equipped with a TC-WAX or a DB-WAX capillary column (internal diameter = 0.25 mm, length = 30 m). GC-MS spectra were recorded on Shimadzu GCMS-QP2010 at an ionization voltage of 70 eV equipped with a DB-WAX capillary column (internal diameter = 0.25 mm, length = 30 m). An acid/base titration was performed by using TOA DKK HM-30G pH meter with TOA DKK GST-5721S electrode.

2.2.2. Syntheses and Characterization of Polyoxometalates

Acetonitrile was dried over CaH_2, distilled and stored under argon. The

commercially available reagents (including organic solvents) were used without further purification. The starting materials of the silicotungstates, $K_8[SiW_{10}O_{36}]\cdot 12H_2O$ and $K_8[\alpha\text{-}SiW_{11}O_{39}]\cdot 13H_2O$, were prepared according to the method described in the literature.[3]

Tetra-*n*-Butylammonium Salt of $[\{\gamma\text{-}SiTi_2W_{10}O_{36}(OH)_2\}_2(\mu\text{-}O)_2]^{8-}$ (TBA-1): $Ti(O)(SO_4)$ (0.16 g, 1.00 mmol) was dissolved in 20 mL of deionized water and then the pH of the solution was adjusted to 1.3 with 70% HNO_3. After stirring the resulting suspension for 3 min at room temperature, $K_8[SiW_{10}O_{36}]\cdot 12H_2O$ (1.50 g, 0.50 mmol) was added in a single step and the continuous stirring of the reaction mixture gave the clear solution within 15 min. An excess amount of $[(n\text{-}C_4H_9)_4N]Br$ (1.00 g, 3 mmol) was added in a single step. After stirring the white suspension for 1 h at room temperature, the resulting white precipitate was collected by the filtration and then washed with an excess amount of H_2O. After the dryness, the crude compound was purified by recrystallization from acetonitrile/H_2O: The solution was kept at 298 K for 24 h to afford the colorless crystals of TBA-**1** (0.64 g; 36% yield). ^{29}Si NMR (53.45 MHz, CD_3CN, 298 K, TMS): $\delta = -84.2$; ^{183}W NMR (11.20 MHz, CD_3CN, 298 K, Na_2WO_4): $\delta = -106.1, -114.0, -131.7$ with an integrated intensity ratio of 1:1:1, respectively; IR (KBr): $\nu = 964, 904, 873, 820, 792, 739, 692, 661, 606, 553, 485, 458$ cm^{-1}; UV/Vis (CH_3CN): λ_{max} (ε) = 252 nm (119685 $mol^{-1}dm^3cm^{-1}$); Positive ion MS (CSI, CH_3CN): *m/z*: 7358 ($[TBA_9\cdot\mathbf{1}]^+$), 3801 ($[TBA_{10}\cdot\mathbf{1}]^{2+}$); elemental analysis calcd (%) for $C_{128}H_{288}O_{78}N_8Si_2Ti_4W_{20}$ ($[(n\text{-}C_4H_9)_4N]_8\cdot\mathbf{1}$): C 21.60, H 4.14, N 1.58, Si 0.79, Ti 2.69, W 51.67; found: C 21.19, H 4.18, N 1.53, Si 0.74, Ti 2.60, W 52.52.

[K(18-crown-6)] Salt of $[\{\gamma\text{-}SiTi_2W_{10}O_{36}(OH)_2\}_2(\mu\text{-}O)_2]^{8-}$ (CEK-1): 20 mL of aqueous solution of $Ti(O)SO_4$ (0.16 g, 1.0 mmol) was adjusted to pH 1.3. To this solution, $K_8[SiW_{10}O_{36}]\cdot 12H_2O$ (1.50 g, 0.50 mmol) was added. The solution was stirred until the solution became clear. 18-crown-6 (0.81 g, 3.0 mmol) was added and the solution was stirred for 15 min to form the white yellow precipitates. Filtration and drying under reduced pressure gave the powder of $[K(18\text{-crown-}6)]_8[\{\gamma\text{-}SiTi_2W_{10}O_{36}(OH)_2\}_2(\mu\text{-}O)_2]$ (CEK-**1**: 1.07 g, 0.154 mmol) in 62 % yield. The single crystal of CEK-**1** suitable for X-ray crystallography was obtained by slow evaporation of the DMSO solution of CEK-**1**. ^1H NMR (270.0 MHz, DMSO-d_6, 298 K, TMS): $\delta = 2.67$ (s, CH_2); $^{13}C\{H\}$ NMR (67.8 MHz, DMSO-d_6, 298 K, TMS): δ

= 69.1 (CH_2); ^{183}W NMR (11.20 MHz, DMSO-d_6, 298 K, Na_2WO_4): δ = −116.07, −118.37, −129.81 with an integrated intensity ratio of 1:1:1, respectively; IR (KBr): ν = 2920, 1473, 1435, 1410, 1388, 1352, 1286, 1251, 1106, 962, 903, 867, 820, 792, 668 cm^{-1}; elemental analysis calcd (%) for $C_{104}H_{220}O_{130}S_4K_8Si_2Ti_4W_{20}$ ([K(18-crown-6)]$_8$·**1**·4DMSO): C 15.75, H 2.80, K 3.95, Si 0.71, Ti 2.42, W 46.45; found: C 15.74, H 3.15, K 3.90, Si 0.71, Ti 2.46, W 46.01.

Tetra-*n*-Butylammonium Salt of [{γ-SiTi$_2$W$_{10}$O$_{36}$(OH)(OMe)}$_2$(μ-O)$_2$]$^{8-}$ (TBA-2): TBA·**1** (2.0 g, 0.28 mmol) was dissolved in 10 mL acetonitrile, followed by the addition of 5 mL of MeOH. After stirring for 30 min at ambient temperature, addition of 100 mL MeOH gave the white precipitate [TBA]$_8$[{γ-SiTi$_2$W$_{10}$O$_{36}$(OH)(OMe)}$_2$(μ-O)$_2$] (TBA-**2**: 1.3 g, 0.18 mmol) in 65 % yield. ^{1}H NMR (270.0 MHz, DMF-d_7, 298 K, TMS): δ = 4.60 (s, 6H, CH_3O), 3.53 (TBA, 64H), 1.88 (TBA, 64H), 1.56 (TBA, 64H), 1.08 (TBA, 96H); ^{13}C NMR (67.8 MHz, DMF-d_7, 298 K, TMS): δ = 62.6 (CH_3O), 49.0 (TBA), 23.8 (TBA), 19.7 (TBA), 13.4 (TBA); ^{29}Si NMR (53.45 MHz, DMF-d_7, 298 K, TMS): δ = −84.5; ^{183}W NMR (11.20 MHz, DMF-d_7, 298 K, Na_2WO_4): δ = −102.2, −113.3, −123.8, −127.1, −131.3, −136.0 with an integrated intensity ratio of 1:2:2:2:1:2, respectively; IR (KBr): ν = 999, 964, 904, 869, 821, 794, 741, 606, 551, 485, 458 cm^{-1}; UV/Vis (CH_3CN): λ_{max} (ε) = 252 nm (135347 mol^{-1}dm^{3}cm^{-1}); Positive ion MS (CSI, CH_3CN): *m/z*: 7387 ([TBA$_9$·**2**]$^+$), 7145 ([TBA$_8$H·**2**]$^+$), 3815 ([TBA$_{10}$·**2**]$^{2+}$), 3699 ([TBA$_9$H·**2**]$^{2+}$); elemental analysis calcd (%) for $C_{130}H_{296}N_8O_{78}Si_2Ti_4W_{20}$ ([(n-C_4H_9)$_4$N]$_8$·**2**): C 21.86, H 4.18, N 1.57; found: C, 20.72; H, 4.05; N, 1.49.

[K(18-crown-6)] Salt of [{γ-SiTi$_2$W$_{10}$O$_{36}$(OH)(OMe)}$_2$(μ-O)$_2$]$^{8-}$ (CEK-2): CEK-**1** (0.16 g, 23.1 mmol) was dissolved in 1 mL DMSO, followed by the addition of 1 mL of MeOH. Vapor diffusion of Et_2O gave the white yellow crystalline solid [K(18-crown-6)]$_8$[{γ-SiTi$_2$W$_{10}$O$_{36}$(OH)(OMe)}$_2$(μ-O)$_2$] (CEK-**2**: 0.06 g, 8.62 mmol) in 37 % yield. ^{1}H NMR (270.0 MHz, DMF-d_7, 298 K, TMS): δ 3.52 (s, 96H, CH_2), 3.28 (s, 6H, *Me*); ^{13}C{H} NMR (67.8 MHz, DMF-d_7, 298 K, TMS): δ 69.4 (s, CH_2), 40.4 (s, CH_3); IR (KBr): ν = 3522, 2999, 2909, 1473, 1455, 1436, 1403, 1352, 1286, 1251, 1106, 1050, 1022, 998, 962, 902, 865, 819, 791, 708, 658 cm^{-1}; elemental analysis calcd (%) for $C_{106}H_{224}O_{130}S_4K_8Si_2Ti_4W_{20}$ ([K(18-crown-6)]$_8$·**2**·4DMSO): C 16.03, H 2.84, K 3.94, Si 0.71, Ti 2.41, W 46.28; found: C 16.44; H 3.34, K 3.59, Si 0.72, Ti 2.40, W 46.17.

Tetra-*n*-Butylammonium Salt of $[\alpha\text{-SiW}_{11}O_{39}]^{8-}$: $K_8[\alpha\text{-SiW}_{11}O_{39}]\cdot 13H_2O$ (15.9 g, 5 mmol) was quickly dissolved in 1 M AcOH/AcONa buffer solution (200 mL). Then, $[(n\text{-}C_4H_9)_4N]Br$ (8 g, 25 mmol) was added to the solution in a single step. The resulting white precipitate was collected by the filtration and then washed with an excess amount of water (3 L). The crude product was purified twice with the precipitation method, followed by the recrystallization to give analytically pure tetra-*n*-butylammonium salt derivative of $[\alpha\text{-SiW}_{11}O_{39}]^{8-}$ (Yield: 37%). IR (KBr): ν = 1005, 963, 956, 910, 800, 737, 547, 533 cm^{-1}; UV/Vis (CH_3CN): λ_{max} (ε) = 259 nm (33000 $mol^{-1}dm^3cm^{-1}$); elemental analysis calcd (%) for $C_{64}H_{152}N_4O_{41}Si_1W_{11}$ ($[(n\text{-}C_4H_9)_4N]_4H_4[\alpha\text{-SiW}_{11}O_{39}]\cdot 2H_2O$): C 20.86, H 4.16, N 1.52, Si 0.76, W 54.89; found: C 21.00, H 4.05, N 1.60, Si 0.80, W 55.32.

Tetra-*n*-Butylammonium Salt of $[\alpha\text{-H}_2\text{SiTiW}_{11}O_{40}]^{5-}$ (TBA-3): The tetra-*n*-butylammonium salt of the mono-vacant α-Keggin silicoundecatungstate $[(n\text{-}C_4H_9)_4N]_4H_4[\alpha\text{-SiW}_{11}O_{39}]\cdot 2H_2O$ (1.55 g (0.4 mmol)) was dissolved in 50 mL of acetonitrile followed by the addition of $TiCl_4$ (66 μL (0.6 mmol)). After stirring the resulting clear pale yellow solution for 1 h at room temperature, H_2O (200 mL) was added in a single step. The resulting white precipitate was collected by the filtration and then washed with an excess amount of H_2O. An analytically pure white powder of $TBA_4[\alpha\text{-H}_2\text{SiTiW}_{11}O_{40}]$ (TBA-**3**) was obtained by the evacuation to dryness at room temperature. ^{29}Si NMR (53.45 MHz, DMSO-d_6, 298 K, TMS): δ = –84.2; ^{183}W NMR (11.20 MHz, DMSO-d_6, 298 K, Na_2WO_4): δ = –89.5, –100.0, –106.6, –110.2, –117.9, –131.4 with an integrated intensity ratio of 1:2:2:2:2:2, respectively; IR (KBr): ν = 963, 915, 880, 800, 651, 546, 530, 386, 333 cm^{-1}; MS (CSI, DMSO/CH_3CN): *m/z*: 3934 ($[TBA_5\cdot(SiTiW_{11}O_{39})]^+$), 3975 ($[TBA_5\cdot(SiTiW_{11}O_{39})\cdot CH_3CN]^+$), 4015 ($[TBA_5\cdot(SiTiW_{11}O_{39})\cdot DMSO]^+$); elemental analysis calcd (%) for $C_{64}H_{146}N_4O_{40}SiTiW_{11}$ ($[(n\text{-}C_4H_9)_4N]_4\cdot$**3**): C 20.72, H 3.97, N 1.51, Si 0.76, Ti 1.29, W 54.5; found: C 20.72, H 3.97, N 1.46, Ti 1.41, W 52.8.

2.2.3. Acid/base Titration

0.1 M acetonitrile/H_2O solution of tetra-*n*-butylammonium hydroxide (TBAOH) was prepared by the dilution of 1.0 M aqueous TBAOH (Aldrich). TBA-**1** (0.406 g,

57 μmol) was dissolved in acetonitrile (30 mL). The acid/base titration was performed under argon at room temperature as follows: To this acetonitrile solution of TBA-**1**, 114 μL of 0.1 M acetonitrile/H_2O solution of TBAOH (0.2 equiv. of **1**) was added with stirring. The measurement of potential was done when the value was stabilized. These operations were repeated 50 times.

2.2.4. Catalytic Oxidation

The catalytic oxidations were carried out with glass tube reactor. A typical procedure was as follows: Catalyst (4 μmol), acetonitrile (6 mL), 30% aqueous hydrogen peroxide (1 mmol), and olefin (5 mmol) were charged in glass tube reactor. The reaction was carried out at 323 K. The reaction solution was periodically sampled and analyzed by GC in combination with mass spectroscopy. The products were identified by the comparison of mass spectra with those of authentic samples. The carbon balance in each experiment was in the range of 95–100%. Remaining hydrogen peroxide after the reaction was analyzed by the $Ce^{4+/3+}$ titration. After the reaction, the catalyst was recovered by the evaporation to dryness followed by washing with ether and *n*-hexane.

2.2.5. X-Ray Crystallography

Diffraction measurement was made on a Rigaku AFC-10 Saturn 70 CCD detector with graphite monochromated Mo Kα radiation (λ = 0.71069 Å; 5 kW) at –180 °C. Data were collected and processed using CrystalClear[11] and HKL2000 for Linux software.[12] Neutral scattering factors were obtained from the standard source. In the reduction of data, Lorentz and polarization corrections were made. Structure analysis was performed by using the CrystalStructure crystallographic structure-solving program package[13] and Win-GX for Windows software.[14] The structures of CEK-**1** and CEK-**2** were solved by heavy-atom Patterson methods (DIRDIF PATTY)[15] and expanded using Fourier techniques (DIRDIF).[16] In the final cycle of full-matrix least-squares refinement on *F*, titanium and tungsten oxygen atoms were refined anisotropically. The structure of TBA-**1** was solved by SHELXS-97 (direct method) and SHELXH-97 (Fourier synthesis and least-squares refinement).[17] Titanium and tungsten atoms were refined anisotropically, and other atoms except hydrogen and

highly disordered carbon atoms of 18-crown-6 were refined isotropically.

2.3. Results and Discussion

2.3.1. Synthesis of Dititanium-Substituted Silicotungstate

The reaction of the potassium salt of $[SiW_{10}O_{36}]^{8-}$ with 2 equiv. of $Ti(O)(SO_4)$ in acidic aqueous solution at ambient temperature and the successive addition of tetra-*n*-butylammonium bromide (= TBABr) yielded the corresponding tetra-*n*-butylammonium derivative (= TBA-**1**) of a desired titanium-substituted silicotungstate. The elemental analysis data indicated the Si:Ti:W molar ratio was 1:2:10 in TBA-**1**. One ^{29}Si NMR signal was observed at −84.2 ppm (Figure 2-1(a)) and the ^{183}W NMR spectrum of TBA-**1** showed three signals at −106.1, −114.0, and −131.7 ppm with the intensity ratio of 1:2:2, respectively (Figure 2-2(a)). This structural symmetry of tungsten atoms suggests that the cluster framework of $[SiW_{10}O_{36}]^{8-}$ maintains the γ-Keggin structure. The positive ion CSI-MS (cold spray ionization mass spectrometry) spectrum of the acetonitrile solution of TBA-**1** exhibited a +1-charged ion peak at m/z = 7358 attributed to $\{((n\text{-}C_4H_9)_4N)_9[H_4Si_2Ti_4W_{20}O_{78}]\}^+$ and the +2-charged peak at m/z = 3801 attributed to $\{((n\text{-}C_4H_9)_4N)_{10}[H_4Si_2Ti_4W_{20}O_{78}]\}^{2+}$ (Figure 2-3). Therefore, **1** could be assigned as the dimer of the di-titanium-substituted γ-Keggin silicotungstate.

The potassium-crown ether clathrate (= $[K(18\text{-crown-}6)]^+$; abbreviated as "CEK") salt derivative of **1** (= CEK-**1**) was also synthesized by addition of 18-crown-6 instead of TBABr to the aqueous reaction mixture of $[SiW_{10}O_{36}]^{8-}$ with 2 equiv. of $Ti(O)(SO_4)$. Both TBA and CEK salts were soluble in polar organic solvents and single crystals of TBA-**1** and CEK-**1** suitable for X-ray analysis were obtained successfully from acetonitrile/H_2O and DMSO, respectively (Table 2-1). The structural properties of the anion parts (= **1**; Figure 2-4) in both crystals were essentially identical (Table 2-2).

An edge-shared dinuclear titanium core, $Ti_2(\mu\text{-}O)_2$, was incorporated into the lacunary site of $[SiW_{10}O_{36}]^{8-}$, and the resulting titanium-substituted γ-Keggin POM fragments, $[SiTi_2W_{10}O_{38}]^{4-}$, were dimerized through oxo ligands giving Ti-O-Ti

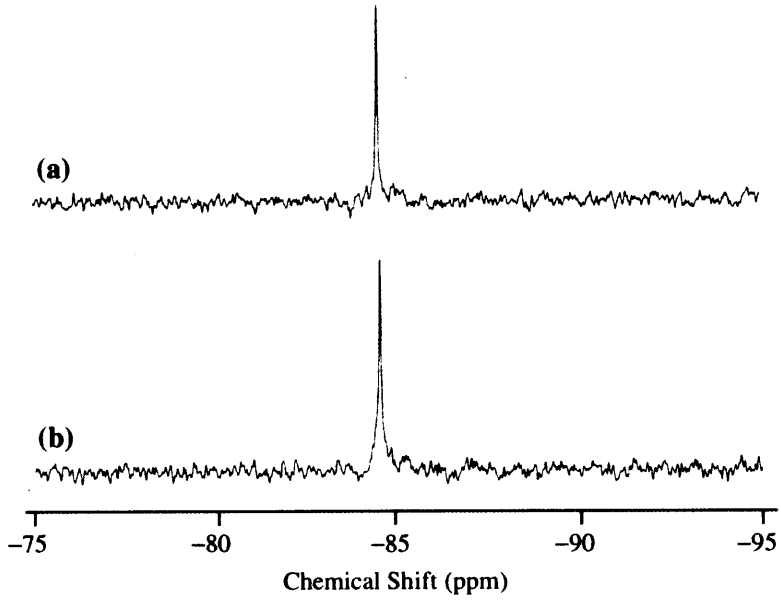

Figure 2-1. ^{29}Si NMR spectra of (a) as prepared TBA-**1** and (b) TBA-**1** recovered after the use for the epoxidation of cyclooctene. After the completion of the epoxidation, the volume of the reaction mixture was reduced by the evaporation. Ether was added to the concentrated solution and the catalyst precipitated was recovered by the filtration.

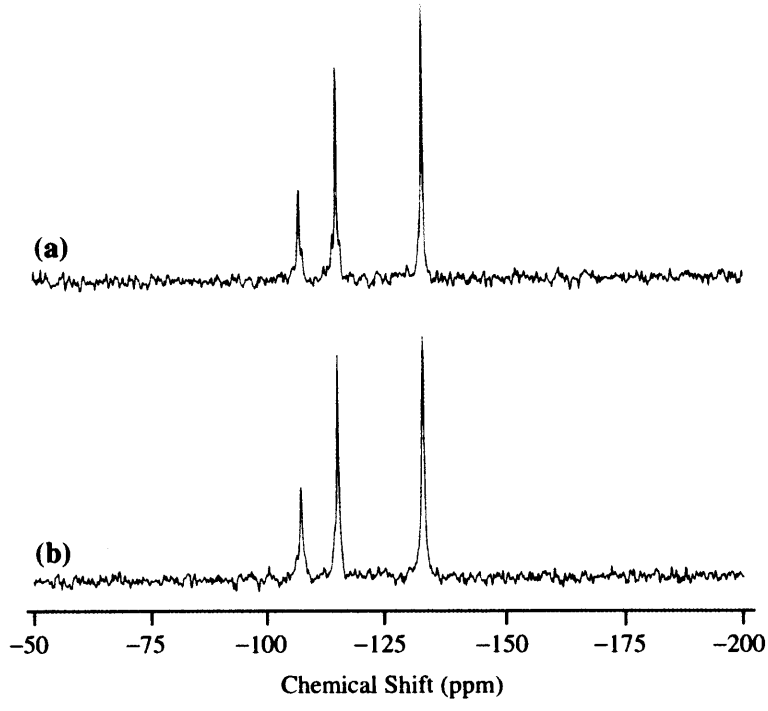

Figure 2-2. ^{183}W NMR spectra of (a) as prepared TBA-**1** and (b) TBA-**1** recovered after the use for the epoxidation of cyclooctene. After the completion of the epoxidation, the volume of the reaction mixture was reduced by the evaporation. Ether was added to the concentrated solution and the catalyst precipitated was recovered by the filtration.

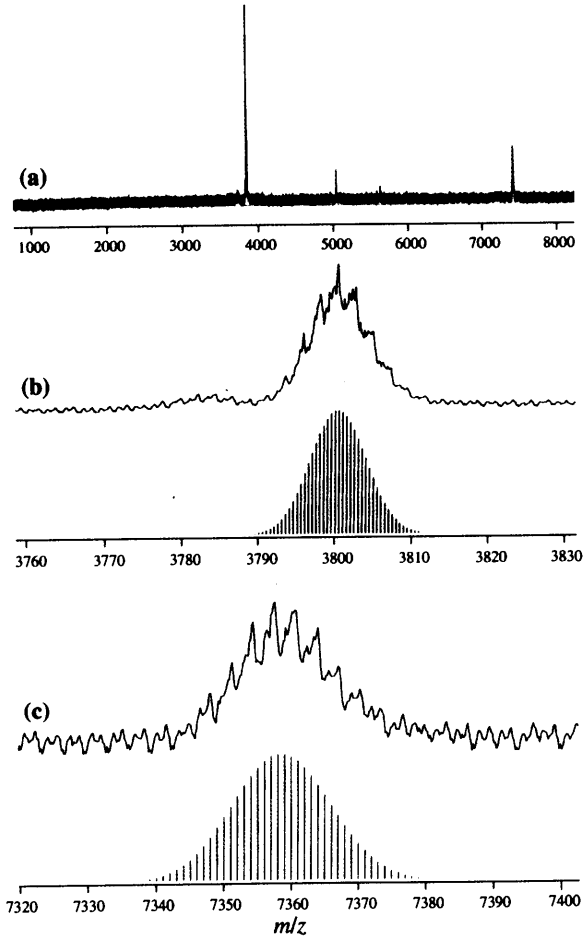

Figure 2-3. Positive ion CSI-MS spectra of TBA-**1** in MeCN ((a) *m/z* 1000–8000, (b) *m/z* 3760–3830, and (c) *m/z* 7320–7400). The lines in (b) and (c) are the calculated pattern of $\{TBA_{10}[H_4Si_2Ti_4W_{20}O_{78}]\}^{2+}$ and $\{TBA_9[H_4Si_2Ti_4W_{20}O_{78}]\}^{+}$, respectively.

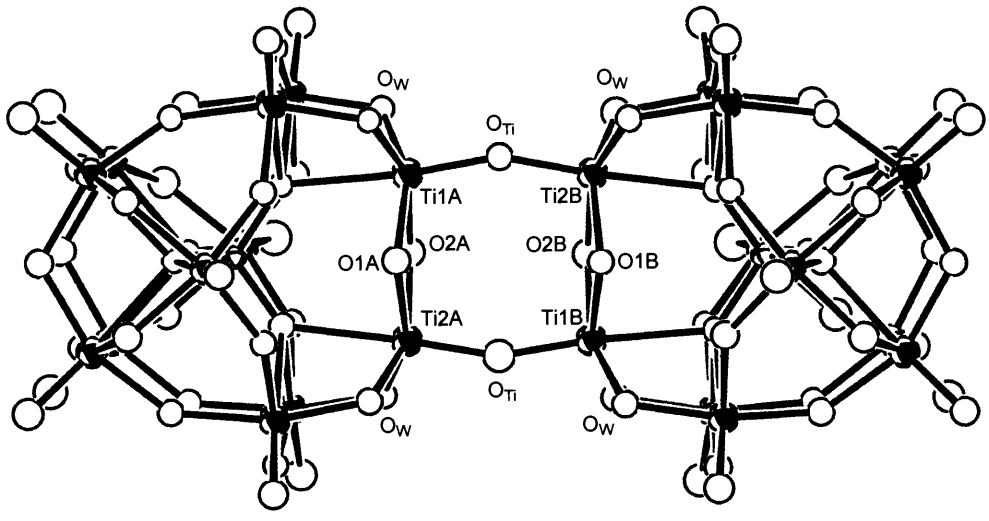

Figure 2-4. ORTEP drawing of $[\{\gamma\text{-}SiTi_2W_{10}O_{36}(OH)_2\}_2(\mu\text{-}O)_2]^{8-}$ (**1**; TBA derivative) drawn at 30 % probability level.

Table 2-1. Crystallographic data for TBA-**1**, CEK-**1**, and CEK-**2**[a]

compound	TBA·**1** ·0.5MeCN	CEK-**1**·2DMSO	CEK-**2**
formula	$C_{258}H_{579}O_{156}N_{17}Si_4Ti_8W_{40}$	$C_{100}H_{212}K_8O_{128}S_2Si_2Ti_4W_{20}$	$C_{98}H_{200}K_8O_{126}Si_2Ti_4W_{20}$
formula weight	14265.94	7764.38	7632.14
crystal system	Pna21 (#33)	Fddd (#70)	C2/m (#12)
space group	orthorhombic	orthorhombic	monoclinic
a (Å)	29.1660(3)	33.2107(3)	45.4319(7)
b (Å)	38.4971(4)	35.4445(4)	17.8884(4)
c (Å)	37.4046(3)	85.0187(8)	15.8179(3)
α (deg)	90.0000	90.0000	90.0000
β (deg)	90.0000	90.0000	96.3280(8)
γ (deg)	90.0000	90.0000	90.0000
V (Å^3)	41998.1(7)	100078.6(17)	12776.9(4)
Z	4	16	2
d_{calcd} (g·cm^{-3})	2.244	2.061	2.036
μ (cm^{-1})	11.132	9.523	9.306
no. of parameters refined	1166	696	301
R	0.0444 (for 25900)[b]	0.0546 (for 18443 data)[c]	0.0602 (for 9127 bata)[c]
wR2[a]	0.1266 (for all 30698 data)	0.0538 (for all 29407 data)	0.0783 (for all 15078 data)

[a] The program packages used for the refinement were SHELXH-97 for TBA-**1** and CrystalStructure for CEK-**1**, and CEK-**2**. [b] For data with $F_0 > 4\sigma(F_0)$. [c] For data with $I > 2\sigma(I)$.

Table 2-2. Selected structural parameters for the anions **1** and **2** (lengthes in Å and angles in deg)

compound	TBA-**1**[a]		CEK-**1**[b]	CEK-**2**[b]
	molecule A	molecule B		
Ti···Ti_{intra}	3.146(6), 3.140(11)	3.140(8), 3.151(8)	3.158(3)	3.176(5)
Ti···Ti_{inter}	3.518(6), 3.502(6)	3.524(6), 3.523(7)	3.523(3)	3.544(5)
Ti-O_R	1.964(17), 2.010(18)	2.009(16), 1.989(18)	1.974(9)	2.009(17)
	2.035(16), 2.000(15)	2.028(15), 1.989(16)	2.008(9)	2.009(19)
	1.969(18), 1.999(16)	2.043(18), 2.013(16)		
	2.035(16), 2.000(15)	1.991(18), 1.990(15)		
Ti-O_{Ti}	1.791(16), 1.78(2)	1.798(16), 1.771(18)	1.804(9), 1.807(9)	1.803(5)
	1.779(19), 1.795(16)	1.820(18), 1.788(16)		
Ti-O_W av.	1.875, 1.851	1.853, 1.902	1.866	1.869
Ti-O_{Si} av.	2.405, 2.369	2.360, 2.338	2.398	2.4151(2)
W-O_{Si} av.	2.332, 2.367	2.330, 2.332	2.345	2.348
W=O av.	1.714, 1.697	1.691, 1.694	1.712	1.699
W-O_{Ti} av.	1.814, 1.906	1.854, 1.892	1.887	1.884
W-O_W av.	1.964, 1.900	1.921, 1.992	1.910	1.923
Si-O av.	1.653, 1.654	1.623, 1.634	1.626	1.631
Ti-O_R-Ti	106.3(8), 100.8(7)	102.1(7), 104.2(7)	106.2(4), 103.5(4)	104.5(12), 104.5(14)
	103.3(7), 103.5(7)	102.8(8), 103.9(7)		
Ti-O-Ti	157.6(10), 159.6(13)	158.7(10), 157.6(11)	154.7(5)	158.8(12)
O_R-Ti-O_R	77.1(7), 75.6(7) 77.3(6), 75.8(7)	76.9(6), 76.5(7) 75.8(7), 77.5(7)	75.1(3), 75.0(3)	75.5(9)

Table 2-2. *(continued)*

compound	TBA-**1**[a]		CEK-**1**[b]	CEK-**2**[b]
	molecule A	molecule B		
O_{Ti}-Ti-O_R	98.5(7),	96.5(7), 99.3(7)	98.8(3),	99.5(7),
	101.9(8)		101.3(3)	99.6(7)
	97.6(9),	100.3(7),	98.8(3),	
	100.0(8)	100.7(7)	101.3(3)	
	98.0(8), 99.7(8)	97.6(8), 99.3(7)		
	98.0(7),	97.8(7), 97.0(7)		
	100.4(7)			
O_{Ti}-Ti-O_W	100.4(8),	100.7(7),	101.6(4),	102.4(6),
	103.6(7)	104.3(8)	101.2(4)	101.1(6)
	100.8(8),	102.6(8),	102.3(4),	
	104.2(8)	102.1(8)	101.1(4)	
	101.4(8),	99.3(7),		
	100.5(8)	103.8(8)		
	102.0(7),	100.3(8),		
	100.9(8)	101.8(7)		
O_W-Ti-O_W	94.8(7), 96.7(7)	94.5(7), 94.8(7)	94.9(4), 95.1(4)	97.7(7)
	95.0(7), 96.0(8)	95.4(7), 94.9(8)		
O_R-Ti-O_W	90.9(7), 88.6(7)	91.6(7), 89.5(7)	92.1(4), 89.8(4)	89.5(8),
				89.3(8)
	92.1(7), 87.6(7)	90.5(7), 89.0(6)		
	92.9(7), 87.9(7)	90.0(7), 91.9(7)		
	91.4(7), 89.2(7)	90.8(7), 90.7(7)		

[a] Molecule A and B are crystallographically independent molecules. [b] Sitting on a crystallographic mirror plane.

linkages. In other words, a cationic tetranuclear titanium center, Ti_4O_6, was supported by two lacunary γ-Keggin anions $[SiW_{10}O_{36}]^{8-}$. The existence of eight counter cations per the dimeric cluster molecule implies that the charge of **1** is –8. The bond valence sum values of titanium (3.43–4.55), tungsten (5.68–6.49) and silicon (3.76–3.90) indicate that the silicotitanotungstate cluster **1** is composed of Ti(IV), W(VI) and Si(IV) ions. Therefore, four protons are associated with the anionic cluster **1** on the basis of the charge balance. Interestingly, the bond valence sum values of O1 and O2 (1.09–1.34) were clearly lower than those of the other oxygen atoms in the Ti-O-Ti linkages (2.09–2.20). These observations suggest that these oxygen atoms in the edge-shared Ti_2O_2 moieties are protonated. The protonation of the oxo ligands at the edge-shared $Ti_2(\mu\text{-}O)_2$ moiety (i.e., $Ti_2(\mu\text{-}OH)_2$ core) is also suggested by the formation of an alkoxo derivative **2**, $[\{\gamma\text{-}SiTi_2W_{10}O_{36}(OH)(OMe)\}_2(\mu\text{-}O)_2]^{8-}$ (see the later section, Scheme 2-1). Therefore, the formulation of **1** can be described as $[\{\gamma\text{-}SiTi_2W_{10}O_{36}(OH)_2\}_2(\mu\text{-}O)_2]^{8-}$.

Recently, the tetrameric Ti-containing silicotungstate composed of β-Keggin subunits, $[\{\beta\text{-}SiTi_2W_{10}O_{39}\}_4]^{24-}$, in which two titanium ions separately locate in each β-Keggin fragment, has been synthesized from $[SiW_{10}O_{36}]^{8-}$ with a similar procedure to that presented herein except for the synthetic temperature. Kortz and co-workers have suggested that the γ-Keggin silicotitanotungstate component (i.e., half unit of **1**) is an initial intermediate and that the subsequent isomerization under relatively high temperature (353 K) in acidic aqueous solution gives the β-Keggin component of the tetrameric silicotitanotungstate (Scheme 2-2).[10] To date, several molecular structures of titanium-substituted POMs including the mono-, di-, and tri-substituted α- or β-isomers of Keggin titanotungstates $[XTi_yW_{12-y}O_{40}]^{n-}$ (X = P, Ge; y = 1, 2, 3) have been reported.[18–22] All of these Keggin POMs have dimeric structures except for the monomeric ($[\alpha\text{-}1,5\text{-}PTi_2W_{10}O_{40}]^{7-}$ and $[\alpha\text{-}PTiW_{11}O_{40}]^{5-}$) and tetrameric ($[\{\beta\text{-}SiTi_2W_{10}O_{39}\}_4]^{24-}$) compounds. In contrast with the previously-characterized compounds, **1** is the first structurally determined di-substituted γ-isomer of titanotungstate, while the molecular structure is dimeric.

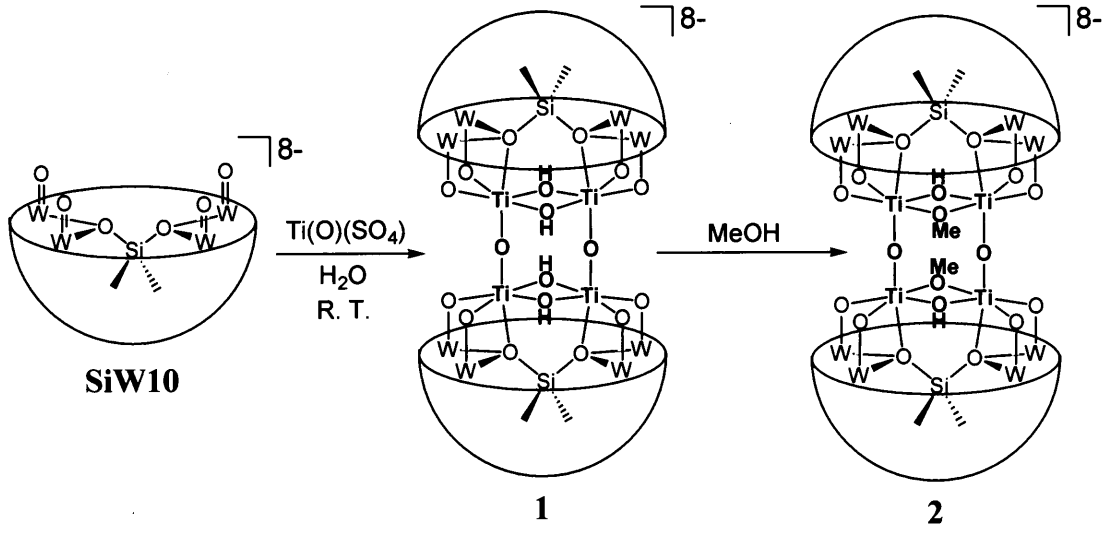

Scheme 2-1. Formation of **1** and **2**.

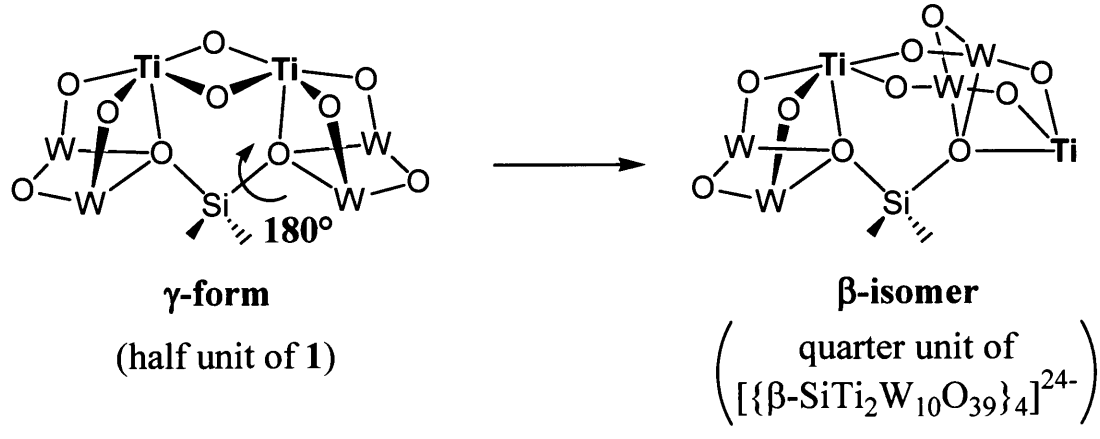

Scheme 2-2. Isomerization of Ti-containing Keggin POM from the γ-form (**1**) to β-isomer.

2.3.2. Formation of Methoxo Derivative

The addition of an excess amount of MeOH to the acetonitrile solution of the TBA salt of **1** resulted in the formation of white precipitates of **2**. The ^{183}W NMR spectrum of the DMF-d_7 solution of the collected white precipitates of **2** exhibited six signals at –102.2, –113.3, –123.8, –127.1, –131.3, and –136.0 ppm with intensities of 1:2:2:2:1:2, respectively, while the ^{29}Si NMR spectrum of the same solution showed one signal at –84.5 ppm (Figure 2-5). These observations suggested that the original C_{2V} symmetry of the γ-Keggin framework of **1** turned to the C_S one in **2**: The same change in the spectral pattern had been observed during the formation of $[\gamma\text{-}SiV_2W_{10}O_{38}(OH)(OMe)]^{4-}$.[23] The positive ion CSI-MS spectrum of the acetonitrile solution of **2** contained the peaks attributed to an alkoxo derivative of **2** (i.e., $[\{\gamma\text{-}SiTi_2W_{10}O_{36}(OH)(OMe)\}_2(\mu\text{-}O)_2]^{8-}$); $\{TBA_9\cdot\mathbf{2}\}^+$ (m/z = 7387), $\{TBA_8\cdot H\cdot\mathbf{2}\}^+$ (7145), $\{TBA_{10}\cdot\mathbf{2}\}^{2+}$ (3815), and $\{TBA_9\cdot H\cdot\mathbf{2}\}^{2+}$ (3699). Therefore, **2** could be assigned as the dimer of the mono-methyl ester derivative of the γ-Keggin silicodititanodecatungstate, and its molecular structure was confirmed by the X-ray crystallography of the CEK salt derivative (see below).

The single crystal of the alkoxo derivative **2**, $[\{\gamma\text{-}SiTi_2W_{10}O_{36}(OH)(OMe)\}_2(\mu\text{-}O)_2]^{8-}$, was obtained by the recrystallization of CEK-**1** in the presence of MeOH. The overall molecular structure of **2** was similar to that of **1** except alkoxy-functionalized sites (Figure 2-6). The dimeric cluster framework was retained in **2**. The alkoxide groups played a role as the bridging ligands of the edge-shared dinuclear titanium sites, giving the $Ti_2(\mu\text{-}OMe)(\mu\text{-}OH)$ core in each γ-Keggin fragment. The Ti-O-Ti linkages connecting two γ-Keggin subunits were remained unchanged when the amount of MeOH reacted with **1** was two times larger than that of **1**, supporting the low reactivity of the Ti-O-Ti linkages.

An acid/base titration of TBA-**1** with tetra-*n*-butylammonium hydroxide (= TBAOH) in acetonitrile exhibited a breakpoint at 2 equiv. with respect to **1**. This fact suggests that (1) two of the four OH moieties in **1** exhibit Brønsted acidity, or (2) the Lewis acidic Ti centers react with OH^-, resulting in the fission of **1** to form the corresponding monomeric γ-Keggin compounds. The former case (i.e., Brønsted acidity of two OH ligands) is consistent with the formation of **2**; the remaining OH^-

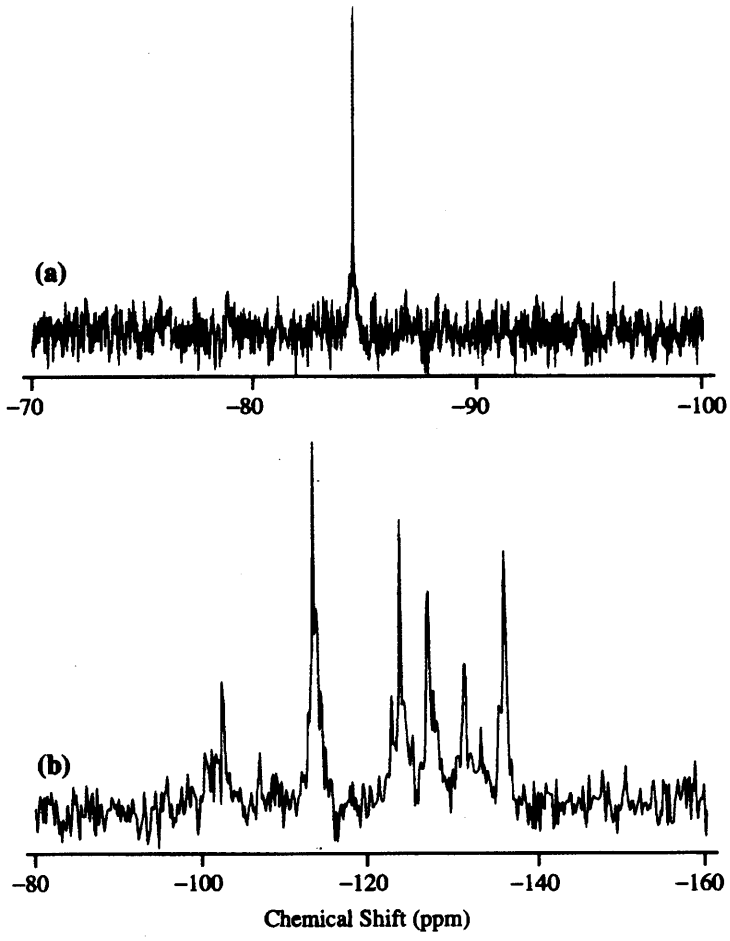

Figure 2-5. ^{29}Si NMR (a) and ^{183}W NMR (b) spectra of TBA salt of **2**.

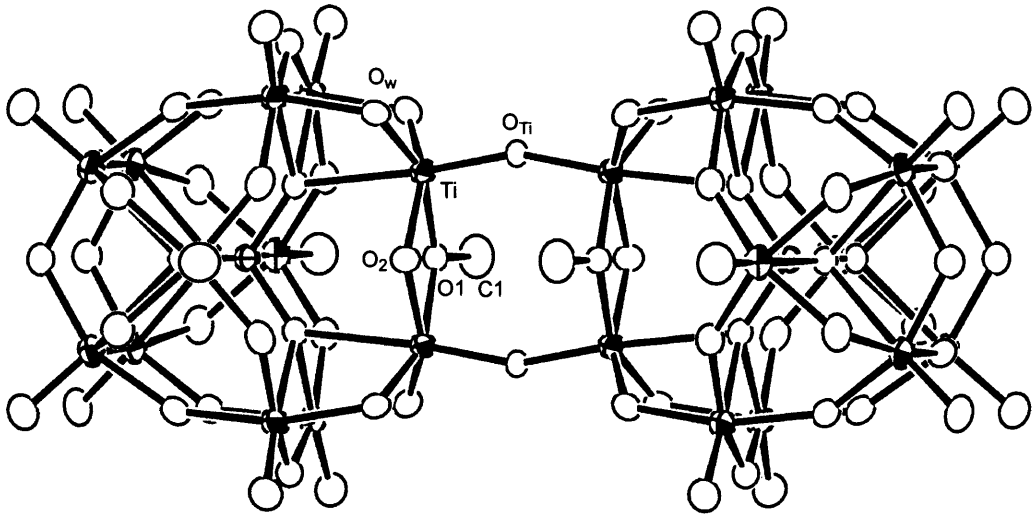

Figure 2-6. ORTEP drawing of $[\{\gamma\text{-}SiTi_2W_{10}O_{36}(OH)(OMe)\}_2(\mu\text{-}O)_2]^{8-}$ (**2**; CEK derivative) drawn at 30 % probability level.

ligands are rather basic enough to react with MeOH and **2** is formed. Recently, it was reported that the reaction of dinuclear $V_2(\mu\text{-}OH)_2$ core of the di-vanadium-substituted γ-Keggin silicotungstate, $[\gamma\text{-}SiV_2W_{10}O_{38}(OH)_2]^{4-}$, with MeOH yielded the corresponding mono-methyl ester containing dinuclear vanadium-μ-hydroxo-μ-alkoxo core, $[\gamma\text{-}SiV_2W_{10}O_{38}(OH)(OMe)]^{4-}$.[23]

2.3.3. Synthesis of Monotitanium-Substituted Silicotungstate

A mono-titanium-substituted Keggin-type silicotungstate, $[\alpha\text{-}H_2SiTiW_{11}O_{40}]^{4-}$ (**3**), was synthesized. The compound **3** was obtained by a similar method to that for the synthesis of the TBA salt of phosphotitanoundecatungstate $[\alpha\text{-}PTiW_{11}O_{40}]^{5-}$.[21a] The reaction of the TBA salt of the mono-vacant α-Keggin type silicoundecatungstate, $[\alpha\text{-}SiW_{11}O_{39}]^{8-}$, with $TiCl_4$ in acetonitrile and the successive addition of water yielded the desired compound **3** as white precipitate. The ^{183}W NMR spectrum of a DMSO solution of **3** exhibited six signals with the intensity ratio of 1:2:2:2:2:2, respectively, suggesting that the **3** has C_S symmetry with the α-Keggin type undecatungstate. The CSI-MS spectrum of the CH_3CN/DMSO solution of **3** showed the peaks attributed to mono-titanium-substituted silicotungstate species; $[TBA_5\cdot(SiTiW_{11}O_{39})]^+$ (m/z = 3934), $[TBA_5\cdot(SiTiW_{11}O_{39})\cdot CH_3CN]^+$ (3975), and $[TBA_5\cdot(SiTiW_{11}O_{39})\cdot DMSO]^+$ (4015). Attempts to synthesize analytically pure **3** were not successful with different synthetic routes: The reaction of $K_8[\alpha\text{-}SiW_{11}O_{39}]$ with titanium(IV) compounds such as $Ti(O)(SO_4)$ and $Ti(SO_4)_2$ in water resulted in the formation of non-titanium-containing silicododecatungstate, $[SiW_{12}O_{40}]^{4-}$.

2.3.4. Mono-Oxygenation of Olefins and Sulfides

First, the epoxidation of cyclooctene was carried out with TBA salts of di- and mono-titanium-substituted silicotungstates **1**, **2**, and **3**, and the TBA salt of fully occupied γ-Keggin silicododecatungstate, $[\gamma\text{-}SiW_{12}O_{40}]^{4-}$ (Table 2-3). The compound TBA-**1** showed high catalytic activity and cyclooctene oxide was obtained in 98% yield (entry 1). The epoxidation did not proceed at all in the absence of the catalyst (entry 5). The mono-titanium-substituted compound **3** and non-substituted compound $[\gamma\text{-}SiW_{12}O_{40}]^{4-}$ were inactive under the present conditions (entries 3 and 4). The

catalytic activity of methanol monoester of **1** (TBA-**2**, 26% yield) was much lower than that of TBA-**1** (entry 2).

Next, effects of solvents on the present epoxidation of cyclooctene were examined. Among solvents tested, acetonitrile was the most effective solvent (98% yield, entry 1). In this case, no stoichiometric formation of acetamide to cyclooctene oxide was observed, showing that the present epoxidation does not proceed via a peroxycarboxyimidic acid intermediate formed by the reaction of acetonitrile and H_2O_2.[24] 1,2-Dichloroethane (54% yield, entry 6) and acetone (44%, entry 7) gave cyclooctene oxide in moderate yield and *N,N*-dimethylformamide was a poor solvent (2%, entry 8). The epoxidation in acetonitrile was inhibited by the addition of a small amount of methanol (0.1 mL) and the yield of cyclooctene oxide decreased to 40% (entry 9).

Table 2-4 shows the results of the epoxidation of various olefins in acetonitrile catalyzed by TBA-**1**. In contrast to porous titanosilicate catalysts, **1** catalyzed the oxygenation of the relatively bulky disubstituted olefines including cyclic compounds such as cyclooctene and 2-norbornene with H_2O_2 (entries 1 and 2). In the case of a non-activated aliphatic terminal olefin of 1-octene, the yield of the corresponding epoxide was very low (entry 7). Geraniol was regioselectively epoxidized at the electron-deficient allylic double bond with small amount of the corresponding aldehyde (entry 8).[25] It has been reported in the Ti-β/H_2O_2 system that an allylic alcohol interacts with the oxidant through the hydrogen bonding of the hydroxyl group that prefer the oxygen transfer to the 2,3-allylic double bond. For the epoxidation of *cis*- and *trans*-olefins, the configurations around the C=C double bonds were completely retained in the corresponding epoxides (entries 4–6). Moreover, the epoxidation rate and selectivity were not changed by the addition of free radical trap, *e.g.*, 2,6-di-*tert*-butyl-4-methylphenol and hydroquinone. These results suggest that the free-radical intermediates are not involved in the present epoxidation.

The present system also catalyzed the sulfoxidation as shown in Table 2-4. It was confirmed that no reaction of aryl sulfides, e.g., 1-methoxy-4-(methylthio)benzene, as well as alkyl sulfides, e.g., methyl *n*-octyl sulfide, proceeded under the same conditions without catalyst. Various kinds of sulfides were selectively mono-oxygenated to the corresponding sulfoxides with high selectivity (≥97%) and high efficiency of hydrogen

peroxide utilization (≥83%). Not only aryl sulfides but also alkyl sulfides could be converted to the corresponding sulfoxides in excellent yield (entries 14 and 15). In the sulfoxidation of aryl sulfides, the reaction rates were affected by the electronic variation due to the substituents on the aromatic rings; electron-donating substituents on aromatic rings accelerated the reaction rates while electron-withdrawing ones retarded the rates (entries 9–13). The fairly good linearity of Hammett plots ($\log(k_X/k_H)$ *vs.* σ plots) suggests that the present oxygenation proceeds via a single mechanism. The slope of the linear line gave a Hammett ρ value of –0.81. The negative Hammett ρ value would be due to the formation of an electrophilic oxidant by the reaction of **1** with H_2O_2. The electronic character of the active oxygen species was examined by the oxidation of thianthrene 5-oxide (SSO).[26] In the present system, the sulfide site of SSO was much more selectively oxidized and the X_{SO} value (= (nucleophilic oxidation)/(nucleophilic + electrophilic oxidation) = $(SSO_2 + SOSO_2)/(SSO_2 + SOSO + 2SOSO_2)$) was 0.03 [Eq. (2-1)]. The low X_{SO} value suggests the formation of an electrophilic oxidant on **1**.

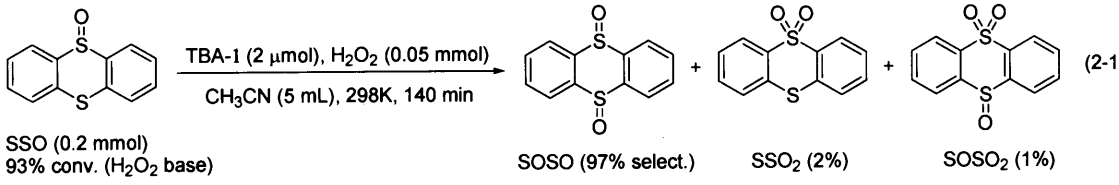

(2-1)

For the competitive epoxidation of *cis*- and *trans*-2-octenes, the ratio of the formation rate of *cis*-2,3-epoxyoctane to that of *trans* isomer (= R_{cis}/R_{trans}) was 21.3. This value is higher than those for the tungstate-hydrogen peroxide systems ($[\gamma\text{-}SiW_{10}O_{34}(H_2O)_2]^{4-}$; 11.5, $NH_2CH_2PO_3H_2/WO_4^{2-}$; 7.3, CPC/$[PW_{12}O_{40}]^{3-}$; 3.7).[4] In the case of $[\gamma\text{-}1,2\text{-}H_2SiV_2W_{10}O_{40}]^{4-}$ with the $V_2(\mu\text{-}OH)_2$ core similar to that with **1**, a very large R_{cis}/R_{trans} value (= 300) for the competitive epoxidation of *cis*- and *trans*-2-octenes was obtained under the conditions of the low olefin concentration (≤ 33.3 mM).[23b] Interestingly, the epoxidation of 3-methyl-1-cyclohexene was highly diastereoselective and gave mainly the corresponding epoxide with the oxirane ring trans to the substituent (anti configuration, entry 3 in Table 2-2). The ^{29}Si and ^{183}W NMR spectra of the catalyst recovered after completion of the epoxidation were not changed and the signals due to the tungstate compounds such as $[\alpha\text{-}SiW_{12}O_{40}]^{4-}$, $[\gamma\text{-}SiW_{10}O_{34}(H_2O)_2]^{4-}$, $[W_2O_3(O_2)_4(H_2O)_2]^{2-}$, and $[H_nWO_2(O_2)_2]^{(2-n)-}$ were not observed (Figures 2-1(b) and 2-2(b)). These results show that the molecular structure of **1** is

preserved during the catalysis. In addition, the first-order dependence of the reaction rate on the concentration of TBA-**1** also supports the idea. Therefore, it is likely that the active electrophilic oxygen species formed by the reaction of **1** with H_2O_2 is embedded in the rigid polyoxometalate framework, resulting in the stereospecificity and diastereoselectivity for the epoxidation.

As above mentioned, the mono-titanium-substituted silicotungstate **3**, was completely inactive for the epoxidation under the present conditions, suggesting that the Ti-O-W and Ti-O centers are not the active sites. The fully occupied silicododecatungstate of $[\gamma\text{-}SiW_{12}O_{40}]^{4-}$ was also inactive, suggesting that the tungsten atoms in **1** do not contribute to the epoxidation. In addition, stereospecificity for the epoxidation of *cis*- and *trans*-olefins by **1** was different from those by tungstate catalysts and no formation of tungstate compounds from **1** during the oxidation. These observations suggest that the catalytic reactions proceed on the multinuclear titanium center of **1**. The methoxo derivative **2** was formed by the dehydrative condensation between the hydroxo group in **1** and methanol as mentioned. Therefore, it is likely that the dehydrative condensation between **1** and hydrogen peroxide to form the hydroperoxo complex proceeds. The reaction of the $V_2(\mu\text{-}OH)_2$ core in $[\gamma\text{-}1,2\text{-}H_2SiV_2W_{10}O_{40}]^{4-}$ with hydrogen peroxide gave $V_2(\mu\text{-}OH)(\mu\text{-}OOH)$ species for the epoxidation of olefins as has been reported.[23b] Similarly, the $Ti_2(\mu\text{-}OH)_2$ core in **1** would react with hydrogen peroxide to form $Ti_2(\mu\text{-}OH)(\mu\text{-}OOH)$ species [Eq. (2-2)]. This idea is supported by the fact that the catalytic activity of **2** was much lower than that of **1**.

$$[\{\gamma\text{-}SiW_{10}Ti_2O_{36}(\mu\text{-}OH)_2\}_2(\mu\text{-}O)_2]^{8-} + 2H_2O_2 \rightarrow [\{\gamma\text{-}SiW_{10}Ti_2O_{36}(\mu\text{-}OH)(\mu\text{-}OOH)\}_2(\mu\text{-}O)_2]^{8-} + 2H_2O \qquad (2\text{-}2)$$

Table 2-3. Epoxidation of cyclooctene with H_2O_2[a]

entry	catalyst	solvent	yield/%	select./%
1	TBA-**1**	acetonitrile	98	>99
2	TBA-**2**	acetonitrile	26	>99
3	TBA-**3**	acetonitrile	3	>99
4[b]	$[\gamma\text{-}SiW_{12}O_{40}]^{4-}$	acetonitrile	<1	–
5	none	acetonitrile	<1	–
6	TBA-**1**	1,2-dichloroethane	54	>99
7	TBA-**1**	acetone	44	>99
8	TBA-**1**	*N*,*N*-dimethylformamide	2	>99
9[c]	TBA-**1**	acetonitrile	40	>99

[a] Reaction conditions: Catalyst (4 μmol), cyclooctene (5 mmol), H_2O_2 (30% aqueous, 1 mmol), solvent (6 mL), 323 K, 3 h. Yields were determined by GC using an internal standard technique. Yield/% = cyclooctene oxide (mol)/ initial H_2O_2 (mol) × 100. [b] TBA salt of $[\gamma\text{-}SiW_{12}O_{40}]^{4-}$ was used. [c] Methanol (0.1 mL) was added.

Table 2-4. Oxygenation of various olefins and sulfides with H_2O_2 catalyzed by TBA-**1**[a]

entry	substrate	product	time (h)	yield (%)	select.(%)
1			3	98	>99
2			10	53	90 (only *exo*)
3			4	64	90 (*syn*/*anti* = 19/81)
4			8	84	98 (only *cis*)
5			10	81	99 (only *cis*)
6			10	12	94 (only *trans*)
7			10	12	91
8[b]	OH	OH	8	91	91
9	MeO	MeO	1	95	99
10			1.5	83	>99
11	F	F	2	84	>99
12	O	O	3	92	98
13	NC	NC	3	96	99
14			3	92	98
15			3	84	99

[a] Reaction conditions for epoxidation: TBA-**1** (4 μmol), olefin (5 mmol), H_2O_2 (30% aq., 1 mmol), MeCN (6 mL), 323 K. Reaction conditions for sulfoxidation: TBA-**1** (2 μmol), sulfide (1 mmol), H_2O_2 (30% aq., 0.2 mmol), MeCN (1 mL), 305 K. Yields and selectivities were determined by GC or ^{1}H NMR using an internal standard technique. Yield/% = epoxide or sulfoxide formed (mol)/ initial H2O2 (mol) × 100. Select./% = epoxide or sulfoxide formed (mol)/ products formed (mol) × 100. [b]Aldehyde was formed (9% select.).

2.4. Conclusion

The novel γ-Keggin silicodititanodecatungstate **1** has been synthesized and its molecular structure was successfully determined. The edge-shared dinuclear Ti sites are protonated to give $Ti_2(\mu\text{-}OH)_2$ cores. The $Ti_2(\mu\text{-}OH)_2$ cores of **1** react with MeOH to give the corresponding alkoxo derivative **2**. The compound **1** is found to be an effective homogeneous catalyst for the oxygen transfer reactions of various substrates including olefins and sulfides. The results for the oxidation of SSO and 3-methyl-1-cyclohexene with **1** show the contribution of rigid non-radical electrophilic oxidant(s) generated on the multinuclear titanium center.

2.5. References

[1] a) Thematic issue on "Polyoxometalates"; *Chem. Rev.* **1998**, *98*, 1–390; b) R. Neumann, *Prog. Inorg. Chem.* **1998**, *47*, 317; c) T. Okuhara, N. Mizuno, M. Misono, *Adv. Catal.* **1996**, *41*, 113; d) C. L. Hill, C. Chrisina, M. P. McCartha, *Coord. Chem. Rev.* **1995**, *143*, 407; e) *Polyoxometalate Chemistry: From Topology via Self-Assembly to Applications* (Eds.: M. T. Pope, A. Müller), Kluwer, Dordrecht, **2001**; f) *Polyoxometalate Chemistry for Nano-Composite Design* (Eds.: T. Yamase, M. T. Pope), Kluwer, Dordrecht, **2002**; g) I. V. Kozhevnikov, *Catalysis by Polyoxometalates*; John Wiley & Sons, Ltd., Chichester, England, **2002**; h) C. L. Hill in *Comprehensive Coordination Chemistry II: Transition Metal Groups 3–6, Vol. 4* (Ed.: A. G. Wedd), Elsevier Science, New York, **2004**, chap. 4.11, pp. 679–759.

[2] a) Y. Nishiyama, Y. Nakagawa, N. Mizuno, *Angew. Chem. Int. Ed.* **2001**, *40*, 3639; b) N. Mizuno, C. Nozaki, I. Kiyoto, M. Misono, *J. Am. Chem. Soc.* **1998**, *120*, 9267; c) N. Mizuno, C. Nozaki, I. Kiyoto, M. Misono, *J. Catal.* **1999**, *182*, 285; d) T. Hayashi, A. Kishida, N. Mizuno, *Chem. Commun.* **2000**, 381.

[3] a) J. Canny, A. Tézé, R. Thouvenot, G. Hervé, *Inorg. Chem.* **1986**, *25*, 2114; b) A. Tézé, G. Hervé, *Inorg. Synth.* **1990**, *27*, 85.

[4] The protonated derivative of $[SiW_{10}O_{36}]^{8-}$, $[SiW_{10}O_{34}(H_2O)_2]^{4-}$, exhibited efficient catalytic activity for olefin epoxidation with H_2O_2 as mentioned in Chapter III: a) K. Kamata, K. Yonehara, Y. Sumida, K. Yamaguchi, S. Hikichi, N. Mizuno, *Science* **2003**, *300*, 964; b) K. Kamata, Y. Nakagawa, K. Yamaguchi, N. Mizuno, *J. Catal.* **2004**, *224*, 224; c) N. Mizuno, K. Yamaguchi, K. Kamata, *Coord. Chem. Rev.* **2005**, *249*, 1944; d) K. Kamata, M. Kotani, K. Yamaguchi, S. Hikichi, N. Mizuno, *Chem. Eur. J.* in press; e) The computational study on the structural nature of $[SiW_{10}O_{34}(H_2O)_2]^{4-}$ has been reported recently: D. G. Musaev, K. Morokuma, Y. V. Geletii, C. L. Hill, *Inorg. Chem.* **2004**, *43*, 7702.

[5] a) J. Canny, R. Thouvenot, A. Tézé, G. Hervé, M. Leparulo-Loftus, M. T. Pope, *Inorg. Chem.* **1991**, *30*, 976; b) K. Wassermann, H.-J. Lunk, R. Palm, J. Fuchs, N. Steinfeldt, R. Stösser, M. T. Pope, *Inorg. Chem.* **1996**, *35*, 3273; c) X.-Y. Zhang, C. J. O'Connor, G. B. Jameson, M. T. Pope, *Inorg. Chem.* **1996**, *35*, 30; d) C. Nozaki, I. Kiyoto, Y. Minai, M. Misono, N. Mizuno, *Inorg. Chem.* **1999**, *38*, 5724.

[6] a) U. Kortz, S. Isber, M. H. Dickman, D. Ravot, *Inorg. Chem.* **2000**, *39*, 2915; b) U.

Kortz, S. Matta, *Inorg. Chem.* **2001**, *40*, 815; c) U. Kortz, Y. P. Jeannin, A. Tézé, G. Hervé, S. Isber, *Inorg. Chem.* **1999**, *38*, 3670.

[7] Examples of homogeneous and heterogeneous systems: a) T. Katsuki, K. B. Sharpless, *J. Am. Chem. Soc.* **1980**, *102*, 5974; b) M. Bonchio, S. Calloni, F. D. Furia, G. Licini, G. Modena, S. Moro, W. A. Nugent, *J. Am. Chem. Soc.* **1997**, *119*, 6935; c) R. D. Oldroyd, J. M. Thomas, G. Sankar, *Chem. Commun.* **1997**, 2025; d) A. Sanjuán, M. Alvaro, A. Corma, H. García, *Chem. Commun.* **1999**, 1641; e) K. Matsumoto, Y. Sawada, B. Saito, K. Sakai, T. Katsuki, *Angew. Chem. Int. Ed.* **2005**, *44*, 4935.

[8] Review articles: a) B. Notari, *Adv. Catal.* **1996**, *41*, 253; b) P. Wu, T. Tatsumi, *Catal. Surv. Asia* **2004**, *8*, 137.

[9] H_2O_2-based catalytic oxidation activities of some Ti-substituted Keggin compounds have been investigated: a) F. Gao, T. Yamase, H. Suzuki, *J. Mol. Catal., A* **2002**, *180*, 97; b) O. A. Kholdeeva, T. A. Trubitsina, R. I. Maksimovskaya, A. V. Golovin, W. A. Neiwert, B. A. Kolesov, X. López, J. M. Poblet, *Inorg. Chem.* **2004**, *43*, 2284; c) C. N. Kato, S. Negishi, K. Yoshida, K. Hayashi, K. Nomiya, *Appl. Catal. A* **2005**, *292*, 97.

[10] F. Hussain, B. S. Bassil, L-H. Bi, M. Reicke, U. Kortz, *Angew. Chem. Int. Ed.* **2004**, *43*, 3485.

[11] a) CrystalClear 1.3.5 SP2: Rigaku and Rigaku/MSC; b) J. W. Pflugrath, *Acta Crystallogr.* **1999**, *D55*, 1718–1725.

[12] Z. Otwinowski, W. Minor, *Processing of X-ray Diffraction Data Collected in Oscillation Mode, Methods in Enzimology, Vol 276* (Eds: Carter, C. W., Jr.; Sweet, R. M.), Academic Press, New York, **1997**, pp. 307–326.

[13] CrystalStructure 3.7.0: Crystal Structure Analysis Package, Rigaku and Rigaku/MSC.

[14] L. J. Farrugia, *J. Appl. Cryst.* **1999**, *32*, 837–838.

[15] P. T. Beurskens, G. Admiraal, G. Beurskens, W. P. Bosman, R. de Gelder, R. Israel, J. M. M. Smits, *The DIRDIF-99 program system, Technical Report of the Crystallography Laboratory*, University of Nijmegen, Netherlands, **1999**.

[16] P. T. Beurskens, G. Admiraal, G. Beurskens, W. P. Bosman, S. Garcia-Granda, R. O. Gould, J. M. M. Smits, C. Smykalla, *The DIRDIF program system, Technical Report of the Crystallography Laboratory*, University of Nijmegen, Netherlands, **1992**.

[17] G. M. Sheldrick, SHELX97, Programs for Crystal Structure Analysis (Release 97 –

2), University of Göttingen, Göttingen (Germany), **1997**.

[18] Di-titanium substituted Keggin compound: K. Nomiya, M. Takahashi, J. A. Widegren, T. Aizawa, Y. Sakai, N. C. Kasuga, *J. Chem. Soc., Dalton Trans.* **2002**, 3679.

[19] Tri-titanium substituted Keggin compounds: a) Y. Lin, T. J. R. Weakley, B. Rapko, R. G. Finke, *Inorg. Chem.* **1993**, *32*, 5095; b) T. Yamase, T. Ozeki, H. Sakamoto, S. Nishiya, A. Yamamoto, *Bull. Chem. Soc. Jpn.* **1993**, *66*, 103; c) K. Nomiya, M. Takahashi, K. Ohsawa, J. A. Widegren, *J. Chem. Soc., Dalton Trans.* **2001**, 2872.

[20] Mono-substituted Keggin compound with dimeric structure: O. A. Kholdeeva, G. M. Maksimov, R. I. Maksimovskaya, L. A. Kovaleva, M. A. Fedotov, V. A. Grigoriev, C. L. Hill, *Inorg. Chem.* **2000**, *39*, 3828.

[21] Titanium-substituted Keggin compounds with monomeric structure: a) W. H. Knoth, P. J. Domaille, D. C. Roe, *Inorg. Chem.* **1983**, *22*, 198; b) T. Yamase, T. Ozeki, S. Motomura, *Bull. Chem. Soc. Jpn.* **1992**, *65*, 1453; c) P. J. Domaille, W. H. Knoth, *Inorg. Chem.* **1983**, *22*, 818; d) T. Ozeki, T. Yamase, *Acta Crystallogr., Sect. C* **1991**, *47*, 693.

[22] Titanium-substituted Wells-Dawson compounds: a) U. Kortz, S. S. Hamzeh, N. A. Nasser, *Chem. Eur. J.* **2003**, *9*, 2945; b) Y. Sakai, K. Yoza, C. N. Kato, K. Nomiya, *Chem. Eur. J.* **2003**, *9*, 4077; c) Y. Sakai, K. Yoza, C. N. Kato, K. Nomiya, *Dalton Trans.* **2003**, 3581; d) K. Nomiya, Y. Arai, Y. Shimizu, M. Takahashi, T. Takayama, H. Weiner, T. Nagata, J. A. Widegren, R. G. Finke, *Inorg. Chim. Acta* **2000**, *300–302*, 285.

[23] a) Y. Nakagawa, K. Uehara, N. Mizuno, *Inorg. Chem.* **2005**, *44*, 14; b) Y. Nakagawa, K. Kamata, M. Kotani, K. Yamaguchi, N. Mizuno, *Angew. Chem. Int. Ed.* **2005**, *44*, 5136; c) Y. Nakagawa, K. Uehara, N. Mizuno, *Inorg. Chem.* **2005**, *44*, 9068.

[24] a) G. B. Payne, P. H. Deming, P. H. Williams, *J. Org. Chem.* **1961**, *26*, 651; b) G. B. Payne, *Tetrahedron* **1962**, *18*, 763; c) S. Ueno, K. Yamaguchi, K. Yoshida, K. Ebitani, K. Kaneda, *Chem. Commun.* **1998**, 295.

[25] W. Adam, A. Corma, A. Martínez, C. M. Mitchell, T. I. Reddy, M. Renz, A. K. Smerz, *J. Mol. Catal. A* **1997**, *117*, 357.

[26] a) W. Adam, D. Golsch, *Chem. Ber.* **1994**, *127*, 1111; b) W. Adam, D. Golsch, *J. Org. Chem.* **1997**, *62*, 115; c) W. Adam, C. M. Mithcell, C. R. Saha-Möller, T. Selvam, O. Weichold, *J. Mol. Catal. A* **2000**, *154*, 251.

Chapter III

Oxygen Transfer Reaction with Hydrogen Peroxide

Catalyzed by Divacant Lacunary Polyoxometalate

3.1. Introduction

Epoxidation of olefins is an important reaction in the laboratory as well as the chemical industry,[1-3] because epoxides are widely used as raw materials for epoxy resins, paints, surfactants, and intermediates in organic syntheses. For example, over 5,000,000 and ~70,000 tons of propylene and butene oxides, respectively, are produced per year.[4] Although a number of epoxidation processes use various catalysts and oxidants, a chlorine-using non-catalytic process (the chlorohydrin process) and catalytic processes based on organic peroxides and peracids are still used extensively (Scheme 3-1).[5] These processes have disadvantages from the economical viewpoint because they are very capital intensive. Furthermore the chlorohydrin process has environmental disadvantages due to the large output of chloride laden sewage. The co-oxidation processes are environmentally acceptable, but the coupling of two products (propylene oxide and styrene or methyl *t*-butyl ether) is commercially undesirable.

In contrast to such classical processes, the catalytic epoxidation with H_2O_2 as an oxidant might offer some advantages because (i) it generates only water as a by-product and (ii) it has a high content of active oxygen species.[6-9] Although transition metal compounds such as metalloporphyrin,[10] titanosilicates,[11] methyltrioxorhenium,[12] tungsten compounds,[13-15] polyoxometalates,[16,17] manganese complexes,[18,19] and non-heme iron complexes[20,21] have been used as effective catalysts for homogeneous and heterogeneous epoxidation with H_2O_2, these systems have some disadvantages; the use of an excess amount of H_2O_2 and low pH in an aqueous phase in the case of the biphasic systems lead to the low efficiency of H_2O_2 utilization, selectivity to epoxides, especially for the water-soluble shorter-chain epoxides, and stereospecificity[10-21] or the kinds of olefins are limited, e.g., due to the small pore size of TS-1.[22] In these contexts, effective catalysts for epoxidation of a wide range of olefins with H_2O_2 are still desired.

The versatility and accessibility of polyoxometalates (POMs) have led to the various applications in the fields of structural chemistry, analytical chemistry, surface science, medicine, electrochemistry, and photochemistry.[23] Especially, the catalytic function of POMs has attracted much attention[24] because their acidic and redox properties can be controlled at atomic or molecular levels. Various catalytic systems for H_2O_2-based epoxidation catalyzed by POMs have been developed. These systems

can be classified into the following two groups according to the structural and mechanistic aspects of POMs (Scheme 3-2).[25]

(i) Catalyst precursors of peroxotungstate or peroxomolybdate species: The monomeric, dimeric, and tetrameric peroxo species are generated by the reaction of POMs with H_2O_2, and the peroxo species can catalyze the epoxidation. The POMs act as catalyst precursors.

(ii) Transition-metal-substituted polyoxometalates: Transition-metal-substituted POMs are oxidatively and hydrolytically stable, and various kinds of catalytically active site can be introduced. The sites influence the catalytic activity and selectivity for the epoxidation.

Polyoxo- and peroxo-tungstates are predominant among simple, soluble metal oxide salts for H_2O_2-based epoxidation, but are sometimes unsuitable for the production of acid-sensitive and/or water-soluble shorter-chain epoxides due to low pH in an aqueous phase. Although Fe, Mn, Co, Zn, Ni-substituted POMs exhibit the high turnover numbers, the efficiency of H_2O_2 utilization, selectivity to epoxides, and activity for the epoxidation of non-reactive terminal olefins should be improved.

The functionality of lacunary POMs as a catalyst precursor of polynuclear peroxo species is interesting because their vacant sites have the possibility to activate H_2O_2 catalytically.[26] In contrast to monomeric or dimeric peroxo species, polynuclear peroxo species are expected to show specific reactivity and selectivity due to the electronic and structural characters. A lacunary phosphotungstate, $Na_7PW_{11}O_{39}$, reacted with H_2O_2 to form tungsten fragments such as $[PO_4\{WO(O_2)_2\}_4]^{3-}$ and $[W_2O_3(O_2)_4(H_2O)_2]^{2-}$. On the other hand, silicotungstates are rather stable in water compared with phosphotungstates and the chemistry has been well established by Tézé and Hervé.[27] In addition, they consist of tungsten elements which are active for homogeneous epoxidation with H_2O_2.[25] While lacunary POMs have been used as precursors for various complexes such as transition-metal-substituted POMs and organic-inorganic hybrid materials,[28] the catalysis by lacunary POMs themselves is scarcely known. Therefore, the development of the epoxidation of olefins catalyzed by lacunary silicotungstates can attain a novel and remarkable oxidation system.

In this chapter, the lacunary Keggin-type silicodecatungstate of $[\gamma\text{-}SiW_{10}O_{34}(H_2O)_2]^{4-}$ (**4**, Figure 3-1), synthesized by the protonation of divacant

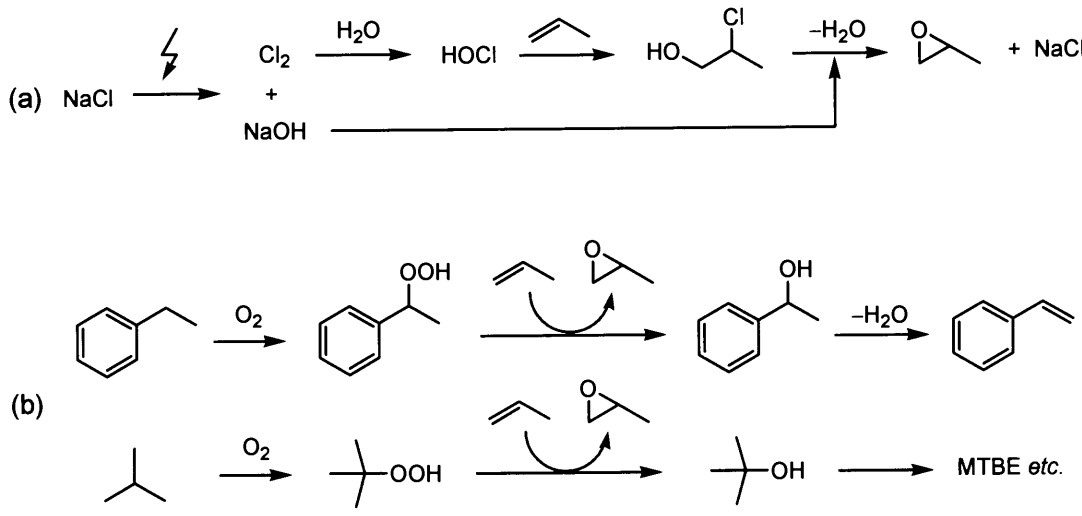

Scheme 3-1. (a) A chlorine-using non-catalytic process (the chlorohydrin process) and (b) catalytic processes based on organic peroxides for epoxidation of propylene.

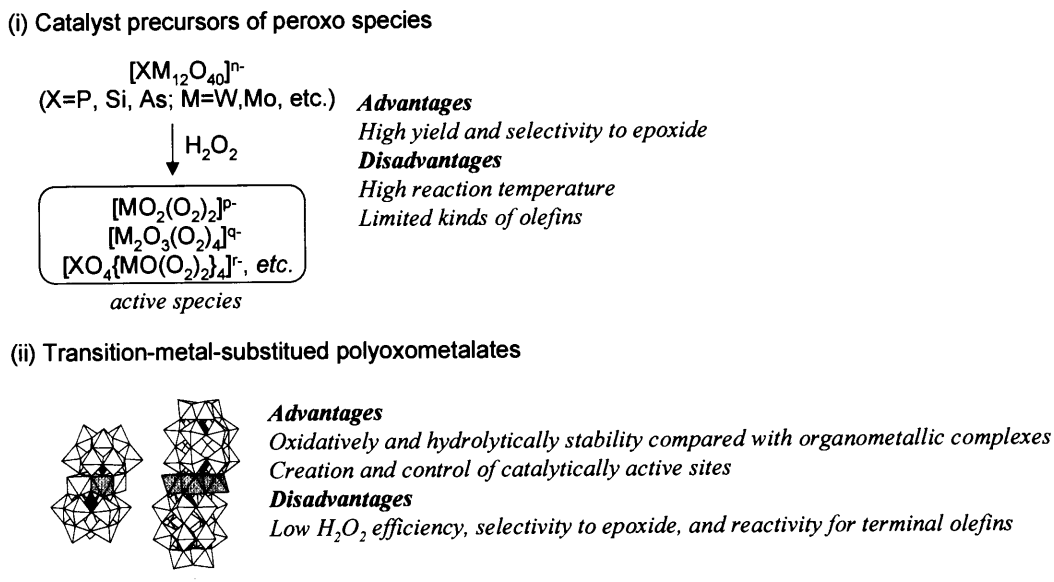

Scheme 3-2. Classification of POMs for H_2O_2-based epoxidation.

lacunary Keggin-type $[\gamma\text{-}SiW_{10}O_{36}]^{8-}$, is used as a catalyst precursor for epoxidation of olefins and oxidation of sulfides with H_2O_2 at 305 K [Eqs. (3-1) and (3-2)]. The catalytic epoxidation by **4** proceeded with ≥99% selectivity to epoxide, ≥99% efficiency of H_2O_2 utilization, high stereospecificity, and the easy recovery of the catalyst.[29]

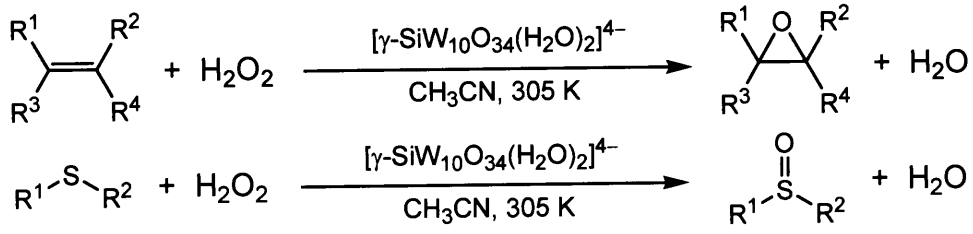

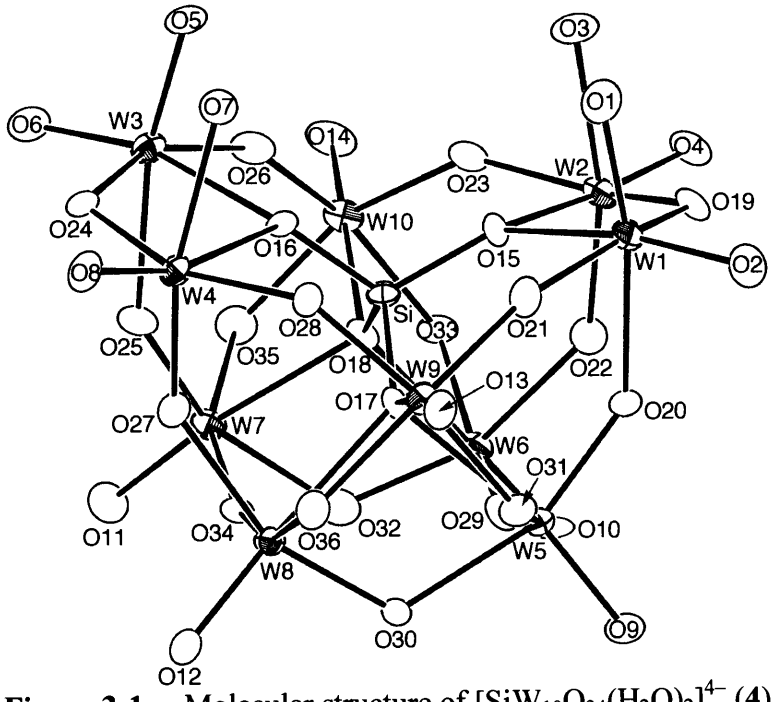

Figure 3-1. Molecular structure of $[SiW_{10}O_{34}(H_2O)_2]^{4-}$ (**4**).

3.2. Experimental

3.2.1. Instruments

IR spectra were measured on a Jasco FT/IR-460 spectrometer Plus using KBr disks. In situ IR spectra were measured on a Mettler Toledo React IR 4000 spectrometer. NMR spectra were recorded at 298 K on a JEOL JNM-EX-270 spectrometer (^{1}H, 270.0 MHz; ^{13}C, 67.80 MHz; ^{29}Si, 53.45 MHz; ^{183}W, 11.20 MHz). Chemical shifts (δ) were reported in ppm downfield from $SiMe_4$ (solvent, $CDCl_3$) for ^{1}H, ^{13}C, and ^{29}Si NMR spectra and Na_2WO_4 (solvent, D_2O) for ^{183}W NMR spectra. UV/Vis spectra were recorded on a Perkin Elmer Lambda 12 spectrometer. GC analyses were performed on Shimadzu GC-14B with a flame ionization detector equipped with a SE-30 packed column and GC-17A with a flame ionization detector equipped with a TC-WAX or a DB-WAX capillary column (internal diameter = 0.25 mm, length = 30 m). HPLC analyses were performed on Agilent 1100 series LC with a UV/Vis detector using a CAPCELL PAK MG C18-reverse phase column (5 μm × 3 mmϕ × 250 mm, SHISEIDO FINE CHEMICALS). Mass spectra were recorded on Shimadzu GCMS-QP2010 at an ionization voltage of 70 eV equipped with a DB-WAX capillary column (internal diameter = 0.25 mm, length = 30 m). CSI-MS spectra were recorded on a JMS-T100LC spectrometer. Typical measurements were as follows: Olifice voltage (90 V and −95 V for positive and negative ions, respectively), sample flow (0.05 $mL \cdot min^{-1}$), solvent ($ClCH_2CH_2Cl$), concentration (0.3 mM), spray temp. (263 K), and ion source temp. (room temp.).

3.2.2. Syntheses and Characterization of POMs

The Keggin-type silicotungstates of $K_4[\alpha\text{-}SiW_{12}O_{40}]\cdot 17H_2O$, $K_8[\beta_2\text{-}SiW_{11}O_{39}]\cdot 14H_2O$, $K_8[\gamma\text{-}SiW_{10}O_{36}]\cdot 12H_2O$, $K_8[\alpha\text{-}SiW_{11}O_{39}]\cdot 13H_2O$, $Na_{10}[\alpha\text{-}SiW_9O_{34}]\cdot$SOLVENT, and $[(n\text{-}C_4H_9)_4N]_4[\gamma\text{-}SiW_{12}O_{40}]$ and the peroxotungstates of $[(n\text{-}C_{12}H_{25})(CH_3)_3N]_2[W_2O_3(O_2)_4(H_2O)_2]$ and $[(n\text{-}C_6H_{13})_4N]_3[PO_4\{WO(O_2)_2\}_4]$ were synthesized by the same procedures.[27,30-32] The tetra-*n*-butylammonium salts of $[\alpha\text{-}SiW_{12}O_{40}]^{4-}$, $[\alpha\text{-}SiW_{11}O_{39}]^{8-}$, $[\alpha\text{-}SiW_9O_{34}]^{10-}$ were prepared by the cation exchange reaction of the alkali metal salts of the corresponding POMs in 1 M CH_3COOH/CH_3COONa buffer solution (pH = 4.7).

Tetra-*n*-Butylammonium Salt Derivative of 4 (TBA-4): The tetra-*n*-butylammonium salt derivative of $[\gamma\text{-}SiW_{10}O_{34}(H_2O)_2]^{4-}$ (TBA-**4**) was prepared by the cation exchange reaction. It has been reported that $[\gamma\text{-}SiW_{10}O_{36}]^{8-}$ was slowly changed to $[\beta_2\text{-}SiW_{12}O_{40}]^{4-}$ in strongly acidic aqueous solution (pH<1).[27,30] Therefore, pH value was adjusted during the synthesis of $[\gamma\text{-}SiW_{10}O_{36}]^{8-}$. $K_8[\gamma\text{-}SiW_{10}O_{36}]\cdot 12H_2O$ (6 g, 2 mmol) was dissolved in 60 mL of H_2O, and the pH of this aqueous solution was carefully adjusted to 2 with HNO_3. After stirring the solution for 15 min at room temperature, an excess amount of $[(n\text{-}C_4H_9)_4N]Br$ (6.46 g, 20 mmol) was added in a single step. The resulting white precipitate of TBA-**4** was collected by the filtration and then washed with an excess amount of H_2O. After the dryness, the crude product was purified twice with the precipitation method (addition of 1 L of H_2O into an CH_3CN solution of TBA-**4** (15 mL)). Analytically pure TBA-**4** was obtained as a white powder. Yield 3.4 g (54 %). Detailed data of TBA-**4**: ^{29}Si NMR (53.45 MHz, CD_3CN/DMSO (2/1 *v/v*), 298 K): $\delta = -83.5$ ($\Delta\nu_{1/2}$ = 4.3 Hz); ^{183}W NMR (11.20 MHz, CD_3CN/DMSO (2/1 *v/v*): 298 K) $\delta = -95.7$ ($\Delta\nu_{1/2}$ = 3.3 Hz), −98.9 ($\Delta\nu_{1/2}$ = 3.3 Hz), −118.2 ($\Delta\nu_{1/2}$ = 4.0 Hz), −119.6 ($\Delta\nu_{1/2}$ = 4.0 Hz), and −195.7 ($\Delta\nu_{1/2}$ = 4.3 Hz) with an integrated intensity ratio of 1:1:1:1:1, respectively; UV/Vis (CH_3CN): λ_{max} (ε) = 275 nm (22000 $mol^{-1}dm^3cm^{-1}$); IR (KBr): ν = 999, 958, 920, 902, 877, 784, 745, 691, 565, 544 cm^{-1}; Raman: ν = 985, 910, 891, 797, 705, 661, 560, 386, 355 cm^{-1}; Positive ion MS (CSI, acetone): *m/z*: 3622.8 ($[(TBA)_5SiW_{10}O_{34}]^+$); Negative ion MS (CSI, acetone): *m/z*: 3137.7 ($[(TBA)_3SiW_{10}O_{34}]^-$); elemental analysis calcd (%) for $C_{64}H_{150}N_4O_{37}SiW_{10}$ ($[(n\text{-}C_4H_9)_4N]_4[\gamma\text{-}SiW_{10}O_{34}(H_2O)_2]\cdot H_2O$): C 22.09, H 4.19, N 1.64, Si 0.80, W 53.24; found: C 22.38, H 4.40, N 1.63, Si 0.82, W 53.53.

Tetra-*n*-Butylammonium Salt Derivative of Diperoxo Polyoxometalate of 5 (TBA-5): The tetra-*n*-butylammonium salt derivative of the diperoxo POM $[\gamma\text{-}SiW_{10}O_{32}(O_2)_2]^{4-}$, TBA-**4**, was isolated as follows: Acetonitrile solution (4 mL) containing tetra-*n*-butylammonium salt of TBA-**5** (0.344 g, 100 μmol) and 20 equiv. 30% aqueous H_2O_2 (2 mmol) with respect to TBA-**5** was vigorously stirred at 273 K. After 2 h, excess diethyl ether (100 mL) was added into the solution. The resulting precipitate was then filtered off, washed with diethyl ether (20 mL × 2), and dried in vacuo to afford 0.339 g (99% yield) of a white powder. ^{29}Si NMR (53.45 MHz,

CD_3CN, 263 K): $\delta = -83.96$ ($\Delta\nu_{1/2} = 0.9$ Hz); ^{183}W NMR (11.20 MHz, CD_3CN, 263 K): $\delta = -117.3$ ($\Delta\nu_{1/2} = 6.5$ Hz), -125.2 ($\Delta\nu_{1/2} = 5.6$ Hz), -146.9 ($\Delta\nu_{1/2} = 6.2$ Hz), -212.5 ($\Delta\nu_{1/2} = 6.6$ Hz), and -548.0 ($\Delta\nu_{1/2} = 12.4$ Hz) with an integrated intensity ratio of 1:1:1:1:1, respectively; IR (KBr): ν = 999, 958, 920, 902, 877, 784, 745, 691, 565, 544 cm^{-1}; Raman: ν = 911, 886, 841, 801, 779, 748, 692, 649, 553, 539, 524, 510, 384 cm^{-1}; Positive ion MS (CSI, $ClCH_2CH_2Cl$): m/z = 3654.8 ($[(TBA)_5SiW_{10}O_{32}(O_2)_2]^+$); elemental analysis calcd (%) for $C_{64}H_{144}N_4O_{36}SiW_{10}$ ($[(n\text{-}C_4H_9)_4N]_4[\gamma\text{-}SiW_{10}O_{32}(O_2)_2]$): C 22.53, H 4.25, N 1.64, Si 0.82, W 53.88; found, C 21.82, H 4.35, N 1.54, Si 0.80, W 53.05.

$K_4[\alpha\text{-}SiW_{12}O_{40}]\cdot 17H_2O$: The potassium salt of silicododecatungstate, $K_4[\alpha\text{-}SiW_{12}O_{40}]\cdot 17H_2O$, was synthesized according to the literature procedure.[27] White crystal: 118 g (68% yield). UV/Vis (H_2O): λ_{max} (ε) = 263 nm (48000 $mol^{-1}dm^3cm^{-1}$); IR (KBr): ν = 1018, 978, 924, 894, 878, 787, 540, 478, 418 cm^{-1}.

$K_8[\beta_2\text{-}SiW_{11}O_{39}]\cdot 14H_2O$: The potassium salt of silicoundecatungstate, $K_8[\beta_2\text{-}SiW_{11}O_{39}]\cdot 14H_2O$, was prepared according to the literature procedure.[27] White powder: 47 g (29% yield). IR (KBr): ν = 946, 879, 859, 737, 539, 462 cm^{-1}.

$K_8[\gamma\text{-}SiW_{10}O_{36}]\cdot 12H_2O$: The potassium salt of silicodecatungstate, $K_8[\gamma\text{-}SiW_{10}O_{36}]\cdot 12H_2O$, was synthesized from the potassium salt of the β_2 isomer, $K_8[\beta_2\text{-}SiW_{11}O_{39}]\cdot 14H_2O$, according to the literature procedure.[27] White powder: 6 g (41% yield). ^{29}Si NMR (53.45 MHz, H_2O/D_2O (4/1 v/v), pH = 3.4, 298 K, TMS): $\delta = -84.91$; ^{183}W NMR (11.20 MHz, H_2O/D_2O (4/1 v/v), pH = 2.9, 298 K, Na_2WO_4): $\delta = -115.7$ ($\Delta\nu_{1/2} = 3.1$ Hz), -145.6 ($\Delta\nu_{1/2} = 2.0$ Hz), -176.9 ($\Delta\nu_{1/2} = 1.8$ Hz) with an integrated intensity ratio of 2:2:1; UV/Vis (H_2O): λ_{max} (ε) = 268 nm (22955 $mol^{-1}dm^3cm^{-1}$); IR (KBr): ν = 988, 942, 906, 866, 820, 745, 668, 598, 558, 530, 480, 444 cm^{-1}.

$Na_{10}[\alpha\text{-}SiW_9O_{34}]\cdot$SOLVENT: The sodium salt of siliconnonatungstate, $Na_{10}[\alpha\text{-}SiW_9O_{34}]\cdot$SOLVENT, was synthesized according to the literature procedure.[27] White powder: 72 g (56% yield). IR (KBr): ν = 982, 936, 864, 808, 706, 556, 528, 500, 486, 436 cm^{-1}.

$[(n\text{-}C_4H_9)_4N]_4[\gamma\text{-}SiW_{12}O_{40}]$: The tetra-$n$-butylammonium salt of $[\gamma\text{-}SiW_{12}O_{40}]^{4-}$ was synthesized according to the published method.[27] The crude product was purified by

recrystallization from acetonitrile/water (6/1 *v*/*v*). The IR spectrum was the same as that reported. IR (KBr): ν = 1006, 971, 910, 872, 839, 796, 768, 703, 553, 538, 522, 488, 461, 414 cm^{-1}; elemental analysis calcd (%) for $C_{64}H_{144}N_4O_{40}SiW_{12}$ ($[(n\text{-}C_4H_9)_4N]_4SiW_{12}O_{40}$): C 20.0, H 3.78, N 1.46; found, C 19.9, H 3.61, N 1.39.

$[(n\text{-}C_6H_{13})_4N]_3[PO_4\{WO(O_2)_2\}_4]$: This compound was synthesized according to the literature procedure.[31] Yield: 1.39 g (50%). ^{31}P NMR (109.25 MHz, CD_3CN, 298 K, H_3PO_4): δ = 4.48 ($^2J_{W\text{-}P}$ = 18.5 Hz); ^{183}W NMR (11.20 MHz, CD_3CN, 298 K, Na_2WO_4): δ = –587.2 ($^2J_{W\text{-}P}$ = 18.4 Hz); IR (KBr): 1093, 1055, 977, 913, 853, 843, 765, 728, 648, 591, 572, 548, 524, 443 cm^{-1}; positive ion MS (CSI, CH_3CN): *m/z*: 2569.0 $[\{(n\text{-}C_6H_{13})_4N\}_4PO_4\{WO(O_2)_2\}_4]^+$; elemental analysis calcd (%) for $C_{72}H_{156}N_3O_{24}PW_4$ ($[(n\text{-}C_6H_{13})_4N]_3[PO_4\{WO(O_2)_2\}_4]$): C 39.05, H 7.10, N 1.90, P 1.40, W 32.22; found: C 38.82, H 6.97, N 1.36, P 1.36, W 33.28.

$[(n\text{-}C_{12}H_{25})(CH_3)_3N]_2[W_2O_3(O_2)_4(H_2O)_2]$: This compound was synthesized by the modification of the reported method;[32] tetra-*n*-hexylammonium ($[(n\text{-}C_6H_{13})_4N]^+$) was replaced by *n*-dodecyltrimethylammonium ($[(n\text{-}C_{12}H_{25})(CH_3)_3N]^+$). The *n*-dodecyltrimethylammonium derivative was obtained in a 50% yield (1.3 g). IR (KBr), 963, 936, 911, 838, 770, 720, 603, 569, 531 cm^{-1}; Raman, 1069, 962, 852, 774, 633, 574, 315 cm^{-1}; positive ion MS (CSI, CH_3CN): *m/z*: 1230.0 $[\{(n\text{-}C_{12}H_{25})(CH_3)_3N\}_2W_2O_3(O_2)_4(H_2O)_2\}]^+$; elemental analysis calcd (%) for $C_{30}H_{68}N_2O_{11}W_2$ ($[(n\text{-}C_{12}H_{25})(CH_3)_3N]_2[W_2O_3(O_2)_4(H_2O)_2]$), C 34.35, H 7.00, N 2.70, W 35.48; found, C 35.53, H 6.92, N 2.66, W 35.43.

3.2.3. Catalytic Oxidation

Procedure for Catalytic Oxidation with Hydrogen Peroxide by TBA-4: The epoxidation of olefins, non-conjugated dienes, and allylic alcohols and oxidation of sulfides were carried out in a 30-mL glass vessel containing a magnetic stir bar. The reaction of gaseous substrates (propylene, 1-butene, and 1,3-butadiene) were carried out with Teflon coated autoclaves. Acetonitrile (Kanto Chemical, >99.5%) was dried and stored over molecular sieves 3A.[33] Substrates were purchased from TCI and Aldrich and used without further purification, except that non-conjugated dienes were purified by the standard procedure.[33] All products were identified by the comparison of GC retention time, mass spectra, and NMR spectra with those of the authentic samples and

the quantifications were carried out by calibrated GC analyses and/or ^{1}H NMR analyses. The carbon balance in each experiment was in the range of 95–100%. Remaining H_2O_2 after the reaction was estimated by potential difference titration of Ce^{3+}/Ce^{4+} (0.1 M of aqueous $Ce(NH_4)_4(SO_4)_4 \cdot 2H_2O$).[34] A typical procedure for the catalytic epoxidation of olefins was as follows: Catalyst containing 80 μmol of tungsten (i.e., TBA-**4**, 8 μmol; $(THA)_3[PO_4\{WO(O_2)_2\}_4]$, 20 μmol; $(DTMA)_2[W_2O_3(O_2)_4(H_2O)_2]$, 40 μmol), solvent ($CH_3CN$, 6 mL), substrate (5 mmol), and an internal standard (naphthalene) were charged in the reaction vessel. The reaction was initiated by the addition of 30% aqueous H_2O_2 (1 mmol). The reaction solution was periodically sampled and analyzed by NMR and GC in combination with mass spectroscopy.

Recycle Experiments: After the reaction, the catalyst was recovered by the evaporation to dryness followed by washing with diethyl ether. In the recycle experiments for epoxidation of cyclooctene with H_2O_2, the used catalyst could be recovered in a >95% yield for each experiments and the quantitative rate for each of the 5 recycle experiments was the same as that for the first run.

Isolation of Epoxide: The isolated yield of cyclooctene oxide was also determined as follows. An acetonitrile (12 mL) solution of reaction mixture (TBA-**4**, 16 μmol; cyclooctene, 10 mmol; H_2O_2, 2 mmol) was stirred at 305 K. The progress of reaction was monitored with the GC analysis and the reaction was terminated after 2 h by the addition of 25 mL of acetonitrile. The volume of the reaction mixture was reduced to 5–10 mL by the evaporation. *n*-Hexane (20 mL) and H_2O (20 mL) were added to this concentrated solution and the precipitated catalyst was removed by the filtration. The organic products solved in the water phase were extracted with *n*-hexane (20 mL × 2). Combined organic phase was washed with saturated aqueous NaCl and then dried over $CaCl_2$. The drying reagent was filtered off through a silica-gel column and the volatile was evaporated to give white solids of cyclooctene oxide (0.221 g, 88% yield).

Competitive Epoxidation of *Cis*- and *Trans*-2-Octenes: The conditions of the competitive epoxidation experiments for 2-octene of *cis*- versus *trans* isomers were as follows. For TBA-**4**: catalyst, 8 μmol; solvent (acetonitrile), 9 mL; oxidant (30% H_2O_2), 1 mmol; substrates (1:1 mixture of *cis* and *trans* isomers), 10 mmol; reaction temperature, 305 K. For $H_3PW_{12}O_{40}$: catalyst, 8 μmol; solvent ($CHCl_3$), 5 mL; oxidant (30% H_2O_2), 3 mmol; substrates (1:1 mixture of *cis* and *trans* isomers), 2 mmol;

reaction temperature, 333 K.

Syntheses of Thianthrene 5-Oxide and Its Oxidation Products: Thianthrene 5-oxide (SSO) was synthesized by the oxidation of thianthrene using HNO_3 according to the reported procedure.[35a] *cis*-Thianthrene 5,10-dioxide (*cis*-SOSO) and *trans*-thianthrene 5,10-dioxide (*trans*-SOSO) were synthesized by the oxidation of SSO using H_2O_2/HCl, and thianthrene 5,5-dioxide (SSO_2) was synthesized by the oxidation of SSO using $KMnO_4$ as previously reported.[35b] Thianthrene 5,5,10-trioxide ($SOSO_2$) was synthesized by the oxidation of SSO_2 catalyzed by TBA-**4** with H_2O_2. The oxidation of SSO_2 was carried out under the following conditions: TBA-**4** (5 μmol), SSO_2 (100 μmol), 30% aqueous H_2O_2 (150 μmol), reaction temperature (298 K), reaction time (24 h). SSO: ^{1}H NMR (270 MHz, $CDCl_3$, 298 K, TMS): δ 7.44 (dt, 2H, J = 1.2, 7.6 Hz), 7.54 (dt, 2H, J = 1.2, 7.6 Hz), 7.62 (dd, 2H, J = 1.2, 7.6 Hz), 7.92 (dd, 2H, J = 1.2, 7.6 Hz); ^{13}C {^{1}H} NMR (67.5 MHz, $CDCl_3$, 298 K, TMS): δ = 124.3, 128.2, 128.8, 129.7, 141.2; elemental analysis calcd (%) for $C_{12}H_8OS_2$: C 62.04, H 3.47; found: C 61.92, H 3.65. SSO_2: ^{1}H NMR (270 MHz, $CDCl_3$, 298 K, TMS): δ = 7.50–7.59 (m, 4H), 7.63–7.68 (m, 2H), 8.19–8.25 (m, 2H); ^{13}C {^{1}H} NMR (67.5 MHz, $CDCl_3$, 298 K, TMS): δ = 125.5, 127.7, 128.7, 132.0, 135.1, 135.3. *cis*-SOSO: ^{1}H NMR (270 MHz, $CDCl_3$, 298 K, TMS): δ = 7.69–7.76 (m, 4H), 8.04–8.11 (m, 4H); ^{13}C {^{1}H} NMR (67.5 MHz, $CDCl_3$, 298 K, TMS): δ = 123.7, 130.8, 138.4. *trans*-SOSO: ^{1}H NMR (270 MHz, $CDCl_3$, 298 K, TMS): δ = 7.63–7.70 (m, 4H), 8.08–8.14 (m, 4H); ^{13}C {^{1}H} NMR (67.5 MHz, $CDCl_3$, 298 K, TMS): δ = 127.8, 131.4, 142.8. $SOSO_2$: ^{1}H NMR (270 MHz, $CDCl_3$, 298 K, TMS): δ = 7.67–7.73 (m, 2H), 7.73–7.84 (m, 2H), 8.12–8.21 (m, 4H); ^{13}C {^{1}H} NMR (67.5 MHz, $CDCl_3$, 298 K, TMS): δ = 125.0, 126.1, 130.7, 133.0, 134.1, 147.8.

Procedure for Oxidation of Thianthrene 5-Oxide: The oxidation products were quantitatively analyzed by HPLC: CAPCELL PAK MG C18-reverse phase column (5 μm × 3 mmϕ × 250 mm, SHISEIDO FINE CHEMICALS), eluent (CH_3OH:CH_3CN:H_2O = 60:15:25), flow rate (0.4 mL/min), column temperature (30 °C), detection at λ = 254 nm, retention times (3.57, 4.69, 4.93, 5.72, 7.73, and 10.7 min for *trans*-thianthrene 5,10-dioxide (SOSO), thianthrene 5,5,10-trioxide ($SOSO_2$), *cis*-SOSO, thianthrene 5,5-dioxide (SSO_2), SSO, and naphthalene (internal standard), respectively).

The reaction conditions (i.e., concentration of substrate, substrate to oxidant ratio, reaction temperature, etc.) were controlled to minimize overoxidation to $SOSO_2$ and then to estimate true electronic nature of the oxidant.[35c] The X_{SO} value was calculated according to the following equation reported,[35c] X_{SO} = (nucleophilic oxidation)/(total oxidation) = $(SSO_2 + SOSO_2)/(SSO_2 + SOSO + 2SOSO_2)$.

3.2.4. ^{18}O-Labeling experiments

$H_2{}^{18}O_2$ (>90% enriched, 2.2% solution in $H_2{}^{18}O$) was obtained from Isotec. $H_2{}^{18}O$ (97.4% ^{18}O enriched) was obtained from MSD Isotopes. $H_2{}^{16}O_2$ (2.2% solution in $H_2{}^{18}O$) was prepared by dilution of concentrated $H_2{}^{16}O_2$ (>95%) with $H_2{}^{18}O$. The ratio of ^{18}O-labeled epoxide to total epoxide for the epoxidation of cyclooctene with TBA-**5** in the presence of $H_2{}^{18}O_2$ was determined by GC-MS analyses. The compound after the reaction of TBA-**5** with $H_2{}^{18}O_2$ (in $H_2{}^{18}O$) was recovered as follows: Acetonitrile solution (260 μL) containing TBA-**5** (4.9 mg, 1.4 μmol) and 2.2% $H_2{}^{18}O_2$ (in $H_2{}^{18}O$, 60 equiv. with respect to TBA-**5**) was vigorously stirred at room temperature. After 10 min, the solution was evaporated and dried in vacuo to afford a white powder.

3.2.5. Kinetic Derivations

The compound TBA-**4** reacts with H_2O_2 to form the diperoxo species of TBA-**5** according to Eq. (3-3). The reaction of TBA-**5** with water did not lead to the formation of TBA-**4**, showing that Eq. (3-3) is irreversible under the present conditions. The diperoxo species of TBA-**5** reacts with H^+ donor such as H_2O_2 to form a reactive species TBA-**6** according to Eq. (3-4).

$$\text{TBA-}\mathbf{4} + 2H_2O_2 \longrightarrow \text{TBA-}\mathbf{5} + 4H_2O \qquad (3\text{-}3)$$

$$\text{TBA-}\mathbf{5} + H^+\text{ donor } (H_2O_2) \overset{K_1}{\rightleftharpoons} \text{TBA-}\mathbf{6} \qquad (3\text{-}4)$$

The reactions in the catalytic cycle consitst of the oxygen tranfer step to olefin from TBA-**6** [Eq. (3-5)] and the regeneration step of TBA-**6** by the reaction of TBA-**7**, where one peroxo oxygen in TBA-**6** is transfered to olefin, with H_2O_2 [Eq. (3-6)].

$$\text{TBA-}\mathbf{6} + \text{olefin} \xrightarrow{k_1} \text{TBA-}\mathbf{7} + \text{epoxide} + H_2O \qquad (3\text{-}5)$$

$$\text{TBA-}\mathbf{7} + H_2O_2 \xrightarrow{k_2} \text{TBA-}\mathbf{6} + H_2O \qquad (3\text{-}6)$$

The concentration of TBA-**6** is expressed by Eq. (3-7). As mentioned in the text, the ^{29}Si and ^{183}W NMR spectra of the isolated TBA-**5** were intrinsically unchanged by addition of excess H_2O_2, suggesting that the equilibrium constant K_1 would be very small. Therefore, initial concentration of TBA-**4** is given by Eq. (3-8).

$$[\text{TBA-}\mathbf{6}] = K_1[\text{TBA-}\mathbf{5}][\text{H}^+ \text{ donor } (\text{H}_2\text{O}_2)] \quad (3\text{-}7)$$

$$[\text{TBA-}\mathbf{4}]_{int} = ([\text{TBA-}\mathbf{5}] + [\text{TBA-}\mathbf{6}] + [\text{TBA-}\mathbf{7}]) \sim [\text{TBA-}\mathbf{5}] \quad (3\text{-}8)$$

When the oxygen tranfer step is rate-determing step, the reaction rate (R_0) is expressed by Eq. (3-9) [Eqs. (3-5), (3-7), and (3-8)]. When the regeneration step is rate-determing step, the concentration of TBA-**6** nealy equals to that of TBA-**7**, R_0 is expressed by Eq. (10) [from Eqs. (3-6)–(3–8)].

$$R_0 = k_1[\text{TBA-}\mathbf{6}][\text{olefin}] = k_1K_1[\text{TBA-}\mathbf{4}]^1[\text{H}^+ \text{ donor } (\text{H}_2\text{O}_2)]^1[\text{olefin}]^1 \quad (3\text{-}9)$$

$$[\text{TBA-}\mathbf{6}] \sim [\text{TBA-}\mathbf{7}] \ll [\text{TBA-}\mathbf{5}]$$

$$R_0 = k_2[\text{TBA-}\mathbf{7}][\text{H}_2\text{O}_2] = k_2K_1[\text{TBA-}\mathbf{4}]^1[\text{H}^+ \text{ donor } (\text{H}_2\text{O}_2)]^1[\text{H}_2\text{O}_2]^1[\text{olefin}]^0 \quad (3\text{-}10)$$

3.2.6. X-ray Crystallography

Colorless single crystals of tetramethylammonium salt derivative of **4** were synthesized according to the procedure for the synthesis of the corresponding tetra-*n*-butylammonium derivative. An aqueous solution (60 mL) of $K_8[\gamma\text{-}SiW_{10}O_{36}]\cdot 12H_2O$ (6 g, 2 mmol), was adjusted to pH = 2 and stirred for 15 min. Then an excess amount of $[(CH_3)_4N]Cl$ (2.27 g, 20 mmol) was added to the solution in a single step. The resulting white precipitate was recrystallized from H_2O to give appropriate single crystals suitable for X-ray analysis. IR (KBr, cm^{-1}): 1000, 957, 918, 894, 872, 780, 710, 637, 599, 566, 544, 491, 455, 406; UV/Vis (H_2O): λ_{max} = 270 (21865 $mol^{-1}dm^3cm^{-1}$); elemental analysis calcd (%) for $C_{16}H_{84}N_4O_{44}SiW_{10}$ ($[(CH_3)_4N]_4[\gamma\text{-}SiW_{10}O_{34}(H_2O)_2]\cdot 8H_2O$): C 6.66, H 2.37, N 1.94, Si 0.97, W 63.67; found: C 6.63, H 2.36, N 1.98, Si 0.93, W 63.33.

Diffraction measurement was made on a Rigaku RAXIS-IV imaging plate area detector with graphite monochromated Mo Kα radiation (λ = 0.71069 Å). Indexing was performed from three oscillation images which were exposed for 5 min. The crystal-to-detector distance was 110 mm. Data collection parameters were as follows:

the oscillation range, 6°; number of oscillation images, 30; and exposed time, 40 min. The data collections were carried out at 213 K. Readout was performed with a pixel size of 100 μm × 100 μm. The data processing was performed on an IRIS Indy computer. A structure analysis was performed on an IRIS O2 computer using the teXsan structure-solving program package.[36] Neutral scattering factors were obtained from the standard source.[37] In the reduction of data, Lorentz and polarization corrections were made. The structure was solved by combination of the direct method (SIR 92) and Fourier synthesis (DIRDIF).[38,39] Least-squares refinements were carried out using SHELXL-97 linked to teXsan.[40] All of the non-hydrogen atoms were refined anisotropically. Crystal Data for $((CH_3)_4N)_4\cdot$**4**: $C_{16}H_{68}O_{40}N_4W_{10}Si$; MW = 2813.22, monoclinic, space Group, $P2_1/n$(#14), a = 11.6628(6) Å, b = 22.2522(8) Å, c = 21.669(1) Å, β = 91.676(1)°, V = 5621.2(5) Å^3, Z = 4, ρcalcd. = 3.324 g/cm^3, μ (Mo Kα) = 205.11, R1 = 0,056 (on F^2) for the unique 8791 data with I > 2.0σ(I) (wR2 = 0.154 for all data) and 674 parameters used for refinement.

3.3. Results and Discussion

3.3.1. Epoxidation of Mono-Olefins and Oxidation of Sulfides

3.3.1.1. Effect of Catalyst

First, the epoxidation of 1-octene with H_2O_2 catalyzed by a series of silicotungstates in acetonitrile at 305 K was examined (Table 3-1). The silicotungstates, $[\alpha\text{-}SiW_9O_{34}]^{10-}$, $[\gamma\text{-}SiW_{10}O_{36}]^{8-}$, $[\alpha\text{-}SiW_{11}O_{39}]^{8-}$, and $[\alpha\text{-}SiW_{12}O_{40}]^{4-}$ were converted to the corresponding tetra-*n*-butylammonium salts by the cation exchange reactions in 1 M CH_3COOH/CH_3COONa buffer solution (pH = 4.7). A divacant lacunary silicodecatungstate, $[\gamma\text{-}SiW_{10}O_{36}]^{8-}$, showed moderate catalytic activity, whereas the other *mono*- and *tri*-vacant lacunary compounds, $[\alpha\text{-}SiW_{11}O_{39}]^{8-}$ and $[\alpha\text{-}SiW_9O_{34}]^{10-}$, as well as a fully occupied silicododecatungstate, $[\alpha\text{-}SiW_{12}O_{40}]^{4-}$, were almost inactive (entries 3–6). The epoxidation did not proceed without catalysts (entry 2). The catalytic activity of $[\gamma\text{-}SiW_{10}O_{36}]^{8-}$ depended on the pH values upon the

Table 3-1. Epoxidation of 1-octene under various reaction conditions[a]

entry	catalyst	oxidant	solvent	yield (%)	selectivity to epoxide (%)	H_2O_2 efficiency (%)
1	TBA-**4**	H_2O_2	acetonitrile	90	99	>99
2	without	H_2O_2	acetonitrile	<1	–	–
3[b]	$[\alpha\text{-}SiW_{12}O_{40}]^{4-}$	H_2O_2	acetonitrile	<1	–	–
4[b]	$[\gamma\text{-}SiW_{12}O_{40}]^{4-}$	H_2O_2	acetonitrile	<1	–	–
5[b]	$[\alpha\text{-}SiW_{11}O_{39}]^{8-}$	H_2O_2	acetonitrile	<1	–	–
6[b]	$[\alpha\text{-}SiW_9O_{34}]^{10-}$	H_2O_2	acetonitrile	<1	–	–
7[c]	$[W_2O_3(O_2)_4(H_2O)_2]^{2-}$	H_2O_2	acetonitrile	25	>99	99
8[d]	$[PO_4\{WO(O_2)_2\}_4]^{3-}$	H_2O_2	acetonitrile	38	>99	92
9	TBA-**4**	TBHP	acetonitrile	<1	–	–
10	TBA-**4**	CHP	acetonitrile	<1	–	–
11	TBA-**4**	H_2O_2	benzonitrile	86	96	95
12	TBA-**4**	H_2O_2	1,2-dichloroethane	71	97	82
13	TBA-**4**	H_2O_2	*n*-butyronitrile	54	98	82
14	TBA-**4**	H_2O_2	acetone	25	99	84
15	TBA-**4**	H_2O_2	chloroform	4	99	11
16	TBA-**4**	H_2O_2	benzene	<1	–	–
17	TBA-**4**	H_2O_2	*n*-hexane	<1	–	–
18	TBA-**4**	H_2O_2	*tert*-butyl alcohol	<1	–	–
19	TBA-**4**	H_2O_2	methanol	<1	–	–
20	TBA-**4**	H_2O_2	dimethylsulfoxide	<1	–	–
21	TBA-**4**	H_2O_2	*N,N*-dimethylformamide	<1	–	–
22[e]	TBA-**4** + imidazole	H_2O_2	acetonitrile	2	>99	95
23[f]	TBA-**4** + pyridine	H_2O_2	acetonitrile	6	>99	>99

[a] Reaction conditions: Catalyst (8 μmol), 1-octene (5 mmol), oxidant (1 mmol), acetonitrile (6 mL), 305 K. Yield and selectivity were determined by GC. Remaining hydrogen peroxide after reaction was estimated by potential difference titration of Ce^{3+}/Ce^{4+} (0.1 M of aqueous $Ce(NH_4)_4(SO_4)_4 \cdot 2H_2O$). Carbon balance for each reaction was greater than 95%. Yield (%) = products (mol)/H_2O_2 used (mol) × 100. H_2O_2 efficiency (%) = products (mol)/consumed H_2O_2 (mol) × 100. [b] Tetra-*n*-butylammonium salt (8 mmol). [c] Dodecyltrimethylammonium salt (40 μmol). [d] Tetra-*n*-hexylammonium salt (20 μmol). [e] Imidazole (16 μmol) was added. [f] Pyridine (16 μmol) was added.

preparation of the corresponding tetra-*n*-butylammonium salts; the catalyst prepared at pH = 2 (TBA-**4**) exhibited the highest activity: Yields after 6 h; 75% (pH = 2) > 52% (pH=1) > 51% (pH = 3, 4) > 32% (pH=0). The compound $[PO_4\{WO(O_2)_2\}_4]^{3-}$ might be protonated by addition of small amount (< 3 equiv. of the compound) of $HClO_4$, as was confirmed by downfield shift of the ^{31}P NMR signal. Further addition of H^+ (over 3 equiv.) resulted in the decomposition of the structure. Therefore, epoxidation of 1-octene was carried out with 2 equiv. of $HClO_4$ added $[PO_4\{WO(O_2)_2\}_4]^{3-}$ catalyst. The yield of 1,2-epoxyoctene and selectivity were 32% and 98%, respectively, and approximately the same as those for non-protonated $[PO_4\{WO(O_2)_2\}_4]^{3-}$ catalyst (38% and >99%, respectively). Therefore, effects of proton were hardly observed for the epoxidation reactions catalyzed by $[PO_4\{WO(O_2)_2\}_4]^{3-}$ under the present conditions in contrast to TBA-**4**. The epoxidation with organic hydroperoxides such as TBHP and cumene hydroperoxide (CHP) did not proceed (entries 9 and 10), in accord with the report that tungsten compounds are not active for oxidation with organic hydroperoxides.[41]

The catalytic activity of TBA-**4** for the epoxidation of 1-octene was compared with peroxotungstates of $[PO_4\{WO(O_2)_2\}_4]^{3-}$ and $[W_2O_3(O_2)_4(H_2O)_2]^{2-}$ on the same loading of tungsten, which have been reported to be effective catalysts for the H_2O_2-based epoxidation.[6,7,9,13,14,15,31,32] In each case, the selectivity to 1,2-epoxyoctane was ≥99%, and TBA-**4** showed the highest activity among the catalysts (entries 1, 7, and 8).

3.3.1.2. Effect of Solvent

Acetonitrile was the most effective solvent (Table 3-1, entry 1). No stoichiometric formation of acetamide with respect to the epoxide was observed, showing that the epoxidation does not proceed via a peroxycarboximidic acid intermediate generated by the reaction of acetonitrile with H_2O_2.[42] Biphasic benzonitrile and 1,2-dichloroethane systems, and homogeneous *n*-butyronitrile and acetone systems gave 1,2-epoxyoctane selectively in moderate to good yields (entries 11–14). Chloroform, benzene, *n*-hexane, methanol, and *tert*-butyl alcohol, in which TBA-**4** was not soluble, were poor solvents (entries 15–19). *N,N*-Dimethylformamide and dimethylsulfoxide were also poor solvents although

TBA-**4** was soluble in these solvents (entries 20 and 21). The addition of only two equiv. imidazole and pyridine with respect to TBA-**4** strongly inhibited the epoxidation in acetonitrile (entries 22 and 23).

3.3.1.3. X-Ray Crystallographic Structure

X-ray crystallographic structural analysis of **4** was performed on a tetramethylammonium salt derivative, and the formulation of **4** could be determined as $[\gamma\text{-}SiW_{10}O_{34}(H_2O)_2]^{4-}$ involving two terminal W–(OH_2) (*aquo* ligand) fragments. Ten tungsten atoms are connected with a central SiO_4 unit, and the structure is classified as γ-Keggin type (Figure 1). The existence of four $(CH_3)_4N^+$ counter cations per **4** implied that the charge of **4** was identified to be –4. The bond valence sum values of tungsten (5.90 to 6.26) and silicon (3.98) indicated that the silicotungstate cluster of **4** was composed of W(VI) and Si(IV) ions.[43] Therefore, four protons are associated with the anionic cluster of **4** on the basis of the charge balance. The bond valence sum values of O3 (0.52) and O7 (0.54) were clearly different from those of the other oxygen atoms (1.58–2.11). Moreover, the bond lengths of W2–O3 and W4–O7 (2.16(1) and 2.14(1) Å, respectively) were notably long in comparison with those of other terminal W=O moieties (1.69(1) to 1.75(1) Å), and such W–O bond elongation was not observed in the previously reported structure of a non-protonated $[\gamma\text{-}SiW_{10}O_{36}]^{8-}$.[30] These observations indicate that two oxygen atoms at vacant sites (i.e., O3 and O7) are *di*-protonated resulting in aquo ligands. The ^{183}W NMR spectrum of TBA-**4** showed five resonance lines at –95.2, –98.8, –118.0, –119.1, –195.5 ppm with 1:1:1:1:1 relative intensities, supporting the structure of **4**.

3.3.1.4. Catalytic activity for Epoxidation of Mono-Olefins

For the oxygenation of *cis*- and *trans*-2-octenes, the configuration around the C=C moiety was retained in the corresponding epoxides. Moreover, *cis*-2-octene was oxygenated much faster than the *trans* isomer; in the competitive oxygenation of *cis*- and *trans*-2-octenes, the ratio of the formation rate of *cis*-2,3-epoxyoctane to that of *trans* isomer (= R_{cis}/R_{trans}) was 11.5. This value is higher than those for the other tungstate-H_2O_2 systems ($H_3PW_{12}O_{40}$: 3.7, $NH_2CH_2PO_3H_2/WO_4^{2-}$: 7.3[15]) and for the stoichiometric epoxidation with organic oxidants such as *m*-CPBA (1.2)[44] and

dimethyldioxirane (8.3).[45] Such a high stereospecific reactivity of TBA-**4** suggests the contribution of a structurally rigid, non-radical oxidant generated on TBA-**4** (probably at a divacant lacunary site).

TBA-**4** could be applicable to the epoxidation of various olefinic substrates (Table 3-2). Bulky cyclic olefins such as cyclopentene, cyclohexene, cyclohexene, 1-methyl-1-cyclohexene, cyclooctene, cyclododecene, and 2-norbornene were epoxidized with ≥99% selectivity and ≥99% efficiency of H_2O_2 utilization (entries 14–21). For some large pore titanium-containing zeolites, hydrolytic decomposition of oxirane rings of the epoxides takes place.[46-50] High yields and selectivity for the epoxidation of cyclooctene, *cis*-2-octene, and *cis*-3-octene were observed under the stoichiometric conditions (i.e., H_2O_2:olefin:TBA-**4** = 125:125:1) (entries 7, 9, and 20). 1,3-Butadiene was epoxidized selectively to give the corresponding mono-epoxide, without the successive epoxidation of the other C=C fragment (i.e., no diepoxide was formed). The most notable feature of the catalytic epoxidation with H_2O_2 mediated by TBA-**4** was that non-activated terminal $C_3 - C_8$ olefins such as propylene, 1-butene, 1-hexene, and 1-octene could be transformed to the corresponding epoxides specifically with high selectivity and efficiency of H_2O_2 utilization (entries 1, 2, 4, and 5). Large-scale experiments (100 fold scaled-up) for propylene and 1-octene showed the same results as for the small-scale experiments in Table 3-2. The decomposition of H_2O_2 to form molecular oxygen was negligible, which reduces the risk of building an explosive atmosphere and simplifying the safety measures needed to insure it. Thus, the catalytic performance of TBA-**4** raises the prospect of using this type of catalyst for the industrial epoxidation.

cis-β-Methylstyrene was converted to *cis*-β-methylstyrene oxide selectively, while a small amount of benzaldehyde was formed by the C=C bond cleavage for the epoxidation of sensitive styrene (entries 22 and 23). The epoxidation of (*1S*)-(−)-α-pinene was also carried out under the same conditions in Table 1. Various unknown by-products except for epoxide were produced (conversion based on, 84 %; epoxide yield, 31 %) and the present epoxidation system is not suitable for the production of acid-sensitive epoxides. These results are consistent with the estimation that H^+ would play an important role in the present epoxidation as mentioned later (section 3.3.3.).

Table 3-2. Epoxidation of various olefins catalyzed by TBA-**4** with H_2O_2[a]

entry	substrate	time (h)	yield (%)	selectivity to epoxide (%)	H_2O_2 efficiency (%)
1[b]	propylene	8	90	>99	>99
2[b]	1-butene	8	88	99	>99
3[b]	1,3-butadiene	9	91	99	99
4	1-hexene	12	80	99	94
5	1-octene	10	90	>99	>99
6[c]	*cis*-2-octene	3	>99	>99	>99
7[c,d]	*cis*-2-octene	10	77	95	89
8[c]	*cis*-3-octene	3	>99	>99	>99
9[c,d]	*cis*-3-octene	10	87	98	99
10[c]	*cis*-2-hexene	2	>99	>99	>99
11[e]	*trans*-2-octene	14	91	>99	99
12	2-methyl-1-pentene	10	98	99	98
13	2-methyl-2-pentene	8	>99	>99	>99
14	cyclopentene	3	>99	>99	>99
15	cyclohexene	6	84	>99	>99
16	cycloheptene	4	>99	>99	>99
17	1-methylcyclohexne	4	95	>99	99
18[f]	2-norbornene	4	>99	99	>99
19	cyclooctene	2	99	>99	>99
20[d]	cyclooctene	24	99	99	99
21[g]	cyclododecene	4	97	>99	>99
22[h]	styrene	12	70	84	98
23[c]	*cis*-β-methylstyrene	4	>99	98	99
24[i]	2-buten-1-ol	14	99	88	99
25[j]	3-methyl-2-buten-1-ol	5	>99	89	>99
26[k]	2-methyl-2-propen-1-ol	13	93	88	94
27[l]	geraniol	4	97	89	97
28[m]	geranyl acetate	8	98	>99	98

[a] Reaction conditions: TBA-**4** (8 μmol), substrate (5 mmol), 30% aqueous H_2O_2 (1 mmol), acetonitrile (6 mL), 305 K. Yield (%) = products (mol)/H_2O_2 used (mol) × 100. H_2O_2 efficiency (%) = products (mol)/consumed H_2O_2 (mol) × 100. [b] Propylene (6 atm), 1-butene (3 atm), 1,3-butadiene (2.5 atm). [c] Only *cis*-epoxide. [d] Olefin (1 mmol). [e] Only *trans*-epoxide. [f] Only *exo* epoxide. [g] Acetonitrile (9 mL). [h] Benzaldehyde (select. 16%) was formed. [i] Substrate: *cis*/*trans* (11/89), epoxy alcohol: *cis*/*trans* (30/70). 2-Butenal (select. 12%) was formed as a by-product. [j] 3-Methyl-2-butenal (select. 11%) was formed as a by-product. [k] 2-Methyl-2-propenal (select. 12%) was formed as a by-product. [l] Only 2,3-epoxide was formed. Geranial (select. 11%) was formed as a by-product. [m] Ratio of 2,3-epoxide to total epoxide was 0.12.

For the epoxidation of primary allylic alcohols, the corresponding epoxy alcohols were selectively obtained with small amounts of α,β-unsaturated aldehydes (entries 24–26). Geraniol was regioselectively epoxidized at the electron-deficient allylic 2,3-double bond without formation of the 6,7-epoxy alcohol (entry 27). On the other hand, geranyl acetate was selectively epoxidized at the electron-rich double bond to give the 6,7-epoxide (entry 28). The π(C=C) HOMO energies of 2-methyl-2-pentene, 3-methyl-2-buten-1-ol, and 3-methyl-2-butenyl acetate were calculated at the HF/6-311G(d,p) level and decreased in the order of 2-methyl-2-pentene (–8.97 eV) > 3-methyl-2-buten-1-ol (–9.25 eV) > 3-methyl-2-butenyl acetate (–9.71 eV). The electron-withdrawing substituents decrease the electron density of the C=C double bond and reduce the π(C=C) HOMO energy, resulting in the decrease of the reactivity of the olefin with electrophilic oxidants. The competitive epoxidation of 2-methyl-2-pentene, 3-methyl-2-buten-1-ol, and 3-methyl-2-butenyl acetate was carried out in order to confirm the template effect of the present epoxidation. The relative rate decreased in the order of 3-methyl-2-buten-1-ol (2.5) > 2-methyl-2-pentene (1.0) > 3-methyl-2-butenyl acetate (0.2). The reactivity order is not consistent with that of the π(C=C) HOMO energies, showing that the template effect reflects the reactivity of these olefins. The template effect was also observed for the epoxidation of geraniol and geranyl acetate. Similar regioselectivities for geraniol and geranyl acetate were observed for the epoxidation with hydrogen catalyzed by the peroxotungstates.[51]

3.3.1.5. Catalytic Activity for Oxidation of Sulfides

The present system also catalyzed the oxidation of sulfides with H_2O_2 (Table 3-3). It was confirmed that the oxidation of alkyl sulfide of methyl *n*-octyl sulfide and aryl sulfide of 1-methoxy-4-(methylthio)benzene did not proceed at all without catalysts under the present conditions. The oxidation of thioanisole proceeded with high selectivity and efficiency of H_2O_2 utilization even under the stoichiometric condition (Table 3-3, entry 2). Various kinds of sulfides were selectively oxidized to the corresponding sulfoxides with high efficiency of H_2O_2 utilization (entries 1–13). The reaction rates were affected by the electronic effects of the substituents on aromatic rings of aryl sulfides (entries 1–9). Not only aryl sulfides but also alkyl ones could be oxidized to the corresponding sulfoxides in excellent yields (entries 10 and 11).

Table 3-3. Oxidation of various sulfides catalyzed by TBA-**4** with H_2O_2[a]

entry	sulfide	time (h)	yield (%)	selectivity to sulfoxide (%)	H_2O_2 efficiency (%)
1	thioanisole	1	98	>99	98
2[b]	thioanisole	2	97	95	99
3	4-(methylthio)toluene	1	>99	>99	>99
4	4-chlorophenyl methyl sulfide	1	97	>99	97
5	4-bromothioanisole	1	>99	>99	>99
6	1-methoxy-4-(methylthio)benzene	1	98	>99	98
7	4-fluorothioanisole	1	95	>99	95
8	4-(methylthio)acetophenone	1	>99	>99	>99
9	4-(methylthio)benzonitrile	1	>99	>99	>99
10[c]	4-nitrothioanisole	1	93	>99	>99
11	ethyl *n*-propyl sulfide	2	84	>99	>99
12	methyl *n*-octyl sulfide	2	94	>99	>99
13	ethyl phenyl sulfide	2	94	>99	94
14	benzyl methyl sulfide	2	98	>99	98

[a] Reaction conditions: TBA-**4** (1.6 μmol), substrate (1 mmol), 30% aqueous H_2O_2 (0.2 mmol), acetonitrile (1.2 mL), 305 K. Yield (%) = products (mol)/H_2O_2 used (mol) × 100. H_2O_2 efficiency (%) = products (mol)/consumed H_2O_2 (mol) × 100. [b] Olefin (1 mmol). [c] Acetonitrile (2.4 mL).

3.3.1.6. Structural Stability

The structural stability of TBA-**4** was confirmed by observation of the reaction mixture with an *in-situ* IR spectrometer. No substantial changes of spectral pattern were observed during the catalytic epoxidation by TBA-**4** with H_2O_2. On the other hand, a mixture $H_3PW_{12}O_{40}$, H_2O_2, and olefin exhibited a drastic change of spectral pattern due to the conversion of $[PW_{12}O_{40}]^{3-}$ to $[PO_4\{WO(O_2)_2\}_4]^{3-}$. The contrast shows that a Si derivative of tetranuclear species (i.e., $[SiO_4\{WO(O_2)_2\}_4]^{4-}$) was not formed in the present catalytic system of TBA-**4**, H_2O_2, olefin, and acetonitrile. The kinetic study revealed the first-order dependence of the reaction rate on the concentration of TBA-**4** (0.36 to 3.81 mM), supporting the idea. Detailed mechanistic aspects of the present epoxidation system are described later (section 3.3.3.).

3.3.2. Epoxidation of Non-Conjugated Dienes

Intramolecular regioselectivity for the epoxidation of dienes that have two electronically and sterically inequivalent double bonds has much information on the active species. Generally, more electron-rich double bonds of dienes are preferably epoxidized when stoichiometric oxidants such as peroxyacids[52] and peroxides[53] or hydroperoxides in the presence of molybdenum compounds[54-56] are used. The effects of steric protection of catalysts for the regioselective epoxidation of non-conjugated dienes have been examined. For example, the highly regioselective epoxidation of more accessible, but less nucleophilic double bonds using sterically hindered metalloporphyrins with NaOCl and PhIO have been developed.[57-60] In contrast to these expensive oxidants, H_2O_2 is an attractive oxidant from the economical and environmental viewpoints because it generates only water as a by-product and has a high content of active oxygen species. Although various catalysts for the regioselective epoxidation of non-conjugated dienes with H_2O_2 have been studied,[10,61-74] the efficiency of H_2O_2 utilization and/or the regioselectivity are still low. Therefore, efficient systems for the regioselective epoxidation of dienes with H_2O_2 are previously unknown.

3.3.2.1. Comparison of Regioselectivity

Table 3-4 shows the epoxidation of various dienes with H_2O_2 in acetonitrile at 305 K catalyzed by TBA-**4**. Under the present reaction conditions, amounts of diepoxides and glycols produced through the hydrolysis were negligible in all cases. Under the stoichiometric conditions (1-methyl-1,4-cyclohexadiene/H_2O_2 molar ratio = 1:1), the total product yield was 61% and the diepoxide was formed. Therefore, the reaction condition in the high ratio of substrate to H_2O_2 was used. For the epoxidation of 1-methyl-1,4-cyclohexadiene (entry 1), the [4,5-epoxide]/[total epoxide] ratio was 0.89 and the more accessible double bond was much more selectively epoxidized. The value was higher than or comparable to those reported for sterically hindered porphyrin systems with NaOCl or PhIO (0.11–0.95)[58,60,75,76] and the mono-cobalt-substituted heteropolytungstate system with O_2 in the presence of aldehydes (0.69)[77] (Table 3-5).

For the epoxidation of *trans*-1,4-hexadiene (entry 2), the terminal double bond was preferably epoxidized. The [terminal epoxide]/[total epoxide] ratio was 0.61 and the

Table 3-4. Epoxidation of dienes catalyzed by TBA-**4** with H_2O_2[a]

entry	diene	time (h)	product (yield (%))	[less substituted epoxide] /[total epoxide]	H_2O_2 efficiency (%)
1		4	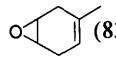 (83)  (10)	0.89	>99
2[b]	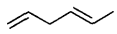	7	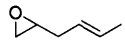 (43) 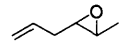 (27)	0.61	81
3[c]	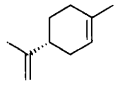	7	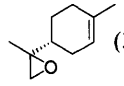 (34) 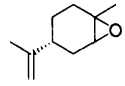 (55)	0.38	93
4	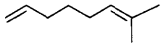	6	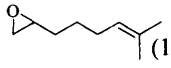 (16) 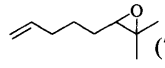 (78)	0.17	>99
5		4	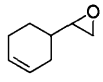 (4) 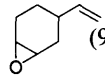 (94)	0.04	98

[a] Reaction conditions: TBA-**4** (8 μmol), diene (5 mmol), 30% aqueous H_2O_2 (1 mmol), acetonitrile (6 mL), reaction temperature (305 K). The reaction conditions were controlled to inhibit the double epoxidation. Yields were determined by gas chromatographic analysis with an internal standard technique. Yield (%) = product (mol) / H_2O_2 used (mol) × 100. Remaining H_2O_2 after the reaction was estimated by potential difference titration of Ce^{3+}/Ce^{4+}. H_2O_2 efficiency = products (mol) / H_2O_2 consumed × 100. [b] Toluene was produced as a by-product (7% yield). [c] Acetonitrile (9 mL).

Table 3-5. Comparison of regioselectivity for the epoxidation of 1-methyl-1,4-cyclohexadiene

system	[4,5 epoxide] /[total epoxide]
TBA-4/H_2O_2 (this work)	**0.89**
m-CPBA	0.08[a]
Mn(TPP)(OAc)/NAOCl/4'-(imidazol-1-yl)acetophenone	0.53[a]
Mn(TTMPP)(OAc)/NaOCl/4'-(imidazol-1-yl)acetophenone	0.70[a]
Mn(TTPPP)(OAc)/NaOCl/4'-(imidazol-1-yl)acetophenone	0.95[a]
$[MnT(3',5'\text{-}G2Ph)P]^+$/PhIO	0.55[b]
$[MnT(3',5'\text{-}G1Ph)P]^+$/PhIO	0.52[b]
$[MnT(2',4',6'\text{-}OMePh)P]^+$/PhIO	0.71[b]
$[MnT(2',4',6'G1AP)P]^+$/PhIO	0.74[b]
$[PW_{11}CoO_{39}]^{5-}$/isobutyraldehyde/O_2 (1 atm)	0.69[c]
m-CPBA	0.07[d]
MnCl(2,7,12,17-tetramethyl-3,8,13,18-tetra[2,6-bis(4-phenyl) -4-fluorophenyl]porphyrin)/NaOCl	0.11[d]
MnCl(2,7,12,17-tetramethyl-3,8,13,18-tetra[2,6-bis(4-phenyl) -4-fluorophenyl]porphyrin)/DMAP/NaOCl	0.33[d]

[a] K. S. Suslick, B. R. Cook, *J. Chem. Soc., Chem. Commun.* **1987**, 200. [b] P. Bhyrappa, J. K. Young, J. S. Moore, K. S. Suslick, *J. Am. Chem. Soc.* **1996**, *118*, 5708; R. Bhyrappa, J. K. Jeffrey, S. Moore, K. S. Suslick, *J. Mol. Catal. A* **1996**, *113*, 109. [c] N. Mizuno, M. Tateishi, T. Hirose, M. Iwamoto, *Chem. Lett.* **1993**, 1985. [d] T. Lai, S. K. Lee, L. Yeung, H. Liu, I. D. Williams, C. K. Chang, *Chem. Commun.* **2003**, 620.

value was much higher than those reported for $Mo(CO)_6$/CHP (0.14)[54] and sterically hindered porphyrin systems with NaOCl or PhIO; Mn(TTPPP)(OAc)/NaOCl (0.35),[60] Mn(T(2',6'-G1APh)P)Cl/PhIO (0.20),[52] Mn(TPP)(OAc)/NaOCl (0.03),[60] and Mn(T(3',5'-G2Ph)P)Cl/PhIO (0.03)[52] (Table 3-6).

The epoxidation of *R*-(+)-limonene (entry 3) easily proceeded to afford a mixture of diastereoisomeric epoxides and the [8,9-epoxide]/[total epoxide] ratio was 0.38. The value was higher than or comparable to those reported for the H_2O_2-based epoxidation; peroxotungstates (<0.03),[61,62,64,71] POMs (<0.01),[65,67] Fe(TDCPN$_5$P)Cl (0.27),[68] MTO/UHP (<0.01),[70] manganese complexes (0.17),[63] stoichiometric reactions such as dimethyldioxirane (<0.01),[53] *m*-CPBA (0.09),[52] benzonitrile/$KHCO_3$/H_2O_2 (0.37),[72] and diisopropylcarbodiimide/$KHCO_3$/H_2O_2 (0.18–0.40).[73,74] Although the regioselectivity for TBA-**4** is lower than the values, reported for sterically hindered porphyrin systems with NaOCl or PhIO (0.62–0.75)[52,60] and various H_2O_2-based systems of Mn(TDCPP)Cl/imidazole (0.59–0.67),[10] $[WZnMn_2(ZnW_9O_{34})_2]^{12-}$ (0.50),[66] and Ti-β (0.55),[69] these systems have ,disadvantages: The use of rather expensive, non-green oxidants such as NaOCl and PhIO, the necessity of excess amounts of oxidant, long reaction time, and high reaction temperature (Table 3-7).

Similarly, the high selectivity to the epoxidation of the electron-poor terminal double bond for the epoxidation of 7-methyl-1,6-octadiene (entry 4) was observed. The [terminal epoxide]/[total epoxide] ratio was 0.17 and the value was much higher than those for the H_2O_2-based epoxidation systems of Al_2O_3/H_2O_2 (<0.01),[78] CF_3CH_2OH/Na_2HPO_4/H_2O_2 (<0.01),[79] and $(CF_3)_2CO$/C_2F_5OH/$NaHPO_4$/H_2O_2 (<0.01) (Table 3-8).[80]

The epoxidation of 4-vinyl-1-cyclohexene (entry 5) proceeded exclusively at the ring position rather than the external position, and the [terminal epoxide]/[total epoxide] ratio of 0.04 was lower than those reported for sterically hindered porphyrin systems with NaOCl or PhIO (0.20–0.73)[58,59] and comparable to dendrimer-metalloporphyrins (0.04–0.11) (Table 3-9).[52] The results of competitive epoxidation of C_6-olefins that have the similar alkyl substituents to the corresponding dienes are in good agreement with the trends of regioselectivity for TBA-**4** (Table 3-10).

The regioselectivity for the epoxidation of various non-conjugated dienes in the

Table 3-6. Comparison of regioselectivity for the epoxidation of *trans*-1,4-hexadiene

system	[terminal epoxide] /[total epoxide]
TBA-4/H_2O_2 (this work)	**0.61**
$Mo(CO)_6$/CHP	0.14[a]
m-CPBA	0.02[b]
Mn(TPP)(OAc)/NaOCl/4'-(imidazol-1-yl)acetophenone	0.02[b]
Mn(TTMPP)(OAc)/NaOCl/4'-(imidazol-1-yl)acetophenone	0.04[b]
Mn(TTPPP)(OAc)/NaOCl/4'-(imidazol-1-yl)acetophenone	0.35[b]
$[MnT(3',5'\text{-}G2Ph)P]^+$/PhIO	0.03[c]
$[MnT(3',5'\text{-}G1Ph)P]^+$/PhIO	0.03[c]
$[MnT(2',4',6'\text{-}OMePh)P]^+$/PhIO	0.03[c]
$[MnT(2',4',6'G1AP)P]^+$/PhIO	0.12[c]

[a] M. N. Sheng, J. G. Zajacek, *J, Org. Chem.* **1970**, *35*, 1839. [b] K. S. Suslick, B. R. Cook, *J. Chem. Soc., Chem. Commun.* **1987**, 200. [c] P. Bhyrappa, J. K. Young, J. S. Moore, K. S. Suslick, *J. Am. Chem. Soc.* **1996**, *118*, 5708; R. Bhyrappa, J. K. Jeffrey, S. Moore and K. S. Suslick, *J. Mol. Catal. A* **1996**, *113*, 109.

Table 3-7. Comparison of regioselectivity for the epoxidation of *R*-(+)-limonene

system	[8,9-epoxide] /[total epoxide]
TBA-4/H_2O_2 (this work)	**0.38**
$[PO_4\{WO(O_2)_2\}_4]^{3-}/H_2O_2$	<0.03[a]
$[HPO_4\{WO(O_2)_2\}_2]^{2-}/H_2O_2$	<0.01[b]
$[Ph_3PCH_2Ph]_2[W_2O_{11}]/H_2O_2$	<0.01[c]
$[PO_4\{WO(O_2)_2\}_4]^{3-}$–amberlite/$H_2O_2$	0.03[d]
$[\alpha\text{-}P_2W_{17}O_{61}Mn(Br)]^{8-}$/PhIO	0.29[e]
$[WZnMn_2(ZnW_9O_{34})_2]^{12-}/H_2O_2$	0.50[f]
$[(Mn(H_2O)_3)_2(WO_2)_2(BiW_9O_{33})_2]^{10-}/H_2O_2$	<0.01[g]
$[(Mn(H_2O))_3(SbW_9O_{33})_2]^{12-}/H_2O_2$	<0.01[g]
$[(Mn(H_2O)_3)_2(Mn(H_2O)_2)_2(TeW_9O_{33})_2]^{8-}/H_2O_2$	<0.01[g]
$[PZnMo_2W_9O_{39}]^{5-}/H_2O_2$	<0.01[h]
$[PW_{11}CoO_{39}]^{5-}/(CH_3)_3CHCHO/O_2$ (1 atm)	0.32[i]
$[PW_{11}CoO_{39}]^{5-}$/isobutyraldehyde/O_2 (1 atm)	0.19[i]
Co(TPP)/$(CH_3)_3CHCHO/O_2$ (1 atm)	0.14[i]
$CoCl_2/(CH_3)_3CHCHO/O_2$ (1 atm)	0.09[i]
$[PW_{11}CoO_{39}]^{5-}$/PhIO	0.12[i]
benzonitrile/K_2CO_3/H_2O_2	0.37[j]
m-CPBA	<0.01[j]
2-nitrobenzenesulfonyl chloride/KO_2	<0.01[k]
FeTTPCl/PhIO	0.05[l]
FeTMPCl/PhIO	0.13[l]
m-CPBA	0.09[l]

Table 3-7. *(continued)*

system	[8,9-epoxide] /[total epoxide]
m-CPBA	0.09[m]
Mn(TPP)(OAc)/NAOCl/4'-(imidazol-1-yl)acetophenone	0.18[m]
Mn(TTMPP)(OAc)/NaOCl/4'-(imidazol-1-yl)acetophenone	0.33[m]
Mn(TTPPP)(OAc)/NaOCl/4'-(imidazol-1-yl)acetophenone	0.61[m]
Mn(TPP)Cl/PhIO	0.12[n]
Mn(TDCPP)Cl/PhIO	0.50[n]
Mn(TDCPP)Cl/PhIO/imidazole	0.59[n]
Mn(TDCPP)Cl/H_2O_2/imidazaole	0.59[n]
Mn(TDCPP)Cl/PhIO/1-methylimidazole	0.56[n]
Mn(TDCPP)Cl/H_2O_2/1-methylimidazole	0.53[n]
Mn(TDCPP)Cl/PhIO/2-methylimidazole	0.71[n]
Mn(TDCPP)Cl/H_2O_2/2-methylimidazole	0.67[n]
MoO_2Cl_2[3-(diethoxyphosphinyl)camphor]/TBHP	<0.01[o]
FeTTPCl/PhIO	0.05[p]
FeTMPCl/PhIO	0.13[p]
FeTTPPPCl/PhIO	0.75[p]
MnTTPPP(OAc)/PhIO	0.36[p]
m-CPBA	0.09[p]
MTO/UHP	<0.01[q]
MTO/H_2O_2	0.34[r]
Ti(O^iPr)$_4$-SiO_2/TBHP	<0.01[s]
[MnT(3',5'-G2Ph)P]$^+$/PhIO	0.38[t]
[MnT(3',5'-G1Ph)P]$^+$/PhIO	0.34[t]
[MnT(2',4',6'-OMePh)P]$^+$/PhIO	0.33[t]
[MnT(2',4',6'G1AP)P]$^+$/PhIO	0.58[t]
$RuCl_2(biox)_2$/isobutyraldehyde/$NaHCO_3$/O_2	<0.01[u]
Ti-β/H_2O_2	0.55[v]
dicyclohexylcarboimide/$KHCO_3$/H_2O_2	0.18–0.40[w]
Ru(TDCPP)(CO)(EtOH)/Cl_2pyNO/HCl	0.63[x]
Ru(TDCPP)(CO)(EtOH)-MCM-41/Cl_2pyNO/HCl	0.23[x]
I/PhIO	0.15[y]
II/PhIO	0.28[y]
III/PhIO	0.39[y]
IV/PhIO	0.43[y]
Mn-dmtacn-SiO_2/H_2O_2	0.17[z]
Mo(O*i*Pr)$_5$-SiO_2/THBP	0.06[aa]
[MoCl{(1*R*,2*S*,5*S*)-8-trimethylsilyloxyl-1-(2-pyridyl) mentholato}(O)$_2$(THF)]/TBHP	0.12[ab]
Fe(TDCPN$_5$P)Cl/PhIO	0.34[ac]
Fe(TDCPN$_5$P)Cl/H_2O_2	0.27[ac]
MnTPPS-PSMP/$NaIO_4$/imidazole	0.24[ad]
Mn-tmtacn /H_2O_2/CH_3COOH	0–0.67[ae]

Table 3-7. (*continued*)

system	[8,9-epoxide] /[total epoxide]
m-CPBA	0.01[af]
MnCl(2,7,12,17-tetramethyl-3,8,13,18-tetra [2,6-bis(4-phenyl)-4-fluorophenyl]porphyrin)/NaOCl	0.33[af]
MnCl(2,7,12,17-tetramethyl-3,8,13,18-tetra[2,6-bis (4-phenyl)-4-fluorophenyl]porphyrin)/DMAP/NaOCl	0.66[af]
Mn(TPP)Cl/O_2/Zn/1-methyl-imidazole/CH_3COOH	0.14[ag]
Mn(TPP)Cl/PhIO	0.13[ag]
dimthyldioxirane	<0.01[ah]

[a] S. Sakaguchi, Y. Nishiyama, Y. Ishii, *J. Org. Chem.* 1996, 61, 5307. [b] L. Salles, C. Aubry, R. Thouvenot, F. Robert, C. D. Morin, G. Chottard, H. Ledon, Y. Jeannin, J. M. Brégeault, *Inorg. Chem.* **1994**, *33*, 871. [c] J. Prandi, H. B. Kagan, H. Mimoun, *Tetrahedron Lett.* **1986**, *27*, 2617. [d] A. L. Villa de P, B. F. Sels, D. E. De Vos, P. A. Jacobs, *J. Org. Chem.* **1999**, *64*, 7267. [e] D. Mansuy, J. F. Bartoli, P. Battioni, D. K. Lyon, R. G. Finke, *J. Am. Chem. Soc.* **1991**, *113*, 7222. [f] R. Neumann, D. Juwiler, *Tetrahedron*, **1996**, *52*, 8781. [g] M. Bösing, A. Nöh, I. Loose, B. Krebs, *J. Am. Chem. Soc.* **1998**, *120*, 7252. [h] S. Tangestaninejad, B. Yadollahi, *Chem. Lett.* **1998**, 511. [h] S. Tangestaninejad, B. Yadollahi, *Chem. Lett.* **1998**, 511. [i] N. Mizuno, M. Tateishi, T. Hirose, M. Iwamoto, *Chem. Lett.* **1993**, 1985. [j] R. G. Carlson, N. S. Behn, C. Cowles, *J. Org. Chem.* **1971**, *36*, 3832. [k] Y. H. Kim, B. C. Chung, *J. Org. Chem.* **1983**, *48*, 1564. [l] J. T. Groves, T. E. Nemo, *J. Am. Chem. Soc.* **1983**, *105*, 5786. [m] K. S. Suslick, B. R. Cook, *J. Chem. Soc., Chem. Commun.* **1987**, 200. [n] P. Battioni, J. P. Renasud, J. F. Bartoli, M. R. Artiles, M. Fort, D. Mansuy, *J. Am. Chem. Soc.* **1988**, *110*, 8462. [o] M. Iyoda, A. Mizusuna, H. Kuroda, M. Oda, *J. Chem. Soc., Chem. Comuun.* **1989**, 1690. [p] K. H. Ahn, J. T. Groves, *Bull. Korean Chem. Soc.* **1994**, *15*, 957. [q] T. R. Boehlow, C. D. Spilling, *Tetrahedron Lett.* **1996**, *37*, 2717. [r] A. M. Al-Ajlouni, J. H. Espenson, *J. Org. Chem.* **1996**, *61*, 3969. [s] C. Cativiela, J. M. Fraile, J. I. Garcia, J. A. Mayoral, *J. Mol. Catal. A* **1996**, *112*, 259. [t] P. Bhyrappa, J. K. Young, J. S. Moore, K. S. Suslick, *J. Am. Chem. Soc.* **1996**, *118*, 5708; R. Bhyrappa, J. K. Jeffrey, S. Moore, K. S. Suslick, *J. Mol. Catal. A* **1996**, *113*, 109. [u] V. Kesavan, S. Chandrasekaran, *J. Chem. Soc., Perkin. Trans. 1.* **1997**, 3115. [v] J. C. van der Waal, M. S. Rigutto, H. van Bekkum, *Appl. Catal. A* **1998**, *167*, 331. [w] G. Majetich, R. Hicks, G. Sun, P. McGill, *J. Org. Chem.* **1998**, *63*, 2564; G. Majetich, R. Hicks, *Synlett* **1996**, 649. [x] C. J. Liu, W. Y. Yu, S. G. Li, C. M. Che, *J. Org. Chem.* **1998**, *63*, 7364. [y] C. K. Chang, C. Y. Yeh, T. S. Lai, *Macromol. Symp.* **2000**, *156*, 117. [z] B. F. Sels, A. L. Villa, D. Hoegaers, D. E. De Vos, P. A. Jacobs, *Top. Catal.* **2000**, *13*, 223. [aa] U. Arnold, R. S. Cruz, D. Mandelli, U. Schuchardt, *J. Mol. Catal. A* **2001**, *165*, 149. [ab] A. A. Valente, I. S. Goncalves, A. D. Lopes, J. E. R. Borges, M. Pillinger, C. C. Romao, X. G. Mera, *New. J. Chem.* **2001**, *25*, 959. [ac] J. F. Bartoli, K. L. Barch, M. Palacio, P. Battioni, D. Mansuy, *Chem. Commun.* **2001**, 1718. [ad] S. Tangestaninejad, M. H. Habib, V. Mirkhani, M. Moghadam, *J. Chem. Res (S).* **2001**, 444. [ae] D. Mandelli, K. B. Voitiski, U. Schuchardt, G. B. Shul'pin, *Chem. Nat. Compd.* **1996**, *38*, 133. [af] T. Lai, S. K. Lee, L. Yeung, H. Liu, I. D. Williams, C. K. Chang, *Chem. Commun.* 2003, 620. [ag] W. Y. Lu, J. F. Bartoli, P. Battioni, D. Mansuy, *New. J. Chem.* **1992**, *16*, 621.

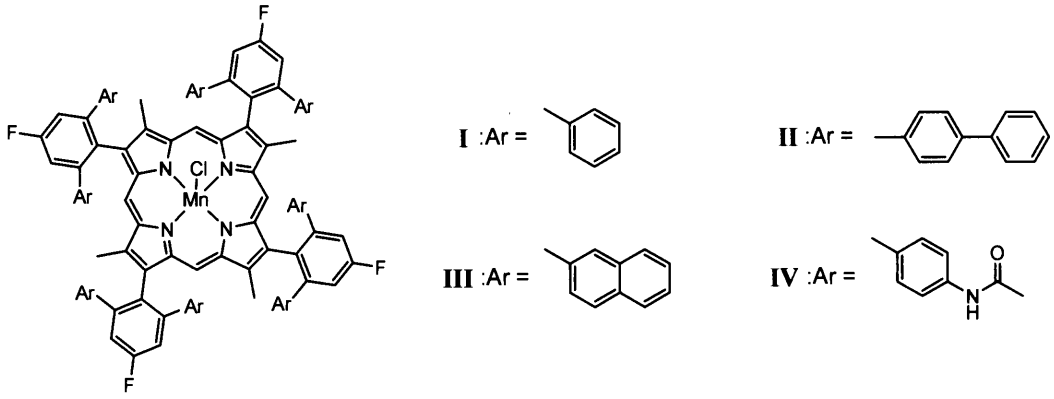

Table 3-8. Comparison of regioselectivity for epoxidation of 7-methyl-1,6-octadiene

system	[terminal epoxide]/[total epoxide]
TBA-4/H_2O_2 (this work)	**0.17**
Al_2O_3/H_2O_2	<0.01[a]
$CF_3CH_2OH/H_2O_2/Na_2HPO_4$	<0.01[b]
$(CF_3)_2CO/C_2F_5OH/H_2O_2/Na_2HPO_4$	<0.01[c]

[a] M. C. A. van Vliet, D. Mandelli, I. W. C. E. Arends, U. Schuchardt, R. A. Sheldon, *Green Chem.* **2001**, *3*, 243. [b] M. C. A. van Vliet, I. W. C. E. Arends, R. A. Sheldon, *Synlett* **2001**, 248. [c] M. C. A. van Vliet, I. W. C. E. Arends, R. A. Sheldon, *Synlett* **2001**, 1305.

Table 3-9. Comparison of regioselectivity for epoxidation of 4-vinyl-1-cyclohexene

system	[terminal epoxide] /[total epoxide]
TBA-4/H_2O_2 (this work)	**0.04**
$Mo(CO)_6$/TBHP	<0.01[a]
m-CPBA	0.02[b]
$(Cl_2CH)_2CO/Na_2HPO_4/H_2O_2$	0.03[c]
m-CPBA	0.03[d]
Mn(TPP)(OAc)/NAOCl/4'-(imidazol-1-yl)acetophenone	0.03[d]
Mn(TTMPP)(OAc)/NaOCl/4'-(imidazol-1-yl)acetophenone	0.05[d]
Mn(TTPPP)(OAc)/NaOCl/4'-(imidazol-1-yl)acetophenone	0.20[d]
$[MnT(3',5'\text{-}G2Ph)P]^+$/PhIO	0.04[e]
$[MnT(3',5'\text{-}G1Ph)P]^+$/PhIO	0.04[e]
$[MnT(2',4',6'\text{-}OMePh)P]^+$/PhIO	0.04[e]
$[MnT(2',4',6'G1AP)P]^+$/PhIO	0.11[e]
$[PW_{11}CoO_{39}]^{5-}$/isobutyraldehyde/O_2 (1 atm)	0.06[f]
$RuCl_2(biox)_2$/isobutyraldehyde/$NaHCO_3/O_2$	<0.01[g]

Table 3-9. (*continued*)

system	[terminal epoxide] /[total epoxide]
I/PhIO	0.39[h]
II/PhIO	0.53[h]
III/PhIO	0.56[h]
IV/PhIO	0.73[h]

[a] M. N. Sheng, J. G. Zajacek, *J. Org. Chem.* **1970**, *35*, 1839. [b] R. G. Carlson, N. S. Behn, C. Cowles, *J. Org. Chem.* **1971**, *36*, 3832. [c] C. J. Stark, *Tetrahedron Lett.* **1981**, *22*, 2089. [d] K. S. Suslick, B. R. Cook, *J. Chem. Soc., Chem. Commun.* **1987**, 200. [e] P. Bhyrappa, J. K. Young, J. S. Moore, K. S. Suslick, *J. Am. Chem. Soc.* **1996**, *118*, 5708; R. Bhyrappa, J. K. Jeffrey, S. Moore, K. S. Suslick, *J. Mol. Catal. A* **1996**, *113*, 109. [f] N. Mizuno, M. Tateishi, T. Hirose, M. Iwamoto, *Chem. Lett.* **1993**, 1985. [g] V. Kesavan, S. Chandrasekaran, *J. Chem. Soc., Perkin. Trans. 1.* **1997**, 3115. [h] C. K. Chang, C. Y. Yeh, T. S. Lai, *Macromol. Symp.* **2000**, *156*, 117.

Table 3-10. Competitive epoxidation of olefins with similar alkyl substituents to the corresponding dienes with H_2O_2 catalyzed by TBA-**4**[a]

entry	corresponding diene	olefin$_1$	olefin$_2$	$R_1/(R_1+R_2)$
1	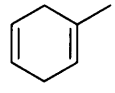	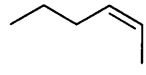	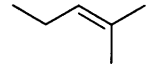	0.88
2	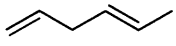	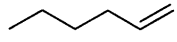	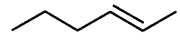	0.61
3	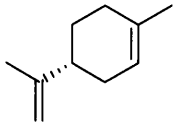	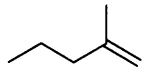	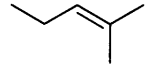	0.47
4	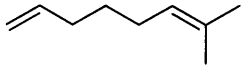	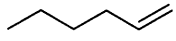	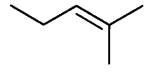	0.28
5	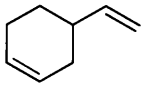	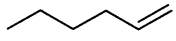	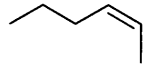	0.06

[a] Reaction conditions: TBA-**4** (8 μmol), olefin$_1$ (5 mmol), olefin$_2$ (5 mmol), 30% aqueous H_2O_2 (1 mmol), acetonitrile (6 mL), reaction temperature (305 K). R_1 and R_2 values were determined from the reaction profiles at low conversion (<10%) of H_2O_2.

present system was compared with those using *m*-CPBA as a stoichiometric oxidant or H_2O_2 in the presence of peroxotungstates of $[PO_4\{WO(O_2)_2\}_4]^{3-}$ and $[W_2O_3(O_2)_4(H_2O)_2]^{2-}$, which have been reported to be effective catalysts for the H_2O_2-based epoxidation.[61,62,64,71] The results are shown in Figure 3-2. In the case of *m*-CPBA, more electron-rich double bonds are preferably oxidized in all cases. Among the tungsten catalysts tested, TBA-**4** showed the highest regioselectivity to the more accessible, but less nucleophilic double bond. In addition, TBA-**4** showed higher TONs than those for $[PO_4\{WO(O_2)_2\}_4]^{3-}$ and $[W_2O_3(O_2)_4(H_2O)_2]^{2-}$. As above mentioned, TBA-**4** was stable under the present reaction conditions and a fully occupied silicododecatungstate, $[\gamma\text{-}SiW_{12}O_{40}]^{4-}$, was inactive for epoxidation, suggesting that the generation of an active oxidant on a divacant lacunary site.

3.3.2.2. Epoxidation of C_6-Olefins

Table 3-11 shows the order of reactivity for epoxidation of a series of C_6-olefins catalyzed by TBA-**4**. The reactivity was decreased in the order of *cis*-2-hexene (13.9) > 2-methyl-1-pentene (3.1) ~ 2-methyl-2-pentene (3.0) > 2,3-dimethyl-2-butene (2.1) > 1-hexene (1.4) > *trans*-2-hexene (1.0). The π(C=C) HOMO energies of C_6-olefins were calculated at the HF/6-311G(d,p) level and decresed in the order of 2,3-dimethyl-2-butene (–8.67 eV) > 2-methyl-2-pentene (–8.97 eV) > *trans*-2-hexene (–9.30 eV) ~ *cis*-2-hexene (–9.32 eV) > 2-methyl-1-pentene (–9.44 eV) > 1-hexene (–9.72 eV). The alkyl substitution increases electron density of the C=C double bond and raises the π(C=C) HOMO energy, resulting in the increase the reactivity of the olefin with electrophilic oxidants without steric hindrance such as peroxyacids, peroxides and peroxo complexes.[81-88] This order is not consistent with that of the π(C=C) HOMO energies of C_6-olefins, but that observed for the epoxidation catalyzed by TS-1, where restricted transition state, shapeselectivity, and diffusion effects were observed.[46] Therefore, the inconsistence of the orders between the π(C=C) HOMO energy and the reactivity would be caused by the steric constraints of the active site of **4**.

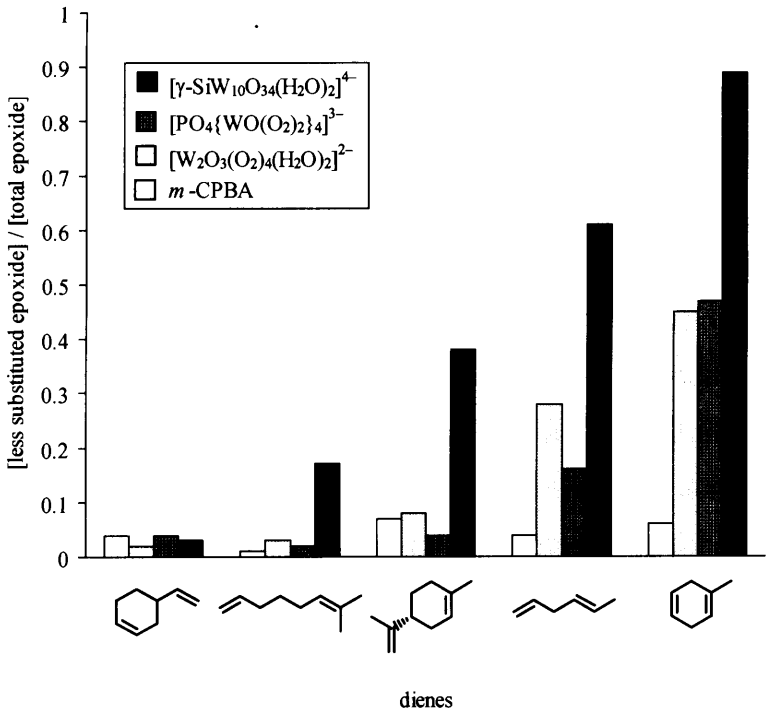

Figure 3-2. Ratio of less substituted epoxides to total epoxides formed by the epoxidation of various dienes.

Table 3-11. Initial and relative rates for the epoxidation of a series of C_6-olefins catalyzed by TBA-**4** with H_2O_2[a]

entry	olefin	R_0 (mM min^{-1})	relative rate[b]
1	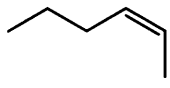	3.08	13.9
2	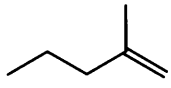	0.68	3.1
3	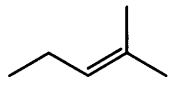	0.68	3.0
4	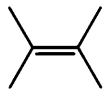	0.47	2.1
5	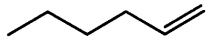	0.30	1.4
6	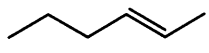	0.22	1.0

[a] Reaction conditions: TBA-**4** (8 μmol), olefin (5 mmol), 30% aqueous H_2O_2 (1 mmol), acetonitrile (6 mL), reaction temperature (305 K). R_0 values were determined from the reaction profiles at low conversion (≤10%) of H_2O_2. [b] The values are ratios of R_0 / R_0 (*trans*-2-hexene).

3.3.3. Reaction Mechanism for Olefin Epoxidation

The activation of hydroperoxides including alkyl hydroperoxides and H_2O_2 by d^0-transition metals has received much attention because group IV–VII metals have been employed for industrial olefin epoxidation with organic hydroperoxides (the Halcon-Arco process). During the last few decades, experimental and theoretical studies on the mechanism of olefin epoxidation have been reported.[85,89-92] It has been accepted for the activation of alkyl hydroperoxide that the oxygen transfer reaction to olefin proceeds via an intermediate η^2-coordination of the peroxide to the Lewis acid metal center, which was structurally characterized in some cases.[93] Recent studies using the molybdenum diperoxo complexes with *tert*-butyl hydroperoxide (TBHP) show that the activation of TBHP by the peroxo complexes with Lewis acid is a key step in the catalytic cycle.[91] An O-O bond polarization of the alkyl peroxide is considered to allow an electrophilic attack to the olefin. For the activation of H_2O_2 with d^0-transition metals, various modes of peroxo species such as $M(\eta^2\text{-}O_2)$,[86,89,90,94] $M(\mu\text{-}\eta^2:\eta^1\text{-}O_2)$,[32,62,95] and M(OOH)[96] have been postulated as active species for the olefin epoxidation depending on the metals and their structures. In this section, the kinetic and mechanistic aspects of the TBA-**4**-catalyzed epoxidation system including the electronic and steric natures of the active oxygen species are described.

3.3.3.1. Electronic and Steric Character of Active Oxygen Species

Although the intramolecular regioselectivity for the epoxidation of non-conjugated dienes that have two electronically and sterically inequivalent double bonds provides much information on the active oxygen species, the regioselectivity estimates both steric and electronic characters of the active oxygen species at the same time. Therefore, the assessment for the steric and electronic characters of the active oxygen species is separated.

First, the electronic characters of the active oxygen species were examined. Figure 3-3 shows Hammett plots ($\log(k_X/k_H)$ versus σ^+) for the competitive oxidation of styrene and *p*-substituted styrenes. The good linearity of Hammett plots suggests that the present epoxidation proceeds via a single mechanism. The negative ρ^+ value of -0.99 agrees with the formation of the electrophilic oxygen species on TBA-**4**.[97] The negative ρ value of -1.09 for a Hammett plot ($\log(k_X/k_H)$ versus σ) for the competitive

oxidation of thioanisole and *p*-substituted thioanisoles also indicates that the nucleophilic sulfide attacks the electrophilic oxygen on the active oxygen species.[98] The electronic character of the active oxygen species formed on TBA-**4** was further examined by using SSO that has been used as a probe of the electronic character of an oxidant (Table 3-12).[99] The oxidation did not proceed without TBA-**4** under the present conditions (entry 4). The results for oxidations of SSO by the tungsten-based complexes showed relatively low X_{SO} values (X_{SO} = (nucleophilic oxidation)/(total oxidation) = (SSO_2 + $SOSO_2$)/(SSO_2 + SOSO + 2$SOSO_2$)) and the sulfide site of SSO was much more selectively oxidized (entries 1–3), showing the electrophilic nature of the active oxygen species. The X_{SO} value for each run in Table 3-12 little changed during the oxidation of SSO (e.g., the X_{SO} value for TBA-**4** was within the range of 0.04–0.06 during the 220-min reaction). The X_{SO} value obtained with TBA-**4** (0.04) was lower than those of tetra-*n*-hexylammonium salt of $[PO_4\{WO(O_2)_2\}_4]^{3-}$ (0.18) and dodecyltrimethylammonium salt of $[W_2O_3(O_2)_4(H_2O)_2]^{2-}$ (0.35), suggesting that the active oxygen species on TBA-**4** is the most electrophilic among these tungstates under the present conditions. The X_{SO} value of TBA-**4** was lower than or comparable to those reported for stoichiometric reagents such as dimethyldioxirane (0.07),[99a] peracetic acid (0.16),[99b] *m*-CPBA (0.13),[99b] HMPT-$MoO(O_2)_2$ (0.16);[35b] and H_2O_2-based catalytic oxidations such as $H_2O_2/HClO_4$ (0.05),[99a] Ti-β (0.07),[99c] Ti-MCM-41 (0.06),[99c] $Na_2WO_4/C_6H_5PO_3H_2/[CH_3(n\text{-}C_8H_{17})_3N]HSO_4$ (<0.01),[99d] and CH_3ReO_3 (0.45).[99e]

The 3-alkyl-substituted cyclohexenes provide a quantitative measure of purely steric effects for the epoxidations, since electronic interactions between the C=C double bond and the allylic substituents are not possible.[100] The higher *trans* diastereoselectivity (*trans/cis* = 81/19) for the epoxidation of 3-methyl-1-cyclohexene by TBA-**4** was higher than those by $[PO_4\{WO(O_2)_2\}_4]^{3-}$ (56/44) and $[W_2O_3(O_2)_4(H_2O)_2]^{2-}$ (55/45) [Eq. (3-9)]. The *trans/cis* ratio for TBA-**4** (81/19) was lower than that of Ti-*β* (92/8) with the steric constraints due to the narrow channels,[100a] and much higher than those of CH_3ReO_3/UHP (49/51),[100a] Ti-MCM-41/TBHP (58/42),[100a] Ti-ITQ-2/TBHP (61/39),[100a] and stoichiometric reagents of *m*-CPBA (48/52)[100c] and dimethyldioxirane (52/48).[100d]

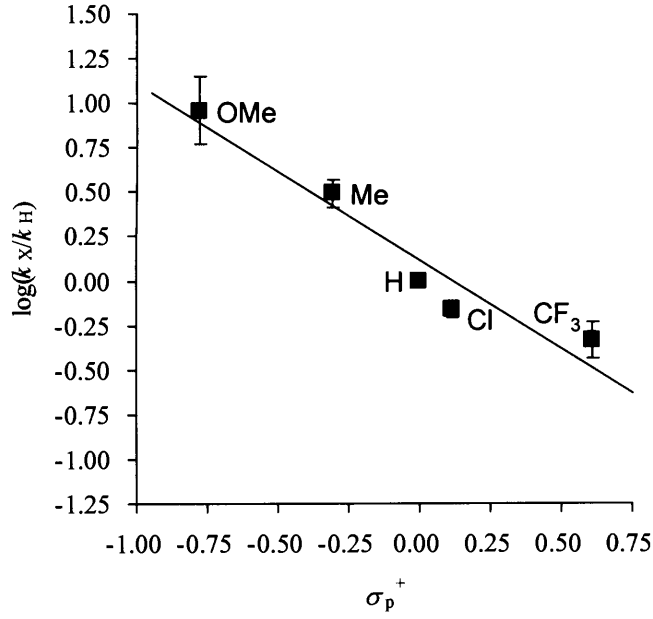

Figure 3-3. Hammett plot for the competitive oxidation of styrene and *p*-substituted styrenes. Reaction rates were estimated by the conversion of substrates. Reaction conditions: Styrene (2.5 mmol), *p*-substituted styrene (2.5 mmol), TBA-**4** (8.0 μmol), 30% aqueous H_2O_2 (1.0 mmol), CH_3CN (6 mL), 305 K. Slope = –0.99 (R^2 = 0.93).

Table 3-12. Oxidation of thianthrene 5-oxide (SSO)[a]

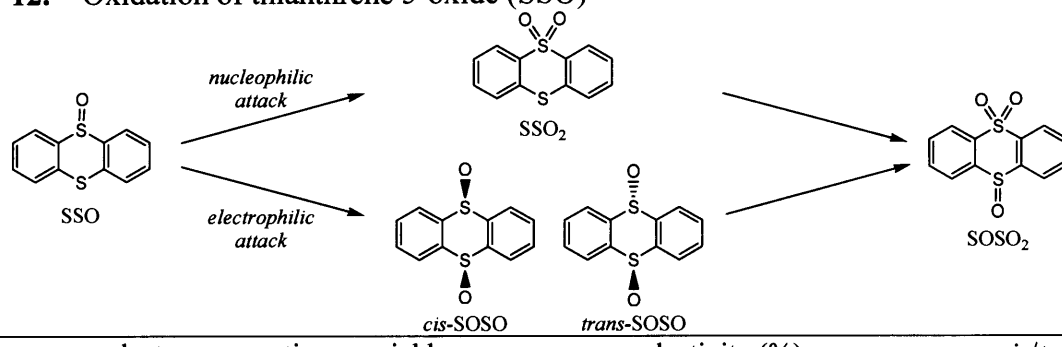

entry	catalyst	time (min)	yield (%)	selectivity (%)				*cis*/*trans*	X_{SO}
				SSO_2	*cis*-SOSO	*trans*-SOSO	$SOSO_2$		
1	TBA-**4**	220	96	2	16	80	1	17/83	0.04
2[b]	$[W_2O_3(O_2)_4(H_2O)_2]^{2-}$	60	80	23	18	40	19	30/70	0.35
3[c]	$[PO_4\{WO(O_2)_2\}_4]^{3-}$	40	>99	8	37	43	12	47/53	0.18
4	without	1440	<1	–	–	–	–	–	–
5[d]	*m*-CPBA	<20	>99	13	29	58	<1	33/67	0.13

[a] Reaction conditions: Catalyst (W: 20 μmol), SSO (200 μmol), acetonitrile (5 mL), 30% aqueous H_2O_2 (50 μmol), 298 K. Yield and selectivity were determined by HPLC analysis with an internal standard technique. Yield (%) = products (mol) / initial oxidant (mol) × 100. X_{SO} = (SSO_2 (mol) + $SOSO_2$ (mol)) / (SOSO (mol) + SSO_2 (mol) + 2 × $SOSO_2$ (mol)). [b] Dodecyltrimethylammonium salt (10 μmol). [c] Tetra-*n*-hexylammonium salt (5 μmol). [d] *m*-CPBA (50 μmol), SSO (200 μmol), chloroform (5 mL), 298 K.

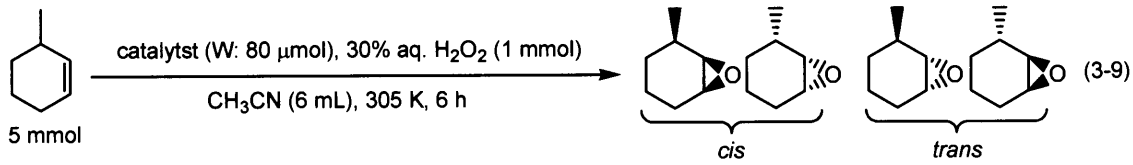

TBA-4: 93% yield (based on H_2O_2), *trans/cis* =81/19
$[W_2O_3(O_2)_4(H_2O)_2]^{2-}$: 93% yield (based on H_2O_2), *trans/cis* =55/45
$[PO_4\{WO(O_2)_2\}_4]^{3-}$: 98% yield (based on H_2O_2), *trans/cis* =56/44

These results for the competitive oxidation of *p*-substituted styrenes, oxidation of SSO, and epoxidation of 3-methyl-1-cyclohexene suggest that the strong electrophilic oxidant species with the steric hindrance is formed by the reaction of TBA-**4** with H_2O_2. The specific regioselectivity for epoxidation of non-conjugated dienes with H_2O_2 by TBA-**4** probably reflects the electronic and steric characters.

3.3.3.2. Reactivity of Divacant Lacunary POM with Hydrogen Peroxide

The time course for the present epoxidation of cyclooctene with H_2O_2 catalyzed by TBA-**4** showed an induction period (ca. 60 min, Figure 3-4). The induction period disappeared upon the pretreatment of TBA-**4** with H_2O_2 (60 min) whereas the induction period (ca. 80 min) was still observed by the pretreatment with cyclooctene. Therefore, the induction period would be caused by the reaction of TBA-**4** with H_2O_2 to form catalytically active species. The γ-Keggin structure of TBA-**4** during the catalysis was stable as previously reported because of the following reasons: (i) The recovered catalyst was recyclable, (ii) no substantial changes were observed for in situ IR and UV/Vis spectra in contrast with the $H_3PW_{12}O_{40}/H_2O_2$ system, (iii) no formation of other tungstate compounds of $[\alpha\text{-}SiW_{12}O_{40}]^{4-}$, $[W_2O_3(O_2)_4(H_2O)_2]^{2-}$, and $[H_nWO_2(O_2)_2]^{(2-n)-}$ after the catalytic reaction was confirmed by ^{29}Si and ^{183}W NMR spectra, and (iv) the reactivity and selectivity of TBA-**4** for the epoxidation of non-conjugated dienes were different from those of peroxotungstate fragments such as $[W_2O_3(O_2)_4(H_2O)_2]^{2-}$ and $[PO_4\{WO(O_2)_2\}_4]^{3-}$. These results show that the induction period is not due to the structural degradation and that the present catalysis does not originate from the tungstates formed by the decomposition of TBA-**4**. On the other hand, a mixture of $H_3PW_{12}O_{40}$, H_2O_2, and an olefin resulted in the decomposition of $[PW_{12}O_{40}]^{3-}$.[101]

Next, the reactivity of TBA-**4** with H_2O_2 was investigated. One new ^{29}Si NMR

signal appeared at −84.1 ppm upon addition of 10 equiv. H_2O_2 (30% aqueous solution) with respect to TBA-**4**, showing the formation of a single species (TBA-**5**) (Figure 3-5(b)). The chemical shift of TBA-**5** was different from that of TBA-**4** (−83.5 ppm, Figure 3-5(a)). The ^{183}W NMR spectrum of TBA-**4** with C_2 symmetry showed five signals at −95.7, −98.9, −118.2, −119.6, and −195.7 ppm with intensity ratio of 1:1:1:1:1, respectively (Figure 3-6(a)). Upon addition of H_2O_2, five new ^{183}W NMR signals appeared at −125.9, −135.4, −155.3, −219.7, and −554.6 ppm with intensity ratio of 1:1:1:1:1, respectively (Figure 3-6(b)). It has been reported for molybdenum and tungsten compounds that the coordination of strong σ donors such as a peroxo group caused upfield shifts of ^{95}Mo and ^{183}W NMR signals.[102] Therefore, the signal at −554.6 ppm is assignable to tungsten atoms with the peroxo ligands. The 1:1:1:1:1 ratio suggests that TBA-**5** also has the C_2 symmetry. The fully occupied silicododecatungstate, $[\gamma\text{-}SiW_{12}O_{40}]^{4-}$, was completely inactive for the catalytic epoxidation. This fact and the specific regioselectivity for epoxidation of non-conjugated dienes by TBA-**4** suggest the formation of an active oxygen species on the divacant lacunary site with the maintenance of γ-Keggin structure.

After the treatment of TBA-**4** with 30% H_2O_2 followed by the addition of an excess amount of diethyl ether, the precipitate was formed. The ^{29}Si and ^{183}W NMR spectra of the precipitate were the same as those of TBA-**5**, showing the successful isolation of TBA-**5** (Figures 3-5(b), 3-6(b), and 3-7). The positive ion cold-spray ionization mass (CSI-MS) spectrum of the isolated compound TBA-**5** showed the most intense parent ion peaks centered at *m/z* 3654.8 with the isotopic distribution (Figure 3-8), which agreed with the calculated pattern of $[(TBA)_5SiW_{10}O_{32}(O_2)_2]^+$.

All these results (^{29}Si NMR, ^{183}W NMR, and CSI-MS spectroscopy) show that the two oxo groups (O^{2-}) are replaced by two peroxo species (O_2^{2-}) on the divacant lacunary site with the retention of γ-Keggin framework. The reaction of reactive triphenylphosphine (1 mmol) with TBA-**5** (20 μmol) in acetonitrile gave 43 μmol of triphenylphosphine oxide, showing two equiv. active oxygen species with respect to TBA-**5**, while the quantitative determination of the amount of active oxygen species by the iodometric titration was unsuccessful due to the interference of the tetra-*n*-butylammonium ions. There are three kinds (**a**, **b**, and **c** in Figure 3-9) of possible sites for the formation of peroxo groups taking account of the C_2 symmetry.

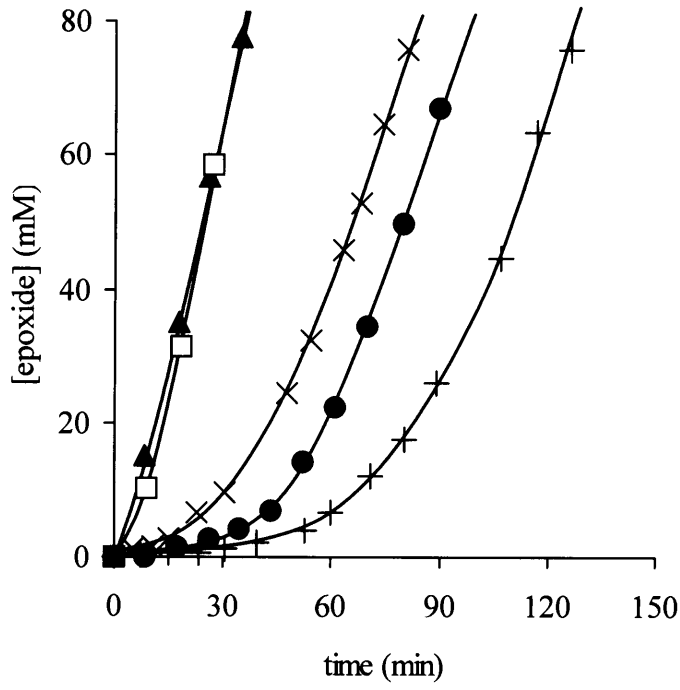

Figure 3-4. Reaction profiles of the epoxidation of cyclooctene with 30% aqueous H_2O_2 catalyzed by TBA-**4**: [TBA-**4**] (1.18 mM), [cyclooctene] (0.74 M), [H_2O_2] (0.15 M), [H_2O] (0.65 M), acetonitrile (6 mL), reaction temperature (305 K). ●: Without pretreatment. ▲: With pretreatment of 30% aqueous H_2O_2 before addition of cyclooctene for 1 h at 305 K. +: With pretreatment of cyclooctene before addition of 30% aqueous H_2O_2 for 60 min at 305 K. □: With addition of $HClO_4$ (0.30 mM) without pretreatment. ×: Using TBA-**5** (1.18 mM) instead of TBA-**4** without pretreatment.

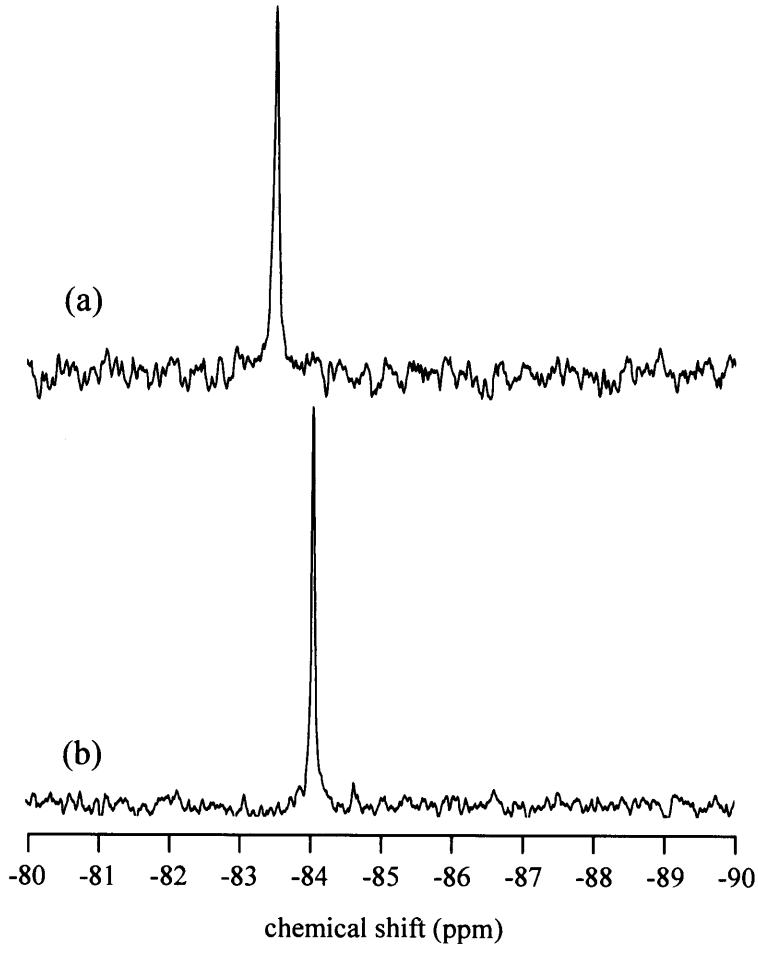

Figure 3-5. ^{29}Si NMR spectra of (a) TBA-**4** in CD_3CN/DMSO-d_6 (2/1, v/v) at 298 K and (b) TBA-**5** in CD_3CN at 263 K (after the treatment of TBA-**4** with 10 equiv. H_2O_2 (30% aqueous solution) with respect to TBA-**4** at 263 K for 3 h).

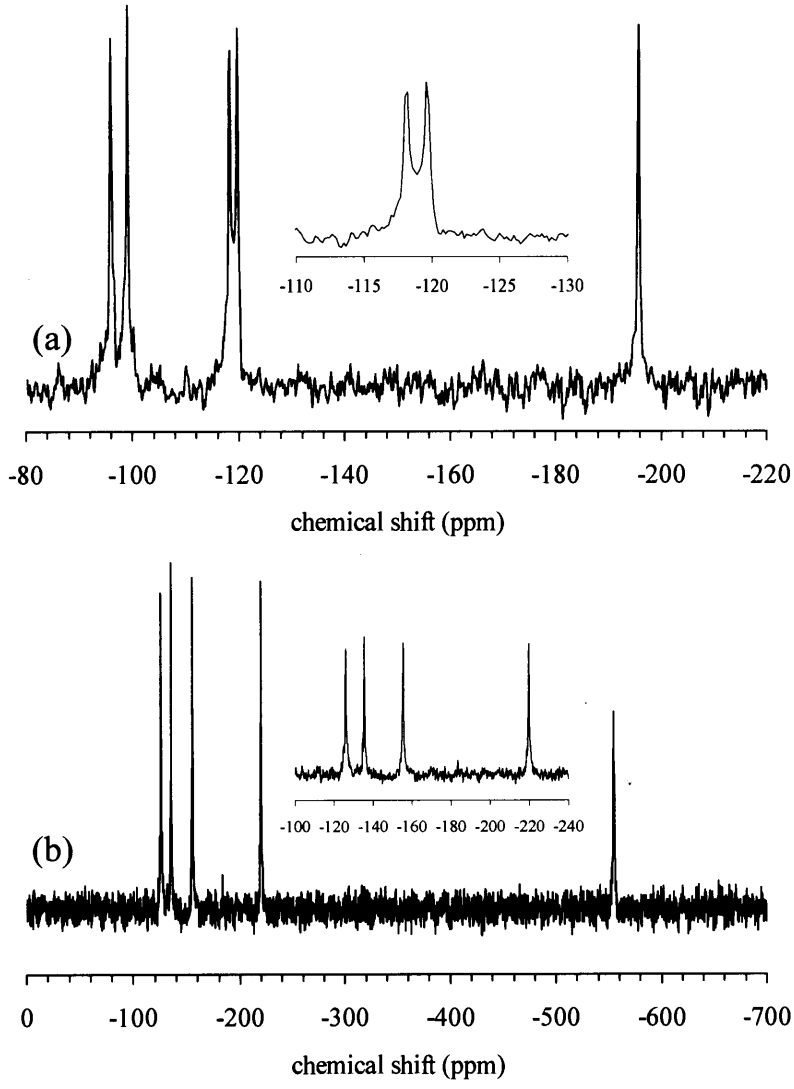

Figure 3-6. ^{183}W NMR spectra of (a) TBA-**4** in CD_3CN/DMSO-d_6 (2/1, v/v) at 298 K and (b) TBA-**5** in CD_3CN at 263 K (after the treatment with 10 equiv. H_2O_2 (30% aqueous solution) with respect to TBA-**4** at 263 K for 3 h).

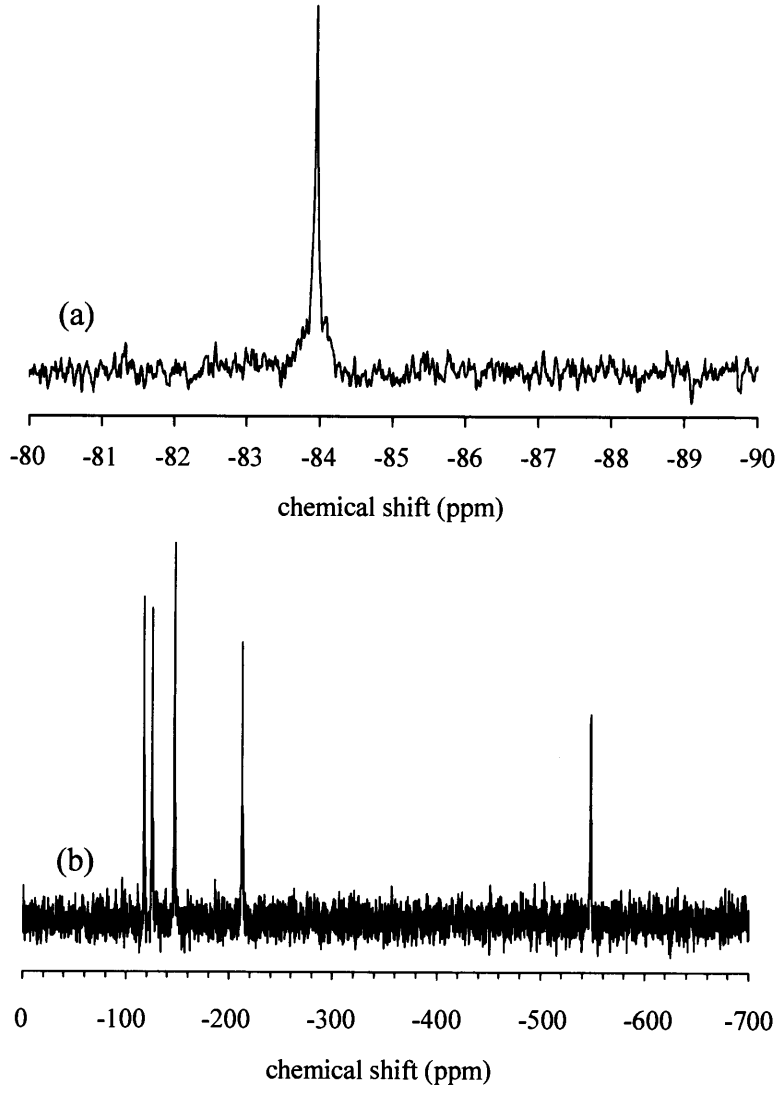

Figure 3-7. (a) ^{29}Si and (b) ^{183}W NMR spectra of the isolated TBA- **5** in CD_3CN at 263 K.

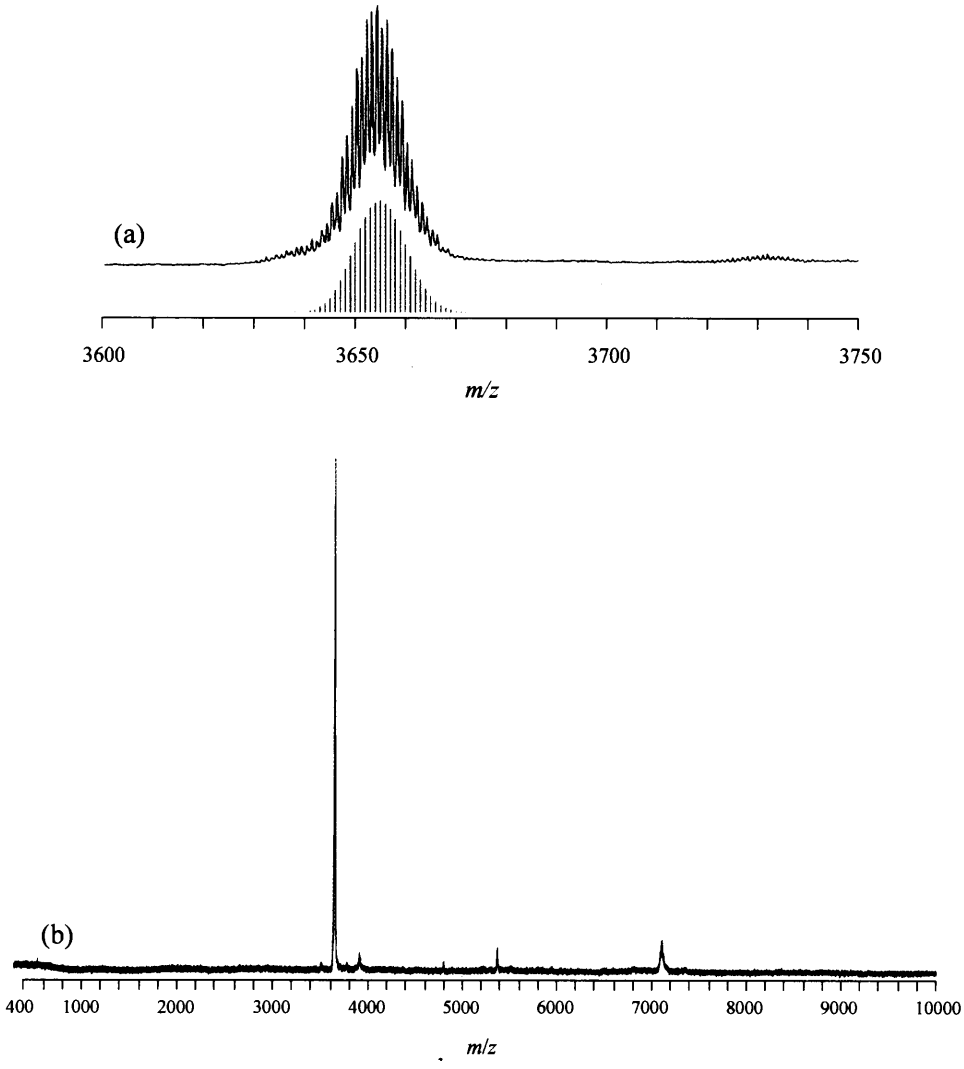

Figure 3-8. (a) Positive ion CSI-MS (*m/z* 3600–3750 (upper) spectrum of TBA-**5** in $ClCH_2CH_2Cl$ (upper) and the calculated pattern of $[(TBA)_5SiW_{10}O_{32}(O_2)_2]^+$ (lower). (b) Positive ion CSI-MS (*m/z* 400–10000) spectrum of TBA-**5** in $ClCH_2C_2Cl$.

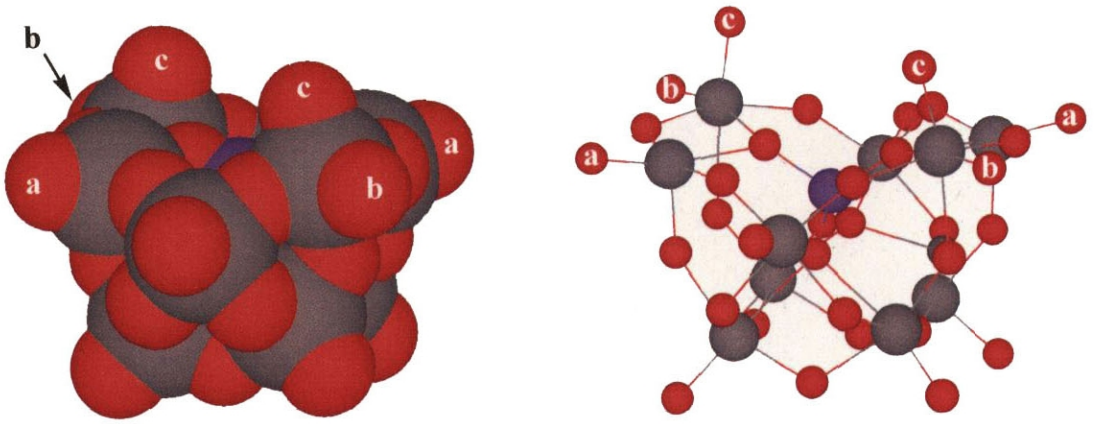

Figure 3-9. Space filling (left) and ball and stick (right) representation of $[\gamma\text{-}SiW_{10}O_{34}]^{4-}$ framework. Purple, gray, and red balls represent silicon, tungsten, and oxygen atoms, respectively.

The strong inhibition of the catalytic reactivity in the presence of coordinative solvents and compounds such as *N,N*-dimethylformamide, dimethylsulfoxide, pyridine, and imidazole suggests that the coordinatively unsaturated sites of $[\gamma\text{-}SiW_{10}O_{34}]^{4-}$, where two aquo ligands in TBA-**4** are eliminated, would play an important role in the activation of H_2O_2. Therefore, the site **a** would be the most probable sites for the formation of the peroxo species. Attempts to obtain crystallographic quality single crystals of $[\gamma\text{-}SiW_{10}O_{32}(O_2)_2]^{4-}$ in acetonitrile, acetone, *N,N*-dimethylformamide, dimethylsulfoxide, dichloromethane, and 1,2-dichloroethane together with vapor diffusion of poor solvents such as diethyl ether, methanol, *n*-hexane, *n*-pentane, and benzene using K^+, $[(CH_3)_4N]^+$, $[(C_2H_5)_4N]^+$, $[(n\text{-}C_3H_7)_4N]^+$, $[(n\text{-}C_4H_9)_4N]^+$, $[(n\text{-}C_4H_9)_3(PhCH_2)N]^+$, $[(n\text{-}C_4H_9)_3(CH_3)N]^+$, $[Ph(CH_3)_3N]^+$, $[Ph_4P]^+$, [K(18-crown-6)]$^+$, [K(dibenzo-18-crown-6)]$^+$, and $[(iso\text{-}C_3H_7)_2NH_2]^+$ as counter cations have yet been unsuccessful. Attempts with the other cations and solvents are in progress.

3.3.3.3. Reactivity of Diperoxo Derivative with Olefins

The stoichiometric epoxidation of cyclooctene with the isolated TBA-**5** hardly proceeded under the same reaction conditions as those in Table 3-1, showing that TBA-**5** is inactive for the present epoxidation. The induction period was still observed

for the epoxidation catalyzed by TBA-**5** with H_2O_2 (Figure 3-4). CSI-MS and in situ IR spectra measured immediately after addition of H_2O_2 (≥20 equiv. with respect to TBA-**4**) were the same as those of TBA-**5**. One ^{29}Si NMR signal at −84.1 ppm was observed at 10 min (150 scans) after addition of H_2O_2 and ^{183}W NMR spectrum of the solution was the same as that of TBA-**5** (5000 scans, 60 min), showing the estimation that the formation of TBA-**5** was completed within 10 min, which were much shorter than ca. 60 min of the induction period. Therefore, it is probable that the reaction of TBA-**5** with H_2O_2 leads to formation of a reactive species (TBA-**6**) and that the induction period observed in the catalytic epoxidation corresponds to the slow formation of TBA-**6** from TBA-**5**. The detection of TBA-**6** by the ^{29}Si and ^{183}W NMR spectroscopy was unsuccessful as shown in Figure 3-10. This is probably because the quantity of TBA-**6** is very small and below the detection limits of ^{29}Si and ^{183}W nuclei (the *S/N* ratio of ^{29}Si and ^{183}W NMR spectra, 7–10). Similarly, the detection of TBA-**6** by *in situ* IR and Raman spectroscopy was unsuccessful. The epoxidation by molybdenum peroxo complexes was initiated by the addition of hydroperoxides and the proton transfer reaction from hydroperoxides to a peroxo ligand was a key step determining the catalytic activity.[91,96c] Similarly, H_2O_2 would work as a proton donor to form a hydroperoxo species (TBA-**6**) such as $(TBA)_3[\gamma\text{-}SiW_{10}O_{32}(O_2)(OOH)]$ through the protonation of TBA-**5** in the present system. The induction period almost disappeared with addition of small amount of $HClO_4$ (0.125–0.250 equiv. with respect to TBA-**4**) (Figure 3-4). In addition, the reaction rates for the epoxidation of cyclooctene in the presence of $HClO_4$ were measured. The good linear correlation between reaction rates and additional amounts of $HClO_4$ was observed as shown in Figure 3-11. All these results support the generation of the hydroperoxo species TBA-**6**. Such an activation mode and different structure may result in a unique reactivity of TBA-**4** compared with $[W_2O_3(O_2)_4(H_2O)_2]^{2-}$ and $[PO_4\{WO(O_2)_2\}_4]^{3-}$.[6] In the presence of TBA-**5** and H_2O_2 (5 equiv. with respect to TBA-**5**), the ratio of less substituted epoxides to total epoxides was 0.87 for the epoxidation of 1-methyl-1,4-cyclohexadiene and the X_{SO} value was 0.03 for the oxidation of SSO, respectively. The respective values well agreed with 0.89 and 0.04 observed for the catalytic reaction with H_2O_2 by TBA-**4**. The agreements show that TBA-**6** is involved in the catalytic cycle.

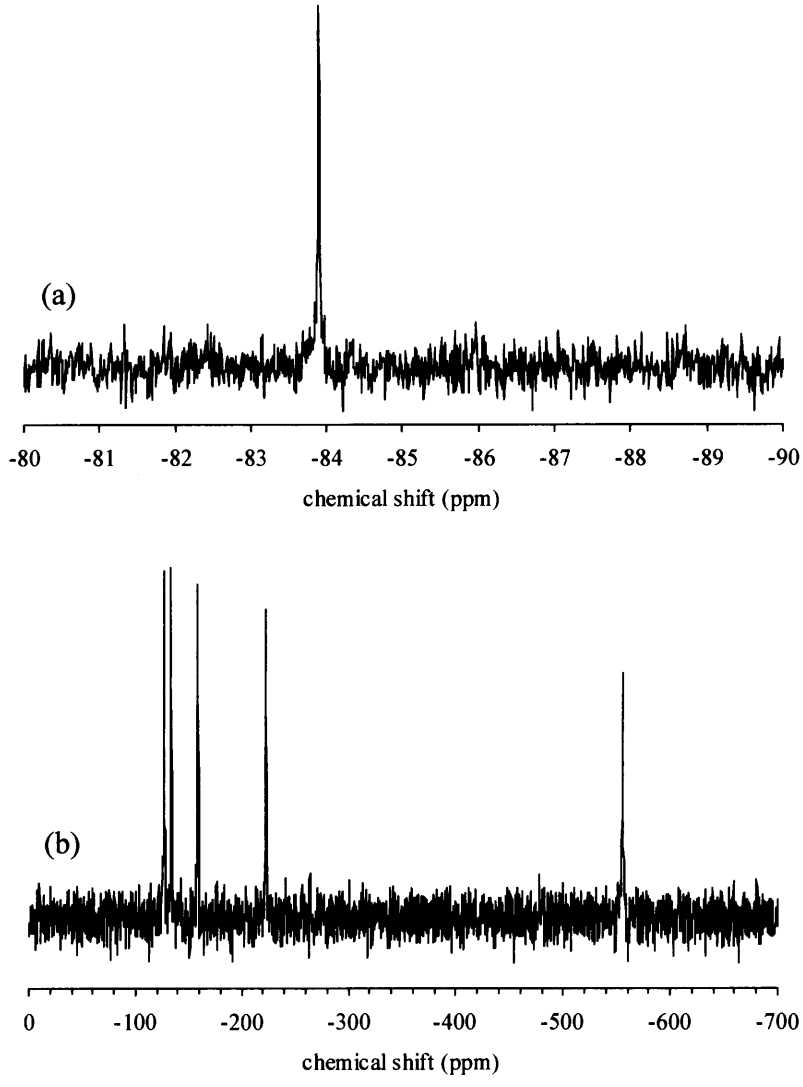

Figure 3-10. (a) ^{29}Si and (b) ^{183}W NMR spectra of isolated TBA-**5** in CD_3CN at 263 K (after addition of 20 equiv. H_2O_2 (88% aqueous solution) with respect to TBA-**5**).

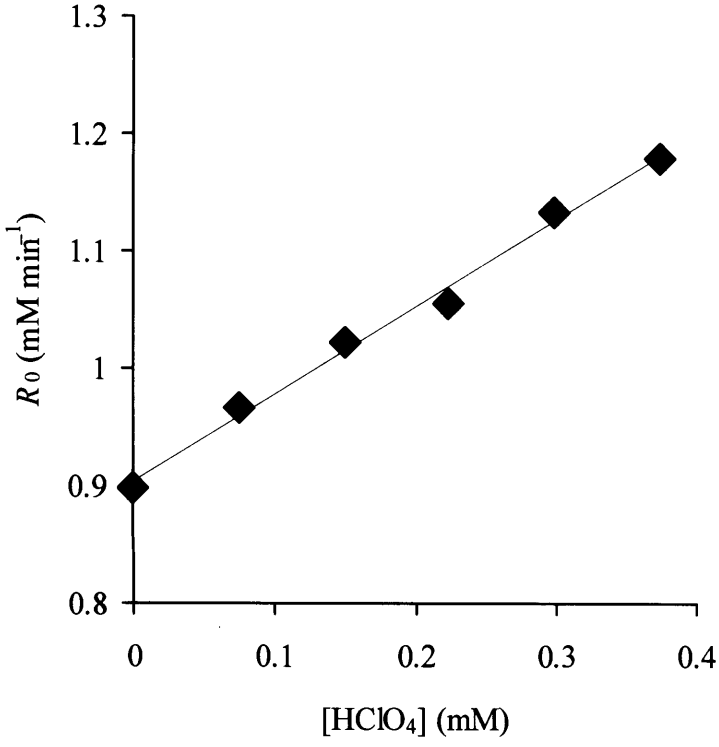

Figure 3-11. Dependences of the reaction rates on the concentrations of additional $HClO_4$: Cyclooctene (0.21 M), TBA-**4** (1.20 mM), H_2O_2 (0.75 M), water (3.38 M), acetonitrile (6 mL), $HClO_4$ (0.07–0.37 mM) 305 K. The epoxidation was initiated by addition of cyclooctene and $HClO_4$ after the pretreatment of TBA-**4** with aqueous H_2O_2 for 60 min at 305 K, and R_0 values were determined from the reaction profiles at low conversions (<10%) of both cyclooctene and H_2O_2. R_0 = 0.74 [$HClO_4$] + 0.90 (R^2 = 0.99).

3.3.3.4. ^{18}O-Labeling Experiments

The origin of oxygen atom incorporated into epoxide was investigated with ^{18}O-labeling experiments. The epoxidation of cyclooctene with TBA-**5** ($(TBA)_4[\gamma\text{-}SiW_{10}O_{32}(^{16}O_2)_2]$) in the presence of 4.5 equiv. $H_2{}^{18}O_2$ (in $H_2{}^{18}O$) with respect to TBA-**5** gave 1,2-epoxycyclooctane with the ^{18}O content of 70 ± 3% (Figure 3-12(a)). No ^{18}O atoms were incorporated into the epoxide with $H_2{}^{16}O_2$ (in $H_2{}^{18}O$) (Figure 3-12(d)), showing that all ^{18}O atoms incorporated into the epoxide originate from $H_2{}^{18}O_2$. The ^{18}O content in the epoxide (^{18}O-labeled epoxide/total epoxide ratio) did not change during the reaction, depended on the amount of $H_2{}^{18}O_2$ used, and agreed with the ^{18}O content in the peroxide ($[H_2{}^{18}O_2]/([H_2{}^{18}O_2] + [W(^{16}O_2)]$ in TBA-**5**)) (inset in Figure 3-12). These facts show the equilibration between $H_2{}^{18}O_2$ and $W(^{16}O_2)$ in TBA-**5**. The CSI-MS spectrum of the compound recovered after the reaction of TBA-**5** with excess (60 equiv. with respect to TBA-**5**) $H_2{}^{18}O_2$ (in $H_2{}^{18}O$) showed the most intense parent ion peaks of $[(TBA)_5SiW_{10}O_{32}(^{18}O_2)_2]^+$ centered at *m/z* 3654.8 + 8.0, whereas the CSI-MS spectrum of the compound recovered after the reaction of TBA-**5** with excess $H_2{}^{16}O_2$ (in $H_2{}^{18}O$) was the same as that of TBA-**5** (Figure 3-13). These facts are in accord with the exchange between $H_2{}^{18}O_2$ and $W(^{16}O_2)$ in TBA-**5**.[103] It is very difficult to distinguish the bands of peroxo species from those of the POM based on the isotopic shifts because the bands related to peroxo species are very weak and overlap with the intense bands of the skeletal vibration of the POM.

3.3.3.5. Reaction Mechanism

On the basis of all the results, the possible reaction mechanism for the epoxidation of olefins with H_2O_2 catalyzed by TBA-**4** (Scheme 3-3) is proposed. First, the compound TBA-**4** reacts with H_2O_2 to form the diperoxo species of TBA-**5** (step 1). The reaction of TBA-**5** with water did not lead to the formation of TBA-**4**, suggesting that step 1 is irreversible. The oxygen transfer reaction from TBA-**5** to C=C bond of the olefin did not occur under the present conditions and TBA-**5** further reacts with H_2O_2 to form the active oxygen species (TBA-**6**) (step 2). These steps probably correspond to the induction period observed in the catalytic epoxidation. The oxygen atom of TBA-**6** transfers to the C=C double bond, giving the corresponding epoxide (step 3). Finally, the regeneration of TBA-**6** by the reaction with H_2O_2 proceeds (step

4).

3.3.3.6. Kinetics

The kinetic data for the present epoxidation were collected after the pretreatment of TBA-**4** with H_2O_2 to make the induction period disappear. A saturation kinetics was observed for the dependence of the reaction rates on the concentration of cyclooctene (0.06–1.15 M, Figure 3-14(a)). The kinetic studies at the low concentration of cyclooctene (0.20 M; i.e., the first-order dependence on the concentration of cyclooctene) showed the first-order dependences of the reaction rates on the concentrations of TBA-**4** (0.29–2.86 mM, Figure 3-14(b)) and H_2O_2 (0.05–0.70 M, Figure 3-14(c)), whereas the first-order and second-order dependences of the reaction rates on the concentration of TBA-**4** (0.29–2.86 mM, Figure 3-15) and on the concentrations of H_2O_2 (0.10–0.70 M, Figure 3-14(d)) were observed at the high concentration of cyclooctene (0.95 M i.e., the zero-order dependence on the concentration of cyclooctene), respectively. These dependences can be explained by the change of the rate-determining step from the oxygen transfer step to C=C double bond (at low concentration of cyclooctene) to the regeneration of TBA-**6** (at high concentration of cyclooctene).

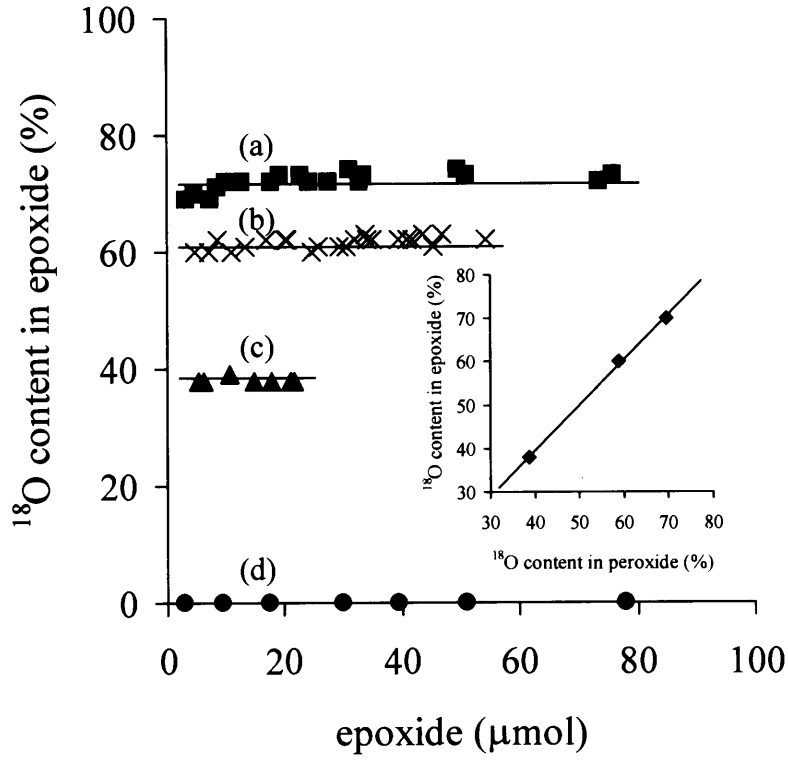

Figure 3-12. Plots of the ratio of ^{18}O contents in the epoxide against the amounts of epoxide formed. The epoxidation of cyclooctene was carried out with 2.2% aqueous hydrogen peroxide. Reaction conditions: TBA-**5** (20 μmol), cyclooctene (1 mmol), CH_3CN (3 mL), 305 K, under 1 atm of Ar. (a) $H_2{}^{18}O_2$ (in $H_2{}^{18}O$, 91 μmol), (b) $H_2{}^{18}O_2$ (in $H_2{}^{18}O$, 56 μmol), (c) $H_2{}^{18}O_2$ (in $H_2{}^{18}O$, 25 μmol), and (d) $H_2{}^{16}O_2$ (in $H_2{}^{18}O$, 91 μmol). Inset: Plots ^{18}O contents in the epoxide against ^{18}O contents in the peroxide. Slope = 1.05 (R^2 = 0.99).

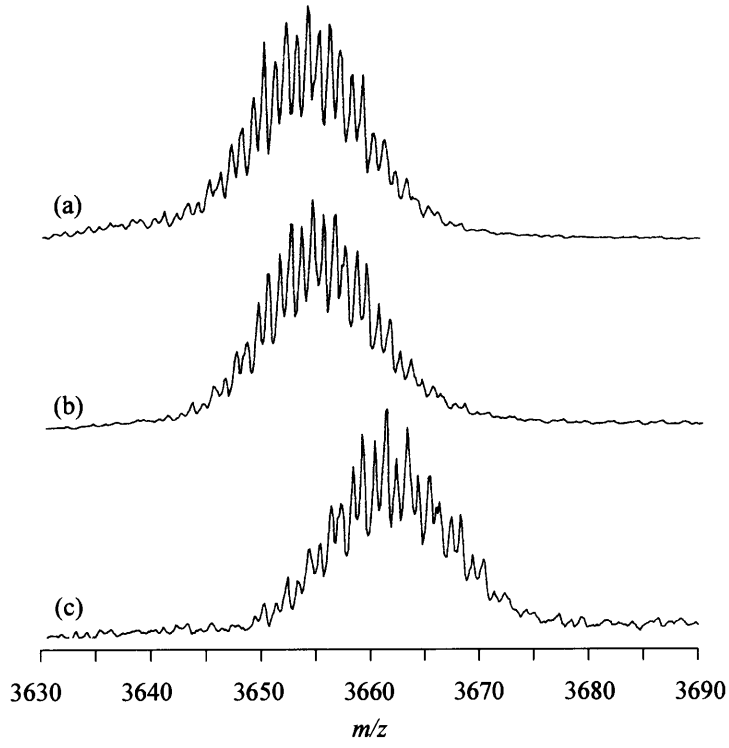

Figure 3-13. Positive ion CSI-MS (*m/z* 3630–3690) spectra of (a) TBA-**5**, (b) the recovered compound after the reaction of TBA-**5** with 2.2% $H_2{}^{16}O_2$ (in $H_2{}^{18}O$, 60 equiv. with respect to TBA-**5**), and (c) the recovered compound after the reaction of TBA-**5** with 2.2% $H_2{}^{18}O_2$ (in $H_2{}^{18}O$, 60 equiv. with respect to TBA-**5**).

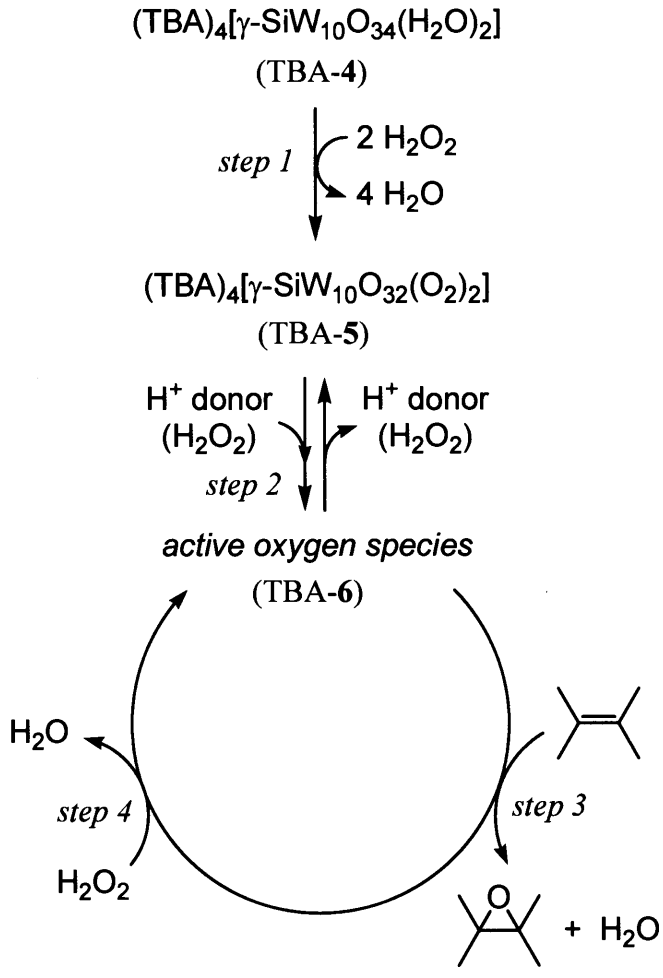

Scheme 3-3. Proposed mechanism for the epoxidation catalyzed by TBA-**4**.

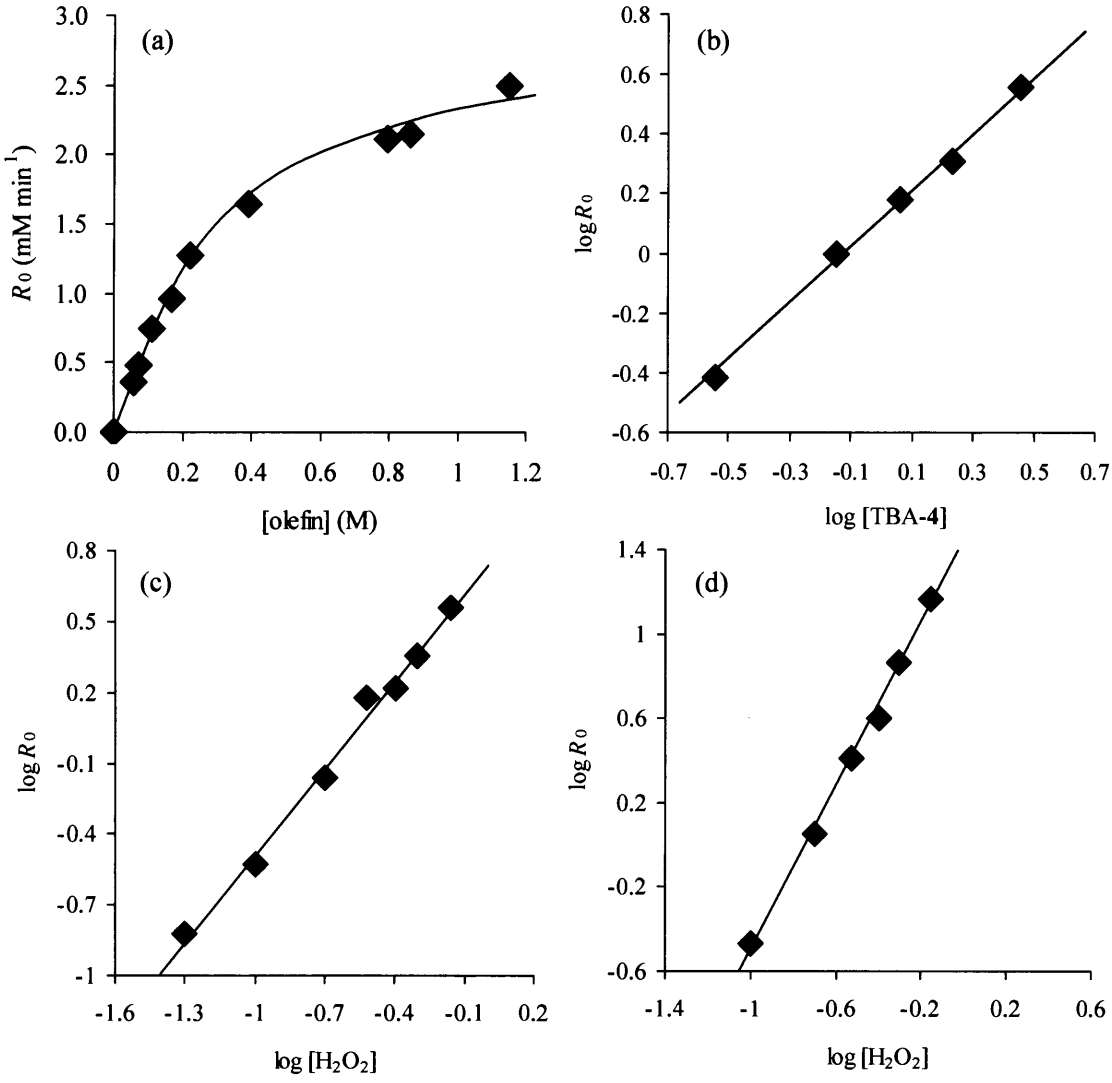

Figure 3-14. Dependences of the reaction rates on the concentrations of (a) cyclooctene, (b) TBA-**4**, and (c and d) hydrogen peroxide: (a) Cyclooctene (0.06–1.15 M), TBA-**4** (1.14 mM), H_2O_2 (0.71 M), H_2O (1.67 M), CH_3CN (7 mL), 305 K; (b) Cyclooctene (0.20 M), TBA-**4** (0.29–2.86 mM), H_2O_2 (0.30 M), H_2O (1.60 M), CH_3CN (7 mL), 305 K; (c) Cyclooctene (0.20 M), TBA-**4** (1.14 mM), H_2O_2 (0.05–0.70 M), H_2O (1.60 M), CH_3CN (7 mL), 305 K; (d) Cyclooctene (0.95 M), TBA-**4** (1.14 mM), H_2O_2 (0.10–0.70 M), H_2O (1.60 M), CH_3CN (7 mL), 305 K. The epoxidation was initiated by addition of cyclooctene after the pretreatment of TBA-**4** with aqueous hydrogen peroxide for 60 min at 305 K, and R_0 values were determined from the reaction profiles at low conversions (<10%) of both cyclooctene and hydrogen peroxide. (b) Slope = 0.95 (R^2 = 0.99). (c) Slope = 1.22 (R^2 = 0.99). (d) Slope = 1.93 (R^2 = 0.99).

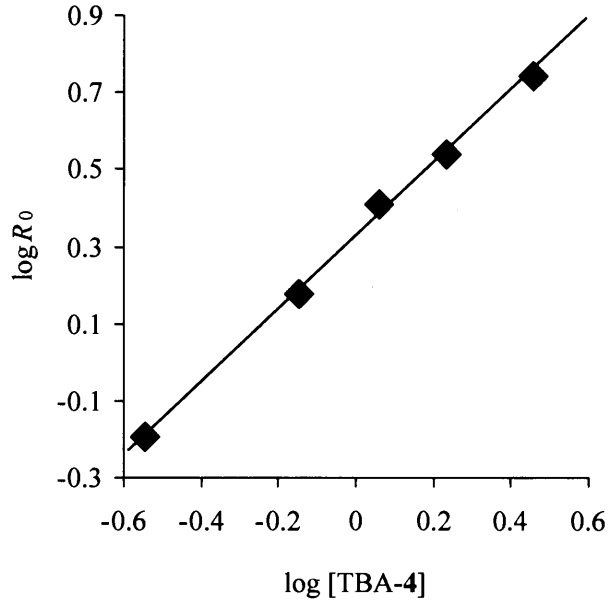

Figure 3-15. Dependences of reaction rates on concentrations of TBA-**4**; Cyclooctene (0.95 M), TBA-**4** (0.29-0.286 mM), H_2O_2 (0.30 M), H_2O (1.60 M), CH_3CN (7 mL), 305 K. The epoxidation was initiated by addition of cyclooctene after the pretreatment of TBA-**4** with aqueous hydrogen peroxide for 60 min at 305 K, and R_0 values were determined from the reaction profiles at low conversions (<10%) of both cyclooctene and hydrogen peroxide. Slope = 0.94 (R^2 = 0.99).

3.4. Conclusion

In conclusion, tetra-*n*-butylammonium salt of silicotungstate compound, $[\gamma\text{-}SiW_{10}O_{34}(H_2O)_2]^{4-}$ (TBA-**4**), which is synthesized by protonation of a divacant lacunary Keggin-type POM of $[\gamma\text{-}SiW_{10}O_{36}]^{8-}$, is found to be an effective homogeneous catalyst for the oxygen transfer reactions of various substrates including olefins, allylic alcohols, and sulfides with high efficiency of H_2O_2 utilization under the mild conditions. The effectiveness of this catalyst is evidenced by high selectivity to epoxide, efficiency of H_2O_2 utilization, high stereospecificity, and the easy recovery of the catalyst from the homogeneous reaction mixture. TBA-**4** exhibits high regioselectivity for epoxidation of non-conjugated dienes which is quite different from those of various classical reagents. These specific regioselectivity and the order of reactivity for epoxidation of a series of C_6-olefins suggest the contribution of active species on the divacant site of the rigid structure of TBA-**4**. The results for the competitive oxidation of *p*-substituted styrenes, oxidation of SSO, and epoxidation of 3-methyl-1-cyclohexene with H_2O_2 catalyzed by TBA-**4** show that the strong electrophilic oxidant species with the steric hindrance is generated. ^{29}Si and ^{183}W NMR and CSI-MS spectra show that the reaction of TBA-**4** with H_2O_2 leads to the generation of the diperoxo species of TBA-**5**. While the isolated compound TBA-**5** is inactive for the stoichiometric epoxidation of cyclooctene, the epoxidation using TBA-**5** proceeds in the presence of H_2O_2. The reaction of TBA-**5** with H_2O_2 would form an active oxygen species (TBA-**6**) and the induction period observed for the catalytic epoxidation mainly corresponds to the formation of TBA-**6**. The kinetic, spectroscopic, and mechanistic investigations show that the present olefin epoxidation proceeds *via* TBA-**6**.

3.5. References

[1] R. A. Sheldon, J. K. Kochi, *Metal Catalyzed Oxidations of Organic Compounds*, Academic Press, New York, **1981**.

[2] C. L. Hill in *Advances in Oxygenated Processes, Vol. 1* (Eds.: A. L. Baumstark), JAI Press, London, **1988**, p. 1-30.

[3] M. Hudlucky, *Oxidations in Organic Chemistry*, ACS Monograph Series, American Chemical Society, Washington, DC, **1990**.

[4] *Chem. Eng. News* September 6, **2004**, *82*, 15.

[5] K. A. Jørgensen, *Chem. Rev.* **1989**, *89*, 431.

[6] B. S. Lane, K. Burgess, *Chem. Rev.* **2003**, *103*, 2457.

[7] R. Noyori, M. Aoki, K. Sato, *Chem. Commun.* **2003**, 1977.

[8] D. E. De Vos, B. F. Sels, P. A. Jacobs, *Adv. Synth. Catal.* **2003**, *345*, 457.

[9] J.-M. Brégeault, *Dalton Trans.* **2003**, 3289.

[10] P. Battioni, J. P. Renaud, J. F. Bartoli, M. Reina-Artiles, M. Fort, D. Mansuy, *J. Am. Chem. Soc.* **1999**, *110*, 8462.

[11] B. Notari, *Adv. Catal.* **1996**, *41*, 253.

[12] C. C. Romão, F. E. Kühn, W. A. Herrmann, *Chem. Rev.* **1997**, *97*, 3197.

[13] C. Venturello, E. Alneri, M. Ricci, *J. Org. Chem.* **1983**, *48*, 3831.

[14] Y. Ishii, K. Yamawaki, T. Ura, H. Yamada, T. Yoshida, M. Ogawa, *J. Org. Chem.* **1988**, *53*, 3587.

[15] K. Sato, M. Aoki, M. Ogawa, T. Hashimoto, D. Panyella, R. Noyori, *Bull. Chem. Soc. Jpn.* **1997**, *70*, 905.

[16] R. Neumann, M. Gara, *J. Am. Chem. Soc.* **1995**, *117*, 5066.

[17] N. Mizuno, C. Nozaki, I. Kiyoto, M. Misono, *J. Am. Chem. Soc.* **1998**, *120*, 9267.

[18] D. E. De Vos, J. L. Meinershagen, T. Bein, *Angew. Chem. Int. Ed. Engl.* **1996**, *35*, 2211.

[19] B. S. Lane, M. Vogt, V. J. DeRose, K. Burgess, *J. Am. Chem. Soc.* **2002**, *124*, 11946.

[20] M. C. White, A. G. Doyle, E. N. Jacobsen, *J. Am. Chem. Soc.* **2001**, *123*, 7194.

[21] K. Chen, M. Costas, L. Que, Jr. *J. Chem. Soc., Dalton Trans.* **2002**, 672.

[22] M. G. Clerici, G. Bellussi, U. Romano, *J. Catal.* **1991**, *129*, 159.

[23] Thematic issue on "Polyoxometalates", *Chem Rev.* **1998**, *98*, 1–389.

[24] a) T. Okuhara, N. Mizuno, M. Misono, *Adv. Catal.* **1996**, *41*, 113; b) N. Mizuno, M. Misono, *Chem. Rev.* **1998**, *98*, 199; c) R. Neumann, *Prog. Inorg. Chem.* **1998**, *47*, 317; d) C. L. Hill, C. Chrisina, M. Prosser-McCartha, *Coord. Chem. Rev.* **1995**, *143*, 407; d) I. V. Kozhevnikov, *Chem. Rev.* **1998**, *98*, 171.

[25] N. Mizuno, K. Yamaguchi, K. Kamata, *Coord. Chem. Rev.* **2005**, *249*, 1944

[26] J. Server-Carrió, J. Bas-Serra, M. E. González-Núnez, A. García-Gastaldi, G. B. Jameson, L. C. W. Baker, R. Acerete, *J. Am. Chem. Soc.* **1999**, *121*, 977.

[27] A. Tézé, G. Hervé, *Inorg. Synth.* **1990**, *27*, 85.

[28] a) M. T. Pope, in *Comprehensive Coordination Chemistry II, Vol. 4* (Eds.: J. A. McCleverty, T. J. Meyer), Elsevier Pergamon, Amsterdam, **2004**, p. 635; b) M. T. Pope, *Heteropoly and Isopoly Oxometalates*, Springer-Verlag, Berlin, **1983**.

[29] a) K. Kamata, K. Yonehara, Y. Sumida, K. Yamaguchi, S. Hikichi, N. Mizuno, *Science* **2003**, *300*, 964; b) K. Kamata, Y. Nakagawa, K. Yamaguchi, N. Mizuno, *J. Catal.* **2004**, *224*, 224; c) K. Kamata, M. Kotani, K. Yamaguchi, S. Hikichi, N. Mizuno, *Chem. Eur. J.* in press.

[30] a) J. Canny, A. Tézé, R. Thouvenot, G. Hervé, *Inorg. Chem.* **1986**, *25*, 2114; b) A. Tézé, J. Canny, L. Gurban, R. Thouvenot, G. Hervé, *Inorg. Chem.* **1996**, *35*, 1001; c) A. Tézé, E. Cadot, V. Béreau, G. Hérvé, *Inorg. Chem.* **2001**, *40*, 2000; d) A. Tézé, M. Michelon, G. Hervé, *Inorg. Chem.* **1997**, *36*, 5666.

[31] C. Venturello, R. D'Aloisio, J. C. J. Bart, M. Ricci, *J. Mol. Catal.* **1985**, *32*, 107.

[32] A. J. Bailey, W. P. Griffith, B. C. Parkin, *J. Chem. Soc., Dalton Trans.* **1995**, 1833.

[33] D. D. Perrin, W. L. F. Armarego, *Purification of Laboratory Chemicals, 3rd ed., Pergamon Press*, Oxford, U.K., **1988**.

[34] A. I. Vogel, *A Textbook of Quantitative Inorganic Analysis Including Elementary Instrumental Analysis*, Longman, New York, **1978**.

[35] a) H. Gilman, D. R. Swayampati, *J. Am. Chem. Soc.* **1955**, *126*, 3387; b) M. Bonchio, V. Conte, M. Assunta, D. Conciliis, F. D. Furia, F. P. Ballistrei, G. A. Tomaselli, R. M. Toscano, *J. Org. Chem.* **1995**, *60*, 4475; c) W. Adam, D. Golsch, F. C. Görth, *Chem. Eur. J.* **1996**, *2*, 255.

[36] teXsan, ver. 1.11, Rigaku Corporation, Tokyo (Japan), **2000**.

[37] *International Tables for X-Ray Crystallography*, Kynoch Press, Birmingham, **1975**, vol. 4.

[38] G. M. Sheldrick, *SHELXS-86*, University of Göttingen, **1986**.

[39] P. T. Beurskens *et al.*, *DIRDIF 92*, University of Nijmegen, **1992**.

[40] G. M. Sheldrick, *SHELXL-97*, University of Göttingen, **1997**.

[41] a) R. A. Sheldon, J. A. Van Doorn, *J. Catal.* **1973**, *31*, 427; b) R. A. Sheldon, J. A. Van Doorn, C. W. A. Schram, A. J. De Jong, *J. Catal.* **1973**, *31*, 438.

[42] G. B. Payne, P. H. Deming, P. Williams, *J. Org. Chem.* **1961**, *26*, 651.

[43] I. D. Brown, D. Altermatt, *Acta Crystallogr.* **1985**, *B41*, 244. Bond valences of hydrogen bonds are not included.

[44] S. Ueno, K. Yamaguchi, K. Yoshida, K. Ebitani, K. Kaneda, *Chem. Commun.* **1998**, 295.

[45] A. L. Baumstark, P. C. Vasquez, *J. Org. Chem.* **1988**, *53*, 3437.

[46] M. G. Clerici, P. Ingallina, *J. Catal.* **1993**, *140*, 71.

[47] T. Blasco, M. A. Camblor, A. Corma, J. P. Pérez-Pariente, *J. Am. Chem. Soc.* **1993**, *115*, 11806.

[48] T. Maschmeyer, F. Rey, G. Sankar, J. M. Thomas, *Nature* **1995**, *378*, 159.

[49] P. T. Tanev, M. Chibwe, T. J. Pinnavaia, *Nature* **1994**, *368*, 321.

[50] P. Wu, T. Tatsumi, *Chem. Commun.* **2002**, 1026.

[51] a) A. L. Villa, B. F. Sels, D. E. De Vos, P. A. Jacobs, *J. Org. Chem.* **1999**, *64*, 7267; b) S. Sakaguchi, Y. Nishiyama, Y. Ishii, *J. Org. Chem.* **1996**, *61*, 5307; c) K. Kamata, K. Yamaguchi, S. Hikichi, N. Mizuno, *Adv. Synth. Catal.* **2003**, *345*, 1193; d) K. Kamata, K. Yamaguchi, N. Mizuno, *Chem. Eur. J.* **2004**, *10*, 4728.

[52] K. S. Suslick, in *The Porphyrin Handbook, Vol 4* (Eds: K. M. Kadish, K. M. Smith, R. Guilard), Academic Press, New York, **2000**, pp. 41.

[53] A. Asouti, L. P. Hadjiarapoglou, *Synlett* **2001**, 1847.

[54] M. N. Sheng, J. G. Zajacek, *J. Org. Chem.* **1970**, *35*, 1839.

[55] U. Arnold, R. S. da Cruz, D. Mandelli, U. Schuchardt, *J. Mol. Catal. A: Chem.* **2001**, *165*, 149.

[56] A. A. Valente, I. S. Gonçalves, A. D. Lopes, J. E. Rodríguez-Borges, M. Pillinger, J. Rocha, C. C. Romão, X. G. Mera, *New. J. Chem.* **2001**, *25*, 959.

[57] J. T. Groves, T. E. Nemo, *J. Am. Chem. Soc.* **1983**, *105*, 5786.

[58] K. S. Suslick, B. R. Cook, *J. Chem. Soc., Chem. Commun.* **1987**, 200.

[59] C. K. Chang, C. Y. Yeh, T. S. Lai, *Macromol. Symp.* **2000**, *156*, 117.

[60] T. S. Lai, S. K. S. Lee, L. L. Yeung, H. Y. Liu, I. D. Williams, C. K. Chang, *Chem. Commun.* **2003**, 620.

[61] S. Sakaguchi, Y. Nishiyama, Y. Ishii, *J. Org. Chem.* **1996**, *61*, 5307.

[62] L. Salles, C. Aubry, R. Thouvenot, F. Robert, C. Dorémieux-Morin, G. Chottard, H. Ledon, Y. Jeannin, J.-M. Brégeault, *Inorg. Chem.* **1994**, *33*, 871.

[63] B. F. Sels, A. L. Villa, D. Hoegaerts, D. E. De Vos, P. A. Jacobs, *Top. Catal.* **2000**, *13*, 223.

[64] A. L. Villa, B. F. Sels, D. E. De Vos, P. A. Jacobs, *J. Org. Chem.* **1999**, *64*, 7267.

[65] S. Tangestaninejad, B. Yadollahi, *Chem. Lett.* **1998**, 511.

[66] R. Neumann, D. Juwiler, *Tetrahedron* **1996**, *52*, 8781.

[67] M. Bösing, A. Nöh, I. Loose, B. Krebs, *J. Am. Chem. Soc.* **1998**, *120*, 7252.

[68] J. F. Bartoli, K. L. Barch, M. Palacio, P. Battioni, D. Mansuy, *Chem. Commun.* **2001**, 1718.

[69] J. C. van der Waal, M. S. Rigutto, H. van Bekkum, *Appl. Catal. A* **1998**, *167*, 331.

[70] T. R. Boehlow, C. D. Spilling, *Tetrahedron Lett.* **1996**, *37*, 2717.

[71] J. Prandi, H. B. Kagan, H. Mimoun, *Tetrahedron Lett.* **1986**, *27*, 2617.

[72] R. G. Carlson, N. S. Behn, C. Cowles, *J. Org. Chem.* **1971**, *36*, 3832.

[73] G. Majetich, R. Hicks, *Synlett* **1996**, 649.

[74] G. Majetich, R. Hicks, G. Sun, P. McGill, *J. Org. Chem.* **1998**, *63*, 2564.

[75] P. Bhyrappa, J. K. Young, J. S. Moore, K. S. Suslick, *J. Am. Chem. Soc.* **1996**, *118*, 5708.

[76] P. Bhyrappa, J. K. Young, J. S. Moore, K. S. Suslick, *J. Mol. Catal. A* **1996**, *113*, 109.

[77] N. Mizuno, M. Tateishi, T. Hirose, M. Iwamoto, *Chem. Lett.* **1993**, 1985.

[78] M. C. A. van Vliet, D. Mandelli, I. W. C. E. Arends, U. Schuchardt, R. A. Sheldon, *Green Chem.* **2001**, *3*, 243.

[79] M. C. A. van Vliet, I. W. C. E. Arends, R. A. Sheldon, *Synlett* **2001**, 248.

[80] M. C. A. van Vliet, I. W. C. E. Arends, R. A. Sheldon, *Synlett* **2001**, 1305.

[81] A. M. Al-Ajlouni, J. H. Espenson, *J. Org. Chem.* **1996**, *61*, 3969.

[82] D. Swern, in *Organic Reactions, Vol 7* (Ed.: R. Adams), Wiley, New York, **1953**, pp. 378.

[83] W. Adam, C. R. Saha-Möller, C. G. Zhao, in *Organic Reactions, Vol 63* (Ed.: L. E.

Overman), Wiley, New Jersey, **2002**, pp. 219.

[84] H. Arakawa, Y. Moro-oka, A. Ozaki, *Bull. Chem. Soc. Jpn.* **1974**, *41*, 2958.

[85] H. Mimoun, M. Mignard, P. Brechot, L. Saussine, *J. Am. Chem. Soc.* **1986**, *108*, 3711.

[86] G. Amato, A, Arcoria, F. Paolo, B, Gaetano, A, Tomaselli, *J. Mol. Catal.* **1986**, *37*, 165.

[87] D. V. Deubel, G. Frenking, H. M. Senn, J. Sundermeyer, *Chem. Commun.* **2000**, 2469.

[88] D. V. Deubel, J. Sundermeyer, G. Frenking, *J. Am. Chem. Soc.* **2000**, *122*, 10101.

[89] a) H. Mimoun, I. S. De Roch, L. Sajus, *Tetrahedron*, **1970**, *26*, 37; b) H. Mimoun, *Angew. Chem. Int. Ed. Engl.* **1982**, *21*, 734.

[90] a) K. B. Sharpless, J. M. Townsend, D. R. Williams, *J. Am. Chem. Soc.* **1972**, *94*, 295; b) O. Chong, K. B. Sharpless, *J. Org. Chem.* **1977**, *42*, 1587.

[91] a) W. R. Thiel, T. Priermeier, *Angew. Chem. Int. Ed. Engl.* **1995**, *34*, 1737; b) W. R. Thiel, *Chem. Ber.* **1996**, *129*, 575; c) A Hroch, G. Gemmecker, W. R. Thiel, *Eur. J. Inorg. Chem.* **2000**, 1107.

[92] D. V. Deubel, G. Frenking, P. Gisdakis, W. A. Herrmann, N. Rösch, J. Sundermeyer, *Acc. Chem. Res.* **2004**, *37*, 645.

[93] a) G. Boche, F. Bosold, J. C. W. Lohrenz, M. Marsch, *Chem. Eur. J.* **1996**, *2*, 604; b) G. Boche, K. Möbus, K. Harms, M. Marsch, *J. Am. Chem. Soc.* **1996**, *118*, 2770; c) H. Mimoun, P. Chaumette, M. Mignard, L. Saussine, J. Fischer, R. Weiss, *New. J. Chem.* **1983**, *7*, 467.

[94] W. A. Herrmann, R. W. Fischer, W. Scherer, M. U. Rauch, *Angew. Chem. Int. Ed. Engl.* **1993**, *32*, 1157.

[95] a) A. C. Dengel, W. P. Griffith, B. C. Parkin, *J. Chem. Soc., Dalton Trans.* **1993**, 2683; b) W. P. Griffith, B. C. Parkin, A. J. P. White, D. J. Williams, *J. Chem. Soc., Dalton Trans.* **1995**, 3131; c) N. M. Gresley, W. P. Griffith, B. C. Parkin, J. P. White, D. J. Williams, *J. Chem. Soc., Dalton Trans.* **1996**, 2039; d) L. Salles, J.-Y. Piquemal, R. Thouvenot, C. Minot, J.-M. Brégeault, *J. Mol. Catal. A: Chem.* **1997**, *117*, 375.

[96] a) H. J. Ledon, F. Varescon, *Inorg. Chem.* **1984**, *23*, 2735; b) I. V. Yudanov, P. Gisdakis, C. Di Valentin, N. Rösch, *Eur. J. Inorg. Chem.* **1999**, 2135; c) G. Wahl, D. Kleinhenz, A. Schorm, J. Sundermeyer, R. Stowasser, C. Rummy, G. Bringmann, C.

Fickert, W. Kiefer, *Chem. Eur. J.* **1999**, *5*, 3237; d) M. G. Clerici, G. Bellusi, U. Romano, *J. Catal.* **1991**, *129*, 159.

[97] a) R. P. Hanzlik, G. O. Shearer, *J. Am. Chem. Soc.* **1975**, *97*, 5231; b) A. L. Baumstark, P. C. Vasquez, *J. Org. Chem.* **1988**, *53*, 3437; c) A. M. Al-Ajlouni, J. H. Espenson, *J. Am. Chem. Soc.* **1995**, *117*, 9243; d) C.-J. Liu, W.-Y. Yu, S.-G. Li, C.-M. Che, *J. Org. Chem.* **1998**, *63*, 7364.

[98] a) J. Arias, C. R. Newlands, M. M. Abu-Omar, *Inorg. Chem.* **2001**, *40*, 2185; b) D. A. Bennett, H. Yao, D. E. Richardson, *Inorg. Chem.* **2001**, *40*, 2996; c) N. S. Venkataramanan, S. Premsingh, S. Rajagopal, K. Pitchumani, *J. Org. Chem.* **2003**, *68*, 7460.

[99] a) W. Adam, D. Golsch, *Chem. Ber.* **1994**, *127*, 1111; b) W. Adam, D. Golsch, *J. Org. Chem.* **1997**, *62*, 115; c) W. Adam, C. M. Mithcell, C. R. Saha-Möller, T. Selvam, O. Weichold, *J. Mol. Catal. A* **2000**, *154*, 251; d) K. Sato, M. Hyodo, M. Aoki, X. Q. Zheng, R. Noyori, *Tetrahedron* **2001**, *57*, 2469; e) W. A. Herrman, R. W. Fischer, J. D. G. Correia, *J. Mol. Catal.* **1994**, *94*, 213.

[100] a) W. Adam, A. Corma, H. García, O. Weichold, *J. Catal.* **2000**, *196*, 339; b) W. Adam, C. M. Mitchell, C. R. Saha-Möller, *Eur. J. Org. Chem.* **1999**, 785; c) G. Bellucci, G. Berti, M. Ferreti, G. Igrosso, E. Mastrorilli, *J. Org. Chem.* **1978**, *43*, 422; d) R. W. Murray, M. Singh, B. L. Williams, H. M. Moncrieff, *J. Org. Chem.* **1996**, *61*, 1830.

[101] D. C. Duncan, R. C. Chambers, E. Hecht, C. L. Hill, *J. Am. Chem. Soc.* **1995**, *117*, 681.

[102] a) O. W. Howarth, *Prog. Nucl. Magn. Reson. Spectrosc.* **1990**, *22*, 453; b) B. Piggott, S. F. Wong, D. Williams, *J. Inorg. Acta* **1988**, *141*, 275; c) H. Nakajima, T. Kudo, N. Mizuno, *Chem. Mater.* **1999**, *11*, 691; d) N. J. Cambell, A. C. Dengel, C. J. Edwards, W. P. Griffith, *J. Chem. Soc., Dalton Trans.* **1989**, 1203.

[103] a) S. B. Brown, P. Jones, K. Prudhoe, *Inorg. Chim. Acta* **1979**, *34*, 9; b) O. Bortolini, F. Di Furia, G. Modena, *J. Am. Chem. Soc.* **1981**, *103*, 3924.

Chapter IV

Epoxidation of Allylic Alcohols in Water with Hydrogen Peroxide Catalyzed by Dinuclear Peroxotungstate

4.1. Introduction

Oxidations of organic compounds are important in industry and synthetic chemistry.[1-3] Stoichiometric oxidants such as dichromate, permanganate, and manganese dioxide are still often used for the transformations.[1-3] The stoichiometric use and disposal of such oxidants are undesirable from the economical and environmental viewpoints. Therefore, much attention has been paid to the use of transition-metal catalysts to achieve the effective oxidation with molecular oxygen and hydrogen peroxide as oxidants.[4-7]

Epoxidation of allylic alcohols is of great importance[8,9] because the epoxides have been used as raw materials for epoxy resins and building blocks for the synthesis of biologically important compounds including natural products,[10,11] and chiral carbons are formed by the epoxidation. Katsuki-Sharpless system with *tert*-butyl hydroperoxide (TBHP) is an important example for the epoxidation of allylic alcohols while the stereoselective epoxidation needs optically active tartrate.[12] Although many methods for the epoxidation of allylic alcohols have been developed, catalytic processes with expensive and environmentally-unacceptable oxidants such as peracids and hydroperoxides in explosive, hazardous, and carcinogenic organic solvents are still widely used.[13] In this context, the developments of efficient catalytic processes using H_2O_2 or O_2 as a green oxidant in non-explosive solvent, especially water, achieve the economical and environmental benefits, and remain challenging.[4-7, 14-17]

Many tungsten-based catalysts have been reported to be active for the epoxidation of allylic alcohols with H_2O_2.[18-28] Most of them need strict pH control with amines or buffers and/or use biphasic procedures because of decomposition of both the allylic alcohols and the epoxides.[18-28] An efficient and simple route for epoxidation of both internal and terminal olefins with H_2O_2 catalyzed by the divacant lacunary silicotungstate, $[(n\text{-}C_4H_9)_4N]_4[\gamma\text{-}SiW_{10}O_{34}(H_2O)_2]$, was reported in chapter III.[29] During the course of the investigation of tungsten-catalyzed oxidation, it was found that use of sodium and potassium salts of lacunary polyoxometalates in water solvent was more efficient and chemoselective for epoxidation of allylic alcohols with H_2O_2 than that of tetra-*n*-butylammonium salt of $[\gamma\text{-}SiW_{10}O_{34}(H_2O)_2]^{4-}$ in organic solvent. *In situ* IR, ^{183}W NMR, and UV/Vis spectroscopy for the reaction of inorganic salts of lacunary polyoxometalates with H_2O_2 in water solvent showed the generation of dinuclear

peroxotungstate, $[W_2O_3(O_2)_4(H_2O)_2]^{2-}$ (**8**). This isolated simple dinuclear peroxotungstate, $K_2[W_2O_3(O_2)_4(H_2O)_2]\cdot 2H_2O$ (K-**8**, Figure 4-1), could act as an effective catalyst for the epoxidation of allylic alcohols using hydrogen peroxide *in water* under mild reaction conditions [Eq. (4-1)].[30] The isolated K-**8** itself has never been used for the catalytic epoxidation of allylic alcohols using hydrogen peroxide in water without additives although K-**8** is a previously known compound. In this chapter, the dinuclear peroxotungstate-catalyzed epoxidation of allylic alcohols with hydrogen peroxide in water including the kinetic and mechanistic aspects of the present epoxidation is reported.

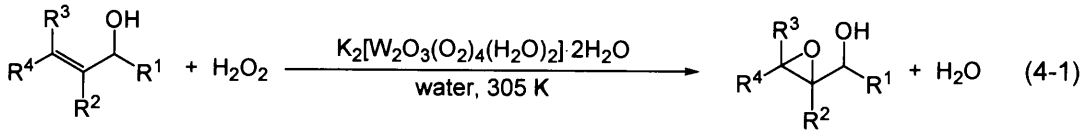

(4-1)

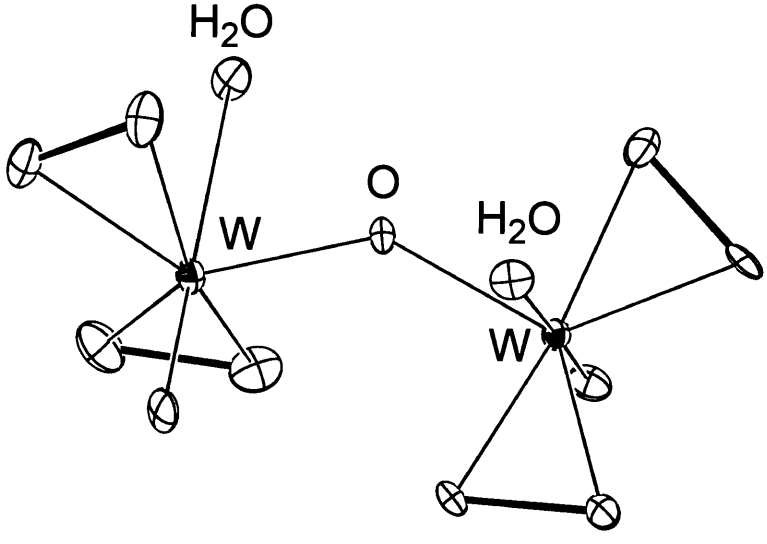

Figure 4-1. Molecular structure of the anion part of $K_2[W_2O_3(O_2)_4(H_2O)_2]\cdot 2H_2O$ (K-**8**).

4.2. Experimental

4.2.1. Instruments

GC analyses were performed on Shimadzu GC-17A with an ionization detector equipped with a TC-WAX capillary column. Mass spectra were determined on Shimadzu GCMS-QP2010 at an ionization voltage of 70 eV. NMR spectra were recorded on JEOL JNM-EX-270. ^{1}H and ^{13}C NMR spectra were measured at 270 and 67.5 MHz, respectively, in $CDCl_3$ or D_2O with TMS as an internal or external standard. ^{183}W NMR spectra of K-**8** were measured at 11.2 MHz in D_2O with Na_2WO_4 (2M D_2O solution) as an external standard. UV-vis spectra were recorded on a Perkin Elmer Lambda 12 spectrometer. IR spectra were measured on Jasco FT/IR-460 Plus using KBr (400–4000 cm^{-1}) or polyethylene disks (below 400 cm^{-1}). *In-situ* IR spectra were measured on a Mettler Toledo React IR 4000 spectrometer.

4.2.2. Materials

The compound K-**8** was synthesized according to the procedure in ref. [31] and characterized by elemental analysis, IR, UV-vis, and ^{183}W NMR spectroscopy, and X-ray crystallographic structural analysis. The characterization results are as follows: Anal. calcd for $K_2[W_2O_3(O_2)_4(H_2O)_2]\cdot 2H_2O$: H, 1.16; O, 34.6; K, 11.27; W, 52.99%. Found: H, 1.12; K, 11.98%; W, 53.19%. IR (400–4000 cm^{-1}: KBr disk; below 400 cm^{-1}: polyethylene disk): ν/cm^{-1} 966 $\nu(W{=}O)$, 854 $\nu(O\text{-}O)$, 764 $\nu_{asym}(W\text{-}O\text{-}W)$, 615 $\nu_{sym}(W(O_2))$, 566 $\nu_{asym}(W(O_2)$, 332 $\nu(W(OH_2))$. UV-vis (H_2O): λ/nm ($\varepsilon/M^{-1}cm^{-1}$) 243 (608). ^{183}W NMR (11.2 MHz, D_2O, Na_2WO_4, 0.3 M, pH = 2.5): δ –704.5. The method[31] for the preparation of the tetra-*n*-hexylammonium derivative of $[W_2O_3(O_2)_4(H_2O)_2]^{2-}$ was modified (i.e., $[(n\text{-}C_6H_{13})_4N]^+$ was replaced by $[(n\text{-}C_{12}H_{25})(CH_3)_3N]^+$) for the synthesis of dodecyltrimethylammonium derivative of **8**. The desired dodecyltrimethylammonium derivative was obtained with a 50% yield. Anal. calcd for $[(n\text{-}C_{12}H_{25})(CH_3)_3N]_2[W_2O_3(O_2)_4(H_2O)_2]$: C, 34.35; H, 7.00; N, 2.70; W, 35.48. Found: C, 35.53; H, 6.92; N, 2.66; W, 35.43. IR (KBr, cm^{-1}): 963, 936, 911, 838, 770, 720, 603, 569, 531. Allylic alcohols of 4-methyl-3-penten-2-ol, (*E*)-3-penten-2-ol, and (*Z*)-3-penten-2-ol were synthesized and confirmed by GC analysis in combination with mass and ^{1}H and ^{13}C NMR spectroscopy as reported

previously.[32-35] All epoxy alcohols are known and have been identified by comparison of their ^{1}H and ^{13}C NMR signals with the literature data.[36-43]

4.2.3. Procedure for Oxidation of Allylic Alcohols

The epoxidation was carried out in a glass vial containing a magnetic stir bar. A typical procedure for the epoxidation of allylic alcohol is as follows: Into a glass vial were successively placed K-**8** (20 μmol), 2-buten-1-ol (5 mmol), H_2O_2 (30% aqueous solution, 5 mmol), and water (6 mL). The reaction mixture was stirred at 305 K for 2 h. After the reaction was finished, the products were extracted by using dichloromethane or *n*-pentane, and the yield and product selectivity were determined by GC or ^{1}H NMR analysis. Recovered aqueous phase was allowed to recycling. Reaction systems are homogeneous except for high-molecular weight alcohol of geraniol (entry 8 in Table 4-3). When the epoxidation of geraniol was carried out with K-**8** under the conditions in Table 4-3, only a 20% yield of 2,3-epoxy geraniol was obtained for 10 h. The epoxidation of geraniol efficiently proceeded by using a lipophilic salt, $[(n\text{-}C_{12}H_{25})(CH_3)_3N]_2[W_2O_3(O_2)_4(H_2O)_2]$, as a catalyst instead of K-**8**. Larger scale reactions (100-mmol scale) were performed via the same procedures as those above described. The turnover frequencies (TOFs) were determined for the initial stage of the epoxidation (~1 h). Reaction conditions for the larger scale reactions were as follows: Allylic alcohol (100 mmol), K-**8** (20 μmol), 30% aq. H_2O_2 (100 mmol), water (120 mL), 305 K, 24 h.

4.2.4. Kinetic Studies

A NMR tube (5 mm diameter) was used as a reactor for the kinetic studies (spin rate, 15 Hz). It was confirmed that the reaction rates were not affected by the spin rates from 10 to 20 Hz. The reaction was periodically monitored by the ^{1}H NMR spectra. Reaction conditions are given in the figure captions (Figures 4-2, 4-3, 4-4, and 4-5). Reaction rates (R_0) for the kinetic studies were determined from the slopes of reaction profiles ($[\text{substrate}]_0$-$[\text{substrate}]_t$ *vs.* time plots) at low conversions (<10%) of the substrate and hydrogen peroxide (initial rate method). The rate constants determined by the slopes of the first-order plots ($-\ln([\text{substrate}]_t/[\text{substrate}]_0$ *vs.* time plots) were in good agreement with those determined by the initial rate method.

4.2.5. Stability of Catalyst

The *in-situ* IR spectra of the reaction solution (2-propen-1-ol (2.0 M), K-**8** (0.1 M), H_2O_2 (2.0 M), water (10 mL), 298 K) were measured with an *in-situ* IR spectrometer to confirm the structure stability of **8**. The band positions and intensities characteristic of K-**8**, *i.e.*, ν(W=O) (966 cm^{-1}) and ν(O-O) (854 cm^{-1}), were periodically monitored. The ν(W-O-W) band could not be observed because of overlap with the intense background of water absorption. No substantial changes in the IR spectra were observed during the catalytic epoxidation. More concentrated solution (2-propen-1-ol (2.0 M), K-**8** (0.3 M), H_2O_2 (2.0 M), D_2O (3 mL)) was used for the ^{183}W NMR measurement because of the lower sensitivity. Under the conditions, the epoxidation of 2-propen-1-ol was completely finished for 20 min. The ^{183}W NMR spectrum showed a signal at –704.5 ppm for the acquisition during catalysis (500 scans, 20 min).

After the epoxidation was completed (reaction conditions in Table 4-1), the products were separated by the extraction with dichloromethane or *n*-pentane and the volume of the aqueous phase was reduced to the half by the evaporation. To the solution, ethanol (20 mL) was added and the precipitate was recovered by the filtration. The stability of the recovered K-**8** was confirmed by the IR (KBr disks) and UV-vis spectra (0.1 mM in H_2O).

4.3. Results and Discussion

4.3.1. Catalytic Epoxidation of Allylic Alcohols

4.3.1.1. Effect of Solvent

Epoxidation of 2-propen-1-ol as a model substrate using 30% aqueous H_2O_2 in various solvents was carried out in the presence of K-**8**. The results are summarized in Table 4-1. The oxidation did not proceed in the absence of K-**8** (entry 2). Water was the most effective solvent for the present epoxidation: 96% Conversion, 99% selectivity to 2,3-epoxy-1-propanol, and 97% efficiency of hydrogen peroxide utilization for the epoxidation of 2-propen-1-ol (entry 1). The use of non-polar toluene, benzene, and dichloromethane solvents (organic/aqueous biphasic system) gave 2,3-epoxy-1-propanol yields of 90, 80, and 63%, respectively (entries 3-5). On the other hand, water-miscible polar acetonitrile (5% yield) and methanol (<1% yield) were poor solvents probably because of the strong coordination to the tungsten center (entries 6 and 7).[44]

4.3.1.2. Effect of Catalyst

The catalytic activity of K-**8** for the epoxidation of 2-propen-1-ol was compared with other tungsten compounds such as H_2WO_4 and K_2WO_4 as shown in Table 4-2. Among tungsten catalysts tested, K-**8** showed the highest yield of the corresponding epoxide: 96% conversion, 99% selectivity to 2,3-epoxy-1-propanol and 97% efficiency of hydrogen peroxide utilization for the epoxidation of 2-propen-1-ol (entry 1). The catalyst precursor of K_2WO_4 showed low catalytic activity due to the non-productive decomposition of hydrogen peroxide, and the efficiency of the H_2O_2 utilization was low (entry 2). In the case of H_2WO_4, the successive hydrolysis of the product of epoxy alcohol to the corresponding triol was dominant while the conversion of 2-propen-1-ol was >99% (entry 3). The selectivity to 2,3-epoxy-1-propanol was increased by the addition of triethylamine to buffer the acidity of the reaction medium (entries 4 and 5).[18,19] However, even in these cases the decomposition of H_2O_2 proceeded to some extent due to the basicity of triethylamine.

Table 1. Oxidation of 2-propen-1-ol with H_2O_2 in various solvents[a]

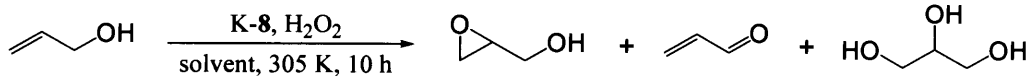

entry	solvent	yield (%)			H_2O_2 efficiency (%)
		epoxide	aldehyde	triol	
1	water	95	1	<1	97
2[b]	water (no catalyst)		no reaction		–
3	toluene	90	2	<1	91
4	benzene	80	<1	<1	90
5	dichloromethane	63	<1	1	79
6	acetonitrile	5	<1	<1	95
7	methanol		no reaction		–

[a] Reaction conditions: Allyl alcohol (5 mmol), K-**8** (100 μmol, 2 mol%), 30% aquesous H_2O_2 (5 mmol), solvent (6 mL), 305 K. Yields were determined by gas chromatography and ^{1}H NMR with an internal standard technique, and based on allyl alcohol. Remaining H_2O_2 after reaction was estimated by potential difference titration of Ce^{3+}/Ce^{4+} (0.1 M of aqueous $Ce(NH_4)_4(SO_4)_4{\cdot}2H_2O$). H_2O_2 efficiency (%) = products (mol)/ consumed H_2O_2 (mol) × 100. [b] Reaction was carried out in the absence of catalyst.

Table 4-2. Oxidation of 2-propen-1-ol with H_2O_2 catalyzed by tungsten compounds [a]

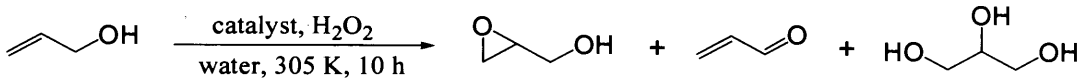

entry	catalytst	yield (%)			H_2O_2 efficiency (%)
		epoxide	aldehyde	triol	
1	K-**8**	95	1	<1	97
2	K_2WO_4	30	<1	<1	32
3	H_2WO_4	<1	<1	>99	>99
4	H_2WO_4-Et_3N (0.29 M)	65	<1	7	76
5	H_2WO_4-Et_3N (0.49 M)	54	<1	1	57
6	without		no reaction		–

[a] Reaction conditions: 2-propen-1-ol (5 mmol), catalyst (W: 200 μmol, 4 mol%), 30% aqueous H_2O_2 (5 mmol), water (6 mL), 305 K. Yields were determined by gas chromatography and ^{1}H NMR with an internal standard technique, and based on 2-propen-1-ol. Remaining H_2O_2 after the reaction was estimated by potential difference titration of Ce^{3+}/Ce^{4+} (0.1 M of aqueous $Ce(NH_4)_4(SO_4)_4{\cdot}2H_2O$). H_2O_2 efficiency (%) = products (mol)/consumed H_2O_2 (mol) × 100.

4.3.1.3. Catalytic Activity for Epoxidation of Allylic Alcohols

Table 4-3 shows the results of epoxidation of various allylic alcohols with 30% aqueous H_2O_2 in the presence of K-**8** without use of the buffer or biphasic system. The pH value of aqueous phase was in the range of 4-5 and no hydrolysis, cleavage, rearrangement of oxirane ring, and allylic oxidation were observed. The catalyst K-**8** was intrinsically stable in the pH range of 2.5–7 as was confirmed by the ^{183}W NMR and IR spectra. The efficiency of the hydrogen peroxide utilization was more than 90% in each case. Oxidation of simple primary allylic alcohols proceeded almost quantitatively and chemoselectively to afford the epoxy alcohols without formation of the corresponding aldehydes and carboxylic acids (entries 1, 2, and 5–7). Larger scale (100 mmol scale) epoxidations of allylic alcohols (K-**8** : H_2O_2 : substrate = 1 : 5000 : 5000) showed turnover frequency (TOF) of 594 h^{-1} and turnover number (TON) of 4200 for 2-buten-1-ol, 442 h^{-1} and 3580 for 3-methyl-2-buten-1-ol, and 167 h^{-1} and 3378 for 2-penten-1-ol [Eq. (4-2)]. These values are higher than those reported to be active for the tungsten-catalyzed epoxidation of internal allylic alcohols with H_2O_2: Na_2WO_4-$NH_2CH_2PO_3H_2$-$[CH_3(n\text{-}C_8H_{17})_3N]HSO_4$ in toluene, 86 h^{-1} (TOF) and 43 (TON);[24] $[C_5H_5N(n\text{-}C_{16}H_{33})]_3PW_{12}O_{40}$ in 1,2-dichloroethane, 5 h^{-1}, 20;[22] $[(n\text{-}C_4H_9)_4N]_2[PhPO_3\{WO(O_2)_2\}]$ in 1,2-dichloroethane, 80 h^{-1}, 40;[23] $\{WZn[M(H_2O)]_2(ZnW_9O_{34})_2\}^{q-}$ (M: Zn^{2+}, Mn^{2+}, Ru^{3+}, Fe^{3+}, etc.) in 1,2-dichloroethane, 167 h^{-1}, 1000;[27,28] Na_2WO_4-phosphate buffer-β-D-fructopyranoside in water, 0.4 h^{-1}, 10.[26] For the epoxidation of *cis*- and *trans*-allylic alcohols, the configurations around the C=C moieties were retained in the corresponding epoxy alcohols (entries 2, 7, and 8). Such a stereospecific epoxidation suggests that the free-radical intermediates are not involved in the epoxidation.

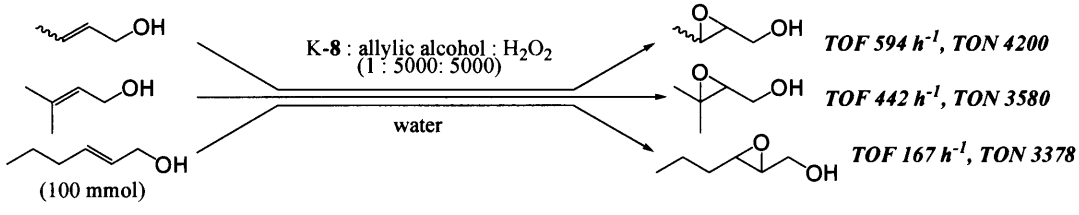

(4-2)

The epoxidation of secondary β,β-disubstituted allylic alcohol (1,3-allylic strained alcohol) proceeded diastereoselectively to form mainly the *threo*-epoxy alcohol (entry 9). Allylic alcohols without 1,3-allylic strain gave *erythro* rich epoxy alcohols (entries 10 and 12). In addition, epoxidation of allylic alcohol, in which 1,3- and 1,2-allylic

strains compete with each other, was more *erythro* selective (entry 13). 2-Cyclohexen-1-ol gave the corresponding epoxy alcohol (>95% *syn* configuration) in a 40% yield together with a 49% yield of 2-cyclohexen-1-one after 12 h under the same conditions as those in Table 4-3. It is noted that the epoxidation of 2-cyclohexen-1-ol was highly stereoselective to give the corresponding epoxy alcohol with oxirane ring *cis* to hydroxyl group (*syn* configuration), while large amounts of α,β-unsaturated ketones were produced for the cyclic allylic alcohols. All these results for the epoxidations of secondary allylic alcohols are similar to those for $VO(acac)_2$/TBHP,[9,45-48] $\{WZn[M(H_2O)]_2(ZnW_9O_{34})_2\}^{q-}/H_2O_2$[27,28], and H_2WO_4/H_2O_2[49] systems in which formation of the metal-alcoholate species in the oxygen transfer step is suggested, and different from those with *m*-CPBA,[5,48] dimethyldioxirane,[5,48] and TS-1/urea-hydrogen peroxide[5,48] systems. In addition, the regioselective epoxidation of geraniol took place at the electron-deficient allylic 2,3-double bond to afford only 2,3-epoxy alcohol in the high yield (entry 8).

No significant changes in the in situ IR spectra were observed during the catalytic epoxidation of 2-propen-1-ol by K-**8** with H_2O_2. In addition, the ^{183}W NMR spectrum of K-**8** after the epoxidation of 2-propen-1-ol showed a signal at –704.5 ppm, which was observed for the as-synthesized K-**8**. IR and UV/Vis spectra of recovered catalyst also suggest the retention of the structure of **8**. These facts show that **8** is stable under the reaction conditions. The first-order dependence of the reaction rate on the concentration of K-**8** as shown in Figure 4-2 supports the idea.

The products could easily be isolated by the simple extraction by using dichloromethane or *n*-pentane after the oxidation since catalyst K-**8** was completely insoluble in these solvents. Actually, no leaching of tungsten into the organic phase was confirmed by inductively coupled plasma atomic emission analysis (ICP-AES). Therefore, the aqueous phase including the catalyst could be recovered without loss of the tungsten species. It is notable that K-**8** can be reused without loss of the catalytic activity, stereospecificity, and chemo-, regio-, and diastereoselectivity for the epoxidation (entries 3, 4, and 10).

Table 4-3. Epoxidation of various allylic alcohols with H_2O_2 in water catalyzed by K-**8**[a]

entry	substrate	time /h	product	yield/ %
1[b]	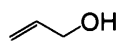	10	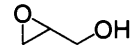	95
2[c]	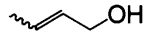	2	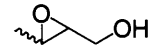	96
3[c,d]	reuse 1	2		97
4[c,d]	reuse 2	2		97
5	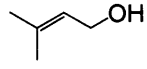	2	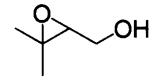	97
6	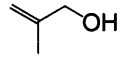	4	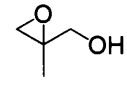	90
7	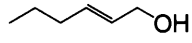	5	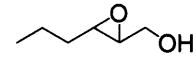	98[e]
8[f]	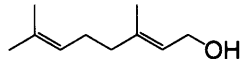	12	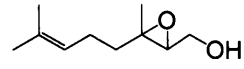	85[e]
9	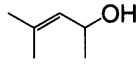	6	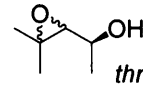 *threo/erythro* = 94/6	85
10[b]	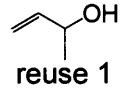	10	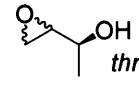	83[g]
11[b,d]	reuse 1	10	*threo/erythro* = 24/76	89[h]
12	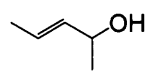	4	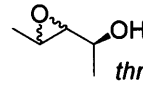 *threo/erythro* = 38/62	83[i]
13	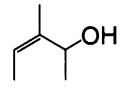	5	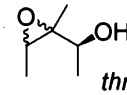 *threo/erythro* = 34/66	77

[a] Reaction conditions: Allylic alcohol (5 mmol), K-**8** (20 μmol, 0.4 mol%), 30% aqueous H_2O_2 (5 mmol), water (6 mL), 305 K. Yields were based on allylic alcohol which were determined by GC and ^{1}H NMR using an internal standard technique. [b] K-**8** (100 μmol, 2 mol%). [c] Substrate: *cis/trans* =13/87, epoxy alcohol: *cis/trans* =13/87. [d] Reuse experiment. [e] Isolated yield. [f] $[(n\text{-}C_{12}H_{25})(CH_3)_3N]_2[W_2O_3(O_2)_4(H_2O)_2]$ (20 μmol) was used as a catalyst. [g] 3-Buten-2-one was produced as a byproduct (7% yield). [h] 3-Buten-2-one was formed as a byproduct (9% yield). [i] 3-Penten-2-one was formed as a byproduct (9% yield).

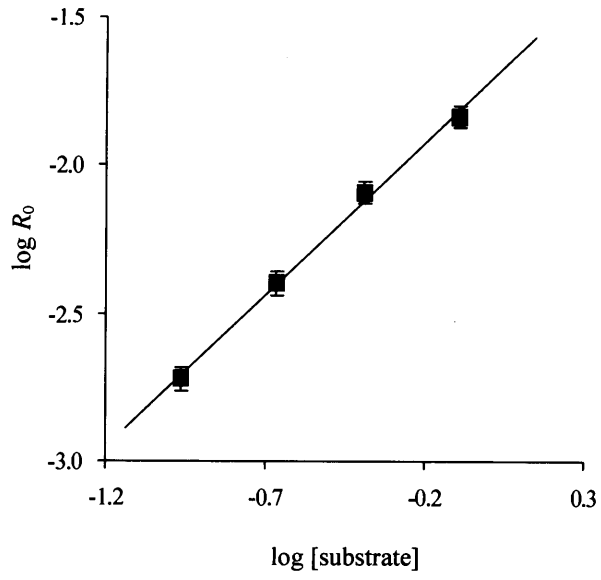

Figure 4-2. Dependence of reaction rate on concentration of 2-buten-1-ol: 2-Buten-1-ol (0.11–0.81 M), K-**8** (2.22 mM), D_2O/H_2O (0.25/0.75 mL), H_2O_2 (0.56 M), 303 K. R_0 values were determined from the reaction profiles at low conversions (<10%) of both 2-buten-1-ol and H_2O_2. Slope = 1.02.

4.3.2. Kinetics and mechanism

The present regioselective epoxidation of allylic alcohol geraniol shows that the allylic hydroxyl function plays an important role in the epoxidation. The need of the hydroxyl functionality is further demonstrated by the complete lack of epoxidation reactivity of the ester and ether derivatives of allyl acetate and 3-methoxy-1-propene. A water/acetonitrile mixed solvent (1/2 vol/vol) was used for the epoxidation to solubilize both the catalyst (K-**8**) and allyl acetate (reaction conditions: Substrate (5 mmol), K-**8** (20 μmol), 30% aqueous H_2O_2 (5 mmol), water/acetonitrile (2/4 mL), 305 K, 24 h). The epoxidation of allyl acetate did not proceed at all, while that of 2-propen-1-ol proceeded to give a 26% yield of 2,3-epoxy-1-propanol under the above conditions. Therefore, the complete lack of epoxidation reactivity of allyl acetate is not caused by the low solubility into an aqueous phase. In this epoxidation, it is

probable that the allylic hydroxyl groups ligate to the tungsten center to form tungsten-alcoholate bond, which prefers the oxygen transfer to the proximal 2,3-allylic double bond rather than to the remote unfunctionalized 6,7-double bond in the case of geraniol. The analogous formation of metal-alcoholate species is suggested at the oxygen transfer step in the allylic alcohol epoxidation systems of $VO(acac)_2$/TBHP, $Ti(O^iPr)_4$/TBHP, $\{WZn[M(H_2O)]_2(ZnW_9O_{34})_2\}^{q-}/H_2O_2$, and H_2WO_4/H_2O_2.[27,28,49] By contrast, non-metal catalyzed *m*-CPBA and dimethyldioxirane systems prefer the epoxidation at 6,7-double bond of geraniol. The selectivity has been explained by the formation of the characteristic hydrogen-bonding in the oxygen transfer step.[27,28] In the present K-**8**-catalyzed system (see-above), the epoxidation of 1,3-allylic strained alcohol proceeded diastereoselectively to give the *threo* diastereoisomer preferentially. The *erythro* selectivity was a little higher in the case of the allylic alcohol without 1,3-allylic strain. These facts are similar to those of $VO(acac)_2$/TBHP and H_2WO_4/H_2O_2 (metal-alcoholate binding mechanism), and different from those of *m*-CPBA and dimethyldioxirane (hydrogen-bonding mechanism). Further, it is noted that the *threo/erythro* ratio in the epoxidation of (*Z*)-3-penten-2-ol catalyzed by K-**8** (*threo/erythro* = 34/66) lies between those for $VO(acac)_2$/TBHP (33/67)[28] and $\{WZn[M(H_2O)]_2(ZnW_9O_{34})_2\}^{q-}/H_2O_2$ (45/55).[28] The stereochemical data suggest that the dihedral angle between the π plane of the double bond and the hydroxy group of the allylic alcohol in the transition-state geometry of the oxygen transfer step for K-**8**-catalyzed epoxidation is 50–70°, in accord with the angle reported for the tungsten-catalyzed epoxidation.[28]

On the basis of these results, a possible catalytic cycle for the present epoxidation is proposed (Scheme 4-1). First, the water ligand of peroxotungstate K-**8** is exchanged by an allylic alcohol to form the tungsten-alcoholate species K-**9** (step 1). The deprotonation of the O-H bond of an allylic alcohol followed by the proton transfer to the peroxo ligand is included in the step 1. The reaction rate for the epoxidation of 2-propen-1-ol decreased with increase in the concentration of protons (Figure 4-3), in accord with the presence of step 1 in Scheme 1. The effect of methanol on the epoxidation of 2-propen-1-ol was examined. The epoxidation was inhibited by the co-existence of methanol and was completely inhibited in the methanol solvent, suggesting that binding of an alcohol functional group to K-**8** is a key step in Scheme 1.

Next, the epoxy alcohol and K-**10** are formed (step 2). Finally, K-**8** is regenerated by the reaction of K-**10** with hydrogen peroxide (step 3). The ^{1}H NMR spectrum of the reaction solution of ethanol (870 mM) catalyzed by K-**8** (50 mM) in D_2O at 305 K after 1 h showed a intense resonance of ethanol together with a set of signals at δ 1.44 (t, ^3J = 5.1 Hz) and δ 2.21 (d, ^3J = 2.5 Hz) due to the methyl protons, at δ 5.35 (q, ^3J = 5.1 Hz) due to the methylene protons, and at δ 9.79 (q, ^3J = 2.5 Hz) due to the formyl proton. The signals at δ 1.44 and δ 5.35 sharply increased followed by the increase in the signals at δ 2.21 and δ 9.79. The signal at δ 2.04 (s) appeared with an induction period and can be assigned to acetic acid. The ^{1}H and ^{13}C NMR spectra of the reaction solution of K-**8** (50 mM) with 2-propen-1-ol (870 mM) in D_2O in the range of 278–305 K showed only resonances of 2-propen-1-ol and 2,3-epoxy-1-propanol, and no resonances due to tungsten-alcoholate species were observed. The signals at δ 2.21 and δ 9.79 can be assigned to acetaldehyde. The ^{1}H NMR signals of the α-protons of tungsten-alcoholate species have been reported in the range of δ 4.8–5.8.[50,51] Therefore, the signal at δ 5.35 can be assigned to the methylene protons of the tungsten-ethoxide species formed through the reaction of ethanol with K-**8**. The signal at δ 1.44 can also be assigned to the methyl protons of the tungsten-ethoxide species. The ^{13}C NMR spectrum showed a resonance at δ 87.9 due to the methylene carbon of the tungsten-ethoxide species.[50.51] These results also suggests the formation of K-**9** during the present epoxidation.

The kinetic studies for the epoxidation of an internal allylic alcohol 2-buten-1-ol showed the reasonable first-order plots for the loss of concentration of 2-buten-1-ol (0.11–0.81 M) (Figure 2). In addition, the first-order dependences of the reaction rate on the concentration of catalyst K-**8** (0.92–4.12 mM) (Figure 4-4) and the zero-order dependence on the concentration of H_2O_2 (0.34–0.78 M) (Figure 4-5) were observed. Kinetic studies on the epoxidation of a terminal allylic alcohol of 2-propen-1-ol also show the first-order dependence of the reaction rate on both concentrations of 2-propen-1-ol (0.31–0.69 M) and catalyst K-**8** (3.8–11.4 mM), and the zero-order dependence on the concentration of H_2O_2 (0.14–0.56 M). Therefore, the reaction rate equation was expressed by following equation [Eq. (4-3)]. R_0 and k are reaction rate and rate constant, respectively. This means that the transition state is composed of one

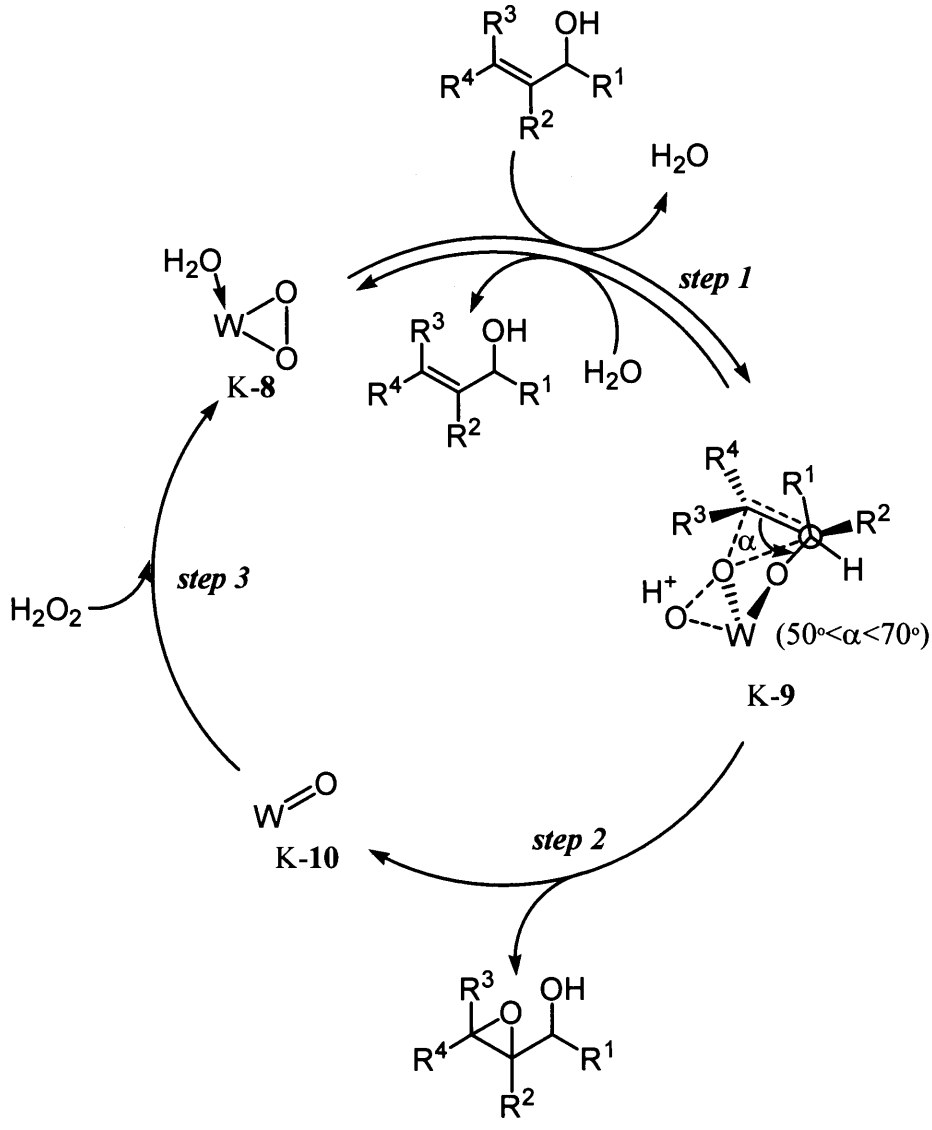

Scheme 4-1. Proposed mechanism for epoxidation of allylic alcohols catalyzed by K-**8**.

molecule of K-**8** and one of an allylic alcohol, but not of H_2O_2.

$$R_0 = -\frac{d[\text{allylic alcohol}]}{dt} = k[\text{K-}\mathbf{8}]^1[\text{allylic alcohol}]^1[H_2O_2]^0 \qquad (4\text{-}3)$$

The dependence of the reaction rate of 2-buten-1-ol on the temperature (Arrhenius plots, 296–328 K) is shown in Figure 4-6. The good linearity of the Arrhenius plots was observed to afford the following activation parameters: E_a = 55.9 kJ·mol^{-1}, ln$A$ = 18.1, $\Delta H^{\ddagger}_{305\ K}$ =53.4 kJ·mol^{-1}, $\Delta S^{\ddagger}_{305\ K}$ = −137.4 J·mol^{-1}·K^{-1}, and $\Delta G^{\ddagger}_{305\ K}$ = 95.3 kJ·mol^{-1}. The dependence of the reaction rate of 2-propen-1-ol on the temperature was also examined to give the following activation parameters: E_a = 68.1 kJ·mol^{-1}, ln$A$ = 20.5, $\Delta H^{\ddagger}_{305\ K}$ =65.6 kJ·mol^{-1}, $\Delta S^{\ddagger}_{305\ K}$ = −117.1 J·mol^{-1}·K^{-1}, and $\Delta G^{\ddagger}_{305\ K}$ = 101.3 kJ·mol^{-1}. The parameters for 2-buten-1-ol was different from those for 2-propen-1-ol while the activation energies (E_a) are in the range of 49–86 kJ·mol^{-1} reported for tungsten-catalyzed epoxidation.[52,53]

When the regeneration rate (step 3) was estimated by tracing the reaction of K-**10** with H_2O_2 by using an *in situ* IR spectrometer, the regeneration was completed within 1 min and the rate was larger than that for the catalytic epoxidation reaction under the same conditions. The zero-order dependence on the concentration of H_2O_2 was observed. These results show that the regeneration of tungsten species K-**10** with H_2O_2 (step 3) smoothly proceeds and is not a rate-limiting step.

The stoichiometric epoxidation of 2-buten-1-ol (1.9 mmol, 0.40 M) with K-**8** (40 μmol) produced 166 μmol of 2,3-epoxy-1-butanol, showing that K-**8** has 4 equiv. active oxygen [Eq. (4-4)]. The rate of stoichiometric epoxidation of 2-buten-1-ol was 8.1×10^{-3} M·min^{-1} and fairly agreed with that of the catalytic epoxidation under the same conditions (8.8×10^{-3} M·min^{-1}); this shows that step 3 is not a rate-limiting step.

(4-4)

Figure 4-7 shows the dependence of the epoxidation rate of 2-propen-1-ol on the content of D_2O (x = [D_2O]/([D_2O] + [H_2O])). The reaction rate was not affected by the presence of D_2O and the proton of the OH group in 2-propen-1-ol was isotopically in equilibrium with the proton in water. These facts show that the deprotonation of O-H bond of an allylic alcohol followed by the protonation of the peroxo ligand is fast and in equilibrium and that the oxygen transfer step from peroxotungstate to an allylic double

bond (step 2) is included in a rate-limiting step in the case of a terminal allylic alcohol. On the other hand, the rate for the epoxidation of an internal allylic alcohol 2-buten-1-ol decreased with increasing the contents of D_2O (Figure 4-8). The decrease in the rate by the presence of D_2O is probably explained as follows: The rate for the 2-buten-1-ol epoxidation was 30 times larger than that for 2-propen-1-ol and therefore the forward process in step 1 would become contributive to a rate-limiting step. The idea is supported by the different activation parameters between 2-propen-1-ol and 2-buten-1-ol.

4.4. Conclusion

In summary, the dinuclear peroxotungstate K-**8** is found to be an effective homogeneous catalyst for the epoxidation of allylic alcohols in water with high efficiency of H_2O_2 utilization. In addition, K-**8** can be reused with retention of the high catalytic activity, stereospecificity and chemo-, regio-, and diastereoselectivity for the epoxidation. The kinetic, spectroscopic, and mechanistic investigation show that the dinuclear peroxotungstate-catalyzed allylic alcohol epoxidation proceeds via the O-H bond deprotonation of allylic alcohols followed by the proton transfer to peroxotungstate/alcoholate formation mechanism.

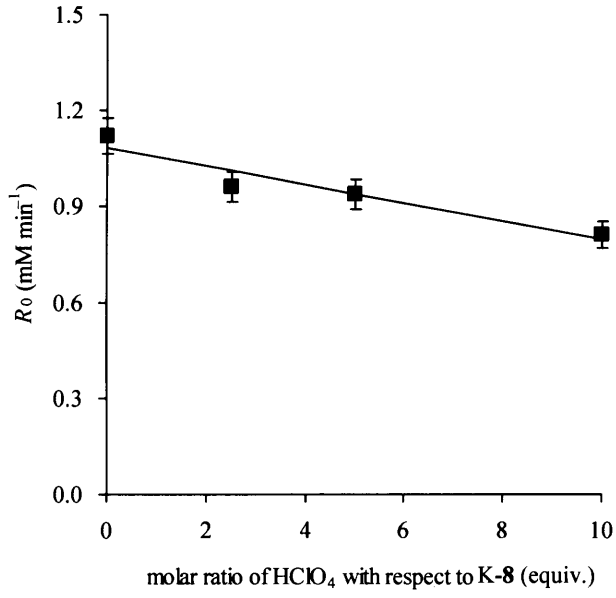

Figure 4-3. Effects of proton on reaction rate for the epoxidation of 2-propen-1-ol: 2-Propen-1-ol (0.37 M), K-**8** (4.5 mM), D_2O/H_2O (0.25/0.75 mL), H_2O_2 (0.52 M), 305 K. R_0 values were determined from the reaction profiles at low conversions (<10%) of both 2-propen-1-ol and H_2O_2.

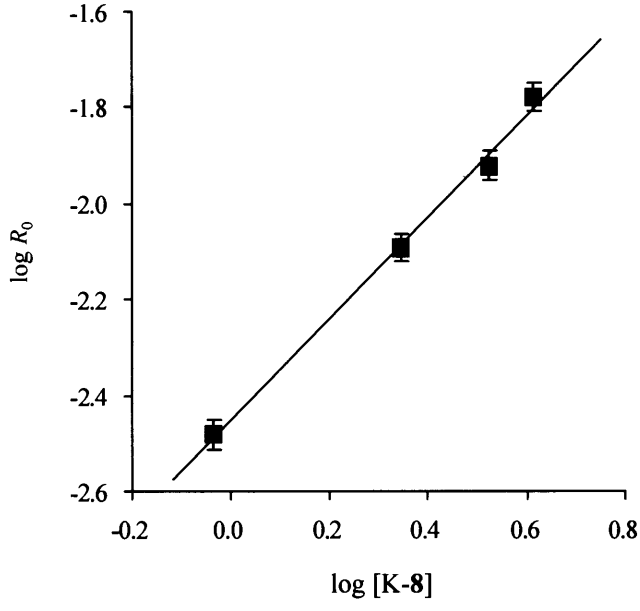

Figure 4-4. Dependence of reaction rate on concentration of K-**8**: 2-buten-1-ol (0.40 M), K-**8** (0.92–4.12 mM), D_2O/H_2O (0.25/0.75 mL), H_2O_2 (0.56 M), 303 K. R_0 values were determined from the reaction profiles at low conversions (<10%) of both 2-buten-1-ol and H_2O_2. Slope = 1.03.

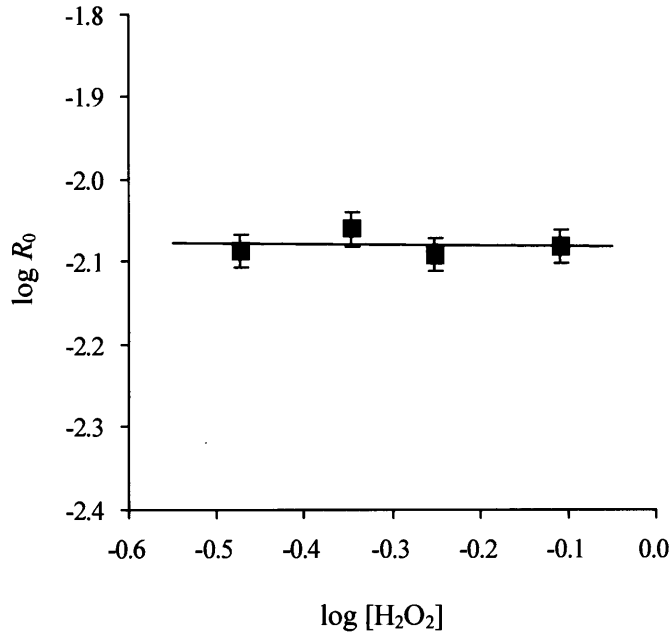

Figure 4-5. Dependence of reaction rate on concentration of hydrogen peroxide: 2-buten-1-ol (0.40 M), K-**8** (2.22 mM), D_2O/H_2O (0.25/0.75 mL), H_2O_2 (0.34–0.78 M), 303 K. R_0 values were determined from the reaction profiles at low conversions (<10%) of both 2-buten-1-ol and H_2O_2. Slope = –0.01.

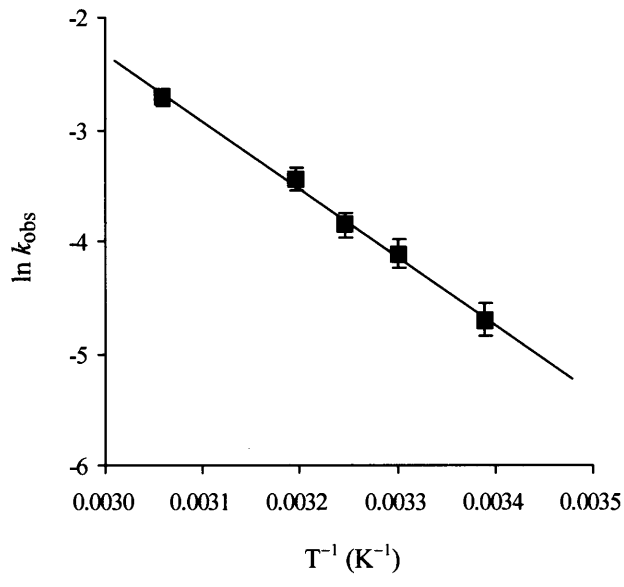

Figure 4-6. Arrhenius plots for the epoxidation of 2-buten-1-ol: 2-Buten-1-ol (0.40 M), K-**8** (2.22 mM), D_2O/H_2O (0.25/0.75 mL), H_2O_2 (0.56 M), 295–328 K. The observed rate constants (k_{obs}) were calculated with the initial rates by using Equation (4-3).

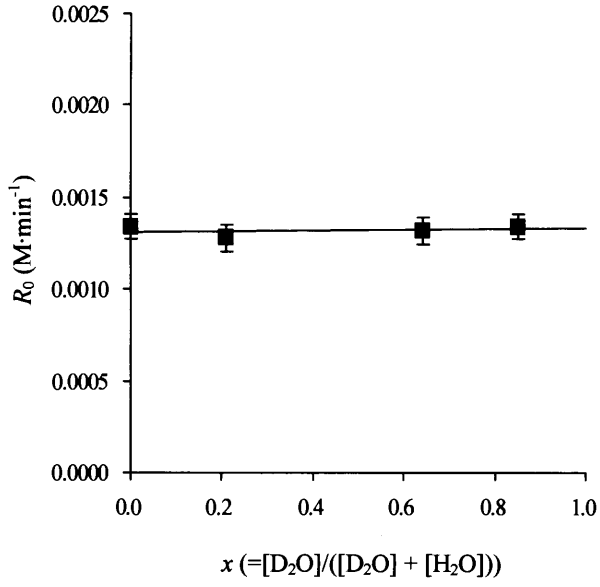

Figure 4-7. Dependence of epoxidation rate of 2-propen-1-ol on the content of D_2O (x = [D_2O]/([D_2O] + [H_2O])): 2-propen-1-ol (0.46 M), K-**8** (11.1 mM), D_2O + H_2O (1 mL), H_2O_2 (0.56 M), 303 K. R_0 values were determined from the reaction profiles at low conversions (<10%) of both 2-propen-1-ol and H_2O_2.

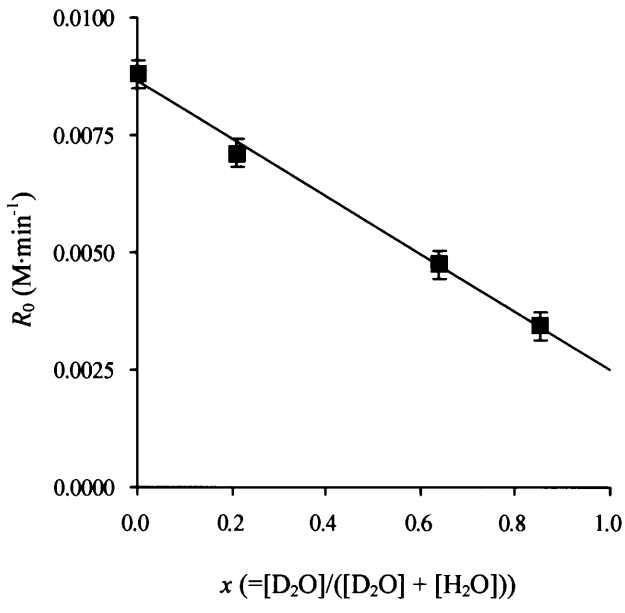

Figure 4-8. Dependence of epoxidation rate of 2-buten-1-ol on the content of D_2O (x = [D_2O]/([D_2O] + [H_2O])). Reaction conditions: 2-Buten-1-ol (0.40 M), K-**8** (2.22 mM), D_2O + H_2O (1 mL), H_2O_2 (0.56 M), 303 K. R_0 values were determined from the reaction profiles at low conversions (<10%) of both 2-buten-1-ol and H_2O_2. Line fit: R_0 = $-0.0061x + 0.0086$ ($r^2 = 0.99$).

4.5. References

[1] R. A. Sheldon, J. K. Kochi, *Metal Catalyzed Oxidations of Organic Compounds*, Academic Press, New York, **1981**.

[2] C. L. Hill in *Advances in Oxygenated Processes, Vol. 1* (Eds.: A. L. Baumstark), JAI Press, London, **1988**, p. 1-30.

[3] M. Hudlucky, *Oxidations in Organic Chemistry*, ACS Monograph Series, American Chemical Society, Washington, DC, **1990**.

[4] P. T. Anastas, J. C. Warner, *Green Chemistry: Theory and Practice*; Oxford University Press, **1998**.

[5] J. H. Clark, *Green Chem.* **1999**, *1*, 1.

[6] R. A. Sheldon, *Green Chem.* **2000**, *2*, G1.

[7] P. T. Anastas, L. B. Bartlett, M. M. Kirchhoff, T. C. Williamson, *Catal. Today* **2000**, *55*, 11.

[8] K. A. Jørgensen, *Chem. Rev.* **1989**, *89,* 431.

[9] W. Adam, T. Wirth, *Acc. Chem. Res.* **1999**, *32*, 703.

[10] P. A. Bartlett, *Tetrahedron* **1980**, *36*, 2.

[11] P. Besse, H. Veschambre, *Tetrahedron* **1994**, *50*, 8885.

[12] T. Katsuki, K. B. Sharpless, *J. Am. Chem. Soc.* **1980**, *102,* 5974.

[13] A. S. Rao, *Comprehensive Organic Synthesis, Vol. 7* (Eds.: B. M. Trost), Pergamon Press, Oxford, **1991**, p.357-387.

[14] G.-J. ten Brink, I. W. C. E. Arends, R. A. Sheldon, *Science* **2000**, *287*, 1636.

[15] Thematic issue on "Green Chemistry", *Acc. Chem. Res.* **2002**, *35*, 685-816.

[16] Thematic issue on "Organic Reaction in Water", *Adv. Synth. Catal.* **2002**, *3-4*, 219-451.

[17] R. Noyori, M. Aoki, K. Sato, *Chem. Commun.* **2003**, 1977.

[18] Z. Racizsewski, *J. Am. Chem. Soc.* **1960,** *82,* 1267.

[19] D. Prat, B. Delpech, R. Lett, *Tetrahedron Lett.* **1986**, *27*, 711.

[20] J. Prandi, H. B. Kagan, H. Mimoun, *Tetrahedron Lett.* **1986**, *27,* 2617.

[21] M. Quenard, V. Bonmarin, G. Gelbard, *Tetrahedron Lett.* **1987**, *28,* 2237.

[22] Y. Ishii, K. Yamawaki, T. Ura, H. Yamada, T. Yoshida, M. Ogawa, *J. Org. Chem.* **1988**, *53,* 3587.

[23] G. Gelbard, F. Raison, E. R. Lachter, R. Thouvenot, L. Ouahab, D. Grandjean, *J,*

Mol. Catal. A **1996,** *114,* 77.

[24] K. Sato, M. Aoki, M. Ogawa, T. Hashimoto, R. Noyori, *Bull. Chem. Soc. Jpn.* **1997**, *70,* 905.

[25] D. Hoegaerts, B. F. Sels, D. E. de Vos, F. Verpoort, P. A. Jacobs, *Catal. Today* **2000**, *60*, 209.

[26] C. Denis, K. Misbahi, A. Kerbal, V. Ferrieres, D. Plusquellec, *Chem. Commun.* **2001**, 2460.

[27] W. Adam, P. L. Alsters, R. Neumann, C. R. Saha-Möller, D. Sloboda-Rozner, R. Zhang, *Synlett* **2002**, 2011.

[28] W. Adam, P. L. Alsters, R. Neumann, C. R. Saha-Möller, D. Sloboda-Rozner, R. Zhang, *J. Org. Chem.* **2003**, *68*, 1721.

[29] a) K. Kamata, K. Yonehara, Y. Sumida, K. Yamaguchi, S. Hikichi, N. Mizuno, *Science* **2003**, *300*, 964; b) K. Kamata, Y. Nakagawa, K. Yamaguchi, N. Mizuno, *J. Catal.* **2004**, *224*, 224; c) N. Mizuno, K. Yamaguchi, K. Kamata, *Coord. Chem. Rev.* **2005**, *249*, 1944; d) K. Kamata, M. Kotani, K. Yamaguchi, S. Hikichi, N. Mizuno, *Chem. Eur. J.* in press.

[30] a) K. Kamata, K. Yamaguchi, S. Hikichi, N. Mizuno, *Adv. Synth. Catal.* **2003**, *345*, 1193; b) K. Kamata, K. Yamaguchi, N. Mizuno, *Chem. Eur. J.* **2004**, *10*, 4728.

[31] N. J. Cambell, A. C. Dengel, C. J. Edwards, W. P. Griffith, *J. Chem. Soc., Dalton Trans.* **1989**, 1203.

[32] S. Krishnamurthy, H. C. Brown, *J. Org. Chem.* **1975**, *40*, 1864.

[33] S. Krishnamurthy, H. C. Brown, *J. Org. Chem.* **1977**, *42*, 1197.

[34] B. Morgan, A. C. Oehlschlager, T. M. Stokes, *J. Org. Chem.* **1992**, *57*, 3231.

[35] H. O. House, S. S. Ro, *J. Am. Chem. Soc.* **1958**, *80*, 2428.

[36] W. Adam, M. Braun, A. Griesbeck, V. Luccini, E. Staab, B. Will, *J. Am. Chem. Soc.* **1989**, *111*, 203.

[37] M. J. Kurth, M. A. Abreo, *Tetrahedron* **1990**, 46, 5085.

[38] H. Pettersson, A. Gogoll, J.-E. Bäckvall, *J. Org. Chem.* **1992**, *57*, 6025.

[39] H. Fuji, K. Oshima, K. Utimoto, *Chem. Lett.* **1992**, 967.

[40] D. F. Taber, J. B. Houze, *J. Org. Chem.* **1994**, *59*, 4004.

[41] D. C. Dittmer, Y. Zhang, R. P. Discordia, *J. Org. Chem.* **1994**, *59*, 1004.

[42] Y. F. Zheng, D. S. Dodd, A. C. Oehlschlager, P. G. Hartman, *Tetrahedron* **1995**, *51*,

5255.

[43] W. Adam, A. Corma, T. I. Reddy, M. Renz, *J. Org. Chem.* **1997**, *62*, 3631.

[44] H. Mimoun, I. S. De Roch, L. Sajus, *Tetrahedron* **1970**, *26*, 37.

[45] K. B. Sharpless, R. C. Michaelson, *J. Am. Chem. Soc.* **1973**, *95*, 6136.

[46] K. B. Sharpless, T. R. Verhoeven, *Aldrichim. Acta* **1979**, *12*, 63.

[47] T. Ito, K. Jitsukawa, K. Kaneda, S. Teranishi, *J. Am. Chem. Soc.* **1979**, *101*, 159.

[48] W. Adam, R. Kumar, T. I. Reddy, M. Renz, *Angew. Chem.* **1996**, *108*, 578; *Angew. Chem. Int. Ed. Engl.* **1996**, *35*, 533.

[49] W. Adam, C. M. Mitchell, C. R. Saha-Möller, *J. Org. Chem.* **1999**, *64*, 3699.

[50] W. Clegg, R. J. Errington, P. Kraxner, C. Redshaw, *J. Chem. Soc., Dalton Trans.* **1992**, 1431.

[51] D. V. Baxter, M. H. Chisolm, S. Doherty, N. E. Gruhn, *Chem. Commun.* **1996**, 1129.

[52] G. G. Allan and A. N. Neogi, *J. Catal.* **1970**, *16*, 197.

[53] D. V. Deubel, *J. Phys. Chem. A* **2001**, *105*, 4765.

General Conclusions

This thesis deals with studies on the catalyst design of polyoxometalate-based compounds for selective oxygen transfer reactions including epoxidation of mono-olefins, non-conjugated dienes, allylic alcohols, and oxidation of sulfides with H_2O_2 as an oxidant. Based on the unique properties of polyoxometalates controllable at atomic and molecular levels (i.e., composition, size, shape, acidity, basicity, and redox potential), the polyoxometalate catalysts could be developed for the above valuable reactions. In addition, the important information on the detailed reaction mechanism and the relationship between the structure of the active site and reactivity can lead to the design of novel homogenous and heterogeneous catalysts, the highly functionalization of the present catalytic system, and the application to more complicated reaction.

In chapter II, a novel dimeric di-titanium-substituted silicotungstate, $[\{\gamma\text{-}SiTi_2W_{10}O_{36}(OH)_2\}_2(\mu\text{-}O)_2]^{8-}$, is synthesized by the introduction of titanium(IV) ions into a divacant lacunary γ-Keggin-type silicotungstate of $[\gamma\text{-}SiW_{10}O_{36}]^{8-}$. An edge-shared dinuclear titanium core, $Ti_2(\mu\text{-}OH)_2$, is incorporated into the lacunary site. The γ-Keggin di-titanium-substituted silicotungstate catalyzes mono-oxygenation reactions such as epoxidation of olefins and sulfoxidation of sulfides with H_2O_2 under mild conditions. On the other hand, the mono-titanium-substituted silicotungstate, $[\alpha\text{-}SiTiW_{11}O_{39}]^{4-}$, and the fully occupied silicododecatungstate, $[\gamma\text{-}SiW_{12}O_{40}]^{4-}$, are inactive. These results suggest that the active sites are not the Ti-O-W, Ti-O, W-O-W, and W=O centers but the dinuclear titanium core of $Ti_2(\mu\text{-}OH)_2$. The molecular structure is preserved during the catalysis because the ^{29}Si and ^{183}W NMR spectra of the catalyst after the oxidation are consistent with those of as-prepared compound. The $Ti_2(\mu\text{-}OH)_2$ core reacts with MeOH to form the corresponding alkoxo derivative, $[\{\gamma\text{-}SiTi_2W_{10}O_{36}(OH)(OMe)\}_2(\mu\text{-}O)_2]^{8-}$. The results for the reaction with methanol, acid-base titration, and stereospecificity show that the $Ti_2(\mu\text{-}OH)_2$ core would react with H_2O_2 to form $Ti_2(\mu\text{-}OH)(\mu\text{-}OOH)$ species as a active oxygen species.

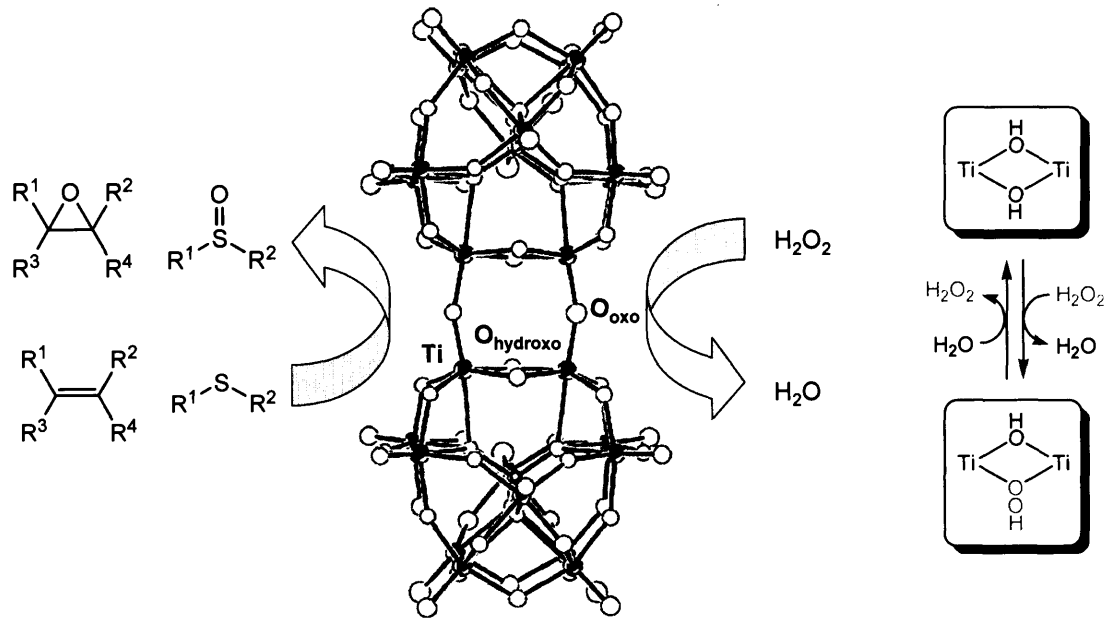

In chapter III, the efficient oxygen transfer reactions of various substrates including olefins, allylic alcohols, and sulfides catalyzed by a novel lacunary silicotungstate of $[\gamma\text{-}SiW_{10}O_{34}(H_2O)_2]^{4-}$, synthesized by the protonation of divacant γ-Keggin type silicotungstate of $[\gamma\text{-}SiW_{10}O_{36}]^{8-}$, are described. The catalytic epoxidation of mono-olefins including non-reactive olefins such as propylene proceeds with ≥99% selectivity to epoxide, ≥99% efficiency of H_2O_2 utilization, high stereospecificity, and easy recovery of the catalyst. For epoxidation of non-conjugated dienes, high regioselectivities which are quite different from those of various classical reagents are observed due to the steric constraints of the active site. The spectroscopic, kinetic, and mechanistic studies show that the activation of H_2O_2 at the lacunary sites involving aqua ligands leads to the generation of the diperoxo species, $[\gamma\text{-}SiW_{10}O_{32}(O_2)_2]^{4-}$, with the maintenance of the γ-Keggin structure and the further protonation of the diperoxo species would form hydroperoxo species as an actual active species. An O-O bond polarization by protonation would allow an electrophilic attack to the olefin. Such strong electrophilic active oxygen species within the rigid structure of lacunary polyoxometalate results in the specific reactivity, regioselectivity, and diastereoselectivity in comparison with the typical stoichiometric oxidants,

mononuclear organometallic compounds, and peroxotungstates.

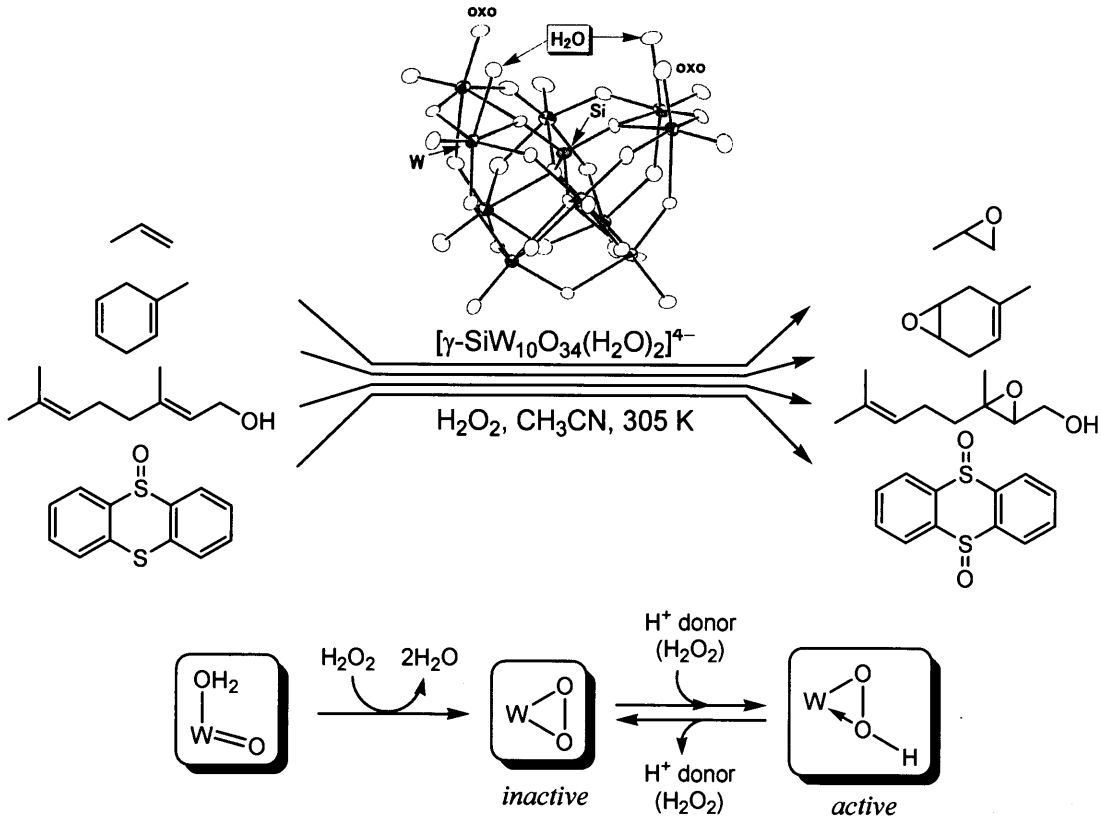

Description in chapter IV is a development of efficient epoxidation of various allylic alcohols in water with H_2O_2 catalyzed by a dinuclear peroxotungstate, $[W_2O_3(O_2)_4(H_2O)_2]^{2-}$. Use of water solvent instead of the explosive, hazardous, and carcinogenic organic solvents provides economical and environmental benefits. The corresponding epoxy alcohols are achieved by using 1 equiv. H_2O_2 with respect to allylic alcohol with high yield, selectivity, efficiency of H_2O_2 utilization. In addition, the catalyst can be reused with retention of the high catalytic activity, stereospecificity and chemo-, regio-, and diastereoselectivity for the epoxidation. The catalytic reaction mechanism including the exchange of the water ligand to form the tungsten-alcoholate species followed by the insertion of oxygen to the carbon-carbon double bond, and the regeneration of the dinuclear peroxotungstate with H_2O_2 is proposed.

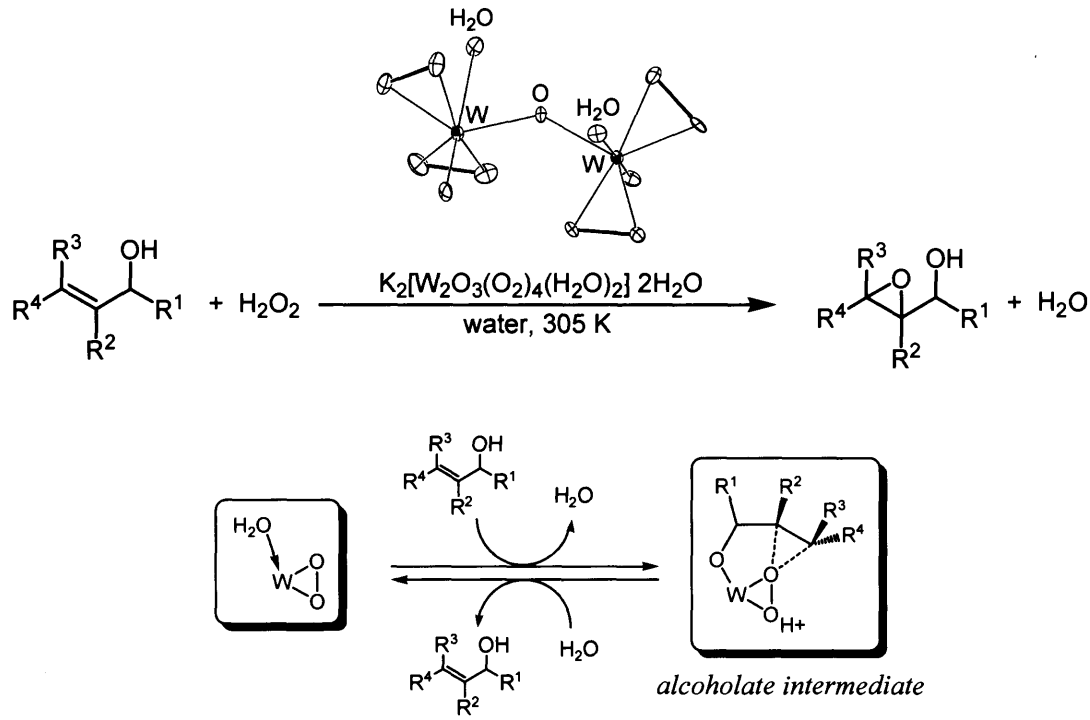

In this thesis, the polyoxometalate-based compounds as highly efficient homogeneous catalysts are designed based on their unique properties. These polyoxometalate catalysts can allow to use "green oxidant" such as H_2O_2 and "green solvent" such as water, which contributes to the solution of the environmental problems. In addition, the high efficiency of H_2O_2 utilization, which means the negligible decomposition of H_2O_2 to form molecular oxygen, reduces the by-products and the risk of building an explosive atmosphere, establishing the simple, efficient, and safe oxidation processes. For the present epoxidation of mono-olefins, non-conjugated dienes, allylic alcohols, and oxidation of sulfides with H_2O_2 as an oxidant, the proton around the catalytically active sites would play an important role in the oxygen transfer step. In the presence of proton (i.e., $Ti_2(\mu\text{-}OH)_2$, H_2O_2, and allylic alcohols), the reaction of the catalyst with H_2O_2 leads to the generation of the most likely hydroperoxide species. In comparison with the classical η^2-peroxo complexes, the hydroperoxo species facilitates a nuclelophilic attack of the substrates such as olefin and sulfide at the peroxo oxygen atom because the peroxo group is polarized by electrophile of proton, resulting in the high catalytic performance.

The specific reactivity and selectivity caused by the unique structure of the functionalized polyoxometalates would be applicable to stereo- and shape-selective organic reactions in the future. Heterogeneous catalysts are more desirable than the homogeneous catalysts from the standpoints of the catalyst/product separation and catalyst recycling. To synthesize heterogeneous catalysts based on polyoxometalates for the liquid-phase oxidation, the following items (1) and (2) are important.

(1) The development of supporting polyoxometalates on appropriate supports without loss of the intrinsic activity and selectivity is challenging and promising.

(2) Complexation of polyoxometalates with appropriate cations to form micro/meso structures would lead to the appearance of the shape selectivity.

List of Publications

[1] Keigo Kamata, Koji Yonehara, Yasutaka Sumida, Kazuya Yamaguchi, Shiro Hikichi, and Noritaka Mizuno,
"Efficient Epoxidation of Olefins with ≥99% Selectivity and Use of Hydrogen Peroxide",
Science, **2003**, *300*, 964–966.

[2] Keigo Kamata, Kazuya Yamaguchi, Shiro Hikichi, and Noritaka Mizuno,
"$[\{W(=O)(O_2)_2(H_2O)\}_2(\mu\text{-}O)]^{2-}$-Catalyzed Epoxidation of Allylic Alcohols in Water with High Selectivity and Utilization of Hydrogen Peroxide",
Advanced Synthesis & Catalysis, **2003**, *345*, 1193–1196.

[3] Keigo Kamata, Yoshinao Nakagawa, Kazuya Yamaguchi, and Noritaka Mizuno,
"Efficient, Regioselective Epoxidation of Dienes with Hydrogen Peroxide Catalyzed by $[\gamma\text{-}SiW_{10}O_{34}(H_2O)_2]^{4-}$"
Journal of Catalysis, **2004**, *224*, 224–228.

[4] Keigo Kamata, KazuyaYamaguchi, and Noritaka Mizuno,
"Highly Selective, Recyclable Epoxidation of Allylic Alcohols with Hydrogen Peroxide in Water Catalyzed by Dinuclear Peroxotungstate",
Chemistry - A European Journal, **2004**, *10*, 4728–4734.

[5] Yuya Goto, Keigo Kamata, Kazuya Yamaguchi, Kazuhiro Uehara, Shiro Hikichi, and Noritaka Mizuno,
"Synthesis, Structural Characterization, and Catalytic Performance of Dititanium-Substituted γ-Keggin Silicotungstate",
Inorganic Chemistry **2006**, *45*, 2347–2356.

[6] Keigo Kamata, Miyuki Kotani, Kazuya Yamaguchi, Shiro Hikichi, and Noritaka Mizuno,
"Olefin Epoxidation with Hydrogen Peroxide Catalyzed by Lacunary Polyoxometalate $[\gamma\text{-}SiW_{10}O_{34}(H_2O)_2]^{4-}$",
Chemistry - A European Journal, **2006**, in press.

<Related Works>

(*Article*)

[7] Noritaka Mizuno, Masaki Hashimoto, Yasutaka Sumida, Yoshinao Nakagawa, and Keigo Kamata,
"Selective Oxidation of Hydrocarbons with Molecular Oxygen Catalyzed by Transition-metal-substituted Polyoxometalates",
Polyoxometalate Chemistry for Nano-Composite Design, Kluwer Academic Publ./Wiley, **2002**, 197–203.

[8] Keigo Kamata, Jun Kasai, Kazuya Yamaguchi, and Noritaka Mizuno,
"Efficient Heterogeneous Oxidation of Alkylarenes with Molecular Oxygen"
Organic Letters, **2004**, *6*, 3577–3580.

[9] Mitsunori Matsushita, Keigo Kamata, Kazuya Yamaguchi, and Noritaka Mizuno,
"Heterogeneously Catalyzed Aerobic Oxidative Biaryl Coupling of 2-Naphthols and Substituted Phenols in Water"
Journal of the American Chemical Society, **2005**, *127*, 6632–6640.

[10] Yoshinao Nakagawa, Keigo Kamata, Miyuki Kotani, Kazuya Yamaguchi, and Noritaka Mizuno,
"Bis(μ-hydroxo) Bridged Di-vanadium-catalyzed Selective Epoxidation of Alkenes with Hydrogen Peroxide",
Angewandte Chemie International Edition, **2005**, *44*, 5136–5140.

(*Book*)

[11] 水野哲孝，鎌田慶吾，山口和也，
「ポリオキソメタレートを用いた分子触媒設計とその酸化触媒作用」，
触媒技術の動向と展望，触媒学会編，**2005**，21–34.

[12] Noritaka Mizuno, Keigo Kamata, and Kazuya Yamaguchi,
"Liquid Phase Oxidations Catalyzed by Polyoxometalates",
Surface and Nanomolecular Catalysis, Taylor and Francis Group, **2006**, 463–492.

(*Review*)

[13] Noritaka Mizuno, Kazuya Yamaguchi, and Keigo Kamata,
"Epoxidaiton of Olefins Catalyzed by Polyoxometalates",
Coordination Chemistry Reviews, **2005**, *249*, 1944–1956.

[14] Noritaka Mizuno, Shiro Hikichi, Kazuya Yamaguchi, Sayaka Uchida, Yoshinao Nakagawa, Kazuhiro Uehara, and Keigo Kamata,
"Molecular design of selective oxidation catalyst with polyoxometalate",
Catalysis Today, **2006**, *117*, 32–36.

Acknowledgements

I wish to express my sincere gratitude to Professor Noritaka Mizuno (The University of Tokyo) for his instructive guidance, invaluable advices, and continuous encouragements throughout the present work. His appropriate supervision leads me to the shortest routs for the goal of the research work. I had an exiting and fruitful time under his attentive guidance. I believe that the experience at Mizuno laboratory is very meaningful for my study and future research work.

I would like to deeply appreciate the judging committee of my thesis, Professor Kazunari Domen (The University of Tokyo), Professor Makoto Fujita (The University of Tokyo), Professor Shiro Hikichi (Kanagawa University), and Professor Masaki Kawano (The University of Tokyo) who gave me valuable and helpful advices for improving and summarizing the present work.

I am grateful to Professor Shiro Hikichi (Kanagawa University) for the X-ray measurements and the helpful suggestions. I am also thankful to Lecturer Kazuya Yamaguchi (The University of Tokyo) for practical advices, technical guidance, and numerous discussions. Without their patient devotions, I will have never finished the present thesis.

I would like to thank Mr. Masahiro Wada, Mr. Yasutaka Sumida, and Dr. Koji Yonehara (Nippon Shokubai Co., Ltd.) for their collaboration and discussion. I have been impressed by their great enthusiasm for researches.

I also wish to appreciate Ms. Chizu Umezu for her kind help in the office works and various problems I met with in daily life.

I wish to thank the past and present members of Mizuno laboratory and CREST project for their suggestions and enjoyable time. I am grateful to Dr. Kazuhiro Uehara and Dr. Syuhei Yamaguchi (Japan Science and Technology Agency (JST)) for the helpful advices and the X-ray structure analyses and Dr. Yoshinao Nakagawa (The University of Tokyo) for the help on quantum chemical calculations. I would like to thank Dr. Takeru Ito (Tokyo Institute of Technology), Dr. Sayaka Uchida (The University of Tokyo), and Mr. Hirotsugu Kano (Sumitomo Chemical Co., Ltd.) for their valuable comments and encouragements. In addition, I appreciate Ms. Miyuki Kotani, Mr. Mitsunori Matsushita, Mr. Jun Kasai, Mr. Yuya Goto, Mr. Atsushi Maniwa, and Mr. Shijiro Kuzuya who made my research life significant and delightful through experiments, discussion, and general support.

Finally, I wish to thank my parents Hiroshi Kamata and Yukiko Kamata, my sister Sachiko Kamata for their continuous encouragement and supports. This thesis is dedicated to my father Hiroshi Kamata who passed away in 2000.

Keigo KAMATA
October, 2006